Abstract volume of the 33rd Himalaya-Karakorum-Tibet Workshop

10-12 September 2018, Lausanne, Switzerland

Editors: Hetényi G, Guillermin Z, Jordan M, Raymond G, Subedi S, Buchs N, Robyr M, Epard JL

DOI: 10.5281/zenodo.1403887

This document contains 184 numbered pages.

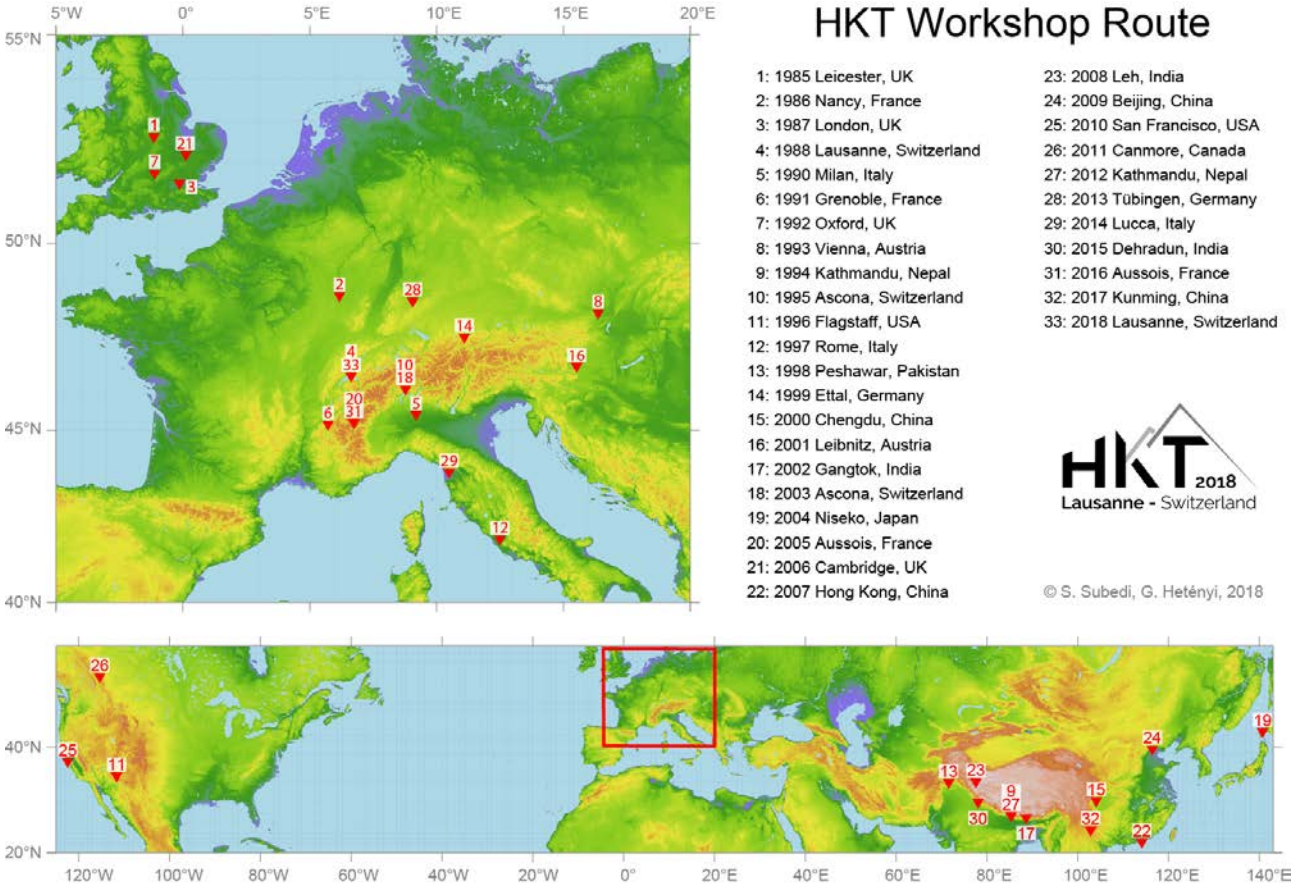

Table of Contents

The abstracts are in alphabetical order according to the first author's last name
Click on titles to access abstracts

Muzaffarabad paleohigh, NW Himalaya, Pakistan: Its impacts on depositional settings and development of Hazara-Kashmir syntaxis

Ahsan N[1], Mahmood T[2], Qayyum A[3], Miraj M[1], Rehman S[4]

[1]Inst. of Geology, Univ. of the Punjab, Lahore, Pakistan [2]OGDCL, Blue Area, Islamabad, Pakistan [3]Dept. of Earth Sciences, Utrecht Univ., The Netherlands [4]Dept. of Earth Sciences, Sargodha Univ., Pakistan

Well-developed sedimentary successions outcrop in Hazara Kashmir Syntaxes (HKS) and its surroundings. In Kashmir Basin a Cambrian sequence represented by Muzaffarabad Formation (Abbottabad Formation) overlies unconformably the Precambrian Dogra Slates (Hazara Formation). A paleohigh, Muzaffarabad Paleohigh (MP), developed probably in Permian after the deposition of shallowing upward algal mat (stromatolitic) dolomite of Muzaffarabad Formation on Precambrian slates in Kashmir Basin. Since its development, MP controlled the tectonic and depositional settings of the entire area.

The fragmentation of Pangaea initiated in late Cambrian and sea water retreated indicating a hiatus of 505 Myr till Danian. Contrary to Kashmir Basin, Permian to Lower Paleocene sequences, punctuated by many unconformities and their correlative conformities, are preserved in Potwar and Hazara basins situated to the west. In late Cretaceous, a basement high developed especially in Hazara and adjoining basins when Indian Plate established its first contact with Kohistan Island Arc and Neotethys retreated. Central parts of HKS (MP and Kashmir Basin) and Hazara Basin again submerged in lower Paleogene. In Kashmir Basin, Hangu Formation initiated deposition over Cambrian-Paleogene composite unconformity in Neothethyan realm.

Hangu Formation, Danian in age, represents a channel deposit in eastern most part of Kashmir Basin and mainly quartz arenite in the northern part of the basin near Muzaffarabad. Transgressive carbonates of middle Paleocene represented by Lockhart Formation overlies Hangu Formation. These carbonates comprise thinly bedded limestone (inner shelf) with intercalated shale in eastern part of Kashmir Basin and massive limestone (outer shelf) in Hazara Basin. Upper Paleocene maximum flooding event covered the entire Indus, Hazara and Kashmir basins whereas area of Kashmir Basin underwent progradational settings. Carbonates of Ypresian Margala Hills Limestone (outer shelf), tidal flat deposits of Eocene Chorgali Formation (carbonates, mudstone, and dolomite) and supra-tidal variegated clays, mudstone and evaporates of Kuldana Formation (marine and nonmarine) were deposited. India and Eurasia collision closed the Neotethys in middle Eocene and Himalayan orogeny started with the deposition of molasses of Rawalpindi group.

Collision related stresses migrated from Main Mantle Thrust (MMT) to south to develop intra-plate thrusts like Main Central Thrust (MCT), Punjal Thrust (PT), Nathia Gali Thrust (NGT) and Main Boundary Thrust (MBT) and strike slip Jhelum Fault on the western margin of MP. MP provided higher basal friction to cause development of a syntaxial bend (HKT) around itself when south directed deformation front reached MP. Ongoing convergence and south directed movement of deformation front developed Himalayan Frontal Thrust. Paleomagnetic studies indicate clockwise rotation in sediments in Kashmir Basin and in Hazara Basin and Potwar Plateau sediments rotated counter-clockwise. This fact suggests that MP being a resistant paleohigh acted as leading edge of the Indian Plate that produced bending of PT, NGT and MBT along its northern margin and along its flanks. Bending of the sedimentary sequence on each side of MP is the reason that causes clockwise rotation along eastern side of MP (Kashmir Basin) and counter-clockwise rotation along western flank of MP (Hazara Basin and Potwar Plateau).

Importance of the Mesozoic geological inheritance in the present structure of the Longmen Shan, Eastern Tibet

Airaghi L[1,2], de Sigoyer J[2], Guillot S[2], Robert A[3], Warren C[4], Deldicque D[5]

[1]ISTeP, Sorbonne Univ., Paris, France [2]ISTerre, Univ. Grenoble-Alpes, France [3]GET, Univ. Paul Sabatier, Toulouse, France [4]The Open Univ., Milton Keynes, UK [5]Laboratoire de Géologie, ENS Paris, France

The Longmen Shan thrust belt (at the eastern border of the Tibetan plateau, Fig. 1) is a tectonically active region as demonstrated by the occurrence of the Mw 7.9 Wenchuan (2008) and Mw 6.6 Lushan (2013) earthquakes in the central and southern part of the belt respectively. The belt lies in a crustal transition zone, between the Sichuan Basin to the east and the Songpan Garze block (Tibetan plateau) to the west. Seismic investigations show that the Tibetan crust is overthickened (> 60 km, Robert et al. 2010). The timing of the crustal thickening is however still debated. The Cenozoic compressional phase (from 30 Ma) unrevealed by low-temperature thermochronology (e.g. Wang et al. 2012) and responsible of a rapid cooling of the belt is indeed related only to a small part of the crustal thickening.

The occurrence of the unexpected recent earthquakes has required a deeper understanding of the temporal evolution of crustal dynamics in the region. To better constrain the calendar of the deformation and crustal thickening we carried out a structural and petro-chronological study in the most exhumed areas of the belt. In the central Longmen Shan, a metamorphic jump of 150-200°C, 5-6 kbar is observed between the metasedimentary Songpan-Garze units in the hanging wall of the major Wenchuan fault (amphibolite-facies metamorphism at T > 500°C) and units in the footwall (T < 380°C, Fig. 1) (Airaghi et al. in revision). Meso-, micro-structures and the folded shape of the paleo-isotherms reveal that the amphibolite-facies metamorphism is coeval with the NE-SW folding (D2 deformation), thickening (up to 30 km) and thrusting of SPG units over the South China block during the Triassic closure of the Paleotethys (de Sigoyer et al. 2014). The Tibetan crust was therefore already thickened at the Late Triassic time. The re-activation of the crystalline massifs (South China basement) at the Lower Cretaceous (ca. 120-140 Ma, Airaghi et al. in press) attests of the long-term thrusting component of the major Wenchuan and Beichuan faults and marks the onset of the dominant basement-involving deformation (D3 deformation). At that time, sedimentary units also experienced a late greenschist metamorphic overprint and E-W folding. In the central Longmen Shan a part of the exhumation therefore precedes the Cenozoic period.

By contrast, in the southern Longmen Shan, no amphibolite-facies metasedimentary rocks are observed (T < 400°C, Fig. 1), suggesting that deep units were never exhumed in this area. The Baoxing crystalline massif is metamorphosed under greenschist-facies conditions (~350°C, ~6 kbar) similar to the ones estimated for the Pengguan massif in the central Longmen Shan (Airaghi et al. 2017; Airaghi et al. in press). However, the new $^{40}Ar/^{39}Ar$ white mica ages date the metamorphism in the southern area at the Early Cenozoic (~80-60 Ma) instead of Early Cretaceous. This suggest that at the long-term scale the Longmen Shan is an asymmetrical belt, with different parts re-activated at different times and experiencing a different geological evolution.

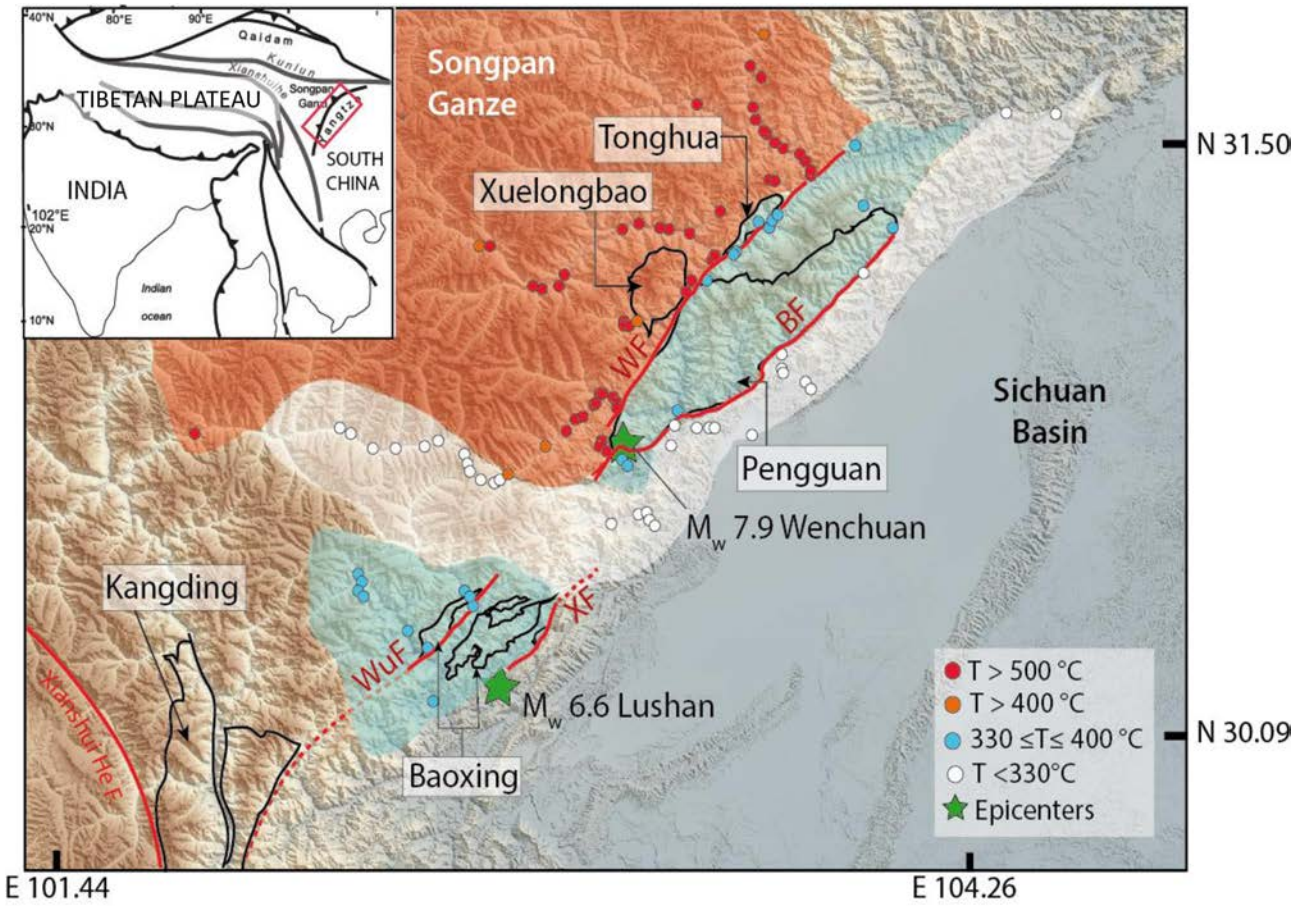

Figure 1. Compilaton map of the maximum temperatures (estimated with the Raman Spectroscopy on Carbonaceous material thermometer) experienced by the rocks of the central and southern Longmen Shan obtained from this study and by Robert et al. (2010). The inset relocates the position of the Longmen Shan in the India-Asia system. WF: Wenchuan fault, BF: Beichuan fault, WuF: Wulong fault, XF: Xiaoguanzi fault. Green stars indicate the location of the epicentres of the 2008 Mw 7.9 Wenchuan and 2013 Mw 6.6 Lushan earthquakes.

References

Airaghi L, de Sigoyer J, Guillot S, Robert A, Deldicque D (in revision) Importance of the Mesozoic geological inheritance in the present structure of the Longmen Shan (eastern Tibet). Tectonics.

Airaghi L, de Sigoyer J, Lanari P, Guillot S, Vidal O, Monié P, Sautter B, Tan X (2017) Total exhumation across the Beichuan fault in the Longmen Shan (eastern Tibetan plateau, China): constraints from petrology and thermobarometry. J Asian Earth Sci 140: 108-121.

Airaghi L, Warren CJ, de Sigoyer J, Lanari P, Magning V (in press) Influence of dissolution/reprecipitation reactions on metamorphic greenschist to amphibolite-facies mica 40Ar/39Ar ages in the Longmen Shan (eastern Tibet). J Metam Geol.

de Sigoyer J, Vanderhaeghe O, Duchene S, Billerot A (2014) Generation and emplacement of Triassic granitoids within the Sonpan Ganze accretionary orogenic wedge in a context of slab retreat accommodated by tear faulting, Eastern Tibetan plateau, China. J Asian Earth Sci 88: 192-216.

Robert A, Pubellier M, de Sigoyer J, Vergne J, Lahfid A, Cattin R, Findling N, Zhu J (2010) Structural and thermal characters of the Longmen shan (Sichuan, China). Tectonophys 491: 165-173.

Wang E, Kirby E, Furlong KP, van Soest M, Xu G, Shi X, Kamp PJJ, Hodges KV (2012) Two-phase growth of high topography in eastern Tibet during Cenozoic. Nat Geosci 5: 540-545.

Climate variability in the Central Indian Himalaya during the last ~15 ka: Evidences of Indian Summer Monsoon variability from multiproxy studies

Ali SN[1], Agrawal S[1], Quamar M[1], Dubey J[1], Chauhan N[2], Bisht P[3], Pandey P[4], Arif M[1], Shekhar M[1], Morthekai P[1], Shukla A[2]

[1]Birbal Sahni Inst. of Paleosciences, India [2]Physical Research Laboratory, Ahmedabad, India [3]Wadia Inst. of Himalayan Geology, Dehradun, India [4]Indian Inst. of Remote Sensing, Dehradun, India

Indian summer monsoons (ISM), is the vital source of precipitation in India and contribute significantly to Asian monsoon system and global climate. By contributing over 80% of the total annual rainfall in India, ISM significantly influences agrarian based Indian socio-economy and is considered as the most significant weather system nourishing the Himalayan glaciers. Abrupt shifts in the ISM on decadal to centennial scales might severely affect Indian socio-economy as observed in the recent past and is associated with the rise and fall of ancient human civilisations. To improve the predictive capabilities of the future ISM variability, characterization of the ISM precipitation before the instrumental period is becoming an urgent need. For proxy based palaeoclimatic reconstructions, climatologically sensitive areas like the transitional zone lying between the dry Trans Himalaya–Tibet towards north and the sub-humid Himalaya towards south that receives high precipitation (amplified signal) during intensified ISM and vice-versa are most suitable in this regard. Keeping these facts in view and to quantify the ISM variability for a monsoon dominated agrarian based Indian socio-economy, we have collected samples from a relict proglacial sedimentary profile situated in the transition zone of higher central Himalaya. Towards this, we have used combined carbon isotope ($\delta^{13}C$), total organic carbon (TOC), magnetic susceptibility (χ_{lf}), loss on ignition (LOI), pollen analysis and aided with Optically stimulated luminescence (OSL) from a ~3.5 m deep sedimentary profile from Kunti Banar valley, Dhauliganga basin, Central Himalaya, India. Based on our proxy records, three major phases of negative and three positive excursions of the ISM in the last ~15 ka have been identified. Prominent negative ISM shift was observed during the Younger Dryas (YD) between ~12.2 and 10.5 ka. While ISM shows an overall weakening during ~8.5 and 2 ka and an increasing trend has been observed during ~10.5 and 8.5 ka and after 2 ka. Surprisingly, our data suggest that the mid Holocene ISM weakening was more severe than that of the younger dryas (YD) in this region. Our reconstructions are broadly in agreement with local as well as regional reconstructions and model simulations.

Seismic full moment tensors for deep earthquakes beneath the Himalayas, and their relevance to metamorphism in the region

Alvizuri C[1], Hetényi G[1]

[1]ISTE, FGSE, Univ. of Lausanne, Switzerland

We present full moment tensors with uncertainties for seismic events in the lower crust beneath the Himalayas in Nepal and Bhutan. This is a region presumed to experience density and volume changes due to metamorphism (eclogitization). We estimate moment tensors for earthquakes in the region to investigate their relation to metamorphism and use the uncertainty estimates to discern among physical mechanisms. The seismic moment tensor is a 3×3 symmetric matrix that represents seismic events within the Earth's crust, including tectonic earthquakes, volcanic events, explosions, and mine collapses. We apply an algorithm that uses seismic waveforms to estimate optimal moment tensors and their uncertainty. The algorithm performs a grid search over the six-dimensional space of moment tensors by generating synthetic waveforms at each grid point and then evaluating a misfit function between the observed and synthetic waveforms. We computed the synthetic waveforms using several 1D structural models for the region. The seismic events considered here were recorded at broadband seismic stations from the GANSSER and HIMNT arrays. We analyse the June 6th, 2013 Bhutan earthquake recorded by the GANSSER array, and a group of events at depths 50-100 km with epicentres within the HIMNT array. In this group the largest event has magnitude Mw 3.6, and the majority have magnitudes 1-2. The waveforms for these events show impulsive first motions, body waves at frequencies above 1 Hz and, for the largest event, surface waves. For each event we utilize all possible waveforms and first motion polarities. Our moment tensor estimates show non-double-couple components, and we discuss their significance in light of the structural and petrological models. If these seismic events are linked to metamorphic reactions such as eclogitization, these results would suggest that the reactions occur at previously undocumented spatial scales.

Using thermochronology to validate a balanced cross section along the Karnali River, far-western Nepal

Battistella C[1], Robinson D[1], McQuarrie N[2], Ghoshal S[2]

[1]Dept. of Geological Sciences, The Univ. of Alabama, Tuscaloosa, USA [2]Univ. of Pittsburgh, USA

Multiple valid balanced cross sections can be produced from mapped surface and subsurface data. By integrating low temperature thermochronologic data, we are better able to predict subsurface geometries. Only one balanced cross section exists along the Karnali River in far western Nepal (Robinson et al. 2006), which does not incorporate thermochronologic data because the data did not exist. Since then, the data published along the Simikot cross section along the Karnali River include muscovite Ar, zircon (U-Th)/He and apatite fission track. In this study, balanced cross sections are reconstructed to determine the kinematics sequence. The cross section is then sequentially deformed in ~10 km increments with flexural loading and erosional isostatic unloading applied to each step. The reconstructed section is then used to create a 2D thermokinematic model that predicts the cooling ages along the section. The modelled cooling ages are compared with the published data and by varying the location of the decollement ramp, shortening rates, and radiogenic heat production the model can be modified to better match the data. Comparison of the modelled cooling ages to the published thermochronologic data along this section indicates that although the cross section is valid and balanced, the suggested fault geometry does not reproduce the observed cooling ages. This fault geometry fails to produce the young uplift imparted by an active ramp in the Lesser Himalaya, indicating a different decollement ramp geometry. By moving this ramp, a more accurate reproduction of the measured cooling ages may result.

Reference

Robinson DM, DeCelles PG, Copeland P (2006) Tectonic evolution of the Himalayan thrust belt in western Nepal: Implications for channel flow models. GSA Bull 118: 865-885.

The 4th HKT Lausanne, 30 years ago: review on local researches in Himalaya and Tibet – In Memory of Maurizio Gaetani

Baud A[1]

[1]Baud Geological Consultant, Lausanne, Switzerland

October 5-8, 1988, we organized with Profs. H. Masson, G. Stampfli and A. Steck the 4th Himalaya-Karakorum-Tibet workshop in Lausanne and we edited the Conference Proceedings, published in Eclogae Geol. Helv., vol. 82,2 (1989). With 90 participants and 35 communications, this fourth meeting confirmed at that time the success of the HKT researches. An exhibition on the Himalayan researches undertaken in Lausanne was also exposed at the University, nearby the meeting.

Initiator of the Lausanne University and Geological Museum research group on Himalaya studies, I participated to excursions, field trips and researches in Ladakh and Zanskar Himalaya (N India) from 1977 to 1983. During 1979 I helped Profs. A. Escher, H. Masson and A. Steck in the organization of the first Eastern Zanskar geotraverse Hemis–Padum. In 1981 I prepared with Prof. M. Gaetani (Milan) a SE–NW geotraverse from Darcha (Lahul) to Thongde (Zanskar) through Sarchu, Phirtse-La and Phugtal. In 1983 I co-organized an expedition with Prof. G. Mascle (Grenoble) and Dr. E. Garzanti (Milano) to carry out detailed stratigraphic sections and tectonic observations in Central Zanskar, N and E of the Spongtang ophiolite Klippe. When in 1985 Western Tibet opened to outsiders, I was the first Westerner geologist to enter in the Kailash area after A. Gansser in 1936 and the first to cross the Western Tibetan plateau from Toling in the Sutlej Valley to Yarkand on the Silk Road. In December 1987 I get the opportunity to work on classical Permian-Triassic boundary sections in the Salt Ranges (Pakistan) and in the Guryul Ravine (Kashmir, India) with Profs. M. Gaetani, J. Marcoux and E.T. Tozer. The main results obtained in collaboration with part of the above mentioned teams, can be summarized as follows:

1. The discovery and definition of large scale SW vergence nappe structure in the Zanskar sedimentary belt (Tethys Himalaya). In spite of strong oppositions and controversies about the nappe theory by autochthonous minded geologists, these geological structures were largely confirmed by detailed field work and mapping by our Italian and British colleagues and the name of the new defined structural units were well adopted by them.
2. A new geological profile through E Zanskar, from Hemis to Padum.
3. Detailed stratigraphic sections of late Cretaceous and early Tertiary sediments of central Zanskar with the geodynamic interpretation of sedimentary record of the northward flight of India.
4. New observations in the Kailash area and along the Sutlej–Yarkand geotraverse.
5. Permian-Triassic isotope stratigraphy in the Salt Ranges and Kashmir.
6. A new geodynamic interpretation and timing of the late Paleozoic rifting.

Deformation of the Indus Basin, Ladakh, NW India

Bhattacharya G[1], Robinson D[1]

[1]Dept. of Geological Sciences, The Univ. of Alabama, Tuscaloosa, USA

The Indus-Yarlung suture zone in Ladakh, northwest India, delineates the collision between the Indian and Asian plates and presents a natural laboratory to test multiple aspects of structural deformation related to continental collision. This study focuses on the structural geology and associated tectonics of the sedimentary basin in the Indus-Yarlung suture zone, called the Indus basin. We investigate the styles of basin deformation in outcrop and regional scales across four sections from western to eastern Ladakh: the Skinning section, the Temesgam section, the Zanskar Gorge and the Upshi-Lato section. Clastic rocks dominate the Indus basin and the conglomerates, with pebble to boulder size clasts, exhibit lateral facies variations. The Indus basin exhibits at least two generations of deformation and constitutes the footwall of the north-vergent Great Counter thrust, which is present along the length of the Himalayan arc. Two primary thrusts, the Choksti and Nimu thrusts, are laterally traceable for more than 150 km along strike in the Indus basin, which is locally cut by multiple thrust faults. The Choksti thrust is a backthrust that dips ~80-90° SSE, and accounts for the vertical isoclinal and overturned folds present in the southern part of the basin. The Nimu thrust dips 55-65° S and accounts for the north-vergent fold-thrust deformation in the northern part of the basin. Structures are predominantly brittle and compressional although limited evidence of extension, overprinted by thrusting, is also present. Reverse drag, normal faults, and step-down slickensides are present in the younger, thrusted Oligocene-Miocene formations of the Indus Group and suggest an extensional regime after deposition and prior to thrusting. Kink folds, doming, and fold interference is observed in the older Late Albian–Early Eocene Tar Group, and in the mélange unit rocks south of the Tar Group. The extensional structures originated when the Greater Indian slab rolled back in Late Oligocene-Early Miocene time causing upper plate extension. The Great Counter thrust was active between ~23-20 Ma and thrusting propagated northward into the Indus basin along the Choksti thrust, which resulted in north-vergent compressional structures. Subsequent erosion of hanging wall block of the Great Counter thrust occurred due to regional uplift, when the Indian plate returned to northward underthrusting mode after Greater Indian slab break-off, leading to a cooling phase between ~19-8 Ma. Thrusting again resumed in Pliocene time between ~6-4 Ma and propagated further northward along the Nimu thrust causing oversteepening of the folds and the Choksti thrust in the south. Pliocene thrusting is likely a local event and is not reported elsewhere in the Indus-Yarlung suture zone.

Low-temperature thermochronology of the Indus basin in NW India: Implications for Miocene cooling

Bhattacharya G[1], Robinson D[1], Orme D[2], Najman Y[3], Olree E[1], Bosu S[1]

[1]Dept. of Geological Sciences, The Univ. of Alabama, Tuscaloosa, USA [2]Dept. of Earth Sciences, Montana State Univ., USA [3]Lancaster Environment Centre, Lancaster Univ., UK

Following the onset of collision between India and Asia in the early Cenozoic, the Indus-Yarlung suture zone became a continental depocenter in northwest India and south Tibet. We present zircon fission-track (ZFT), and apatite and zircon (U-Th)/He (AHe and ZHe) thermochronologic data from sedimentary rocks of the Indus basin, which runs > 450 km through the Indus suture zone in northwest India and record the thermo-tectonic events after the onset of India-Asia plate collision. Sedimentation began in the basin in the Late Albian and continued to at least Late Miocene time (~6 Ma). Using ZFT ages and thermal modelling of ZHe ages, we show that maximum burial temperatures in the basin did not exceed 280°C in the deeper Tar Group and remained below 200°C in the shallower Indus Group. Our oldest ZHe ages, integrated with published depositional ages from the Indus basin, require that motion along the Great Counter thrust in northwest India began after ~23 Ma and ended by ~20 Ma. After regional backthrusting, cooling of the basin was achieved in two phases- a) in Miocene time (ca. 19-8 Ma), based on interpretation and thermal modelling of our ZHe ages, and b) in Pliocene time (ca. 3.3-2.3 Ma), which is evident from our limited AHe dataset. We interpret that the Miocene cooling was caused by erosion of the Great Counter thrust hanging wall due to regional uplift caused by northward underthrusting of the continental Indian plate following Greater Indian slab break-off at ~20 Ma. Local shallow crustal burial (< 2 km) by thrusting also occurred in Early Pliocene time in the northern part of the Indus basin and subsequent erosion exhumed the rocks. Subduction dynamics of the Indian plate in Miocene time controlled the regional tectonics of the Indus basin through deposition and exhumation.

Pamir tectonic evolution and associated environmental changes recorded since 40 Ma in the western Tarim Basin, Aertashi section

Blayney T[1], Dupont-Nivet G[2,3], Najman Y[1], Proust JN[2,4], Meijer N[3], Roperch P[4], Sobel E[3], Millar I[5], Guo Z[6]

[1]Lancaster Environment Centre, Lancaster Univ., UK [2]CNRS, France [3]Inst. of Earth and Environmental Science, Univ. of Potsdam, Germany [4]Geosciences Rennes, Univ. of Rennes, France [5]ERC Isotope Geosciences Laboratory, BGS Keyworth, Nottingham, UK [6]Key Laboratory of Orogenic Belts and Crustal Evolution, Peking Univ., Beijing, China

At the western syntaxis of the India-Asia collision, the northward indentation of the Pamir salient into the Tarim Basin is the focus of controversial models linking lithospheric to surface and atmospheric processes. Competing models have been proposed involving either continental subduction or delamination of the Asian slab presently south dipping under the Pamir. The Tarim Basin also hosts the Taklimakan desert, a key tracer of environmental changes. The age of this desert formation remains, however, controversial with estimates ranging from 26-22 Ma to 3 Ma.

Here we report tectonic and climatic events recorded in the most complete and best-dated sedimentary sequences from the western Tarim Basin flanking the eastern Pamir (the Aertashi section), based on sedimentology, provenance and paleoenvironmental proxies constrained by our magnetostratigraphic analyses.

Increased tectonic subsidence and a shift from marine to continental deposition at 41 Ma indicate far-field deformation from the south affecting Tarim. A sediment accumulation hiatus from 24.3 to 21.6 Ma followed by deposition of proximal conglomerates is linked to fault propagation into Tarim, which may relate to coeval break-off of the Indian slab later followed by roll-back of the south-dipping Eurasian slab. From 21.6 to 15.0 Ma, increasing accumulation of fining upwards clastics is interpreted as the expression of a major dextral transtensional system linking the Kunlun to the Tian Shan ahead of the northward Pamir indentation. At 15.0 Ma, the appearance of North Pamir-sourced conglomerates followed at 11 Ma by Central Pamir-sourced volcanics, coincide with growth-strata and clockwise vertical-axis rotation, associated with activation of a local east-vergent thrust wedge. Together, this enables to interpret that Pamir indentation had started by 24.3 Ma, reached the study location at 15.0 Ma, and had passed it by 11 Ma. This provide kinematic constraints on tectonic models involving intracontinental subduction and delamination.

More arid conditions prevailed already at 41 Ma, and then at 37 Ma, following the stepwise westward retreat of the Proto-Paratethys Sea that previously covered the desert and provided moisture. Sand dunes appeared ca. 34 Ma linked to the ca. 100 m sea-level drop of the Eocene-Oligocene transition implying further sea retreat and aridification. From ca. 30 Ma onwards, the appearance of smectite and from ca. 18 Ma to 15 Ma, the combined appearance of kaolinite with increasing weathering indices, magnetic susceptibility, and organic carbon isotope, are assessed with respect to westerly moisture seasonality and the orographic effect of the formation of the Pamir and Tian Shan orogens.

Luminescence dating and landscape evolution of the Himalaya, Nepal

Bouscary C[1], King G[1], Herman F[2], Biswal R[2], Chanard K[3], Lavé J[4], Hetényi G[2]

[1]Inst. of Geological Sciences, Univ. of Bern, Switzerland [2]FGSE, Univ. of Lausanne, Switzerland [3]LAREG, IGN, Univ. Paris Diderot, France [4]CRPG, CNRS, Univ. of Lorraine, Nancy, France

The 2015 Gorkha earthquake in Nepal, which caused widespread devastation and loss of life, reveals some gaps in our understanding of the deformation of the Himalaya. Here we quantify the exhumation rates in Nepal, which are linked to the processes of deformation, using luminescence thermochronometry.

The Himalaya mountain belt is the result of compressional orogeny due to the continental collision between the Indian and the Eurasian tectonic plates. Different north-dipping crustal-scale thrusts accommodate this convergence. In this project, we analyse samples collected across one of the most tectonically significant structures in the Himalayan orogen, the Main Central Thrust (MCT), which comprises one of the key high strain zones in the Himalaya and has accommodated at least 100 km of shortening. By quantifying exhumation rates on both sides of the MCT, the long-term deformation across this major thrust can be assessed.

Optically Stimulated Luminescence (OSL)-thermochronometry is a recently developed very-low-temperature thermochronometer, sensitive to temperatures of 30-100°C, based on optically stimulated luminescence dating of quartz and feldspar minerals. It offers the potential for tight constraint of cooling histories over recent – Quaternary – timescales and provides high-resolution cooling histories beyond the range of other thermochronometric systems. Applying this new technique to feldspar extracts of a set of samples from the Nepalese-Himalaya will provide insights into the cooling and thus exhumation/erosion history of the Himalayan fold-and-thrust belt.

Preliminary results indicate variations in exhumation rates between the different samples of the Himalayan range in Nepal. These data imply tectonic differences, providing controls on the tectonic history – fault evolution – of this region, which is at a colliding plate margin, with implications for the related seismic hazard.

Chasing a moving target: The age of the Main Central Thrust

Braden Z[1], Godin L[1], Kellett D[2], Yakymchuk C[3], Cottle J[4]

[1]Dept. of Geological Sciences and Geological Engineering, Queen's Univ., Kingston, Canada [2]Geological Survey of Canada, Dartmouth, Canada [3]Earth and Environmental Sciences, Univ. of Waterloo, Canada [4]Dept. of Earth Science, Univ. of California, Santa Barbara, USA

Crustal shortening is accommodated during continental collision along major thrust faults and shear zones. When these shear zones activate in different parts of an orogen is central to the understanding of how orogenic systems evolve. The Main Central thrust (MCT) is one of the major thrust systems in the Himalaya, yet, available timing constraints of its activity vary greatly along the length of orogen. From the Himalayan hinterland to the foreland, the MCT is exposed multiple times by broad open folds that form the Karnali klippe in western Nepal. Three comparable exposures of the MCT (Searle et al. 2008) were sampled to study shear zone evolution in the southward transport direction. Despite first order similarities, detailed geochronology reveals significant differences in timing of deformation and metamorphism along each exposure of the MCT.

In all three exposures, quartz microstructures reveal similar, progressive changes in deformation mechanism with structural position from the middle of the metamorphic core to the immediate footwall of the MCT. The core and the immediate hanging wall of the MCT show grain boundary migration quartz recrystallization, while the MCT footwall shows bulging recrystallization around relict quartz grains. Quartz crystallographic orientation analyses confirm a pervasive south-directed sense of shear. Opening angle thermometry yields temperatures of deformation ≥ 500°C ± 50°C within the hinterland MCT high strain zone and temperatures of 425°C ± 50°C in the foreland MCT.

Phase equilibria modelling yields comparable peak pressure-temperature conditions in the lower metamorphic core in the hinterland and on the north flank of the Karnali klippe of ca. 700-650°C, 1.1-0.8 GPa. Peak temperatures decrease by 100-50°C from the lower metamorphic core towards the base of the MCT high strain zone. Peak temperatures also decrease towards the foreland. Pressure conditions on the foreland MCT remain unconstrained.

(U-Th)/Pb petrochronology yields monazite crystallization ages as early as 47 Ma in the lower metamorphic core on the north flank, with decreasing ages down section towards the base of the MCT. Melt crystallization began ca. 35 Ma and lasted until 18 Ma (Braden et al. 2017). In contrast, the oldest recorded monazite crystallization in the hinterland is 18 Ma with melt crystallization beginning ca. 14 Ma and lasting until ~8 Ma (Braden et al. 2017). U/Pb zircon geochronology on a sheared kyanite-bearing leucocratic pod from the base of the MCT high strain zone in the hinterland constrains south-directed deformation to as recently as 8 Ma (Braden et al. 2018). This ductile thrusting in the hinterland MCT occurred out-of-sequence with respect to the foreland MCT, along which ductile deformation was complete by 17 Ma. $^{40}Ar/^{39}Ar$ thermochronology on white mica indicates recrystallization/cooling of the foreland MCT zone below 350-400°C by 17 Ma, the north flank of the klippe by 14 Ma, and the hinterland by 6 Ma (Fig. 1).

There is no single age for the MCT in western Nepal. MCT activity is better described as prolonged and diachronous in the transport direction. Ductile deformation propagated in the Oligocene from hinterland to foreland. The foreland MCT segment cooled first, in the early Miocene, while the still-hot hinterland MCT segment reactivated in the late Miocene.

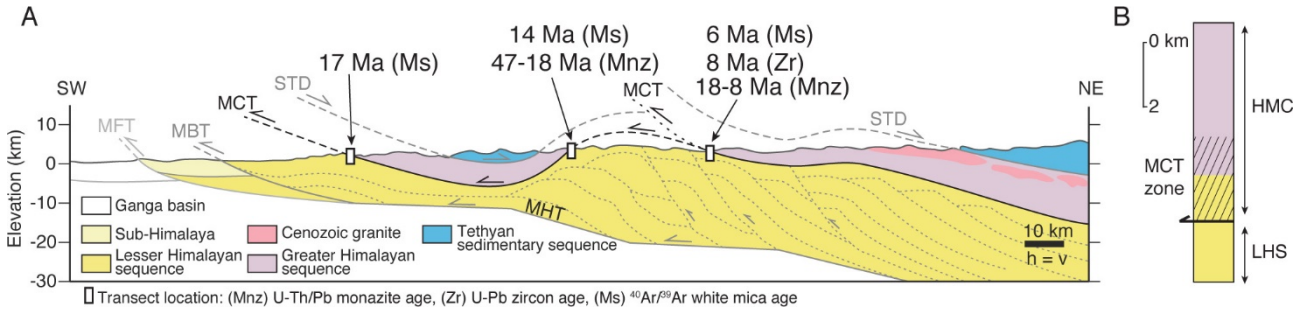

Figure 1. A) Cross-section through the western Nepal Himalaya, modified from Soucy La Roche et al. 2018. Each of the three dated transects includes multiple samples from the hanging wall to the footwall of the MCT, as shown in B. B) Structural column illustrating the location of the MCT and the vertical span of dated samples. HMC: Himalayan metamorphic core, LHS: Lesser Himalayan sequence.

References

Braden Z, Godin L, Cottle JM (2017) Segmentation and rejuvenation of the Greater Himalayan sequence in western Nepal revealed by in situ U-Th/Pb monazite petrochronology. Lithos 284-285: 751-765.

Braden Z, Godin L, Cottle J, Yakymchuk C (2018) Renewed late Miocene (< 8 Ma) hinterland ductile thrusting, western Nepal Himalaya. Geology 46: 503-506.

Searle MP, Law RD, Godin L, Larson KP, Streule MJ, Cottle JM, Jessup MJ (2008) Defining the Himalayan Main Central Thrust in Nepal. J Geol Soc 165: 523-534.

Soucy La Roche R, Godin L, Cottle J, Kellett DA (2018) Preservation of the early evolution of the Himalayan middle crust in foreland klippen: Insights from the Karnali klippe, west Nepal. Tectonics 37: TC4847.

U-Pb zircon ages from a suprasubduction zone ophiolite, Nidar, NW Himalaya, India: Incipient arc magmatism in fore-arc oceanic crust

Buchs N[1], Epard JL[1], Müntener O[1]

[1]ISTE, FGSE, Univ. of Lausanne, Switzerland

The Nidar Ophiolite is a suprasubduction zone ophiolite exposed in the Indus-Tsangpo suture zone in the Western Himalayas (Thakur and Virdi 1979; Mahéo et al. 2004). It represents a remnant of the Neo-Tethys Ocean located between the Indian and Eurasian margins before the Himalayan collision at around 50 Ma.

The Nidar Ophiolite consists of an upper mantle unit dominated by harzburgites and dunites. These ultramafics are overlaid by an oceanic crustal sequence composed of isotropic and layered gabbros, pillow lavas and lava flows, that are associated to lower Cretaceous radiolarites (Zyabrev et al. 2008). The gabbros are intruded by km-scale immature arc-related bodies containing, wehrlites, clinopyroxenites, hornblende-gabbros, pegmatitic gabbros, porphyritic sub-volcanic rocks and plagiogranites. New LA-ICPMS U/Pb zircon ages of four plagiogranite samples from three different outcrops display concordant and overlapping lower Cretaceous ages of 132.6 ± 1.6 Ma to 129.7 ± 1.6 Ma without any evidence of inherited cores. The εHf values of the dated zircons are ranging from +13 to +15 and are representative of a juvenile mantle reservoir.

Those new zircon ages coupled to field and geochemical data constrain the magmatic evolution of the Nidar Ophiolite, which was formed by at least during two magmatic events in a suprasubduction zone environment: (i) phase 1 magmatism corresponds to the formation of an oceanic crust of poorly constrained age (Ahmad et al. 2008) in fore-arc setting and (ii) phase 2 magmatism is characterized by the intrusion of incipient arc magmatism into pre-existing oceanic crust during the Late Valanginian to Early Hauterivian.

References

Ahmad T, Tanaka T, Sachan HK, Asahara Y, Islam R, Khanna PP (2008) Geochemical and Isotopic Constraints on the Age and Origin of the Nidar Ophiolitic Complex, Ladakh, India: Implications for the Neo-Tethyan Subduction along the Indus Suture Zone. Tectonophys 451: 206-224.

Mahéo G, Bertrand H, Guillot S, Villa IM, Keller F, Capiez P (2004) The South Ladakh ophiolites (NW Himalaya, India): an intra-oceanic tholeiitic arc origin with implication for the closure of the Neo-Tethys. Chem Geol 203: 273-303.

Thakur VC, Virdi NS (1979) Lithostratigraphy, Structural Framework, Deformation and Metamorphism of the Southeastern Region of Ladakh, Kashmir Himalaya, India. Himalayan Geology 9: 63-78.

Zyabrev SV, Kojima S, Ahmad T (2008) Radiolarian biostratigraphic constraints on the generation of the Nidar Ophiolite and the onset of Dras arc volcanism: tracing the evolution of the closing Tethys along the Indus–Yarlung-Tsangpo suture. Stratigraphy 5: 99-112.

U-Pb zircon ages in the Upshi Molasse at Martselang, Indus Molasse, Ladakh

Buchs N[1], Epard JL[1], Steck A[1]

[1]ISTE, FGSE, Univ. of Lausanne, Switzerland

The Indus Molasse is a key formation to decipher the kinematic evolution of the Indus suture zone. It is deposited in a basin located south of the Ladakh batholith and north or on top of the accretion prism and of the rising North Himalayan Nappes. At the north-eastern edge of the basin, the Molasse is transgressive on the Ladakh batholith. In the Gongmarula–Hemis–Karu section, these deposits are named the Upshi Molasse (Frank et al. 1977). The Hemis Molasse is thrust towards the north on top of the Upshi Molasse and metamorphized under prehnite-pumpellyite facies during the Late Eocene (Steck et al. 1993; Steck 2003).

Steck et al. (1993) described pyroclastic deposits at Martselang in the Upshi Molasse. These breccias, made up of angular felsic material, have been sampled; zircons have been separated and dated using U-Pb, LA-ICPMS method. The age obtained on a homogeneous group of 9 zircons is 59.6 ± 0.1 Ma; one zircon gives an older age of 88.4 ± 2.4 Ma. It demonstrates that the age of the Upshi Molasse is syn- or post- 59.6 Ma (syn- or post-Selandian, Paleocene) if it is assumed in a first case that the zircons have a monogenic volcanic origin, or, in a second case, they are of a purely detrital origin from the batholith. The Upshi Molasse is therefore not the equivalent of the Maastrichtian Basgo Formation (Van Haver 1984; Garzanti and van Haver 1988) found in a similar tectonic position, 25 km NW of Leh. If the batholith material in the studied samples is sub-contemporaneous to its deposition due to a pyroclastic phreatic explosion, it would imply that the Upshi Molasse is older than the post 47.1 ± 0.1 Ma (Lutetian, Eocene) Chumathang Molasse (St-Onge et al. 2010) located 70 km E of Upshi.

References

Frank W, Gansser A, Trommsdorff V (1977) Geological observations in the Ladakh area (Himalayas). A preliminary report. Schweiz Min Petr Mitt 57: 89-113.

Garzanti E, van Haver T (1988) The Indus clastics: fore-arc basin sedimentation in the Ladakh Himalaya (India). Sediment. Geology 59: 237-249.

Steck A (2003) Geology of the NW Himalaya. Eclogae Geol Helv 96: 147-196.

Steck A, Spring L, Vannay JC, Masson H, Stutz E, Bucher H, Marchant R, Tièche JC (1993) Geological transect across the Northwestern Himalaya in eastern Ladakh and Lahul (A model for the continental collision of India and Asia). Eclogae Geol Helv 86: 219-263.

St-Onge MR, Rayner N, Searle MP (2010) Zircon age determinations for the Ladakh batholith at Chumathang (Northwest India): Implications for the age of the India–Asia collision in the Ladakh Himalaya. Tectonophys 495: 171-183.

Van Haver T (1984) Etude stratigraphique, sédimentologique et structurale d'un bassin d'avant arc: exemple du bassin de l'Indus, Ladakh, Himalaya. Thèse, Univ. Scientifique et Médicale de Grenoble, 204 p.

Duration of inverted metamorphic sequence formation across the Himalayan Main Central Thrust, Sikkim, NE India

Burg JP[1], Moulas E[2], Tajcmanová L[1], Cioldi S[1]

[1]Geological Inst., Dept. of Earth Sciences, ETH Zurich, Switzerland [2]ISTE, FGSE, Univ. of Lausanne, Switzerland

This study investigates the tectonic setting and the timescale of inverted isograds related to crustal-scale thrusting at the MCT in the Sikkim region, northeast India. The aim is to contribute to the understanding of the link between mechanical and thermal evolution of major thrust zones and to clarify the nature and the origin of orogenic heat by applying garnet diffusion modelling.

Garnet compositional zoning is used as a gauge for rate estimates of element diffusion within the mineral. Convectional geothermobarometry based on phase equilibria using garnet chemical compositions indicates an inverted thermal- and a normal pressure-gradient from the structural bottom to top of the footwall of the MCT. Inverse-fitting numerical model considering Fractionation and Diffusion in GarnEt (FRIDGE) was applied to find a best fit for a P-T path. Such an inverse fitting model generates compositional profiles of garnet from a given bulk rock composition assuming chemical fractionation and simultaneous diffusion along a P-T-t path. Simulations were then compared with measured garnet profiles. The P-T path was then adapted until the mismatch between calculated and observed profile is minimized.

The abrupt compositional changes in most of the analysed garnets is appropriate for simple diffusion modelling at the peak temperature. This approach helps constraining the maximum time spent near peak conditions. Results indicate 3 to 6 Ma long high-temperature metamorphic conditions. This short duration does not permit complete thermal re-equilibration but allows preservation of inverted metamorphic gradients. Zircon SHRIMP ages measured in MCT migmatites indicate that peak temperature conditions were reached between ca. 18 and 15 Ma.

Considering the normal pressure gradient, the narrowness (3 up to 5 km) of high grade rocks (kyanite- and sillimanite-zone) and the short duration of peak-T conditions, we contend that viscous-heating explains localized and short-lived metamorphic conditions along crustal thrust zones like the MCT.

Dating the High Himalayan Discontinuity and the Main Central Thrust in the Marshyangdi Valley, Central Nepal, by in-situ U-Th-Pb monazite petrochronology

Carosi R[1], Montomoli C[2], Cottle J[3], Iaccarino S[1], Tartaglia G[1], Visonà D[4]

[1]Univ. of Torino, Italy [2]Univ. of Pisa, Italy [3] Dept. of Earth Science, Univ. of California, Santa Barbara, USA [4]Univ. of Padova, Italy

The mid-crust of the Himalaya is represented by the Greater Himalayan Sequence (GHS), one of the major tectonic units of the Himalayan belt exposed for nearly ~2500 km. It has been considered as a coherent tectonic unit since long time, bounded by the South Tibetan Detachment to the top and the Main Central Thrust to the bottom. However, integrated studies by different techniques allow to recognise several high-temperature shear zones in the core of the GHS along the belt, with top-to-the S-SW sense of shear (High Himalayan Discontinuity: HHD (Montomoli et al. 2013; 2015; Iaccarino et al. 2015; Carosi et al. 2018). U-Th-Pb in situ monazite petrochronology provides ages older than the Main Central Thrust, along the same structural profile. Data on the pressure (P) and temperature (T) evolution testify that these shear zones affected the tectono-metamorphic history of the belt and different P-T conditions have been recorded in the hanging-wall and footwall of the HHD. This tectonic feature running for several hundreds of kilometres is documented in several sections of Western and Central-Eastern Nepal dividing the GHS in two different portions. We present the results of a transect in the GHS of Marshyangdi valley (Manaslu massif) (Pêcher 1989). Close the transition between sillimanite-bearing gneiss and kyanite-bearing gneiss, few km north of Syangie village, we identified a high-temperature ductile shear zone with kinematic indicators pointing to a top-to-the S sense of shear.

U-Th-Pb in situ analysis on monazite, joined with chemical compositional maps, performed by LASS at Santa Barbara (California) on samples from the shear zone and its footwall provided ages ranging from ~8 to 43 Ma. The age of the HHD in the Marshyangdi valley is constrained between ~27 and 18 Ma, in very good agreement with the ages of the HHD detected along strike in the GHS (Montomoli et al. 2013; 2015; Carosi et al. 2018), before the later activation of the Main Central Thrust along the same section (Catlos et al. 2001; Gibson et al. 2016) constrained at ~16-13 Ma.

The occurrence of the HHD, detected by structural analysis and petrochronology, in the Marshyangdi valley allows us to fill a gap in the recognition of the HHD between Western and Central-Eastern Nepal.

References

Carosi R, Montomoli C, Iaccarino S (2018) 20 years of geological mapping of the metamorphic core across Central and Eastern Himalayas. Earth Sci Rev 177: 124-138.

Catlos EJ, Harrison TM, Kohn MJ, Grove M, Ryerson FJ, Manning CE, Upreti BN (2001) Geochronologic and thermobarometric constraints on the evolution of the Main Central Thrust, central Nepal Himalaya. J Geophys Res 106: 16177-16204.

Gibson R, Godin L, Kellett D.A, Cottle JM, Archibald D (2016) Diachronous deformation along the base of the Himalayan metamorphic core, west-central Nepal. GSA Bull 128: 860-878.

Iaccarino S, Montomoli C, Carosi R, Massonne HJ, Langone A, Visonà D (2015) Pressure–temperature–time–deformation path of kyanite-bearing migmatitic paragneiss in the Kali Gandaki valley (Central Nepal): Investigation of Late Eocene–Early Oligocene melting processes. Lithos 231: 103-121.

Montomoli C, Carosi R, Iaccarino S (2015) Tectonometamorphic discontinuities in the Greater Himalayan Sequence: a local or a regional feature? Geol Soc London Spec Publ 412: 25-41.

Montomoli C, Iaccarino S, Carosi R, Langone A, Visonà D (2013) Tectonometamorphic discontinuities within the Greater Himalayan Sequence in Western Nepal (Central Himalaya): insights on the exhumation of crystalline rocks. Tectonophys 608: 1349-1370.

Pêcher A (1989) The metamorphism in the central Himalaya. J Metam Geol 7: 31-41.

Structural setting of the Yalaxiangbo Dome, SE Tibet, China

Chen J[1], Carosi R[1], Cao H[2], Montomoli C[3], Iaccarino S[1], Langone A[4], Li G[2]

[1]Univ. of Torino, Italy [2]Inst. of Geology, Chinese Academy of Geological Sciences, Beijing, China [3]Univ. of Pisa, Italy [4]CNR, Ist. di Geoscienze e Georisorse, Pavia, Italy

The Yalaxiangbo gneiss dome (SE Tibet) in eastern Himalaya is one of the major metamorphic culminations in the Tethyan Himalayan Sequence, referred to as North Himalayan Gneiss Domes (NHGD). It comprises three main tectonic units separated by an upper ductile/brittle and a lower ductile detachment. The upper tectonic unit, above the upper ductile/brittle detachment, includes unmetamorphosed to low-grade metamorphic Triassic-Lower Cretaceous slate and metapsammite of the Tethyan Himalayan Sequence. The middle tectonic unit, sandwiched between the upper and lower detachments, consists of mylonitic granite, staurolite-garnet-two mica schist and biotite-plagioclase gneiss affected by the ductile top-to-the north extensional shear of the lower detachment. The lower tectonic unit consists of mylonitic gneiss, leucogranite plutons, dikes, and sills.

By integrating macro-/micro-structural analyses, petrographic and Laser Ablation Inductively Coupled Plasma-Mass Spectrometer (LA-ICP-MS) in situ U-(Th)-Pb monazite geochronological data from selected samples affected by ductile shear, we constrain the activity of the lower detachment at ca. 18 and the shearing along the upper detachment later than ca. 15 Ma (Chen et al. 2018). The detachment system is made up by two different shear zones activated in different times and at different structural levels and our data are in agreement with a migration of the deformation from the lower portions to the upper ones (Cottle et al. 2015, Kellett and Grujic 2012, Iaccarino et al. 2017, Montemagni et al. 2018). The kinematic, geochronology and petrologic features of the Yalaxiangbo detachments are similar to the South Tibetan Detachment system, which crops out in southern Tibet.

References

Chen J, Carosi R, Cao H, Montomoli C, Iccarino S, Langone A, Li G (2018) Structural setting of the Yalaxiangbo dome, SE Tibet (China). Ital J Geosci 137: 330-347.

Cottle JM, Searle MP, Jessup MJ, Crowley JL, Law RD (2015) Rongbuk re-visited: Geochronology of leucogranites in the footwall of the South Tibetan detachment system, Everest region, southern Tibet. Lithos 227: 94-106.

Iaccarino S, Montomoli C, Carosi R, Montemagni C, Massonne HJ, Langone A, Visonà D (2017) Pressure-Temperature-Deformation-Time Constraints on the South Tibetan Detachment System in the Garhwal Himalaya (NW India). Tectonics 36: 2281-2304.

Kellett DA, Grujic D (2012) New insight into the South Tibetan detachment system: Not a single progressive deformation. Tectonics 31: TC2007.

Montemagni C, Iaccarino S, Montomoli C, Carosi R, Jain AK, Villa IM (2018) Age constraints on the deformation style of the South Tibetan Detachment System in Garhwal Himalaya. Ital J Geosci 137: 175-187.

Mitigation of carbon loss in the northern permafrost region through stratospheric aerosol geoengineering implement

Chen Y[1], Zhang Z[1]

[1]Beijing Normal Univ., Beijing, China

Permafrost regions in the Northern Hemisphere include boreal Asia, Europe, North America, areas of Tibet and various mountainous regions. According to an observationally-based estimate of integrated C in the northern permafrost region, the surface soil C stock (0-3 m) is nearly 1.035 ± 150 Pg C (1015 g). Climate warming, as a result of human activities, causes permafrost regions to thaw and release carbon to the atmosphere, representing the shift from a carbon sink to a carbon source. Geoengineering, the intentional large-scale manipulation of the environment in order to mitigate global warming, may be an attractive proposition to slow on-going carbon loss from permafrost. We use soil temperature data from seven Earth system models with NCSCD's soil carbon data to predict the spatial-temporal variation of carbon stocks in permafrost regions under RCP4.5 scenario and stratospheric aerosol Geoengineering(G4) from the Geoengineering Model Intercomparison Project between 2020-2090. The prediction is based on a simplified, data-constrained approach proposed as PInc-Panther, and the effect of Geoengineering to mitigate permafrost thaw and reduce carbon loss is evaluated. The rebound effect after Geoengineering stops is also discussed. We find a pattern of "summer gain, autumn loss" for the cyclical changes of soil C stock, and the major contribution of Geoengineering has been to mitigate the deepening of permafrost degradation.

Late Miocene-Pleistocene evolution of India-Eurasia convergence partitioning between the Bhutan Himalaya and the Shillong Plateau: New evidences from foreland basin deposits along the Dungsam Chu section, Eastern Bhutan – In memory of Gwladys Govin

Coutand I[1], Barrier L[2], Govin G[3], Grujic D[1], Hoorn C[4], Dupont-Nivet G[5], Najman Y[3]

[1]Dept. of Earth Sciences, Dalhousie Univ., Halifax, Canada [2]Inst. de Physique du Globe de Paris, Univ. Paris Diderot, CNRS, Paris, France [3]Lancaster Environment Centre, Univ. of Lancaster, UK [4]Inst. for Biodiversity and Ecosystem Dynamics, Univ. of Amsterdam, The Netherlands [5]Geosciences Rennes, Univ. of Rennes, France

The Shillong Plateau is a unique basement-cored uplift in the foreland of the eastern Himalaya that accommodates part of the India-Eurasia convergence since the late Miocene. It was uplifted in the late Pliocene to 1600 m, potentially inducing regional climatic perturbations by orographically condensing part of the Indian Summer Monsoon (ISM) precipitations along its southern flank. As such, the eastern Himalaya-Shillong Plateau-ISM is suited to investigate effects of tectonics, climate, and erosion in a mountain range-broken foreland system. This study focuses on a 2200 m thick sedimentary section of the Siwalik Group strategically located in the lee of the Shillong Plateau along the Dungsam Chu at the front of the eastern Bhutan Himalaya. We have performed magnetostratigraphy constrained by vitrinite reflectance and detrital apatite fission track dating, combined with sedimentological and palynological analyses. We show that (1) the section was deposited between ~7 and 1 Ma in a marginal marine deltaic transitioning into continental environment after 5 Ma, (2) depositional environments and paleoclimate were humid with no major change during the depositional period indicating that the orographic effect of the Shillong Plateau had an unexpected limited impact on the paleoclimate of the Bhutanese foothills, and (3) the diminution of the flexural subsidence in the basin and/or of the detrital input from the range is attributable to a slowdown of the displacement rates along the Main Boundary Thrust in eastern Bhutan during the latest Miocene-Pleistocene, in response to increasing partitioning of the India-Eurasia convergence into the active faults bounding the Shillong Plateau.

Seismic and aseismic slip on the Main Himalayan Thrust: Bayesian modelling accounting for prediction uncertainties

Dal Zilio L[1], Jolivet R[2]

[1]Inst. of Geophysics, Dept. of Earth Sciences, ETH Zurich, Switzerland [2]Laboratoire de Géologie, ENS Paris, France

Most of the convergence rate across the Himalayan arc has been shown to be absorbed by slip along a major basal thrust fault: the Main Himalayan Thrust (MHT). In this context, the geodetic strain measured across the arc can be used to determine the pattern of interseismic coupling and estimate the return period of large earthquakes. A coupling map already exists (Stevens and Avouac 2015), which indicates that the MHT is locked from the surface to a distance of approximately 100 km down dip. However, these results are obtained assuming a planar fault in a purely elastic and infinitely long half-space. These assumptions can thus strongly impact inferences of seismogenic coupling. For instance, the 2015 Mw 7.8 Gorkha earthquake revealed a potential key role of fault geometry and heterogeneous strain in controlling the rupture propagation along MHT. Hence, what controls the arrest of the rupture is not yet clear since the fault appears fully locked during the pre-seismic period. Going forward, we need a robust coupling model to understand its spatial relationship to interseismic, preseismic, and postseismic slip, which will provide better insights into the mechanical behaviour of the MHT.

Here we address this issue by proposing a new coupling model obtained from the joint inversion of multiple observations (GPS and levelling data) in a fully Bayesian framework. This approach allows to evaluate the population of plausible coupling models given geodetic data and forward problem uncertainties. We first explore a few simple forward models to derive first order conclusions on the extent of interseismic plate coupling. Then we perform a Bayesian exploration to evaluate in greater detail the range of possible models of plate coupling and assess the variability allowed by the interseismic velocity. Our approach is exempt from any smoothing and allows us to assess the extent of any purported shallow slip deficit as constrained by available geodetic data. In addition, we account for uncertainty in the assumed elastic structure used to compute the Greens functions. Thus, our solution includes the ensemble of all plausible models that are consistent with our prior information and fit the available observations within data and prediction uncertainties. These models, combined with the size, location, and frequency of large Himalayan earthquakes, can provide new insights on where and when aseismic creep is taking place, and what fraction of the long-term slip rate it accounts for. Our goal is not only to obtain a trustworthy coupling distribution but also to produce realistic estimates of uncertainty, which can impact our interpretation and assessment of future rupture processes.

Reference

Stevens VL, Avouac JP (2015) Interseismic coupling on the main Himalayan thrust. Geophys Res Lett 42: 5828-5837.

Uncertainty analysis for seismic hazard: A case study for NE India region

Das R[1], Wason H[2]

[1]National Research Center for Integrated Natural Disaster Management, Chile [2]IIT Roorkee, India

The probabilistic seismic hazard assessment (PSHA) is considered to be the most preferred methodology for estimation of seismic hazard and can be viewed as catering to the need of defining compatible earthquake input for seismic engineering design. It is well established that uncertainties exist in probabilistic seismic hazard assessment studies; the main sources being earthquake catalogue, seismic source zones configuration and individual strong motion attenuation relations, amongst others. Some studies have been carried out recently by different researchers to investigate these uncertainties in seismic hazard assessment but the effect of uncertainty due to earthquake catalogue is addressed very little in the literature. In the present study, we examine the effect of uncertainty due to earthquake catalogue in probabilistic seismic hazard maps (10% and 0.5% probability of exceedance in 50 years) for Northeast India region, which is one of the most active seismic regions, encompassed by 87°-98° N longitude and 20°-30° E latitude. The uncertainty in seismic hazard estimation has been obtained using a Monte Carlo approach. Quantification of uncertainty is done in terms of Coefficient of Variation (CoV). The overall variability of earthquake catalogues and strong ground motions and their sensitivity are investigated using the logic tree approach.

Seismic hazard has been computed by performing hazard computations at a grid interval of 0.1°×0.1° covering the entire Northeast India region. Peak ground acceleration (PGA) and spectral acceleration (Sa) values have been evaluated at bedrock level corresponding to probability of exceedance (PE) of 10% and 0.5% in 50 years. These exceedance values correspond to return periods of 475 years and 10’000 years, respectively. For 475 years return period, mean values for PGA, Sa at 0.2 sec and 1.0 sec spectral periods vary between 0.01g to 0.32g, 0.02g to 0.656g and 0.02g to 0.178g, respectively. For 10’000 years return period, mean values for PGA, Sa at 0.2 sec and Sa at 1.0 sec are found to vary between 0.02g to 0.68g, 0.05g to 1.48g and 0.16g to 0.42g, respectively. Mean CoV values for PGA of 475 years and 10’000 years return periods are observed to be 0.21 and 0.15, respectively. Mean CoV values for Sa at 0.2 sec and 1.0 sec of 475 years and 10’000 years return periods are found to be 0.177 and 0.127, and 0.287 and 0.42, respectively. A decreasing trend of CoV has been observed with increasing return period. The seismic hazard results obtained in this study will be useful for engineering seismology applications in the region.

Principal joint sets and geomorphic markers in NW Bhutan

De Palézieux L[1], Leith K[1], Löw S[1]

[1]*Geological Inst., Dept. of Earth Sciences, ETH Zurich, Switzerland*

With large alluvial plains, narrow gorges, prominent knick points, and chains of terraces or cut-off ridges, the deeply-incised valleys in Bhutan reflect an environment of diverse erosional activity. Topography ranges from 97 m to 7570 m, with characteristic postglacial landscapes typically located above ca. 4200 m. The lower latitudes below ca. 3000 m show high relief and terraced or linear hillslopes indicative of a fluvial origin.

The present-day tectonic activity of the region is not well known; however, recent publications suggest more seismic activity than previously thought at least in the southern parts of the country (Hetényi et al. 2016) and exhumation rates around 1.4 mm/yr in Western Bhutan (Portenga et al. 2015). Literature regarding the geomorphological setting of the region is equally sparse, with a few publications discussing soil ages (e.g. Caspari et al. 2007), river terraces (Motegi 2001), and landsliding (Dunning et al. 2009).

Over the course of two field campaigns in NW Bhutan we have mapped geomorphological markers such as terraces, knickpoints, and slope instabilities and gathered information regarding the local structural setting, such as orientation, size and infill of joints and faults and their relationship to the local topography and geomorphology. Combining these two sets of information allows us to come up with a (rough) characterization of the geomorphology of the region, both in its recent tectonic and erosional activity.

References

Caspari T (2005) The soils of Bhutan: parent materials, soil forming processes, and new insights into the paleoclimate of the eastern Himalayas. Doctoral dissertation. Technische Univ. München.

Dunning SA, Massey CI, Rosser NJ (2009) Structural and geomorphological features of landslides in the Bhutan Himalaya derived from Terrestrial Laser Scanning. Geomorphology 103: 17-29.

Hetényi G, Le Roux-Mallouf R, Berthet T, Cattin R, Cauzzi C, Phuntsho K, Grolimund R (2016) Joint approach combining damage and paleoseismology observations constrains the 1714 A.D. Bhutan earthquake at magnitude 8 ± 0.5. Geophys Res Lett 43: 10695-10702.

Motegi M (2001) GLOF Sediments and Geology of River Terraces in Wangdi Phodrang District, Bhutan. J Geogr 110: 17-31.

Portenga EW, Bierman PR, Duncan C, Corbett LB, Kehrwald NM, Rood DH (2015) Erosion rates of the Bhutanese Himalaya determined using in situ-produced 10Be. Geomorphology 233: 112-126.

Generation and emplacement of Triassic granitoids within the Songpan Garze accretionary-orogenic wedge from different sources, mantle-derived and crust-derived, Eastern Tibetan plateau, China

Deschamps F[1], de Sigoyer J[2], Duchêne S[1], Bosse V[3], Vanderhaeghe O[1]

[1]GET, Univ. Paul Sabatier, Toulouse, France [2]ISTerre, Univ. Grenoble-Alpes, France [3]Laboratoire Magmas et Volcans, Univ. Blaise Pascal, Clermont-Ferrand, France

The Songpan Garze (SG) unit located in the central Tibetan plateau, represents an emblematic site where the thickening of the crust began during Triassic time and results from successive steps since that time. On its eastern border we document the first stage of thickening from 240 to 180 Ma related to the closure of Paleotethys, and to the formation of an accretionary-orogenic wedge emplaced on the western passive margin of the South China craton. This huge SG wedge formation leads to extensive metamorphism at the base of the wedge, and to syn-orogenic magmatic emplacement, displaying a diversity of petrologic and geochemical characteristics: I-type low- to high-K calc-alkaline, A-type alkaline, and S-type peraluminous granitoids intruded in upper Triassic sediments.

To better understand the relationships in between metamorphism and the genesis of magmatism in the SG unit, we present a comprehensive petrological, geochemical, and geochronological study of the granitoid intrusive in the Triassic metasediments. We focus this study on two neighbouring and emblematic granitoid plutons Markam and Taiyanghe, separated by less than 2 km intrusive into Songpan Garze metasediments. (i) The main volume of the Markam pluton is dominated by an S-type peraluminous medium- to coarse-grained granite (Qtz+Pl+Kfs+Bt+Ms+Grt+Chl+Tur) which was emplaced over a period of 30 Myr from 231 to 200 Ma based on U-Pb zircon ages, (peak at 207 Ma) at an estimated minimum depth of ~11 km (300 MPa) (based on the metamorphic contact observed in the hosted rocks). Markam granites ($0.709405 < {}^{87}Sr/{}^{86}Sr(t) < 0.711113$; $-9.02 < \varepsilon Nd(t) < -7.99$) result from the melting of the Songpan Garze metasediments under amphibolite facies conditions at a depth of at least 20 km (based on the petrological study of xenolithes). (ii) The main volume of the Taiyanghe pluton is dominated by I-type, high-K calc-alkaline, fine- to coarse-grained diorite and syenodiorite (Qtz+Pl+Kfs+Bt+Amp±Chl±Grt), and was emplaced over a period of ~40 Myr (239-202 Ma) at an estimated minimum depth of about 11 km. Taiyanghe rocks have isotopic signatures ($0.708037 < {}^{87}Sr/86^{Sr}(t) < 0.708665$; $-6.27 < \varepsilon Nd(t) < -3.62$) typical of magmas resulting from partial melting of an ultramafic source under eclogite facies conditions and without any reliable chemically influenced of the SG metasediments. This magmatic series has experienced limited fractional crystallization from the parental magma, leading to the formation of a (Pl+Amp)-rich cumulate. The Taiyanghe pluton also includes I-type, low-K calc-alkaline hornblende-gabbros (Amp(Hbl)+Pl+Qtz+Bt), corresponding to residual mush during the differentiation of the Taiyanghe magmas.

These data added to the study of A-type alkaline granite (Nyanbayaoche, Rilong, Zhalaokun, Zhandakun) emplaced in the same range of ages, at 3 km depth, associated to the melting of undepleted mantle mixed with a South China crust, provide evidence that the Triassic plutons intruding the Songpan Garze accretionary-orogenic wedge result from partial melting at different levels of mantle and crustal protoliths leading to magmas that show limited interactions despite their nearby emplacement, over a 40 Myr period.

Remelting of Neoproterozoic Dalhousie and Dhauladhar granite during Cambro-Ordovician: Constraints from in situ U-Pb zircon geochronology, Himachal Pradesh, NW Himalaya

Dhiman R[1], Singh S[1]

[1]Dept. of Earth Sciences, IIT Roorkee, India

A widespread Pan-African magmatism has been found in the Higher Himalayan Crystallines (HHC) which has southern limit at senso-stricto the Main Central Thrust (MCT). This magmatism is thought to represent a part of large thermo-magmatic episode in the fragmented Gondwana of Afghanistan, Australia and Antarctica and is associated with a mega-zone of crustal extension, thinning, and melting of lower crust. The Lesser Himalayan Granitic Belt (LHGB) that lies just north of the MCT, geographically falls within the Lesser Himalaya although they belong to the Higher Himalayan sequences. The Dalhousie and Dhauladhar Granites also form a part of the LHGB in Himachal Pradesh, exposed close to Jutogh/Main Central Thrust (MCT) between Kaplas, Dalhousie, Mandi and Karseog. The granites from Dalhousie and the Dhauladhar area are coarse-medium grained, mylonitized and with porphyritic biotite, as well as fine-grained potassic, calc-alkaline and peraluminous granites. Both the granites are showing similar mineral assemblages, and contain K-feldspar, plagioclase, and biotite. An attempt has been made to integrate new U-Pb zircon geochronology by SHRIMP and LAMC-ICP-MS on Dalhousie and Dhauladhar granite. The “outer band” of Dhauladhar granites in Himachal Pradesh have always been considered as the mylonite zone which is an extension of Garh Formation or Kulu-Bajura Thrust Sheet and has been dated as 1850 Ma (Paleoproterozoic) body. However, the in situ U-Pb zircon dates by SHRIMP and LA-MC-ICPMS analysis reveal reworking of Neoproterozoic (magmatic core) during Cambro-Ordovician (magmatic rim) time. The geochronological data suggest recycling of older crust during Neoproterozoic and Cambro-Ordovician time. Presence of zircon core ages between 1220 Ma and 670 Ma suggest derivation of zircon rims, aged 460 Ma, by intra-crustal melting. We suggest that Cambro-Ordovician continental magmatism was built on the Greater Himalayan sequence and can be correlated with amalgamation of Gondwanaland over granite formed during Rodinian breakup during Neoproterozoic time. This new data on Neoproterozoic magmatic body also support detrital zircon source within Greater India domain.

Seismotectonics of Bhutan and its foreland: New insights from the GANSSER passive seismic experiment

Diehl T[1], Singer J[2], Hetényi G[3], Grujic D[4], Clinton J[1], Giardini D[2], Kissling E[2]

[1]Swiss Seismological Service, ETH Zurich, Switzerland [2] Inst. of Geophysics, Dept. of Earth Sciences, ETH Zurich, Switzerland [3]ISTE, FGSE, Univ. of Lausanne, Switzerland [4]Dept. of Earth Sciences, Dalhousie Univ., Halifax, Canada

The instrumental record of Bhutan is characterized by a lower seismicity compared to other parts of the Himalayan arc. To understand this low activity and its impact on the seismic hazard, the temporary GANSSER seismic network was installed in Bhutan for 22 months between 2013 and 2014. Recorded seismicity, earthquake moment tensors and local earthquake tomography reveal along-strike variations in structure and crustal deformation regime. A thickened crust imaged in western Bhutan suggests lateral differences in stresses on the Main Himalayan Thrust (MHT), potentially affecting the interseismic coupling and deformation regime. Sikkim, western Bhutan and its foreland are characterized by strike-slip faulting in the Indian basement. Strain is particularly localized along a NW-SE striking mid-crustal fault zone reaching from Chungthang in northeast Sikkim to Dhubri at the northwestern edge of the Shillong Plateau in the foreland. The dextral Dhubri-Chungthang fault zone (DCF) causes segmentation of the Indian basement and the MHT between eastern Nepal and western Bhutan and connects the deformation front of the Himalaya with the Shillong Plateau by forming the western boundary of the Shillong block. The Kopili fault, the proposed eastern boundary of this block, appears to be a diffuse zone of mid-crustal seismicity in the foreland. In eastern Bhutan we image a seismogenic, flat portion of the MHT, which might be either related to a partially creeping segment or to increased background seismicity originating from the 2009 Mw 6.1 earthquake. In western-central Bhutan clusters of micro-earthquakes at the front of the High-Himalayas indicate the presence of a mid-crustal ramp and stress build-up on a fully coupled MHT. The area bounded by the DCF in the west and the seismogenic MHT in the east has the potential for M7-8 earthquakes in Bhutan. Similarly, the DCF has the potential to host M7 earthquakes as documented by the 2011 Sikkim and the 1930 Dhubri earthquakes, which were potentially associated with this structure.

Slope activity and processes in the Himalaya of Northern Bhutan

Dini B[1], Manconi A[1], Löw S[1]

[1]*Geological Inst., Dept. of Earth Sciences, ETH Zurich, Switzerland*

Bhutan is a small Himalayan country, located between India and Tibet. Its territory is characterised by active tectonics, erosion and extreme topographic gradients as well as highly varied climatic zones. Such geographical setting makes for a landscape prone to geological mass movements. In this project we focus on 1) fundamental contributions to scientific knowledge regarding processes conditioning large rock slope movements in the High Himalaya of Bhutan and 2) landslide hazard assessment by exploiting the state-of-the art in Differential Interferometry of Synthetic Aperture Radar (DInSAR) image processing and post-processing.

We analysed high resolution optical images (GoogleEarth) and high resolution DTM (ALOS World 3D) in order to detect unstable slopes with clear geomorphological features. Moreover, we processed satellite-based radar images (2 Envisat ASAR tracks and 4 ALOS Palsar-1 frames) with DInSAR techniques, covering an observation period between August 2005 and March 2011. Validation of specific cases was carried out with more recent data (ALOS Palsar-2 and Sentinel-1, between September 2014 and July 2017). Specifically, we generated more than 500 differential wrapped interferograms and analysed them individually for actively deforming areas. Successively, we created a weight based on acquisition parameters and number of observations for each individual object, in order to generate a likelihood of activity. We also processed 5 of the available tracks with the SBAS (Small Baseline Subset) approach and obtained velocity and displacement maps which were also analysed for potentially active areas and displacement time series.

We thus obtained a large inventory of rockslides and rock glaciers (more than 1300 objects) based on optical images and two inventories based on DInSAR information containing more than 1000 objects classified by landslide type including: 1) rockslides, 2) rock glaciers, 3) moraines, 4) talus or slope debris. The underlying driving processes were systematically investigated through the analysis of the time series trends. For this purpose, we also analysed the seasonal cycles within the time series and identified two cycles that were interpreted as uncorrected atmospheric delays. Outside of such atmospheric cycles we were able to detect spatially well constrained areas characterised by seasonal cycles likely caused by reversible ground deformation. This, combined with the analysis of the overall trends seen in the time series, allowed for the classification of the processes driving slope instability: 1) gravitational, 2) reversible related to permafrost freeze and thaw and 3) reversible related to groundwater recharge and depletion.

The extent of the investigated area (roughly 8000 km^2) and the amount of systematically analysed data are unprecedented. We show how to generate a classification of instabilities types and processes and to maximise the extraction of information on slope instability for an extensive and largely inaccessible region.

Paleogeographic and paleoenvironmental reconstructions of the India-Asia collision

Dupont-Nivet G[1,2], Meijer N[2], Kaya M[2], Westerweel J[1,3], Tardif D[4], Barbolini N[5], Rohrmann A[2], Aminov J[6], Licht A[7], Poblete F[8], Roperch P[3], Hoorn C[5], Proust JN[3], Fluteau F[4], Donnadieu Y[9], Guillot S[10], Guo Z[11], Aung D[12]

[1]CNRS, France [2]Inst. of Earth and Environmental Science, Univ. of Potsdam, Germany [3]Geosciences Rennes, Univ. of Rennes, France [4]Inst. de Physique du Globe de Paris, France [5]Inst. for Biodiversity and Ecosystem Dynamics, Univ. of Amsterdam, The Netherlands [6]Inst. of Geology, Earthquake Engineering and Seismology, Academy of Sciences of the Republic of Tajikistan [7]Dept. Earth and Space Sciences, Univ. of Washington, Seattle, USA [8]Inst. de Ciencias de la Ingeniería, Univ. de O'Higgins, Rancagua, Chile [9]CEREGE, Aix-Marseille Univ, Aix en Provence, France [10]ISTerre, Univ. Grenoble-Alpes, France [11]Key Laboratory of Orogenic Belts and Crustal Evolution, Peking Univ., Beijing, China [12]Dept. of Geology, Univ. of Yangon, Myanmar

Despite decades of research in the Himalaya-Karakorum-Tibet and surrounding regions, the geodynamic setting of the India-Asia collision and the associated tectonic growth and uplift of the Tibetan Plateau remain fundamentally unresolved. Consequently, the timing, forcing mechanisms and interactions cannot be unambiguously assessed between associated regional paleoenvironmental changes (monsoons, aridification), land-sea distribution, surface processes, paleobiogeographic evolution and global carbon cycle.

We review here the mid-term progress of the ERC MAGIC project (Monsoons in Asia caused Greenhouse to Icehouse Change?) aiming at better understanding the evolution of India-Asia collision by integrating regional geodynamic constraints, well-dated paleoenvironmental proxy records and climate modelling. MAGIC focuses on the Paleogene period that includes the early collision and plateau growth, associated regional development of monsoons and westerlies over the Proto-Paratethys Sea and the global Greenhouse to Icehouse cooling. Our work focuses on three areas constraining Asian paleoenvironments including results not presented here but in several other contributions to this meeting:

In Myanmar paleomagnetic results provide geodynamic context (Westerweel et al. this meeting) and new dating of magmatic rocks and sediments along with additional detrital geochronology and basin analysis of the Burmese subduction margin and implications for the history of India-Asia convergence.

Along the Eastern Tibetan Plateau margin paleomagnetic reconstruction of the Qiangtang latitudinal displacement (Roperch et al. this meeting), the combination of leaf wax stable isotope and pollen for paleoaltimetry and paleoenvironmental reconstructions (Rohrmann et al. this meeting) and the extended lacustrine paleoenvironmental records enable us to better constrain the evolution of the Tibetan Plateau growth and its implications for paleoenvironmental changes.

In westernmost China and Tajikistan, the Proto-Paratethys sea fluctuations and the sedimentary records of Pamir tectonic evolution are now precisely dated enabling us to constrain driving mechanisms and paleoenvironmental consequences (Blayney et al. this meeting; Kaya et al. this meeting).

Here we present a new multi-proxy record from NE Tibet now extended in time from 50 to 25 Ma. This record enables to precisely track moisture sources from monsoons and westerlies and identify their driving factors and, in particular, their link to global changes associated with the Eocene-Oligocene transition. This together with the other MAGIC results, allow for a comprehensive paleogeographic and paleoenvironmental reconstructions of the India-Asia collision zone that are

used to constrain initial climate modelling experiments presented elsewhere by Tardif et al. (this meeting) which permit validation of hypotheses on paleoenvironment-climate interactions.

References

Blayney T, Dupont-Nivet G, Najman Y, Meijer N, Proust JN, Sobel E, Millar I, Guo Z (2018) Pamir tectonic evolution and associated environmental changes recorded since 40 Ma in the western Tarim Basin, Aertashi section. HKT meeting (this volume).

Kaya MY, Dupont-Nivet G, Proust JN, Roperch P, Bougeois L, Meijer N, Frieling J, Fioroni C, Altıner SO, Vardar E, Stoica M, Mamtimin M, Guo Z (2018) Paleogene evolution of the proto-Paratethys Sea in Central Asia (Tarim Basin, western China), driving mechanisms and paleoenvironmental consequences. HKT meeting (this volume).

Rohrmann A, Barbolini N, Meijer N, Yang Z, Dupont-Nivet G (2018) High central Tibet at the onset of Indo-Asian collision derived from leaf-wax hydrogen and palynology data. HKT meeting (this volume).

Roperch P, Dupont-Nivet G, Guillot S, Goussin F, Huang W, Replumaz A, Yang Z, Guo Z (2018) Tibetan Plateau paleolatitude and tectonic rotations: paleomagnetic constraints. HKT meeting (this volume).

Tardif D, Fluteau F, Donnadieu Y, Le Hir G, Ladant JB, Poblete F (2018) Influence of paleogeography on asian Cenozoic climate. HKT meeting (this volume).

Westerweel J, Roperch P, Licht A, Dupont-Nivet G, Win Z, Poblete F, Huang H, Littell V, Swe HH, Thi MK, Hoorn MC, Aung DW (2018) First paleomagnetic constraints on the latitudinal displacement of the West Burma block. HKT meeting (this volume).

Understanding the relationship between the surface topography and subsurface geometry of the Main Himalayan Thrust in Central Nepal through numerical landscape evolution models

Eizenhöfer P[1], McQuarrie N[1], Ehlers T[2], Ghoshal S[1]

[1]Univ. of Pittsburgh, USA [2]Univ. of Tübingen, Germany

A major goal in tectonic geomorphology is to understand the degree to which topography of active mountain ranges reflects subsurface fault activity. The Main Himalayan Thrust (MHT) has evolved through the development and migration of active ramps and faults, and thus the location of active rock uplift and foci of increased erosion over the past ca. 20 Ma. This evolution is preserved on the present-day surface as age and distribution of different thermochronometers, but also is expressed in the elevation, relief, and morphology of the topographic surface. The sequential restoration of balanced cross sections presents a method to reconstruct past locations and magnitudes of structurally induced uplift and exhumation in space and time. By assigning viable convergence rates to each step of deformation during the reconstruction we can provide a kinematic model that can be integrated in landscape evolution algorithms such as CASCADE. This model set up allows us to link ramp and fault activity to a discrete topographic response and explore how the geometry of fault structures, the location of ramps and the rates of faulting affect the modelled topography, long-term topographic evolution, and the potential to preserve legacy landscapes in present-day topography. In this study we evaluate different proposed geometries for the MHT in the Central Nepal Himalaya (e.g. hinterland dipping duplex, foreland dipping duplex, antiformal stack, out-of-sequence thrust) and analyse the impact of the locations of active ramps and fault evolution in each model on the predicted topography over time. Quantitative geomorphic metrics such as river channel steepness indices are further utilized to compare the modelled topography to topographic metrics measured in the Himalayas today. Our modelling results show a landscape that is significantly shaped by both the location of ramp uplift and the continuous southward horizontal displacement of uplifted topography. Regions of active rock uplift above ramps are characterized by an across-strike asymmetry in their relief and topography across the main drainage divide. A wide region of increased river channel steepness indices extends over tens of kilometres southwards away from the region of active rock uplift. The same region shows southwardly displaced convergence-parallel interfluves that retain legacy high elevations that remember and record uplift over the active ramp. Thus, we argue that the interpretation of geomorphic markers of uplift at convergent orogens requires consideration of horizontal displacement magnitude and rate. This geomorphic-kinematic model approach can provide additional constraints to quantitatively evaluate given fault geometries and kinematics and test their ability to reproduce the evolution of modern landscapes over geologic time.

Functioning of a small “landslide catchment” and its geomorphic impacts: The Ghatte Khola, Myagdi District, Nepal Himalaya

Fort M[1]

[1]*Univ. Paris Diderot, France*

Small river catchments play a major role in the overall denudation of the Himalayas, because they may generate extreme, geomorphic events. I consider here their potential impacts on the morphology and functioning of trunk rivers, and indirectly on infrastructure and settlements located along the valley floor.

My case study, the Ghatte Khola, is an intermittent tributary of the Kali Gandaki (Myagdi District, Western Nepal) affected by occasional debris flow events. The cause of the debris flows is a persistent planar slide zone (dip slope) that is reactivated by pre- or monsoon heavy rainfall on the upper, forested catchment. As a result, the narrow channel of the upstream part of the tributary is temporary clogged by landslide masses, until sudden, landslide outburst floods occur. Downstream, where the channel is entrenched across a 5-8 m thick debris fan, the functioning of successive debris flows has caused bank erosion and stream channel widening. At the junction with the Kali Gandaki (see photo below), the flows sometimes aggrade debris volumes large enough to impede the Kali Gandaki for a few hours and cause the level of this major river to rise more than 5 m upstream. During the last 40 years, pulsed aggradations transferred erosion point to the opposite (left bank) side of the Kali Gandaki. This ephemeral, yet threatening behaviour of the stream, occurs quite frequently, every two or three years, according to field investigations (geomorphic mapping, sediment analysis, repeated photographs), completed by interviews with villagers.

Eventually, I show that such moderate to high-magnitude/frequency events are very efficient to foster sediment fluxes and create temporary sediment storages in major river network, a fact that is to be considered prior to any new settlement and road design. In the Kali Gandaki valley, the road open in 2007 is now planned to become a 2-way metal road, as an annex of the new “Silk Road” that will cross Mustang down to Lumbini at the Indian border and called “the Kali Gandaki corridor”. In this context, the functioning of such a “landslide catchment” and the ongoing construction of a new bridge create potential new hazards to infrastructure and will increase the functional, social, and economic vulnerability.

Expedition 354 on the Bengal fan: Implications on Neogene erosion regime and climate

France-Lanord C[1], Spiess V[2], Feakins S[3], Galy V[4], Galy A[1], Huyghe P[5], Yoshida K[6]

[1]CRPG, CNRS, Univ. of Lorraine, Nancy, France [2]GeoB, Bremen Univ., Germany [3]Dept. of Earth Science, Univ. of Southern California, Los Angeles, USA [4]Woods Hole Oceanographic Inst., USA [5]ISTerre, Univ. Grenoble-Alpes, France [6]Shinshu Univ,. Matsumoto, Japan

In Himalaya, the monsoon precipitations exert a primary control on erosion. From its intensity depends the extension of the glacier cover, landslide activity, river incision, vegetation cover, and export of sediments towards the floodplain. The monsoon also exerts a primary control on the chemical erosion as weathering rates are clearly dependent upon river discharge.

In the floodplain, sediment export also is tightly controlled by climate. The seasonality and intensity of the monsoon allow to reach discharge high enough to ensure the efficiency of river transport to the delta (Lupker et al. 2011). This efficient transport also acts as a limiting factor for weathering as it reduces residence time in the floodplain. The comparison between the Ganga with a large floodplain and the Brahmaputra with a narrow floodplain and comparatively lower residence time confirms that Himalayan weathering is limited by transport.

Recent IODP Expedition 354 in the Bengal fan (France-Lanord et al. 2016) generated a comprehensive record of Himalayan erosion over the Neogene and Quaternary. It documents the interplay between Himalayan tectonic and climate. The Bengal fan is predominantly composed of detrital turbiditic sediments originating from Himalayan rivers, and transported through the delta and shelf canyon, supplying turbidity currents loaded with a wide spectrum of grain sizes. Turbiditic deposition makes that record at a given site is discontinuous which was the reason for an E-W transect approach. Expedition 354 drilled seven sites along a 320 km E-W transect at 8°N allowing the restitution of an almost complete record of Himalayan erosion at the scale of the Neogene.

Turbiditic sediments have clear Himalayan origin and close mineralogical and isotopic analogy with those of the modern Ganga-Brahmaputra river sediments. Major and trace element geochemistry show relatively stable compositions throughout the Neogene and Quaternary. They reveal a very weak regime of chemical weathering with no significant variation through time. Concentrations in mobile elements such as Na and K relative to Al are significantly higher than in modern sediments and suggest that weathering or soil erosion is amplified in the modern time. Low weathering of the sediments at 8°N indicates that erosion was dominated by physical processes and that transport was rapid enough to prevent evolution of particles in the floodplain. In the modern Himalaya, low weathering is achieved primarily by landslides and rapid transfer through the floodplain, i.e. limited recycling of sediment deposited in the floodplain. Both processes are favoured by the seasonality and the intensity of the monsoon. On the organic side, carbon isotopic analyses of organic matter in turbidites clearly reveal its continental origin. The hydrogen isotopic composition of leaf-wax compounds reveals low δD since Early Miocene, indicative of significant amount effect i.e. Monsoon. Overall, the low weathering intensity suggests that comparable erosion regime was established since at least Early Miocene.

References

France-Lanord C, Spiess V, Klaus A, Schwenk T, Expedition 354 Scientists (Eds.) (2016) Proceedings of the International Ocean Discovery Program, 354. IODP.

Lupker M, France-Lanord C, Lavé J, Bouchez J, Galy V, Métivier F, Mugnier JL (2011) A Rouse-based method to integrate the chemical composition of river sediments: Application to the Ganga basin. J Geophys Res 116: F04012.

Evaluation of stable isotopic composition of Nepalese rivers before and after the Mw 7.8 Gorkha earthquake

Gajurel A[1], France-Lanord C[2], Lupker M[3], Lavé J[2], Rigaudier T[2]

[1]Dept. of Geology, Tribhuvan Univ., Kathmandu, Nepal [2]CRPG,CNRS, Univ. of Lorraine, Nancy, France
[3]Geological Inst., Dept. of Earth Sciences, ETH Zurich, Switzerland

Stable isotopic studies (H and O) have been continuously performing from the major large rivers like Kosi and Narayani as well as their small tributaries to understand the water cycle from yearly isotopic record in relation with direct precipitation. Here we present a set of data, mostly from the southern Himalayan flank, including daily sampling of rivers in Narayanghat, Khudi, Marshyandi, Trisuli and Kosi as well as precipitation water data since the pre-Gorkha Earthquake (Mw 7.8) of 25 April 2015. For the precipitation at a given location, data are marked by strong seasonal contrast (e.g. Zhang et al. 2001, Gajurel et al. 2006) probably related to source of moisture and amount effect.

Strong seasonality in oxygen isotopic composition of river water (4-5‰) in the catchment of Narayani River in the Himalaya in 2010 is recorded. In contrast, the composition evolves much more stable with a slight tendency to increase during the monsoon in 2015. The Kosi data set of 2015 shows a variation in δ18Osmow from -12‰ to -8‰, and for the δD_{SMOW} from -80‰ to -50‰ (Fig. 1). The data set situated on line $\delta D = 7.7 \times \delta^{18}O + 7.7‰$) is close to the GMWL. The seasonal trend in $\delta^{18}O$ generates an offset particularly between June-July and August that influence on river isotopic composition. The river isotopic compositions are progressively depleted in heavy isotopes during the monsoon reflecting the seasonal evolution of precipitation, however, it is buffered by the ground water reservoir. At the beginning and end of the monsoon, the contrast between precipitation and ground water is large and precipitation events generate scattered river variations depending on direct runoff to ground water supply, however, such trend is not always observed particularly after 2015 Gorkha earthquake.

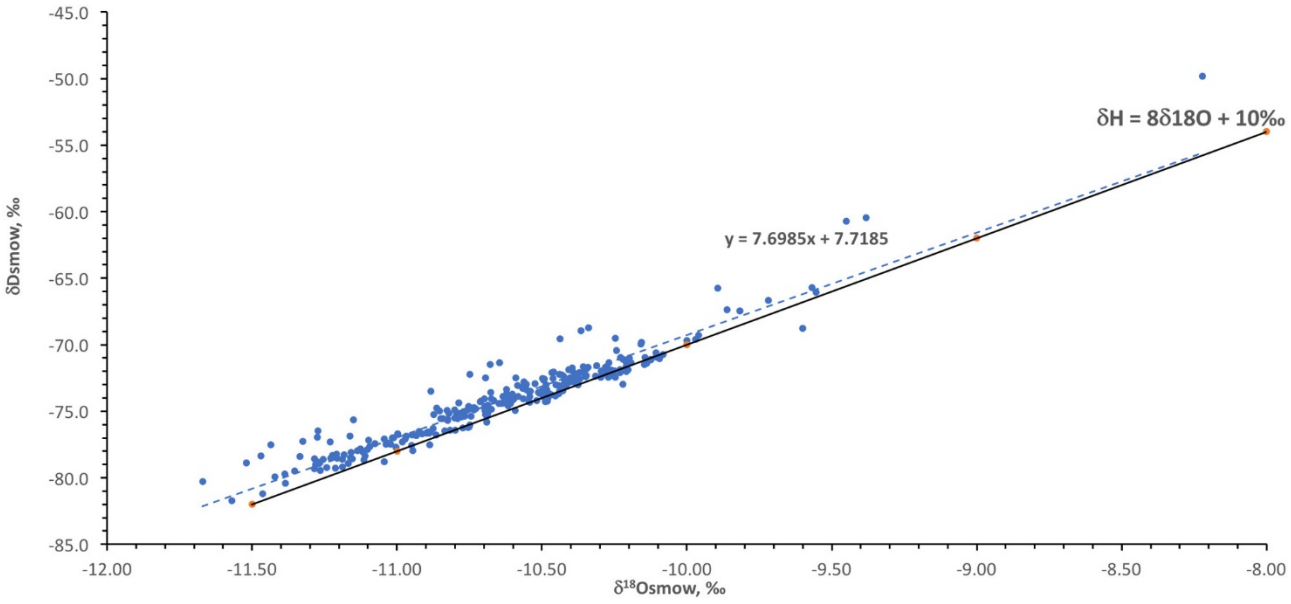

Figure 1.

References

Gajurel AP, France-Lanord C, Huyghe P, Guilmette C, Gurung D (2006) C and O isotope compositions of modern freshwater mollusc shells and river waters from the Himalaya and Ganga plain. Chem Geol 233: 156-183.

Zhang X, Masayoshi N, Koji F, Yao T, Han J (2001) Variation of precipitation δ18O in Langtang Valley, Himalayas. Science in China 44: 769-778.

Early Permian palynomorphs from the Saltoro Formation, Shyok Suture Zone, Northern Ladakh, India

Gautam S[1], Upadhyay R[2], Das M[1], Behera B[1]

[1]Fakir Mohan Univ., Nuapadhi, Balasore, India [2]Dept. of Geology, Kumaun Univ., Nainital, India

We report the presence of Early Permian (Sakmarian-Artinskian) palynomorphs from the sedimentary rocks of the Shyok Suture Zone, exposed along Shyok River Valley in northern Ladakh, India. The palynomorphs bearing sedimentary rocks belong to the Saltoro Formation (Hundri Formation) of the Shyok Suture Zone. The characteristic taxa recorded in the assemblage are: *Arcuatipollenites*, *Barakarites*, *Caheniasaccites*, *Crescentipollenites*, *Corisaccites*, *Faunipollenites*, *Hamiapollenites*, *Ibisporites*, *Lacinitriletes*, *Lahirites*, *Parasaccites*, *Platysaccus*, *Plicatipollenites*, *Potonieisporites*, *Primuspollenites*, *Rhizomaspora*, *Scheuringipollenites*, *Striatites*, *Striatopodocarpites*, *Verticipollenites*, *Vesicaspora* and *Tetraporina*. The presently recorded palynoflora reveals a typical early late Permian age and may be affiliated to those described from the Gondwana of the Peninsular India. Thus, based on present findings it could be suggested that the metasedimentary tectonic slivers (Saltoro Formation) of the Shyok Suture Zone did received Gondwanic sediments during and after Permian from the Peri-Gondwanan Karakoram block. The Karakoram block belongs to the Cimmerian microcontinent that accreted to the southern margin of Asia prior to the India-Asia collision.

Tectonic implications of 15 Ma meteoric water infiltration in the South Tibetan Detachment, Mt. Everest, Himalaya

Gébelin A[1], Jessup M[2], Teyssier C[3], Cosca M[4], Law R[5], Brunel M[5], Mulch A[6]

[1]School of Geography, Earth and Environmental Sciences, Plymouth Univ., UK [2]Dept. of Earth and Planetary Sciences, Univ. of Tennessee, Knoxville, USA [3]Earth Sciences, Univ. of Minnesota, Minneapolis, USA [4]USGS, Central Mineral and Environmental Resources Science Center, Denver, USA [5]Dept. of Geosciences, Virginia Tech, Blacksburg, USA [6]Senckenberg Biodiversity and Climate Research Centre, Frankfurt/Main, Germany

We document infiltration of deuterium-depleted fluids (D_{water} < -120 ‰) in the South Tibetan Detachment (STD) mylonitic footwall over a minimum duration of ca. 2 Myr between 17 and 15 Ma where recrystallized hydrous minerals equilibrated with low-D (meteoric) water and therefore, recorded the hydrogen isotope composition of water present during deformation. The origin of fluids and the timing of fluid flow was determined by using a combination of hydrogen isotope (D) and $^{40}Ar/^{39}Ar$ geochronology measurements performed on hydrous silicates from mylonites collected over 200 m of structural section in the STD footwall at Rongbuk Valley, near Mount Everest.

Synkinematic biotite record high-temperature isotopic exchange with deuterium-depleted water (D_{water} = -150 ± 5 ‰) that infiltrated the ductile segment of the STD during mylonitic deformation. The presence of low-D meteoric water in the STD mylonitic footwall is further supported by hornblende and chlorite with very low D values of -183 ‰ and -162 ‰, respectively. The presence of low- D meteoric water in the STD footwall raises the question of how these fluids penetrated the crust down to the ductile segment of the STD at 15 Ma.

Here, we propose that the presence of such fluids at depth is consistent with a model involving syn-convergent stretching/extension of the upper crust, high topography and high (paleo-) geothermal gradient (Fig. 1). Based on previous paleoaltimetry estimates demonstrating that a topographic high characterized the Mt Everest region (Gébelin et al. 2013) and southern Tibet (Spicer et al. 2003, Ding et al. 2017) during the middle Miocene, we suggest that extension did occur in the Tethyan Himalayan sequence as a result of gravitational instability that induced a rotation of the maximum principal compressive stress in the upper part of the crust from a north-south horizontal direction to a near vertical orientation. As a consequence, steep E-W striking brittle normal faults soling down on to the STD developed in the upper crust during top-to-the-north normal sense motion on the underlying STD and served as conduits for surface-derived fluids to penetrate the crust down to the brittle-ductile transition at least between 17 and 15 Ma. Crustal thickening, partial melting, and intrusion of leucogranites in the STD footwall would have provided the necessary high heat flow to induce and sustain buoyancy-driven fluid convection in the mylonitic STD footwall. Following the end of activity on the STD, this continued topographic load was expressed by E-W extension along the Himalayan arc from the late Miocene to the present.

These results are also supported by synkinematic biotite, hornblende, and muscovite with low D values of -190 ‰, -181 ‰, and -167 ‰, respectively, that crystallized in the high strain STD footwall along a N-S transect located 100 km further east (Nyalam region).

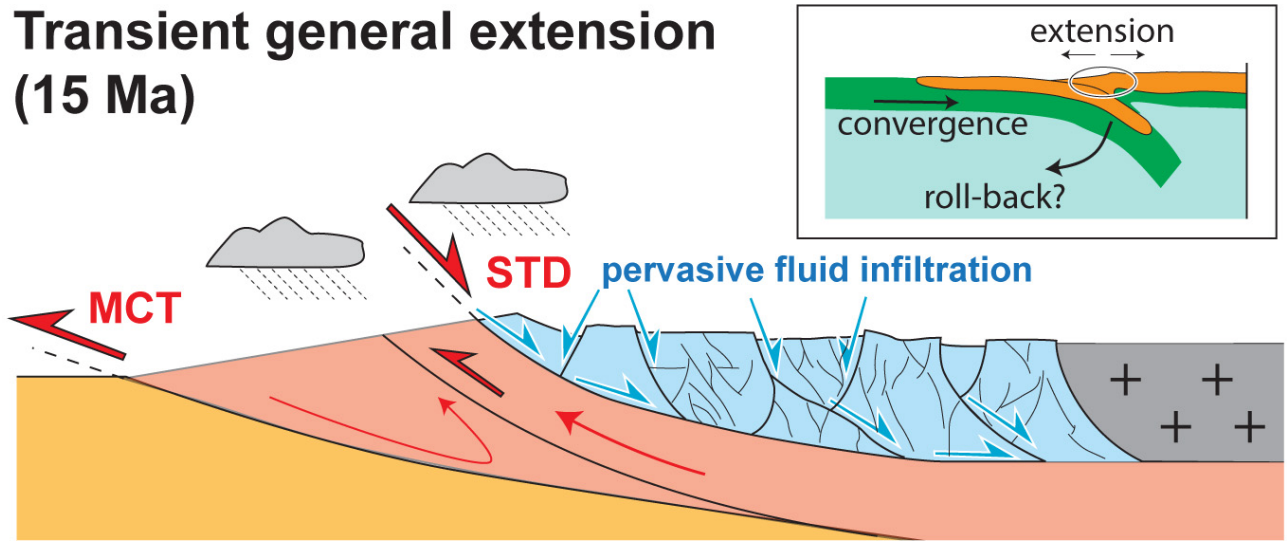

Figure 1.

References

Ding L, Spicer RA, Yang J, Xu Q, Cai F, Li S, Lai Q, Wang H, Spicer TEV, Yue Y, Shukla A, Srivastava G, Ali Khan M, Bera S, Mehrotra R (2017) Quantifying the rise of the Himalaya orogeny and implications for the South Asian monsoon. Geology 45: 215-218.

Gébelin A, Mulch A, Teyssier C, Jessup MJ, Law RD, Brunel M (2013) The Miocene elevation of Mount Everest. Geology 41: 799-802.

Spicer RA, Harris BBW, Widdowson M, Herman AB, Guo S, Valdes PJ, Wolfe JA, Kelley SP (2003) Constant elevation of southern Tibet over the past 15 million years. Nature 421: 622-624.

Source characterisation of NW Himalaya and its surrounding region: Geodynamical implications

Ghangas V[1], Mishra O[1]

[1]Ministry of Earth Sciences, India

Source characterisation of NW Himalaya and its surrounding region has been made by analysing high quality data-set of 87 events (2.2 ≤ Mw ≤ 4.9) recorded during January 2009 to December 2014 by total of 12 stations (Fig. 1) consisted of three components short period (10 stations) and broad-band seismographs (2 stations) with sampling rate of 50 sps with Nyquist frequency of 25 Hz.

Based on rigorous analysis of the corrected source spectrum, the values of spectral parameters such as low frequency spectral level (Ω_0), corner frequency (f_c), high-cut frequency (f_{max}), and kappa (κ), different source parameters (seismic moment M_0, source radii r, stress drop Δσ and moment magnitude Mw) of the events has been estimated using Brune model (1970). In this study it is observed that there is a systematic variation of source dimension in terms of the source radii of the circular fault vary from 4 m to 975 m with distinct changes in the static stress drops calculated for a given constant stress of 0.1 bar, 1 bar, 10 bar and 100 bars that varied from 0.38 to 99 bars. It is observed that there is a close correlation between the source radius and seismic moment (M_0) in which a sharp variation of seismic moment depicts changes from 2.64×10^{19} to 2.32×10^{23} dyne.cm with increase of the source radii. We infer that variability in stress drop for seismic moment is attributed to different seismic sources of varying strengths. Our results suggest that stress drop of the events have good correspondence with source depth, indicating the shear stress regime in the brittle crust having linear relationship with Δσ and source depth with significant changes of stress drop which assumed higher value with very large variability in depth, which in turn suggests the presence of intricate subsurface seismogenic sources beneath the NW Himalaya and its surrounding region. A scaling relation between seismic moment and corner frequency is established for the region as: $M_0 = 7\times10^{22}\ fc^{-2.9}$, which is in good unison to Garhwal and Kumaon Himalaya, indicating that NW Himalaya source zone is similar to that of Garhwal and Kumaon Himalaya region and its propensity to earthquake genesis predominantly bears analogous source mechanism to that of Garhwal and Kumaon Himalaya region.

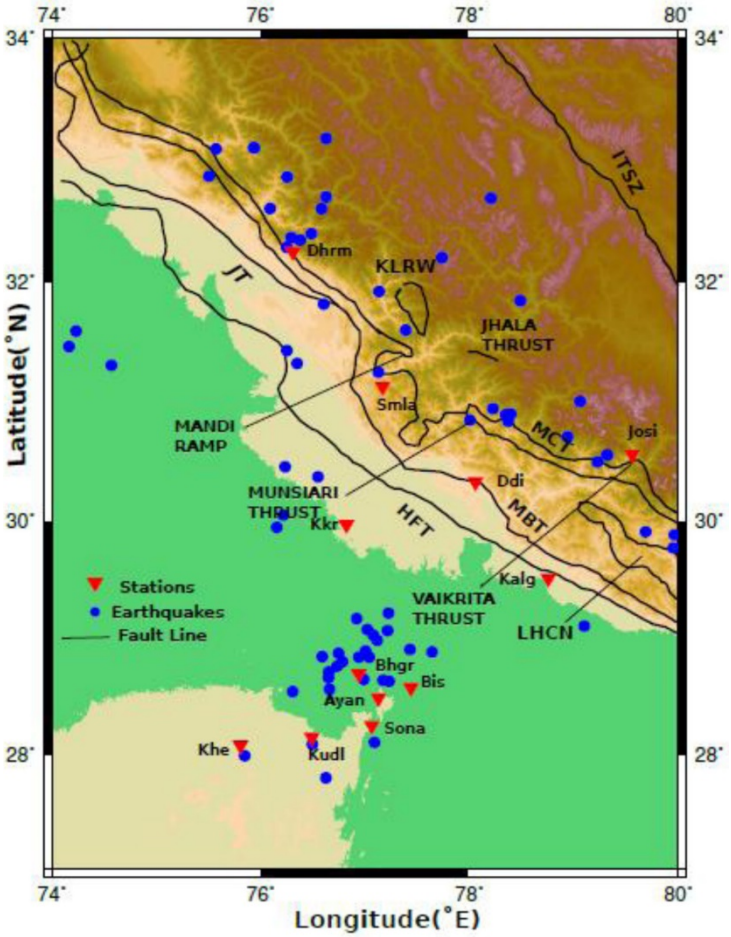

Figure 1. Map showing tectonic features of the NW Himalaya. Tectonic features (lines) are shown and include: Main Boundary Thrust (MBT); Main Central Thrust (MCT), Himalayan Frontal Thrust (HFT), Munsiari thrust, Vaikrita thrust; Jammu thrust (JT), Lesser Himalayan Crystalline Nappe (LHCN), Kullu-Larji-Rampur Window (KLRW), Jhala thrust. Filled triangles depict the network stations and filled circles shows the epicentres (source: ISC).

Reference

Brune JN (1970) Tectonic stress and the spectra of seismic shear waves from earthquakes. J Geophys Res 75: 4997-5009.

Structural evolution of Kohat and Potwar fold thrust belts in Pakistan: New evidence from low temperature thermochronology

Ghani H[1,2], Sobel ER[1], Zeilinger G[1], Glodny J[3], Zapata S[1]

[1]Inst. of Earth and Environmental Science, Univ. of Potsdam, Germany [2]Dept. of Earth and Environmental Science, Bahria Univ., Islamabad, Pakistan [3]GFZ Potsdam, Germany

The Kohat and Potwar fold thrust belts in Pakistan represent the outermost external zone of the Himalayan fold and thrust system. The Main Boundary Thrust (MBT) and the Main Frontal Thrust (MFT) mark the northern and southern boundaries respectively. In order to better understand the sequence of deformation, and the kinematics of fold and thrusts in the Kohat and Potwar fold thrust belts, we have constructed balanced cross-sections and conducted Apatite U-Th-Sm/He(AHe) and Apatite fission track (AFT) dating. We have systematically sampled Cambrian to Pliocene sandstones from different stratigraphic sections in the Salt, Surghar and Kohat Ranges. The data from the Kohat fold thrust belt suggest totally reset AHe and AFT ages. The clustered AHe data from the Salt Range suggest totally reset ages and the broad range of AFT results suggests partially reset ages. Combining our thermochronology data with our structural reconstructions, we interpret the deformation history as follows: 1) synchronous movement on the MBT and out of sequence movement on the western part of the MFT in the Surghar Range at ~12 Ma, 2) to the south of the MBT in the Kohat fold and thrust belt, AHe ages date cooling while uplifting above the duplex: at 5 Ma on the Lachi thrust, 3 Ma on Shakardarra-Karak thrust 3) At 5 Ma, a second episode of out-of-sequence deformation occurred on the MFT, in the Salt Range. The spatial distribution of AHe and AFT ages in combination with the structures shown in balanced sections suggest that the deformation south of MBT did not uniformly propagate towards south. Instead the deformation was active on different structures at different time causing an out of sequence evolution of the Kohat and Potwar fold and thrust belts.

Fault structure and earthquake dynamics of the 2015 Mw 7.8 Gorkha earthquake in Nepal using aftershocks recorded by the NAMASTE, a dense local seismic network

Ghosh A[1], Mendoza M[1], Li B[1], Karplus M[2], Nabelek J[3], Sapkota S[4], Adhikari L[4], Klemperer S[5], Velasco A[2]

[1]Univ. of California, Riverside, USA [2]Univ. of Texas, El Paso, USA [3]Oregon State Univ., Corvallis, USA [4]Dept. of Mines and Geology, Kathmandu, Nepal [5]Stanford Univ., USA

We designed and installed a 45-stations seismic network right after the 2015 Mw 7.8 Gorkha earthquake. It covered the entire rupture area of the mainshock in Nepal. This dense local network was operational for approximately one year and recorded a prolific aftershock sequence. In addition, we combined four teleseismic arrays to image rupture propagation using a backprojection algorithm. It shows unilateral along-strike eastward rupture, but with significant complexity near the end when rupture bifurcated around a stronger patch that eventually failed to produce the largest aftershock of this event. Thousands of well constrained aftershock locations reveal distinctly heterogeneous seismicity pattern in 3D with strong along-strike variation. Eastern part of the rupture is much more active than the western part and show a wider earthquake distribution along-dip. We quantitatively analyse the distribution of earthquakes to interpret fault structure in this part of the Himalaya. Based on the aftershock distribution, we infer that the MHT is characterized by two gently northerly dipping planes with both horizontal and vertical separation. The updip upper plane is subhorizontal while the downdip lower plane dips 8º NNE. They are connected by a complex cluster of seismicity. This cluster shows several steeply dipping planes resembling a duplex structure. Therefore, we conclude that MHT in this part of the Himalaya is characterized by two gently north dipping planes connected by a duplex structure, which may contribute to the rupture complexity of the Gorkha mainshock.

Determining sub-surface geometry by integrating transport-parallel distribution of cooling ages, surface geology and data from the 2015 Gorkha earthquake

Ghoshal S[1], McQuarrie N[1], Robinson D[2]

[1]Univ. of Pittsburgh, USA [2] Dept. of Geological Sciences, The Univ. of Alabama, Tuscaloosa, USA

Cooling ages measured at the surface are a function of the cumulative path taken by rocks from burial to exhumation. The geometry and location of ramps, as they develop through time, determine areas of active uplift and increased exhumation rates, exerting a first-order control on the distribution of cooling ages. We propose that the distribution of cooling ages at the surface can be used in conjunction with subsurface constraints provided by seismicity to constrain the present geometry of an orogen and provide insight into its temporal development.

We test this hypothesis in the Central Nepal Himalayas, where the 2015 Gorkha earthquake ruptured and illuminated the geometry of the Main Himalayan Thrust (MHT) along the rupture path. The location and depth of the hypocentre, along with the orientation of the rupture plane highlighted that previous estimates of the MHT needed to be revised. After the earthquake, updated solutions for the MHT still show varying geometries, suggesting that additional constraints are required to distinguish between them.

We test the effect of subsurface geometry on cooling ages through forward modelling of a series of sequentially restored balanced cross-sections created along transects in Central Nepal. The resulting kinematics are input into a thermokinematic model (PECUBE) to evaluate the relationship between subsurface geometry and predicted cooling ages. Central Nepal boasts a large, well-distributed thermochronological dataset, which can be used to constrain permissible subsurface geometries. The new cross-sections were drafted along a section line oriented along the Budhi Gandaki valley. We also evaluate a published cross-section, drafted on a section line ~40 km to the east. We test how the location of the active ramp affects cooling ages, using the decollement estimates proposed after the Gorkha earthquake. Due to the lack of surface exposure of the Lesser Himalayan duplex in Central Nepal, we evaluate and test different duplex geometries and kinematics (e.g. foreland-dipping vs. hinterland-dipping) to observe their effect on cooling ages across strike. Since the distribution of cooling ages is dependent on how the geometry has developed over time, this provides insight into how these different geometries affect the development of cooling ages at the surface and helps constrain a viable model for duplex formation. We also tested the sensitivity of the modelled cooling ages to a variety of additional model parameters (e.g. crustal heat production and thrust sheet velocities) to identify viable solutions for the region.

We propose a new cross-sectional geometry for Central Nepal that is able to match the geology at the surface, reproduce the observed distribution of cooling ages, and match known subsurface constraints following the earthquake.

Rapid denudation at the Dhauladhar range front, Himachal Pradesh, India

Godard V[1], Mahéo G[2], Mukherjee S[3], Sterb M[4], Maleappane É[1], Leloup H[5], Team ASTER[1]

[1]Aix-Marseille Univ., France [2]Univ. of Lyon 1, France [3]IIT Bombay, India [4]ENS Lyon, France [5]CNRS, France

Assessing along-strike variability in deformation patterns along the Himalayan arc is of primary importance to decipher the relative contribution of the main tectonic structures in accommodating the India-Eurasia convergence. In active mountain ranges a dynamic coupling exists between tectonic and denudation, with high rates of rock uplift along thrust faults usually coincident with high denudation and exhumation rates (e.g. Kirby and Whipple 2012). From that perspective, surface processes provide a way to investigate the spatial distribution of tectonic uplift and test different possibilities for the geometry and slip rates of the associated structures, even though simultaneous variations in the climatic boundary condition can interfere in the interaction between tectonic and erosion.

Significant along-strike variability has been reported along the Himalayan arc, in terms of geometry of the structures and intensity for both external and internal forcings. One of the most peculiar long-wavelength feature of the range is the Kangra reentrant (Himachal Pradesh, India) in the western part of the arc. This area displays (1) a wide sub-Himalayan zone, (2) noticeable changes in the orientation of the structures and (3) very high topographic gradients at the Dhauladhar front range. Recent studies have highlighted the occurrence of significant out-of-sequence deformation at various times scales in the Kangra reentrant (Mukherjee 2015; Dey et al. 2016; Thiede et al. 2017), suggesting that this area could significantly depart from deformation regimes determined in other well documented regions (e.g. Avouac 2003).

We present 25 new ^{10}Be-derived denudation rates from the Chamba region in Himachal Pradesh and in particular the southern front the Dhauladhar range, where the Main Boundary Thrust has been identified as an active structure from the analysis of thermochronological data, as well as from the Ravi and Beas rivers. Calculated denudation rates range from 0.2 to 3 mm/yr, with the highest rates localized along the front of the Dhauladhar range (1-3 mm/yr range). The data also display significant along-strike variability and denudation rates appear to taper down below 1 mm/yr at the NW and SE tips of the range. Our data provide further support for sustained uplift of the Dhauladhar range at millennial time-scales and the existence of significant out-of-sequence deformation in this part of the Himalayan arc.

References

Avouac JP (2003) Mountain building, erosion, and the seismic cycle in the Nepal Himalaya. Adv Geophys 46: 1-80.

Dey S, Thiede RC, Schildgen TF, Wittmann H, Bookhagen B, Scherler D, Strecker MR (2016) Holocene internal shortening within the northwest Sub-Himalaya: Out-of-sequence faulting of the Jwalamukhi Thrust, India. Tectonics 35: 2677-2697.

Kirby E, Whipple KX (2012) Expression of active tectonics in erosional landscapes. J Struct Geol 44: 54-75.

Mukherjee S (2015) A review on out-of-sequence deformation in the Himalaya. In: Mukherjee S, Carosi R, van der Beek P, Mukherjee BK, Robinson D (Eds.) Tectonics of the Himalaya. Geol Soc London Spec Publ 412: 67-109.

Thiede R, Robert X, Stübner K, Dey S, Faruhn J (2017) Sustained out-of-sequence shortening along a tectonically active segment of the Main Boundary thrust: The Dhauladhar Range in the northwestern Himalaya. Lithosphere 9: 715-725.

Varied thermo-rheological structure, mechanical anisotropy, and lithospheric deformation of the southeastern Tibetan Plateau

Gong W[1], Jiang X[1]

[1]Ocean Univ. of China, Qingdao, China

To investigate the lithospheric structure and deformational pattern, we construct two thermo-rheological models using two integrated geophysical profiles along the southeastern Tibet. The lithosphere of the Chuandian block is warmer on average than that of the surrounding areas. The estimated rheological strength changes from a strong jelly sandwich regime into a weak “crème brûlée” regime going from the Indochina block and South China plate to the Chuandian block.

According to Pms and SKS splittings, the crust-mantle is decoupled in the south of 26°N. Given that a strong load-bearing layer at the topmost part of the upper mantle beneath the Indochina block, the decoupling may occur below the topmost mantle. The fast Pms polarization directions are almost parallel to GPS velocity vectors in the South China plate and Indochina block, suggesting a vertical coherent deformation in the crust with a jelly sandwich regime. However, the fast Pms polarization directions are at high angles to GPS velocity vectors in the Chuandian block, indicating the decoupling within the crust. This deformation is consistent with a “crème brûlée” regime in this block.

The observations of seismic energy release and crustal isostatic state can contribute to an intensive understanding of the crustal deformation. The release of earthquake energy is concentrated in the upper-middle crust beneath the Chuandian block, which presents a weak lower crust. In the South China plate and Indochina block, the thickness of the seismogenic layer is identical to the Moho depth, implying a mechanically strong crust. The isostatic crustal thickness is almost identical to the Moho depth in the South China plate, suggesting that the crust is in Airy isostatic equilibrium. However, the isostatic crustal thicknesses beneath the Chuandian block and Indochina block are thinner and thicker than the Moho depth, respectively. The isostatic undercompensation of the crust beneath the Chuandian block might be caused by thickening of the weak middle-lower crust and little upper crustal shortening. This indicates that the middle-lower crust is entirely decoupled from upper crust. It is consistent with a “crème brûlée” rheological regime and the discrepancy between the Pms splitting and GPS velocity vectors in the southern Chuandian block. The isostatic overcompensation of the crust beneath the Indochina block may be correlated with rapid uplift and intense denudation process of the surface. However, the middle-lower crust cannot deform just like the form of thickening in the Chuandian block. It is mechanically coupled to the upper crust.

Based on the comparison between geophysical and geological observations in the central-northern Tibet and the Chuandian block, we can infer that the crustal deformational pattern may be more complex than the crustal channel flow contributed by the topography-induced horizontal pressure gradient. Driven by the weak layers shown by thermo-rheological structure, seismic energy release, crustal isostatic state and seismic anisotropy, a significant decoupling within the crust in the southern Chuandian block is observed. However, the layers with aqueous fluids and partial melting are only distributed in part of place or channels that can be observed by seismic and magnetotelluric observations.

Inverted temperature fields: Peak metamorphic and deformational temperatures across the Lesser Himalayan Sequence

Grujic D[1], Ashley K[2], Coble M[3], Coutand I[1], Kellett D[4], Larson K[5], Whipp D[6], Whynot N[1]

[1]Dept. of Earth Sciences, Dalhousie Univ., Halifax, Canada [2]Univ. of Texas, Austin, USA [3]Stanford Univ., USA [4]Geological Survey of Canada, Dartmouth, Canada [5]Univ. of British Columbia, Okanagan, Canada [6]Univ. of Helsinki, Finland

The inverted metamorphism associated with the Main Central thrust zone in the Himalaya has been historically attributed to a number of tectonic processes. Here we show that there is actually a composite peak and deformation temperature sequence that formed in succession via different tectonic processes. Deformation partitioning seems to have played a key role, and the magnitude of each process has varied along strike of the orogen.

To explain the formation of the inverted metamorphic sequence across the Lesser Himalayan Sequence (LHS) in eastern Bhutan, we used Raman spectroscopy of carbonaceous material (RSCM) to determine the metamorphic peak temperatures and Ti-in-quartz thermobarometry to determine the deformation temperatures, combined with thermochronology including published apatite and zircon (U-Th)/He and fission-track data, and new and published $^{40}Ar/^{39}Ar$ dating of muscovite.

RSCM results indicate that there are two peak temperature sequences separated by a major thrust within the LHS. The internal (northern) temperature sequence shows an apparent inverted peak temperature gradient of 12 °C/km; in the external (southern) sequence, peak temperatures are constant across the structural sequence. To reconcile these results, we suggest that pervasive ductile deformation within the upper LHS and along the Main Central thrust zone at its top stopped at ~11 Ma at which time the deformation shifted and focused within the external duplex and the Main Boundary thrust.

Formation of a rain shadow: O and H stable isotope records in authigenic clays from the Siwalik Group in Eastern Bhutan

Grujic D[1], Govin G[2], Barrier L[3], Bookhagen B[4], Coutand I[1], Cowan B[1], Hren M[5], Najman Y[2]

[1]Dept. of Earth Sciences, Dalhousie Univ., Halifax, Canada [2]Lancaster Environment Centre, Lancaster Univ., UK [3]Univ. Paris Diderot, France [4]Inst. of Earth and Environmental Science, Univ. of Potsdam, Germany [5]Univ. of Connecticut, Storrs, USA

We measure the oxygen and hydrogen stable isotope composition of authigenic clays from Himalayan foreland sediments (Siwalik Group), and from present day small stream waters in eastern Bhutan to explore the impact of uplift of the Shillong Plateau on rain shadow formation over the Himalayan foothills. Stable isotope data from authigenic clay minerals (< 2 μm) suggests the presence of three palaeoclimatic periods during deposition of the Siwalik Group, between ~7 and ~1 Ma. The mean $\delta^{18}O$ value in palaeo-meteoric waters, which were in equilibrium with clay minerals, is ~2.5‰ lower than in modern meteoric and stream waters at the elevation of the foreland basin. We discuss the factors that could have changed the isotopic composition of water over time and we conclude that: (a) The most likely and significant cause for the increase in meteoric water $\delta^{18}O$ values over time is the “amount effect”, specifically, a decrease in mean annual precipitation. (b) The change in mean annual precipitation over the foreland basin and foothills of the Himalaya is the result of orographic effect caused by the Shillong Plateau’s uplift. The critical elevation of the Shillong Plateau required to induce significant orographic precipitation was attained after ~1.2 Ma. (c) By applying scale analysis, we estimate that the mean annual precipitation over the foreland basin of the eastern Bhutan Himalayas has decreased by a factor of 1.7-2.5 over the last one to three million years.

Stress transfer and connectivity between the Bhutan Himalaya and the Shillong Plateau

Grujic D[1], Hetényi G[2], Cattin R[3], Baruah S[4], Benoit A[3], Drukpa D[5], Saric A[1]

[1]Dept. of Earth Sciences, Dalhousie Univ., Halifax, Canada [2]ISTE, FGSE, Univ. of Lausanne, Switzerland [3]Geosciences Montpellier, Univ. of Montpellier, France [4]CSIR, North East Inst. of Science and Technology, Jorhat, India [5]Dept. of Geology and Mines, Thimphu, Bhutan

Within the northern Indian Plate, the Shillong Plateau is a peculiar geodynamic terrane, hosting significant seismic activity outboard the Himalayan belt. This activity is often used as an argument to explain apparent reduced seismicity in the Bhutan Himalayas. Although current geophysical and geodetic data indicate that the Bhutan Himalayas accommodate more deformation than the Shillong Plateau, we aim to quantify the extent to which the two geodynamic regimes are connected and potentially interact through stress transfers. We compiled a map of major faults and earthquakes in the two regions and computed co-seismic stress transfer amplitudes. Our results indicate that the Bhutan Himalayas and the Shillong Plateau are less connected than previously suggested. Major earthquakes in either of the two regions mainly affect transverse faults connecting them, causing up to ~40 bar Coulomb stress change; however, this effect is clearly less on thrust faults of the either region (up to 1 bar only). The Mw 8.25 1897 Assam earthquake that affected the Shillong Plateau did not cause a stress shadow on the Main Himalayan Thrust in Bhutan as previously suggested. Similarly, the Mw 8 ± 0.5 1714 Bhutan earthquake had negligible impact on stress accumulation on thrust faults bounding the Shillong Plateau. Furthermore, the main process shaping the regional stress patterns continues to be interseismic loading with complex boundary conditions in a diffuse deformation field involving the Bengal Basin and Indo-Burman Ranges. While both the Bhutan Himalayas and the Shillong Plateau exhibit a compressional regime, their stress evolutions are more weakly connected than hypothesized. Although our modelling suggests lateral increase in stress interactions, from west (less) to east (more), in the Bhutan Himalayas, a clearer picture will only emerge with better constrained fault geometries, slip rates, crustal structure, and seismicity catalogues in the entire region of distributed deformation.

Metasomatism soft mantle and growth of the Tibet Plateau

Guillot S[1], Goussin F[1], Cordier C[1], Boulvais P[2], Roperch P[2], Schulmann K[3], Dupont-Nivet G[4], Guo Z[5], Replumaz A[1]

[1] ISTerre, Univ. Grenoble-Alpes, France [2]Geosciences Rennes, Univ. of Rennes, France [3]EOST, Univ. of Strasbourg, France [4]Inst. of Earth and Environmental Science, Univ. of Potsdam, Germany [5]Key Laboratory of Orogenic Belts and Crustal Evolution, Peking Univ., Beijing, China

The timing and mechanism of the Tibet Plateau formation remain elusive. Whether the bulk of its formation really occurred during the Cenozoic, either by continuous and homogeneous thickening of the whole lithosphere followed by mantle delamination, or by localized continental subductions reactivating ancient suture zones, are questions yet to be assessed. Here we report mantellic phlogopite and magmatic carbonates preserved in Eocene potassic rocks from Eastern Qiangtang bringing direct evidence that the lithospheric mantle in Central Tibet had been hydrated and CO_2-enriched prior to the India-Asia collision. Rheological calculations suggest that such metasomatized mantle would have been extremely weak but buoyant enough to prevent sinking into the deep mantle. The slow seismic anomaly beneath Central Tibet would image a weakened lithosphere of normal thickness rather than an asthenospheric upwelling resulting from any delamination. This soft and buoyant inherited Tibetan lithosphere may have permitted the growth of the Tibet Plateau by underthrusting of stronger Indian and Asian continental slabs.

Crustal configuration and Moho geometry in the NW Himalaya and Ladakh-Karakoram collision zone based on receiver function study

Hazarika D[1], Wadhawan M[1], Paul A[1], Kumar N[1]

[1]*Wadia Inst. of Himalayan Geology, Dehradun, India*

The northwest Himalaya and Ladakh–Karakoram zone outline the western extremity of the Himalayan–Tibetan orogenic system which provides unique opportunity to study the interaction of the Indian and Eurasian plates. The geometry of Moho and inter-crustal features have been investigated beneath a profile consisting of 29 seismological stations extending from the Indo-Gangetic plain (IGP) to the eastern Ladakh-Karakoram zone passing across the Satluj valley of northwest Himalaya. The study reveals ~44 km crustal thickness beneath the Himalayan Frontal Thrust (HFT), and it gradually increases to ~62 km beneath the Tethyan Himalaya (TH) and ~80 km beneath the Karakoram Fault zone. About 3-4 km thick sedimentary column is inferred beneath the stations located over the IGP. A gentle north dipping structure of the Main Himalayan Thrust (MHT) is imaged between the Sub and Higher Himalaya in contrast to the reported ramp structure of the MHT beneath the Garhwal and Nepal Himalaya. The ramp structure is, however, identified further north, beyond the South Tibetan Detachment in Satluj valley. The depth of the MHT varies from ~16 to 27 km across the Sub, Lesser, and Higher Himalaya, and it increases to ~38 km beneath the TH forming a ramp. This is significantly a different structure of the MHT beneath the Satluj valley, which is attributed to the effect of underthrusting Delhi-Hardwar Ridge, a transverse structure to the Himalayan arc. Conspicuously, no strong or large earthquake is observed during 1964-2017 in this segment of the Himalayan Seismic Belt.

Strong azimuthal variation of crustal structure is observed in the Indus suture zone (ISZ), the zone which marks the collision and subsequent subduction of both the Tethyan oceanic plate and Indian continental plate beneath Eurasia. The teleseismic waves piercing the ISZ do not show clear P-to-S (Ps) converted phase at the depth of Moho. In contrast, the waves piercing the Karakoram zone, Ladakh batholith and the Tethyan Himalayan region south of the ISZ clearly show the Moho converted Ps phase and corresponding inverted models reveal variation of crustal thickness from ~75 km beneath the Tso Morari Crystalline complex to ~80 km beneath the Karakoram fault zone. A prominent intracrustal low-velocity zone (IC-LVZ) is detected beneath the Ladakh-Karakoram zone within the depth range ~15-40 km. The observed IC-LVZ is interpreted as due to the presence of fluid/partial melt. This study provides compelling evidence that the mid-crustal low-velocity zone does extend across the suture zone, into the Tethyan Himalaya. The contact between this serpentinized ultramafic rocks and the eclogitized Indian continental crust in the suture zone is identified at ~47-50 km depth beneath Ladakh-Karakoram zone.

Clustering of rock avalanches and rock avalanche deposits along the Main Central Thrust and within the Higher Himalayan Crystalline Sequence, Sikkim

Hermanns RL[1], Morken O[1], Sengupta A[2], Penna I[1], Gupta V[3], Kumar Bhasin R[4], Dehls J[1]

[1]Geological Survey of Norway, Trondheim, Norway [2]IIT Kharagpur, India [3]Wadia Inst. of Himalayan Geology, Dehradun, India [4]Norwegian Geotechnical Inst., Norway

First field investigations on the hazard analysis for seismically triggered rock slope failures along the Gangtok Yumthang / Lachen trans-Himalayan highways reveal two clusters of rock slope failure deposits. This transect crosses the Main Central Thrust (MCT) between the Lesser Himalayan Sequence (LHS) in the South and the Higher Himalayan Crystallin Sequence (HHCS) in the North. This transect also crosses climatic boundaries from humid in the south characterized by rainforest vegetation up to the mountaintops into a much dryer Tibet plateau like environment north of the first range crossing 5000 m altitude. The climate zones run in the area parallel to the MCT however offset to the north by about 25 km.

The southern cluster bracket the MCT as a ca. 20 km wide belt and deposits occur in similar quantity in the LHS and the HHCS. This cluster contains two historic rock avalanches. The older occurred in the night from September 10th to 11th, 1983 and killed about 200 soldiers. No triggering or conditioning event is reported for this event. The second is the Dzongu rock avalanche that occurred on August 13th, 2016 on a sunny day with no external trigger. However, local people reported that the slope had frequent rock fall activity for several years that increased after the M6.8 Nepal/Sikkim border earthquake from September 18th, 2011. This coincides with a deformation zone becoming visible at the back scarp on satellite images. Rock fall activity further accelerated following eyewitnesses 15-20 days prior to the event. The rock avalanche formed a dam that has not breached catastrophically since formation and it is under video surveillance. To the same cluster belong 19 boulder deposits. These are formed by boulders up to ~30 m in diameter, that form steps in the lower valley flanks. These steps are all settled, and the rainforest got partly removed. The steps often correspond to steps on the opposite slope. Furthermore, are the slopes above the deposits spoon shaped and drainage systems on the slopes are poorly developed and not canalized, interpreted thus to be the deposits of prehistoric rock avalanches.

The second cluster occurs to the north in the rather arid climate zone between the villages of Lachung and Yumthang. One historic rock avalanche occurred in the area reported by locals to have been triggered by the M7.3 earthquake of May 12th, 2015 with the epicentre at the Chinese border between Kathmandu and Mt. Everest that was the strongest aftershock of the April 25th Gorkha earthquake. This coincides with bracketing satellite images published on GoogleEarth. This rock avalanche dammed the valley and caused an air-blast destroying the pine forest for 300 m ahead of the deposit. The rock avalanche is directly overlying an older rock-avalanche deposit of larger extend. Seven further deposits with similar characteristics were found between both villages.

We sampled rock boulder deposits for cosmogenic nuclide age determination to get a better understanding of the frequency of these events that will be part of our hazard analysis.

Geophysical and petrological assessment of the partially molten plutons, Lhasa Block

Hetényi G[1], Pistone M[1], Nabelek PI[2], Baumgartner LP[1]

[1]ISTE, FGSE, Univ. of Lausanne, Switzerland [2]Geological Sciences, Univ. of Missouri, Columbia, USA

Zones of partial melt in the middle crust of Lhasa Block, southern Tibet, have been geophysically observed as seismically reflective “bright spots”. These plutons bear important relevance for geodynamics as they have been used to invent and support channel-flow models in the Himalaya-Tibet orogen.

Here we assess the spatial abundance, melt fractions, and plausible longevities of these crustal “bright spots”. We establish lower and upper bounds on these characteristics using a joint geophysical-petrological approach.

Geophysical imaging constrains the average abundance of partial melt zones to 5.6 km^3 per surface-km^2 (minimum: 3.1 km^3/km^2, maximum: 7.6 km^3/km^2 over the mapped area). Physical properties detected by field geophysics and interpreted by laboratory measurements constrain the volume of partial melt to be between 5 and 26%.

We evaluate the viability of these estimates with petrological modelling using a combination of mineral-melt phase equilibria and thermal modelling based on published geotherms, crustal bulk rock compositions and water contents consistent with the Lhasa Block. These simulations determine: (a) the physico-chemical conditions of melt generation at the base of the Tibetan crust and its transport and emplacement in the middle crust; (b) the melt percentage produced at the source, transported, and emplaced to form the observed “bright spots”. Two main mechanisms are considered: (1) flux melting produced during mineral dehydration reactions in the underthrusting Indian lower crust; (2) dehydration-melting reactions caused by heating within the Tibetan crust. We find that both mechanisms demonstrate first-order match in explaining the formation of the partially molten “bright spots”. Moreover, to match the amounts of partial melt, a combination of the two mechanisms may be required.

Thermal modelling shows that the Lhasa Block plutons have only small amounts of melt and only for geologically short timescales (< 1 Myr), if not continuously fed. We also demonstrate that the observed spatial abundance of partial melt zones and the current input rate of new material to the bottom of the Tibet crust needed to generate the melts are sustainable.

In summary, the short life span and small sizes compared to the Tibetan Plateau suggests that the partially molten zones in the middle crust are ephemeral and local features. These characteristics are inconsistent with both large lateral extent and continuity, as well as permanence of channel flow transport within the Tibetan crust.

Structural controls of the seismicity revealed by the Himalaya-Karnali network experiment in Western Nepal

Hoste-Colomer R[1], Bollinger L[1], Lyon-Caen H[2], Bhattarai M[3], Koirala B[3], Gupta R[3], Kandel T[3], Timsina C[3], Corentin C[1], Adhikari L[3]

[1]CEA, France [2]Laboratoire de Géologie, ENS Paris, France [3]Depth. of Mines and Geology, Kathmandu, Nepal

According to historical chronicles as well as preliminary paleoseismological trenches, the latest devastating great earthquake in Western Nepal happened more than 500 years ago in 1505 A.D. (e.g. Sapkota 2011, Hossler et al. 2016). Despite its inescapable repeat in the future, the seismic behaviour of the Main Himalayan Thrust fault segments ruptured during this earthquake are poorly known. Among others, large uncertainties remain on the downdip extent and geometry of the locked fault zone and its lateral variations as well as their relations with large and great earthquake ruptures.

A first temporary seismic experiment, the “Himalaya-Karnali-Network” (Hi-KNet), was therefore deployed for two years in western Nepal in order to image the thrust at depth and reveal the behaviour of the seismicity along the brittle-ductile transition zone. A total of 15 temporary seismic stations were installed above the main seismic belts in Chainpur-Bhajang and Karnali region, complementarily to the Regional Seismological Network.

More than 2000 local earthquakes were located below the network during the first year of experiment. Most of these events were clustered within pluri-kilometric long swarms that lasted a few days or weeks. The finest relocations of the local earthquakes reveal a complex pattern of along strike variations of the seismicity. Most clusters develop at the intersection between the megathrust and contacts between Lesser Himalayan tectonic slivers (Fig. 1). Some of the seismic swarms migrate with time.

Altogether, the swarms and individual earthquakes reveal ramps and flat geometry of the megathrust. Some of these structures, among them the largest active ramps, are likely to partially control the rupture of intermediate to large earthquakes.

The structural segmentation revealed by the seismicity leads us to propose a fault model involving intermediate, large and great earthquakes in West Nepal.

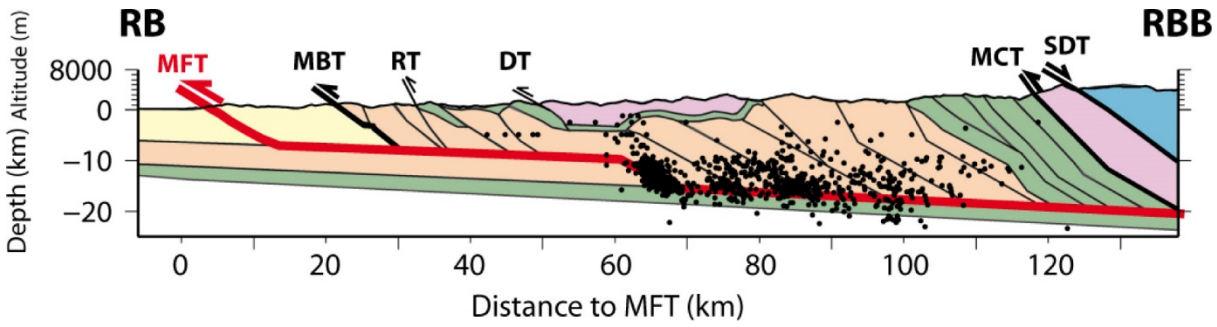

Figure 1. Chainpur-Bahjang section through the seismicity (Hoste-Colomer 2017). Black dots correspond to the hypocenters of the local earthquakes located within a 20 km-swath of the Chainpur section in 2015. Balanced geological cross section from Robinson et al. (2006).

References

Hossler T, Bollinger L, Sapkota SN, Lavé J, Gupta RM, Kandel TP (2016) Surface ruptures of large Himalayan earthquakes in western Nepal: evidence along a reactivated strand of the Main Boundary Thrust. Earth Planet Sci Lett 434: 187-196.

Hoste-Colomer R (2017) Variations latérales de sismicité le long du megachevauchement himalayen au Népal. PhD thesis, Paris Science et Lettres Research Univ., 230 p. Available at: https://tel.archives-ouvertes.fr/tel-01797590

Robinson DM, DeCelles PG, Copeland P (2006) Tectonic evolution of the Himalayan thrust belt in western Nepal: Implicaitons for channel flow models. Geol Soc Am Bull 118: 865-885.

Sapkota SN (2011) Surface rupture of 1934 Bihar-Nepal earthquake: implications for seismic hazard in Nepal Himalaya. Phd Thesis, IPGP.

Cross faults and their role in Himalayan tectonics: The Benkar Fault, an example from the Khumbu region, Nepal

Hubbard M[1], Gajurel A[2], Seifert N[1]

[1]Dept. of Earth Sciences, Montana State Univ., USA [2]Dept. of Geology, Tribhuvan Univ., Kathmandu, Nepal

Though thrust faults and, more recently, extensional faults, have been the dominant topic in Himalayan structural geology literature, there is another type of structure that may be equally important to the mountain building process in the Himalaya. These structures are the transverse faults that are highly oblique/perpendicular to the strike of the thrusts and the South Tibetan Detachment System (STDS). Previous workers have discussed the importance of the Yadong Fault on the western border of Bhutan as well as the Gish and Kosi faults in the Sikkim region (Wu et al. 1998; Mukul et al. in press). Further west the bounding faults of the Thakola Graben are transverse to the range, as are the bounding faults of the Leo Pargil Dome (Langille et al. 2014). A number of these structures are clearly extensional, but other structures of this orientation appear to have a strike-slip sense of displacement. We present here a newly-recognized structure from eastern Nepal, the Benkar Fault (see map below). This structure has a linear trace possibly extending from south of Salleri in the Lesser Himalaya to the lower Khumbu glacier in the Greater Himalaya and possibly into Tibet. Though there is a geomorphic expression of the fault, there is no major difference in average elevation across the fault as seen in the Thakola Graben or along the Yadong Fault. The Benkar fault zone is roughly 3 km wide and strikes N30-50E with a steep southeast dip. Foliation on the high peaks adjacent to the structure appears to be displaced with a southeast-side-down sense of shear. Locally, alignment of sillimanite provides a lineation that plunges shallowly to the southwest. Ductile fabric asymmetries determined in thin-section suggest a normal, right-lateral sense of shear. In a number of places, however, there are brittle fault fabrics with left-lateral, normal kinematics suggesting multiple episodes of deformation. To the east, the Gish and Kosi faults are faults of similar length and orientation. Timing of displacement for all of these faults is yet to be determined. Future work aims to gain an understanding of the structural history with a goal of understanding the relation of these cross faults to the major east-west striking thrust faults and normal faults. Cross faults could be expressions of lateral ramps, tear faults, or could be related to a large-scale, east-west extension that has been documented in Tibet.

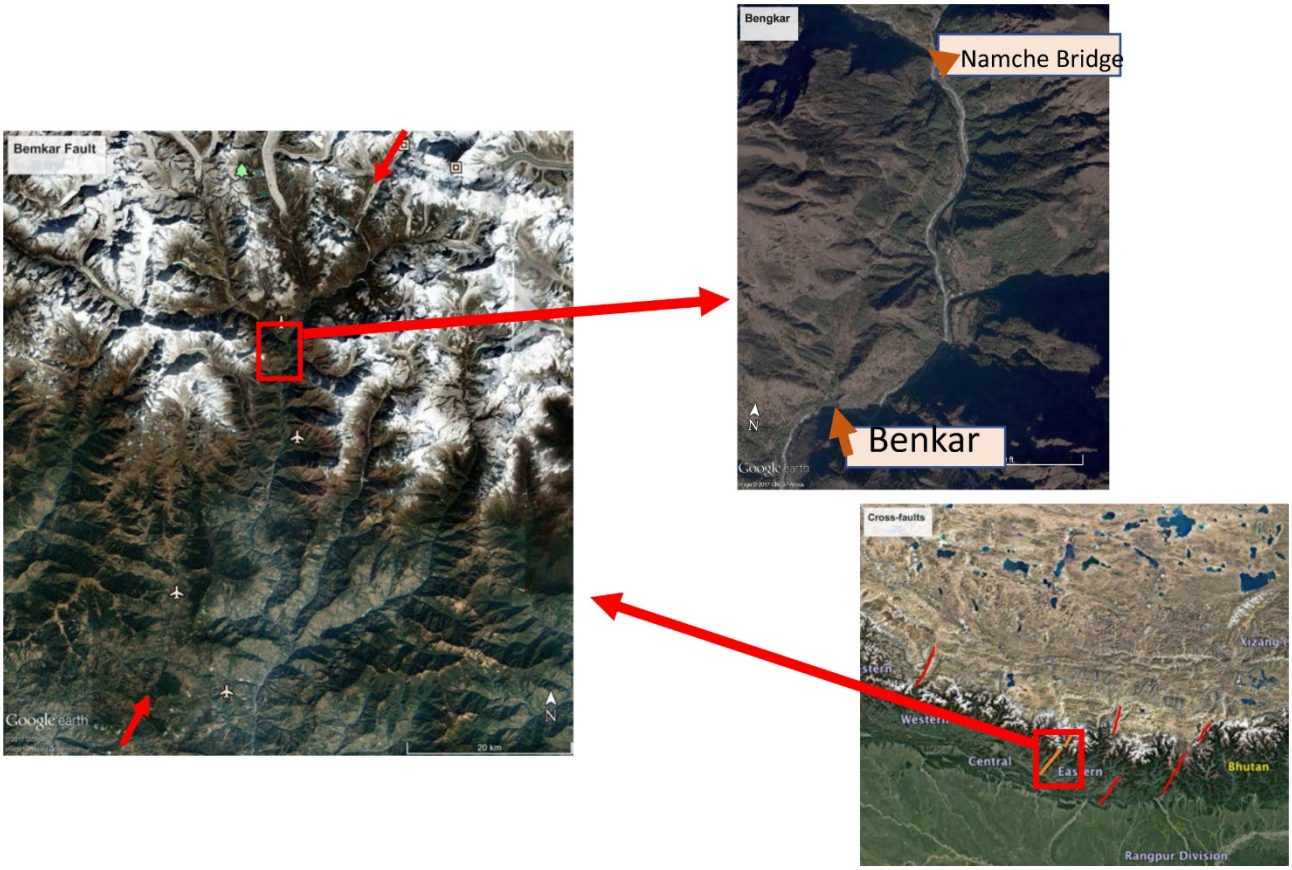

References

Langille JM, Jessup MJ, Cottle J, Ahmad T (2014) Kinematic and thermal studies of the Leo Pargil Dome: Implications for synconvergent extension in the NW Indian Himalaya. Tectonics 33: 1766-1786.

Mukul M, Jade S, Ansari K, Matin A, Joshi V (in press) Structural insights from Global Positioning System measurement in the Darjiling-Sikkim Himalaya. J Struct Geol.

Wu C, Nelson KD, Wortman G, Samson SD, Yue Y, Li J, Kidd WSF, Edwards MA (1998) Yadong cross structure and South Tibetan Detachment in the east central Himalaya (89°-90°E). Tectonics 17: 28-45.

Assessing provenance, exposure timing, and emplacement processes of large exotic boulders in central Himalayan river valleys

Huber M[1], Gallen S[2], Lupker M[1], Haghipour N[1], Christl M[1], Gajurel A[3]

[1]Geological Inst., Dept. of Earth Sciences, ETH Zurich, Switzerland [2]Colorado State Univ., Fort Collins, USA
[3]Dept. of Geology, Tribhuvan Univ., Kathmandu, Nepal

Tectonically active landscapes develop equilibrium and steady state topography by balancing rock uplift and erosion over long timescales (> 1 Myr) (e.g. Willett and Brandon 2002). On shorter timescales (≤ 10^5 yr) landscape evolution is characterized by phases of erosion and aggradation induced by changes in climatic forcing and threshold behaviour (e.g. Schumm 1979).

In central Himalayan river valleys, numerous large boulders (> 10 m in diameter) lie on or are contained within Quaternary river terraces, active floodplains or the modern river bed (Fig. 1). Their lithology frequently differs from the surrounding bedrock and reveals that they are derived from rock units outcropping > 10 km of kilometres upstream. The large boulders show evidence of fluvial rounding, crescentic percussion marks and are located 2000 m lower in elevation than the terminal moraines associated with the last glacial maximum (LGM) (e.g. Owen and Benn 2005). The exact transport mechanisms of such exceptionally large grain sizes remain unknown and may be linked to reoccurring catastrophic mass-wasting events. This study aims to constrain the timing and processes that lead to emplacement of these exotic boulders.

(1) The boulder size of 16 boulders was used to estimate paleo-discharges in two valleys of central Nepal (Trishuli and Sunkoshi) based on different literature fluid flow approaches (e.g. Alexander and Cooker 2016). These estimates indicate discharges in the order of 10^4 to 10^5 m^3/s are necessary to mobilize the surveyed boulders.

(2) ^{10}Be exposure ages of these boulders show ages up to 10.2-14.2 ka BP for two boulders in the Sunkoshi but also show clustering of emplacement at ca. 4.5-5.5 ka BP in both valleys (Fig. 1). Exposure dating implies a re-occurrence interval > 10^3 yrs for such large magnitude events.

The ages documented in this study were compared to dated glacial landforms, alluvial deposits and earthquake occurrence in central Himalaya (e.g. Abramowski et al. 2003, Pratt-Sitaula et al. 2004, Bollinger et al. 2014) as well as terrestrial climate records of the Indian monsoon influenced region (e.g. Wang et al. 2002, Sarkar et al. 2015). Correlation between boulder exposure ages, shift on monsoon governed climate regime, and glacial retreat suggests linkage of emplacement to mid-Holocene climate transition after an Early Holocene climate optimum (EHCO). We reason that the mid-Holocene weak monsoon induced wide-spread glacier retreat and may have led to high magnitude Glacial Lake Outburst floods (GLOFs) responsible for large scale boulder emplacement in central Himalayan river valleys. We therefore propose that large floods causing valley aggradation may occur during onsets of weak monsoon phases and may be linked to glacier dynamics.

Figure 1. Top left: Boulders lying on a tributary fan south of Devighat, Trishuli valley. The valley widens here substantially. Top right: Boulder appears sub-angular sitting on top of terrace deposit at Betrawati, Trishuli valley. In the background peaks rise >5000 m. Bottom left: Narrow part of Sunkoshi river after its confluence with Balephi Khola. Bottom right: Largest boulder surveyed in this study in Sunkoshi valley with a maximum diameter of 36 m and an estimated weight of 35'000 tons consists of gneiss lithology, minimum travel distance ~15 km. ^{10}Be surface exposure ages in ka BP. Coordinates of viewpoints given on each photo.

References

Abramowski U, Glaser B, Kharki K, Kubik P, Zech W (2003) Late Pleistocene and Holocene paleoglaciations of the Nepal Himalaya: 10Be surface exposure dating. Zeitschr f Gletscherkunde u Glazialgeologie 39: 183-196.

Alexander J, Cooker MJ (2016) Moving boulders in flash floods and estimating flow conditions using boulders in ancient deposits. Sedimentology 63: 1582-1595.

Bollinger L, Sapkota SN, Tapponnier P, Klinger Y, Rizza M, van Der Woerd J, Tiwari D, Pandey R, Bitri A, Bes de Berc S (2014) Estimating the return times of great Himalayan earthquakes in eastern Nepal: Evidence from the Patu and Bardibas strands of the Main Frontal Thrust. J Geophys Res 119: 7123-7163.

Owen LA, Benn DI (2005) Equilibrium-line altitudes of the Last Glacial Maximum for the Himalaya and Tibet: an assessment and evaluation of results. Quat Int 138: 55-78.

Pratt-Sitaula B, Burbank DW, Heimsath A, Ojha T (2004) Landscape disequilibrium on 1000-10'000 year scales Marsyandi River, Nepal, central Himalaya. Geomorphology 58: 223-241.

Sarkar S, Prasad S, Wilkes H, Riedel N, Stebich M, Basavaiah N, Sachse D (2015) Monsoon source shifts during the drying mid-Holocene: Biomarker isotope based evidence from the core "monsoon zone" (CMZ) of India. Quat Sci Rev 123: 144-157.

Schumm SA (1979) Geomorphic thresholds: the concept and its applications. Trans Inst Br Geogr 4: 485-515.
Wang R, Scarpitta S, Zhang S, Zheng M (2002) Later Pleistocene/Holocene climate conditions of Qinghai–Xizhang Plateau (Tibet) based on carbon and oxygen stable isotopes of Zabuye Lake sediments. Earth Planet Sci Lett 203: 461-477.
Willett SD, Brandon MT (2002) On steady states in mountain belts. Geology 30: 175-178.

Impact of mantle dynamics on Himalayan tectonics, morphology, climate, and biosphere

Husson L[1], Replumaz A[1], Webb A[2], van der Beek P[1], Condamine F[3], Mac Kenzie R[2], Sepulchre P[4]

[1]ISTerre, CNRS, Univ. Grenoble-Alpes, France [2]Earth Sci. Dept, Hong-Kong Univ., Hong-Kong [3]Geosciences Montpellier, CNRS, Univ. of Montpellier, France [4]LSCE, CNRS, Univ. Versailles, St. Quentin, France

Fast uplift and exhumation of the Himalaya and Tibet and fast subsidence in the foreland basin portray the primary Neogene evolution of the Indian-Eurasian collision zone. We relate these events to the relative northward drift of India over its own slab. Our mantle-flow model derived from seismic tomography shows that dynamic topography over the southward-folded Indian slab explains the modern location of the foreland depocenter. Back in time, our model suggests that the stretched Indian slab detached from the Indian plate during the indentation of the Eurasian plate and remained stationary underneath the northward-drifting Indian continent. We model the associated southward migration of the dynamic deflection of the topography and show that sediment-compensated dynamic subsidence has amounted to ~6000 m in the foreland basin since 15 Ma, while the dynamic surface uplift of the Himalaya amounted to ~1000 m during the early Miocene. These results indicate that mantle flow is a fundamental ingredient of Himalayan-Tibet dynamics, and invite to reconsider the canonical lithosphere-scale mechanisms for both the uplift history of the Himalaya and subsidence of its foreland basin. The impact of mantle dynamics can be tracked at various levels of the Himalayan orogeny. In the crust, it modifies the force balance and may activate or seal major fault activity. By setting the surface elevation, it alters the morphology and modifies surface processes. Last, dynamic uplift of the surface modifies the climate and biosphere.

Himalayan exhumation rates since 12 Ma from detrital apatite fission-track thermochronology, Middle Bengal Fan, IODP Expedition 354

Huyghe P[1], Bernet M[1], Galy A[2], Naylor M[3], Cruz J[4]

[1]ISTerre, Univ. Grenoble-Alpes, France [2]Univ. of Lorraine, Nancy, France [3]Univ. of Edinburgh, UK [4]Florida State Univ., USA

Apatite fission-track analysis of turbidites collected in the middle part of the Bengal Fan (IODP expedition 354) reveals the occurrence of a dominant age population (P1) with < 1 Myr lag-time since at least 12 Ma and indicating exhumation rates of up to 4 km/Myr. This major and persistent population shows that the exhumation is mainly controlled by the mid-crustal ramp geometry of the Main Himalayan Thrust which produces a high erosion zone above its rapidly exhumed hanging wall. The inferred constant exhumation rate is not affected by Late Miocene or Quaternary variations of the Indian Summer Monsoon at the broad Ganga and Brahmaputra catchment scale and on Ma time-scales.

Inverted metamorphic gradient in large-hot orogens: The case of the Main Central Thrust zone in the Alaknanda-Dhauli Ganga Valleys, Garhwal Himalaya, India

Iaccarino S[1], Montomoli C[2], Carosi R[1], Montemagni C[3], Massonne HJ[4], Jain A[5], Villa I[3], Visonà D[6]

[1]Univ. of Torino, Italy [2]Univ. of Pisa, Italy [3]Univ. of Milano-Bicocca, Italy [4]Univ. Stuttgart, Germany [5]IIT Roorkee, India [6]Univ. of Padova, Italy

In the Alaknanda-Dhauli Ganga valleys (Garhwal Himalaya, NW India) a complete and well-exposed structural section of the Himalayan belt is present (Jain et al. 2014) starting from the Lesser Himalayan Sequence (LHS), up to the Tethyan Himalayan Sequence. This portion of the belt is a classical area where sheared rocks of the Main Central Thrust zone (MCTz) between the LHC and the Greater Himalayan Sequence (GHS) have been mapped. Classically, the MCTz in this area is mapped as bounded by two discrete thrust-sense shear zones, the Vaikrita Thrust at the top and the Munsiari Thrust at the bottom. Moreover, despite this zone was characterized by geochemical, isotopical and geochronological data (e.g. Ahmad et al. 2000), structural, microstructural and petrofabric constraints (e.g. Valdiya 1980; Jain et al. 2014, Hunter et al. 2018; Hunter et al. in press) and petrologic estimates (Spencer et al. 2012; Thakur et al. 2015), there are still some open questions regarding, for instance, the MCT location and its structural evolution.

In this contribution a detailed meso- and micro-structural and petrological reappraisal along the MCTz transect is presented, focusing also on the distribution of index-minerals and the relationship between blastesis and deformation.

The metamorphic evolution of selected key-samples along the MCTz has been reconstructed after detailed electron microprobe work using multi-equilibrium geothermobarometry, P-T grids and equilibrium assemblage diagrams. U-(Th)-Pb in situ monazite geochronology allowed us to put an absolute temporal constraint both on the prograde metamorphic history and on the exhumation-related metamorphic overprint of the upper part of the MCTz. Particularly along the MCTz, a clear inverted metamorphic gradient (from ca. 500 up to ca. 700°C) is well constrained and also discernible by the distribution of Al-rich minerals (e.g. chloritoid, staurolite, kyanite) in sheared quartzites. Particularly, “peak” temperatures obtained by this work along the MCTz, are only partially in agreement with the (lower) T suggested by microstructural-based thermometry. These new P-T-D-t data, joined with the data available in the geological literature, shed new light on the tectono-metamorphic evolution of the Himalayan metamorphic core in this portion of the belt.

References

Ahmad T, Harris N, Bickle M, Chapman H, Bunbury J, Prince C (2000) Isotopic constraints on the structural relationships between the Lesser Himalayan Series and the High Himalayan Crystalline Series, Garhwal Himalaya. GSA Bull 112: 467-477.

Hunter NJR, Weinberg RF, Wilson CJL, Luzin V, Misra S (in press) Microscopic anatomy of a “hot-on-cold” shear zone: Insights from quartzites of the Main Central Thrust in the Alaknanda region (Garhwal Himalaya). GSA Bull.

Hunter NJR, Weinberg RF, Wilson CJL, Law RD (2018) A new technique for quantifying symmetry and opening angles in quartz c-axis pole figures: Implications for interpreting the kinematic and thermal properties of rocks. J Struct Geol 112: 1-6.

Jain AK, Shreshtha M, Seth P, Kanyal L, Carosi R, Montomoli C, Iaccarino S, Mukherjee PK (2014) The Higher Himalayan Crystallines, Alaknanda–Dhauli Ganga Valleys, Garhwal Himalaya, India. J Virtual Explorer 47: Paper 8.

Spencer CJ, Harris RA, Dorais JM (2012) The metamorphism and exhumation of the Himalayan metamorphic core, eastern Garhwal region, India. Tectonics 31: TC1007.

Thakur SS, Patel SC, Singh AK (2015) A P-T pseudosection modelling approach to understand metamorphic evolution of the Main Central Thrust Zone in the Alaknanda valley, NW Himalaya. Contribution Mineral Petrol 170: 1-26.

Valdiya KS (1980) Geology of the Kumaun Lesser Himalaya. Wadia Inst. of Himalayan Geology, Dehra Dun, India, 249p.

1.74 Ga crustal melting after rifting at the northern Indian margin: Investigation of mylonitic orthogneisses in the Kathmandu area, Central Nepal

Imayama T[1], Arita K[2], Fukuyama M[3], Yi K[4], Kawabata R[1]

[1]Okayama Univ. of Science, Japan [2]Hokkaido Univ., Japan [3]Akita Univ., Japan [4]Korea Basic Science Inst., Daejeon, R. of Korea

Mylonitic orthogneisses in the Kathmandu area, central Nepal have been investigated using whole-rock and mineral chemistry, Rb-Sr isotopes, and zircon U-Pb age dating. Zircon REE patterns determined from orthogneisses are characterized by enriched HREE patterns and the prominent Eu anomaly, indicating a magmatic origin. The U-Pb zircon age dating revealed that ca. 1.74 Ga felsic magmatism occurred in this area. Temperatures of 705-765°C were calculated using the Ti-in-zircon thermometer and are typical crustal melting temperatures for felsic magmatism. Whole-rock data from most orthogneisses in this and previous studies fall between the “syn-collisional” and “post-collisional” fields on the tectonic discrimination diagram, whereas a few orthogneisses represent rift-related magmatism. Very high Sr isotopic ratios (0.865-3.585) and high Th and U concentrations for all orthogneisses in this study represent components of old crust. These occurrences indicate that mylonitic orthogneisses are largely of crustal origins. This and previous studies are indicative of at least two Paleoproterozoic magmatic episodes: ca. 1.92-1.90 Ga rift-related magmatism and 1.84-1.74 Ga crustal melting. Considering the absence of a Paleoproterozoic collision in the Himalaya, the later crustal melting may have been accompanied by burial of the Indian basement during thermal subsidence after rifting, producing the high geothermal gradient in the middle crust. This study indicates that the two-stage Paleoproterozoic magmatism in Nepal occurred along the northern passive margin of the Indian basement during and/or after the breakup of the Columbia supercontinent.

Tourmaline and micas as petrogenetic minerals: Preliminary study from two-mica Mansehra Granite, KPK, Pakistan

Irum I[1,2], Altenberger U[1], Zeilinger G[1], Günter C[1], Ghani H[1,2]

[1]Inst. of Earth and Environmental Science, Univ. of Potsdam, Germany [2]Dept. of Earth and Environmental Sciences, Bahria Univ., Islamabad, Pakistan

The Mansehra Granite Complex (MGC) is exposed over a large area in the Lesser Himalayas of Pakistan. It is intruded into the Precambrian Tanawal Formation and is bounded to the east by the Himalayan western syntaxis and to the west by the Swat Metamorphic Complex. The focus of the study presented here is the chemistry of tourmaline and biotite and their association and significance as a petrogenetic indicator for the evolution of Mansehra Granitic Complex. Combined with observations of field relations and the analysis of the whole rock petrography, the Mansehra Granitic Complex is subject of a detailed structural and petrological investigation. The MGC has a mega-porphyritic texture on a large scale and is comprising micas and tourmalines with sufficient chemical variation for differentiating the magmatic phases. The phenocrysts size in some sections range from 0.5 to 9 mm. Both fine grained magmatic and high-temperature deformation textures, such as strong foliation, types are locally present. The granites are strongly peraluminous and tourmaline is associated with two types of mineral assemblages: 1) Quartz + K-feldspar + Plagioclase + Muscovite +Chlorite ± Biotite ± Garnet ± Andalusite, and 2) Quartz + Plagioclase + Muscovite ± Garnet ± Biotite. Biotite granite is the abundant variety in comparison to the tourmaline-rich granites. Those granites having the major amount of tourmaline have less or no biotite, and vice versa. The tourmaline in the Mansehra granites is typically of varying colour and composition, showing brownish, zoned and coarse grains or brown to bluish coloured and zoned grains. The tourmaline is of schorlitic composition and present in association with muscovite. Several factors control the stability of tourmaline in felsic magmas, like boron content of the melt, the amount of Al_2O_3, FeO, MnO, MgO, whole rock composition, temperature, oxygen fugacity, aH_2O and fluctuating environmental conditions. Biotite constitutes the important mafic mineral in Mansehra granites and ranges in size from fine to coarse grained. It shows prominent pleochroic halos in several sections and is altered to chlorite across and along the grain. These halos have subhedral to euhedral crystals of zircon and prismatic crystals of apatite in several sections. The saturation of biotite is dependent on the FeO, MgO, K_2O, and Al_2O_3 in granitic melt while its stability is related to the oxygen fugacity, temperature, and pressure conditions. The generation of compositional phase diagrams is ongoing work in order to determine the relationship between tourmaline and micas in the granitic rocks. So far, the petrography and mineral chemistry suggests distinct stability fields for tourmaline rich and biotite rich granites.

Three stages of cooling found in Mount Everest massif since 15 Ma based on thermochronologic studies and their implications

Iwano H[1], Danhara T[1], Takigami Y[2], Sakai H[3]

[1]Kyoto Fission-Track Co., Japan [2]Kanto Gakuen Univ., Yokohama, Japan [3]Kyoto Univ., Japan

Sakai et al. (2005) first reported the Yellow Band, top of the metamorphic rocks of Mount Everest massif, was rapidly cooled down at 14.7 Ma. To see how the inside had cooled down, we performed zircon and apatite fission-track (FT) and muscovite Ar/Ar analyses of the Higher Himalayan Crystallines (HHC) including leucogranite along the southern slope of Mount Everest, E. Nepal. Seventeen samples were collected from the metamorphosed Yellow Band under the Qomolangma Detachment (QD; 8,300 m a.s.l.) to the Main Central Thrust (MCT; 2000 m a.s.l.) near Jubing. Here we adopt a structural distance from QD or MCT for samples instead elevation. In the HHC between QD and MCT, we found three stages of cooling history based on the relationship between zircon and apatite FT ages. The first stage is a rapid cooling zone at the topmost (QD to ~1.5 km below) of HHC has a simultaneity of zircon and apatite FT ages (15~14 Ma) indicating a cooling rate of >> 100 °C/Myr. This is supported by unimodal distributions of confined-track length in zircon. The second one is a slow cooling zone (1.5 to 7 km below from QD) has a significant difference of FT ages up to 10 million years among the two minerals from the same rock sample. A cooling rate of 12 °C/Myr is given in this zone. The resulting broad and skewed track-length distributions in zircon support the slow cooling history. The third is a relatively fast cooling zone (40-50 °C/Myr) that corresponds to the lower half of HHC in which the 10 km-thick massif has constant zircon and apatite FT ages being 5-3 Ma and 1.5-0.8 Ma, respectively. All the above fission-track age and length data are reasonably explained only by a model that the Mount Everest massif had cooled perpendicular to the structures (QD and MCT), not along elevation. Especially, the cooling pattern of the third zone cannot be explained by uplift. In other words, the exhumation of Mount Everest massif had stopped at least earlier than 5 Ma. From interpolation between muscovite Ar/Ar ages and apatite FT ages, the closure temperature for the retention of fission tracks in zircon is estimated to be ~250°C at the cooling rate of 50 °C/Myr In this presentation, we will show temporal changes of cooling profile of HHC in the Mount Everest region since 15 Ma.

Reference

Sakai H, Sawada M, Takigami Y, Orihashi Y, Danhara T, Iwano H, Kuwahara Y, Dong Q, Cai H, Li J (2005) Geology of the summit limestone of Mount Qomolangma (Everest) and cooling history of the Yellow Band under the Qomolangma detachment. The Island Arc 14: 297-310.

Cryptic structures vs. channel flow: Yet another false dichotomy

Jamieson R[1], Beaumont C[2]

[1]Dept. of Earth Sciences, Dalhousie Univ., Halifax, Canada [2]Dept. of Oceanography, Dalhousie Univ., Halifax, Canada

Cryptic structures within the Greater Himalayan Sequence have received considerable attention recently (e.g. Cottle et al. 2015; Carosi et al. 2016; Goscombe et al. 2018). They are "cryptic" in the sense that discontinuities within this apparently continuous metamorphic sequence have been revealed from a range of structural and metamorphic criteria, including abrupt, foliation-parallel lithological changes and significant contrasts in pressure-temperature-time-deformation (P-T-t-D) histories over short distances.

Numerical models for the Himalayan-Tibetan system published more than a decade ago (e.g. Beaumont et al. 2001; Jamieson et al. 2006) predict that cryptic structures should have developed within the Greater Himalayan Sequence (GHS) and Main Central Thrust (MCT) zone during early thrusting and subsequent metamorphism and exhumation accompanying channel flow. In model HT111 (Jamieson et al. 2006), originally vertical “protolith” boundaries (Fig. 1a) become strongly attenuated, transposed, and imbricated during transport beneath the plateau and exhumation at the flank of the model orogen. These boundaries, which separate ductile thrust sheets formed during construction of the model orogen, survive burial, transport in the mid-crustal channel, and exhumation at the plateau flank (Fig. 1b, c). Because they are syn-metamorphic, and therefore affected by structural reworking and metamorphic overprinting, the natural equivalents of these boundaries may be difficult to detect from field observations alone. However, contrasting model P-T-t paths and peak metamorphic ages (broad loops, older ages at higher structural levels; tight hairpins, younger ages at lower structural levels) reflect the contrasting trajectories of the corresponding model materials through the orogen. During the later stages of model evolution, material emerging from beneath the plateau is juxtaposed with newly accreted material across a first-order discontinuity corresponding to the model "MCT" of Jamieson et al. (2004). However, equivalent discontinuities also form during the assembly of the model “GHS” as footwall material is accreted deep in the crust, forming finite-thickness ductile thrust sheets that are then transported through the model orogen. Basal accretion generally follows a normal in-sequence progression with older structures at the top, although some out-of-sequence thrusts may be generated during exhumation. The accumulation of these accreted sheets and their bounding cryptic structures, in combination with their differential transport in response to velocity gradients within the orogen, contributes to the tectonic assembly of the GHS and the inverted metamorphic sequence characteristic of the MCT zone.

The question of whether the presence of cryptic structures is or is not compatible with channel flow represents a false dichotomy, reminiscent of the “channel vs. wedge” debate of a few years ago (e.g. Beaumont and Jamieson 2010). The model results demonstrate that cryptic structures are entirely compatible with channel flow and are a predictable consequence of the way metamorphic sequences in crustal-scale ductile thrust zones, including the GHS, are constructed.

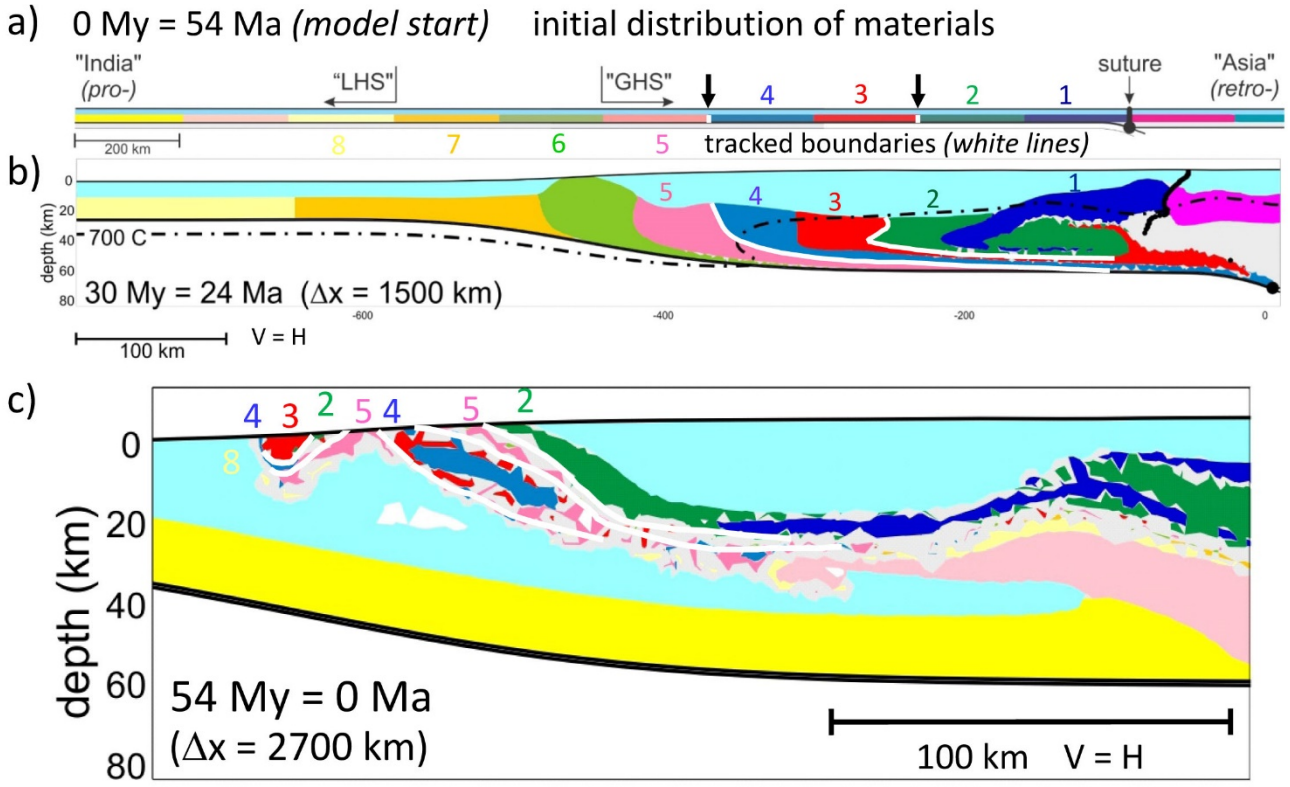

Figure 1. Development of cryptic structures in model HT111 (after Jamieson et al., 2006). a) Initial distribution of materials. Coloured blocks with identical material properties, separated by vertical markers, are used to track model "protolith" materials and boundaries through the orogen. b) Model orogen after 30 Myr of convergence, showing early deformation of originally vertical boundaries. c) Model orogen after 54 Myr of convergence, showing tracked materials and boundaries as they appear at the model surface following channel flow and exhumation. Numbers correspond to coloured blocks; white lines show boundaries.

References

Beaumont C, Jamieson RA (2010) Himalaya-Tibetan orogeny: Channel flow versus (critical) wedge models, a false dichotomy? Abstracts, HKT Workshop, San Francisco, USGS Open File Report 2010-1099.

Beaumont C, Jamieson RA, Nguyen MH, Lee B (2001) Himalayan tectonics explained by extrusion of a low-viscosity crustal channel coupled to focused surface denudation. Nature 414: 738-742.

Carosi R, Montomoli C, Iaccarino S, Massonne HJ, Rubatto D, Langone A, Gemignani L, Visonà D (2016) Middle to late Eocene exhumation of the Greater Himalayan Sequence in the Central Himalayas: Progressive accretion from the Indian plate. GSA Bull 128: 1571-1592.

Cottle JM, Larson KP, Kellett DA (2015) How does the mid-crust accommodate deformation in large, hot collisional orogens? A review of recent research in the Himalayan orogen. J Struct Geol 78: 119-133.

Goscombe B, Gray D, Foster DA (2018) Metamorphic response to collision in the Central Himalayan Orogen. Gondwana Res 57: 191-265.

Jamieson RA, Beaumont C, Medvedev S, Nguyen MH (2004) Crustal channel flows: 2. Numerical models with implications for metamorphism in the Himalayan-Tibetan orogen. J Geophys Res 109: B06407.

Jamieson RA, Beaumont C, Nguyen MH, Grujic D (2006) Provenance of the Greater Himalayan Sequence and associated rocks: Predictions of channel flow models. Geol Soc London Spec Publ 268: 165-182.

Multispectral and geomorphological detection and field validation of lithologies relevant to glacier dynamics in High Mountain Asia

Kargel J[1], Haritashya U[2], Karki A[3], Furfaro R[4], Shugar D[5], Regmi D[6], Watson S[4]

[1]Planetary Science Inst., Tucson, USA [2]Univ. of Dayton, USA [3]Nepal Electricity Authority, Kathmandu, Nepal [4]Univ. Arizona, Tucson, USA [5]Univ. Washington Tacoma, USA [6]The Himalayan Research Expeditions Pvt. Ltd., Kathmandu, Nepal

Bedrock lithological differences in the Everest-Lhotse area (Nepal) and the Aru Mountains (Tibet) are mappable by satellite multispectral reflectance analysis. These mountain bedrock units are also expressed on the surfaces of glaciers draining from them (supraglacial debris; also, mud expressed from glacier beds through ice avalanches). Glacier dynamics involving lake formation, glacier thinning, calving in the Everest area, and ice avalanches in the Aru Mountains appear to be connected to particular lithologies. We will present examples to show how rock units can be mapped via satellite and connected to geologic map data and glacier processes. The mapping approaches we are developing support studies of glacier and landslide dynamics, aiming to discover how rock lithologies relate to particular processes and to the characteristics of glaciers, ice avalanches, and landslides. Our methodology involves analysis of ASTER and Landsat 8 OLI multiband spectra, in some cases one or the other, in other cases a composite.

In a companion abstract (this volume), Karki and Kargel offer a working hypothesis that variability in lithology and contrasts of mechanical properties of rocks and minerals in a landslide have large influences on the landslide processes during runout and in the characteristics of landslide deposits, such as whether river-impacting landslides can form a transient or long-term metastable dam or cannot readily form a dam at all. Kääb et al. (2018) recently used remote sensing to detect unusual lithological compositions (for glacierized mountains) of rocks at two Tibetan glaciers that underwent catastrophic detachment on low-angle slopes.

The lithologies of major bedrock units of bedrock in the Mount Everest-Lhotse area are readily mapped by satellite multispectral reflectance analysis. These mountain bedrock units are also expressed on the surfaces of glaciers draining from them (supraglacial debris and mud expressed from glacier beds through glacier ice avalanches), and furthermore, some glacier dynamics involving lake formation, thinning, and calving appear to be connected to particular lithologies.

The colours of supraglacial debris connect back to the lithologies exposed on the mountains (Fig. 1). Mass wasting from the mountain sides deposits debris on the glacier surface, which then flows toward the terminus. As the glacier descends to lower elevations, melting takes place. Some evidence supports a role of particular types of debris in facilitating the initiation and growth of supraglacial ponds. The physical link might involve differences in albedo or thermal conductivity (hence, effects on ice melting related to the surface thermal boundary conditions of debris laden zones and the thermal structure of the debris layer); or different rock debris particle shapes and sizes (hence, propensity to plug englacial conduits and affect water retention and drainage).

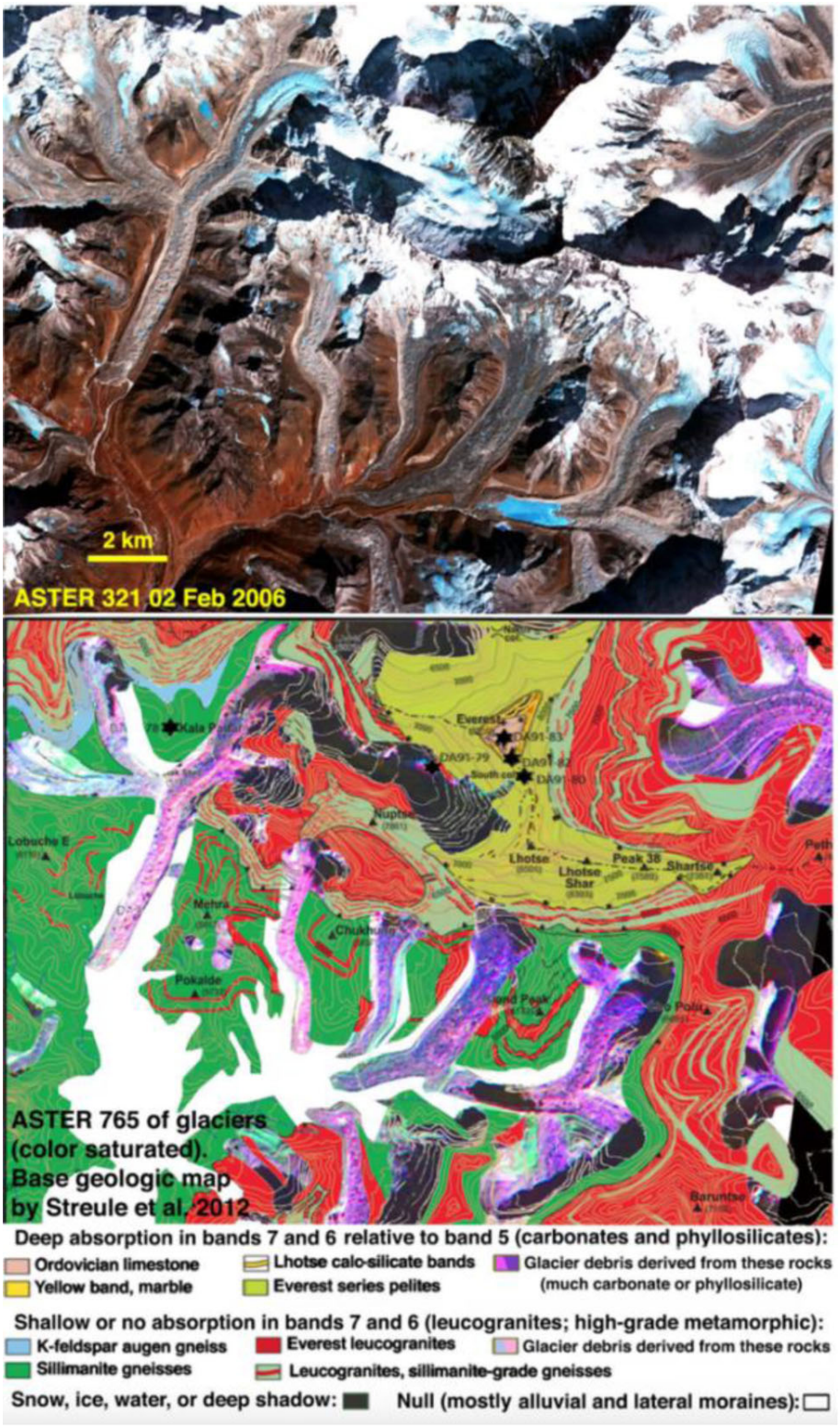

Figure 1. Top: ASTER VNIR bands 3-2-1 image near Everest, colour and contrast stretched. Bottom: Clip of glaciers in this ASTER scene, rendered as a partially colour-saturated RGB from SWIR bands 7, 6, and 5, overlain of a geologic map. White areas are null: mainly alluvial deposits and moraines. Debris-covered glaciers show as hues of purple, magenta, and cyan, depending on lithology.

Reference

Kääb A et al. (2018) Massive collapse of two glaciers in western Tibet in 2016 after surge-like instability. Nat Geosci 11: 114-120.

Geological and lithological controls on landslides relevant to Nepal's hydroelectric power: The case of the Jure landslide

Karki A[1], Kargel J[2]

[1]Nepal Electricity Authority, Kathmandu, Nepal [2]Planetary Science Inst., Tucson, USA

Impacts of landslides and ice avalanches directly into dams, reservoirs, power plants, pipelines, transmission lines, highways, bridges, and villages, and river blockages, upstream inundation, and downstream outburst floods pose threats to the region's mountain dwellers and economic development. In Nepal, the Himalaya provide one of the most world's foremost regions of high hydroelectric power potential but also is an actively uplifting mountain belt with a severe suite of natural mountain hazards, including earthquakes, landslides, debris flows, ice and snow avalanches, and glacier lake outburst floods. On August 2nd, 2014, 25 km SSW of the border village of Kodari, the Jure landslide occurred. 5.05 Mm^3 of rock collapsed and killed 156 people, destroyed 115 houses, buried a stretch of the Araniko Highway (Khanal and Gurung, 2014), and dammed the Bhotekoshi (river), making a lake, which lasted 12 hours before natural breaching, by which time it exceeded 2 km length (Acharya et al. 2016) and ~55 m depth. The lake inundated the Sanima hydroelectric power station and affected seven power plants, taking 65 MW of power offline (http://sanimahydro.com.np/sanimahydro/?url=project&id=22). The landslide scar plus deposit is > 1260 m long, > 500 m wide, and has 800 m of elevation loss.

The initiation and development of the Jure landslide offers insights into landslide conditioning and triggers. Landslide-controlling roles of slope, seismicity, river undercutting, rainfall, freeze-thaw, and forest cutting, and burning are well known. Lithology dependent mechanical properties of bedrock also constitute important controls on landslides and avalanches but are less commonly considered in landslide susceptibility assessments. Lithologic properties, bedding, and structural joints and faults control shear planes, groundwater movement, weathering, and weakening of bedrock; and the production, permeability, and creep of soils related to oversaturation, wetting-drying, and freeze-thaw. We hypothesize that the variation of lithology-dependent geotechnical properties is one key to landslide/avalanche susceptibility, the growth of landslides to large volumes, and the effectiveness of landslides to dam rivers (Fig. 1). We have undertaken field and laboratory investigations of rock mechanical properties – following Budathoki (2016) – and the geologic structure and topography of the Jure landslide, Nepal (Bhote Koshi Valley) to initiate a test of this hypothesis. Geologically, the landslide lies in the Kuncha Formation of the Nawakot Group (Budathoki 2016). Major landslide materials are phyllite, mica schist, and metasandstone, and minor graphitic schist, quartz veins, and metabasic-lava of the Kuncha formation. Water flow through discontinuities and major cracks have caused long-term degradation of rock bridges and widening of joints. The Jure landslide deposit, where observed, is boulder- and cobble-supported with large pore spaces filled by sand and pebble matrix. Such a deposit structure was a key to the transient damming by this landslide. In our preliminary assessment (Fig. 1), the landslide's space-filling sedimentological structure and its wide variations of particle grain sizes, lithological compositions, and geotechnical properties of rocks are all interrelated.

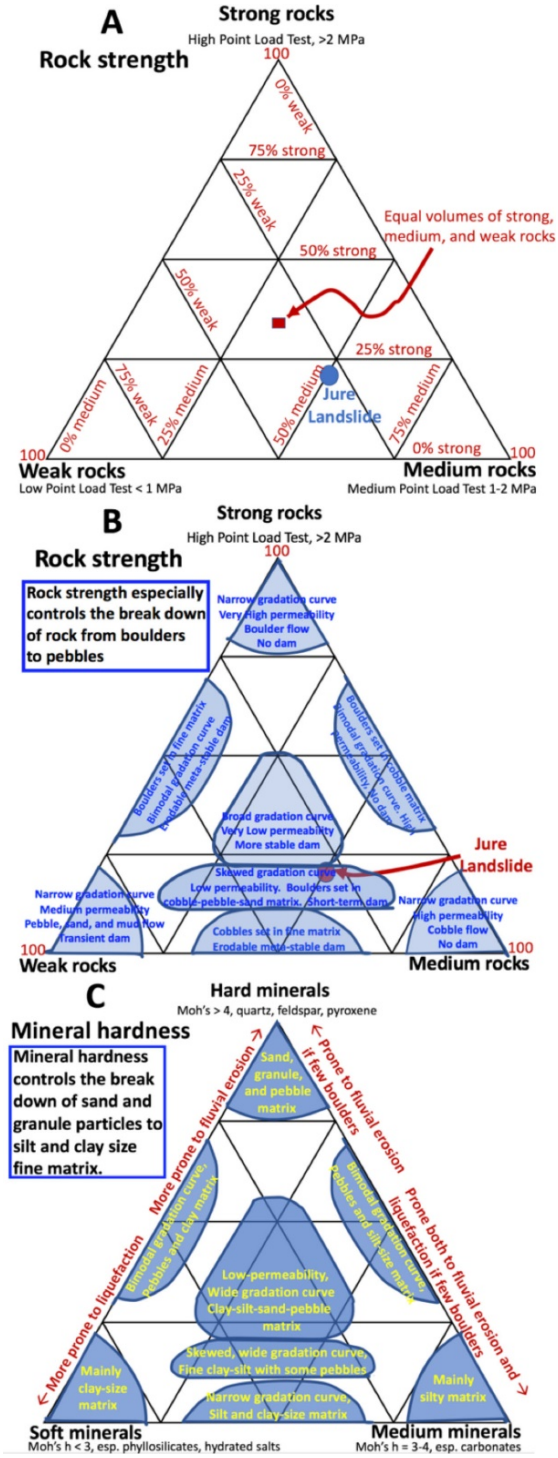

Figure 1. Working hypothesis: Rock strength controls landslide breakdown of rocks from boulders to pebbles (A and B); and mineral hardness controls the breakdown of fine matrix material (C).

References

Acharya TD, Mainali SC, Yang IT, Lee DH (2016) Analysis of Jure landslide dam, Sindhupalchowk using GIS and remote sensing. International Archives of the Photogrammetry, Remote Sensing and Spatial Information Sciences, Vol. XLI-B6, XXIII ISPRS Congress, 12-19 July 2016, Prague.

Budathoki R (2016) Cause and Mechanism of 2014 Jure Rock Avalanche in Sindhupalchowk District, Central Nepal. MSc thesis, Dept. of Geology, Tribhuvan Univ.

Khanal RR, Gurung DR (2014) ICIMOD Rapid Field Investigation of the Jure Landslide Site, Jure, Sinhupalchowk District, Nepal. Online resource, www.icimod.org/resource/14483, last accessed 24 May 2018.

Paleogene evolution of the proto-Paratethys Sea in Central Asia, Tarim Basin, western China: Driving mechanisms and paleoenvironmental consequences

Kaya M[1], Dupont-Nivet G[1,2,3], Proust JN[2], Roperch P[2,3], Bougeois L[4], Meijer N[1], Frieling J[5], Fioroni C[6], Özkan Altıner S[7], Vardar E[7], Stoica M[8], Mamtimin M[9], Zhaojie G[3]

[1]Inst. of Earth and Environmental Science, Univ. of Potsdam, Germany [2]Geosciences Rennes, CNRS, Univ. of Rennes, France [3]Key Laboratory of Orogenic Belts and Crustal Evolution, Peking Univ., Beijing, China [4]Rectorat de l'Académie de Montpellier, Ministère de l'Éducation Nationale, France [5]Dept. of Earth Sciences, Utrecht Univ., The Netherlands [6]Univ. Modena e Reggio Emilia, Italy [7]Dept. of Geological Engineering, Middle East Technical Univ., Ankara, Turkey [8]Dept. of Geology, Faculty of Geology and Geophysics, Univ. of Bucharest, Romania

Climate modelling and proxy studies suggest that Cenozoic Asian climate has been governed by the combination of Asian monsoons driven by Tibetan Plateau uplift and global climate and westerly moisture modulated by fluctuations of the proto-Paratethys Sea. As part of the ERC MAGIC project, we focus on the evolution of the proto-Paratethys Sea which covered a vast area extending from the Mediterranean Tethys to the Tarim Basin in western China during Cretaceous and Paleogene times before it retreated westward and isolated into the Paratethys Sea. Transgressive and regressive episodes of the proto-Paratethys Sea have been previously recognized but their timing, extent, and depositional environments remain poorly constrained, especially for the early Paleogene. This hampers understanding of their driving mechanisms (tectonic and/or eustatic) and their contribution to Asian environmental changes. Here we present a new chronostratigraphic framework based on biostratigraphy and magnetostratigraphy, and a detailed paleoenvironmental analysis for the proto-Paratethys sea incursions in the southwestern Tarim Basin during the Paleogene. A major regional restriction event marked by the exceptionally thick shelf evaporites of the Aertashi Formation is assigned a Danian-Selandian age (~63 Ma and ~59 Ma). This is followed by a marine incursion with a transgression estimated as early Thanetian (~59 Ma) and a regression within the Ypresian (~52-53 Ma) in the Qimugen Formation. The next incursion as its transgression in the Kalatar Formation is now constrained as early Lutetian (~47-46 Ma), complementing previous work that identified its regression at 41 Ma and the last sea incursion in the Bartonian (38-37 Ma). We find most sea-level fluctuations (3rd order) are coeval with regional tectonic events – the onset India-Asia collision (59-52 Ma) and the Indian slab break off (47-41 Ma) – suggesting far-field tectonic effects on the intra-cratonic basin. The transgressive/regressive cycles are also time-equivalent with the reported humid and arid phases in Central Asia, thus strengthening the role of proto-Paratethys as an important moisture source for the Asian interior.

Geodynamical models of the lithospheric-scale evolution of the Hindu Kush and Pamir and implications for the Himalayan-Tibetan orogen

Kelly S[1], Beaumont C[2], Butler J[3]

[1]Dept. of Earth Sciences, Dalhousie Univ., Halifax, Canada [2]Dept. of Oceanography, Dalhousie Univ., Halifax, Canada [3]Geological Survey of Newfoundland and Labrador, Canada

Like many collisional orogens, the Himalayan-Tibetan (H-T) orogen, including the Pamir and Hindu Kush, contains exotic terranes (e.g. Songpan Garze, Qiangtang, Lhasa and lateral equivalents) accreted to Asia prior to terminal continent-continent collision with India. However, the ways in which the properties of these terranes precondition the ensuing style of collisional orogeny in this and other orogens remain poorly understood. Building on results from Kelly et al. (2016) and Li et al. (2016), we use 2D thermomechanical finite element models to examine in particular how the style of collision changes in response to variations in the strength and the lithospheric mantle density of these accreted terranes, as well as the density of the pro-lithospheric mantle, which determines its propensity to subduct or compress the accreted terranes and retro-lithosphere.

We start by considering models that are consistent with the evolution of the Hindu Kush and Pamir because the current state of lithospheric-scale cross sections through these regions is reasonably well documented. For the Pamir, models evolve self-consistently through several emergent phases, namely: 1) Oceanic subduction; 2) Subduction and breakoff of the Greater India rifted margin; 3) Indentation/advancing subduction by India causing shortening of the accreted Asian terranes; 4) Shortening of the crust and delamination of the weakest terrane mantle lithosphere (Pamir); 5) Subduction of Indian mantle lithosphere, and; 6) Crustal shortening of the Alai and Tien Shan terranes and partial delamination of the Alai mantle lithosphere leaving a south dipping mantle slab, as observed beneath the Pamir. We attribute the contrasting geodynamics of the Hindu Kush mainly to thinner Indian crust which makes Indian lithosphere subduction easier and results in the opposite subduction polarity, as observed beneath the Hindu Kush. The models also display “convective” removal of mantle lithosphere through entrainment by the subducting Indian mantle lithosphere.

We can translate what we have learned from Pamir models eastward to address the coeval evolution of the western and central H-T orogen and we will discuss models that satisfy its tectonic and magmatic evolution.

The modelled variations in the properties of the accreted terranes’ lithospheric mantle can be interpreted to reflect metasomatism/hydration during earlier oceanic subduction beneath the terranes prior to or during accretion. Strongly metasomatized/hydrated (i.e. dense and weak) mantle is easily removed thereby facilitating later flat-slab underthrusting. By implication, the evolution of the H-T system is strongly conditioned by the properties of the lithospheric mantle of the previously accreted terranes. In particular, crustal deformation in these models is often strongly coupled to shortening/removal of lithospheric mantle which may account for the apparently enigmatic behaviour in which the Tibetan orogen develops in steps (e.g. early Qiangtang deformation), each focussed in a particular terrane and reflecting strength contrasts among the terranes.

References

Kelly S, Butler JP, Beaumont C (2016) Continental collision with a sandwiched accreted terrane: Insights into Himalayan–Tibetan lithospheric mantle tectonics? Earth Planet Sci Lett 455: 176-195.

Li ZH, Liu M, Gerya T (2016) Lithosphere delamination in continental collisional orogens: A systematic numerical study. J Geophys Res 121: 5186-5211.

Seismotectonics of NE Afghanistan

Kufner SK[1], Kakar N[2,3], Schurr B[1], Yuan X[1], Metzger S[1], Shamal S[3]

[1]GFZ Potsdam, Germany [2]Norwegian Afghanistan Committee [3]Kabul Univ., Afghanistan

The Pamir-Hindu Kush region of Tajikistan and NE Afghanistan stands out due to its worldwide unique zone of intense intermediate depth seismicity, accommodating frequent Mw 7+ earthquakes with hypocentres reaching down to 250 km depth. Here, we present seismological data allowing to characterize the active deformation within the Pamir-Hindu Kush mountains and the Tajik-Afghan basin at the northwestern tip of the India-Asia collision zone.

Contradicting the plate tectonic paradigm, intermediate depth seismicity within the Pamir-Hindu Kush region occurs far away from any (paleo-)oceanic basin and continental lithosphere appears to subduct by itself in a north-south compressional regime, imposed by the northward advancing Indian continent. Since 2008, we operated different temporary seismic deployments within this remote region which allowed us to postulate Asian subduction beneath the Pamir and oppositely oriented Indian subduction and ongoing break-off beneath the Hindu Kush. Due to sparse station coverage in Afghanistan it was so far not possible to resolve the lateral termination of this break-off, nor its connection to the crustal structures and seismicity on top.

Starting in autumn 2017, we set up a 15-sites covering seismic network in NE Afghanistan within a joint project of GFZ Potsdam and the Norwegian Afghanistan Committee. The network is situated on top of the nest of intermediate depth seismicity and further west in the Afghan platform. The stations are equipped with short period Mark seismometers and Cube data recorders. The current temporary network is planned to operate until January 2019. Here, we show preliminary results on ongoing seismic deformation, derived from data recorded by these stations together with results on crustal seismicity in the Tajik basin from our earlier deployments. The obtained hypocentre distribution suggests a spatial correlation between the sub-crustal termination of the subducting slab and the region of most pronounced crustal seismicity.

Mapping the crustal architecture by surface wave and ambient noise tomography in the Himalaya-Karakoram-Tibet region

Kumar N[1], Babu V[1], Verma S[1], Hazarika D[1], Yadav D[1]

[1]Wadia Inst. of Himalayan Geology, Dehradun, India

Surface wave data is used to investigate the sub-surface lithosphere structure beneath the western part of Himalaya-Tibet collision zone including Karakoram fault. We extracted group velocities for the period range of 6 to 60 s of fundamental mode of Rayleigh and Love wave using Frequency Time Analysis (FTAN) technique (Herrmann 2013). Data of shallow focused (depth < 50 km) over 300 earthquakes of M > 4.0 is used of 40 broadband seismographs. Variable trends of dispersion curves are observed in different directions of the study region and the 2D tomography group velocity maps are obtained at 1º grid separation using inversion technique (Yanovskaya and Ditmar 1990). Observed period range has high spatial variation of velocity, lower period has very low velocity for the paths passing through the sedimentary strata such as the Indo-Gangetic plains. In the intermediate period (25-40 s) the paths passing through the India-Tibet collision and Tibetan plateau also has low velocity compared to other parts. It clearly indicates partial melting and partly fluid filled zones in the middle and lower crust. Local dispersion curves are extracted from 2D tomographic maps at 1° grid spacing which are inverted to construct 1D shear wave velocity at each node using non-linear inversion technique (Herrmann 2013). Different profiles aligned to N-S direction, NW-SE perpendicular to the major tectonic features and along the strike of the Karakoram fault are taken to formulate the shear wave velocity structure. The inverted shear wave velocity for the upper part of the lithosphere indicates variable depth of the Moho discontinuity, ~40 km beneath the Indo-Gangetic plains towards south that increases to 75-80 km on the boundary of India-Eurasia plates. The similar observations are for the part of Tibetan plate (Wittlinger et al. 2004).

We also performed ambient noise tomography for the NW Himalaya region using data of 31 broadband seismic stations. The ray paths sample the Himalayan region, the south Tibetan detachment zone and the Indo-Tsangpo suture zone. The spatial regional difference for group velocities are mapped for the periods in the range 4-40 s for Rayleigh and Love waves. The 2D tomography maps of fundamental mode has larger variations depicted for the Rayleigh waves rather mainly for the paths passing close to India-Tibet tectonic boundary. This study based on latest data gives new detail of sub-surface structural setup of the western part of Himalaya highlighting a low velocity mid-crustal layer characterized by an absence of lower crustal seismicity below decollement plane. A clear discontinuity within the physical properties mimics a possible decollement plane that could transfer sizeable earthquakes. Specifically, a minimum value of Rayleigh wave velocity close to the decollement zone is reported and may likely correspond to mineral anisotropy while its existence to the lower part can be due to partial melting as per previous finding.

References

Herrmann RB (2013) Computer programs in seismology: An evolving tool for instruction and research. Seismol Res Lett 84: 1081-1088.

Rapine R, Tilmann F, West M, Ni J, Rodgers A (2003) Crustal structure of northern and southern Tibet from surface wave dispersion analysis. J Geophys Res 108: 2120.

Wittlinger G, Vergne J, Tapponnier P et al. (2004) Teleseismic imaging of subducting lithosphere and Moho offsets beneath western Tibet. Earth Planet Sci Lett 221: 117-130.

Yanovskaya TB, Ditmar PG (1990) Smoothness criteria in surface-wave tomography. Geophys J Int 102: 63-72.

Tectonic evolution of the Yarlung Suture Zone: Subduction controlled crustal deformation

Laskowski A[1]

[1]*Dept. of Earth Sciences, Montana State Univ., USA*

Geologic records of Tibetan mountain building along the Yarlung suture zone are essential for understanding the processes that created the Tibetan Plateau. I present results from field mapping, structural analysis, and geo/thermochronology applied to three field areas: the Lopu Range in southwestern Tibet, the Lazi region in south-central Tibet, and the Dazhuka region in southeastern Tibet. This research provides a semi-continuous record of Neo-Tethyan subduction and India-Asia collision from Jurassic to recent time. The data primarily address the following questions: 1) What was the structure of the Asian margin prior to collision? 2) When did India-Asia collision initiate? 3) What happened to the suture zone after collision? 4) What is going on along the suture zone today? U-Pb geochronologic data and field relationships suggest that subduction initiated along the suture zone during Middle Jurassic to Early Cretaceous time and was followed by Early Cretaceous forearc extension during emplacement of the Yarlung suture zone ophiolites. Basal forearc strata in the Lopu Range have a maximum depositional age of 97 ± 1 Ma and were deposited atop the Yarlung suture zone ophiolites. Detrital zircon data from metasedimentary rocks structurally below and south of Bainang terrane subduction-accretion mélange indicate mixed, Indian and Asian provenance at ~62 Ma, supporting early Paleocene onset of India-Asia collision. The youngest Gangdese arc granitoids intruded subduction-accretion mélange between 49-37 Ma, interpreted as recording southward subduction zone migration after collision initiation. Crosscutting relationships, U-Pb geochronologic data, and zircon (U-Th)/He thermochronologic data indicate that the south-dipping Great Counter thrust system deformed suture zone assemblages between 23 and 16 Ma. Zircon (U-Th)/He data and a U-Pb age of a crosscutting dike indicate that E-W extension initiated by 16 Ma in the Lopu Range region. Based on interpretation of compiled thermochronologic data and regional structural geology, we hypothesize that ongoing contraction is actively uplifting the Gangdese Range, fuelling N-S striking rifts that are localized to the Gangdese Range between the Lopu Range and Lazi regions. Geologic constraints from this research were integrated with geophysics and regional tectonic data to construct a lithospheric-scale kinematic model. The temporal correlation between changes in upper-plate deformation and changes in subduction behaviour suggest that subduction processes controlled deformation along the Yarlung suture zone.

Giant landslide deposits and the modalities of their removal by fluvial sediment export in the central Himalayas

Lavé J[1], Benedetti L[2], Valla P[3], Guérin C[4], France-Lanord C[1]

[1]CRPG, CNRS, Univ. of Lorraine, Nancy, France [2]CEREGE, Aix-Marseille Univ, Aix en Provence, France
[3]Inst. of Geological Sciences, Univ. of Bern, Switzerland [4]CEA, France

Slope failures and deep seated landslides are usually considered as the most efficient processes for hillslope erosion in active orogens. Erosion in the Narayani basin in central Himalaya (Nepal) confirms such assertion, with in addition the probable predominance of the very large landslides in the erosive budget of the range. In the High Himalayan part of this basin, a number of pluri-kilometric giant landslides have been described and involve up to ten cubic kilometres mass wasting (e.g. Weidinger et al. 2002).

In this contribution, we discuss how the fluvial network does respond to such massive and sudden supply of debris. We base our analysis on several cases, documented by sedimentologic and geomorphologic observations, lithologic counting, geochemical tracing (down to the Ganga plain), and ^{14}C, CRN or IRSL dating.

Three types of deposits and therefore of sediment export modalities have been identified: (1) in case of coarse debris deposit, long term stability of the dam inducing filling of the upstream lake followed by upstream sediment by-pass and slow re-incision of the massive dam; (2) catastrophic dam failure followed by massive debris flow(s) runout, leading to massive terraces building over tens of kilometres; or (3) gradual but very efficient fluvial removal of the landslide deposits. The third case occurs when bedrock fracturing and crushing during landslide fall has strongly reduced the average debris size, as observed in a giant landslide in the Annapurnas range. In that case, because the steep Himalayan rivers are usually in strong over capacity or largely underloaded with fine to medium-size sediment, there can evacuate up to several cubic kilometres of landslide deposits in one or two centuries. The coarsest part of the exported material is temporarily stored through aggradation in the massive Lesser Himalayan fill terraces because river gradient drops suddenly when river exits the High Himalaya, whereas the finest fraction is exported very rapidly further downstream, outside of the range. Once a large portion of the landslide debris has been eroded in the source deposit, river quickly returns to over-capacity conditions and to its long term or background conditions, and fill terraces are rapidly re-incised (re-erosion of the fill terrace occurs at rates incommensurate with long term bedrock downcutting rate).

The two most important results of the presented Himalayan examples indicate first that erosion of giant landslides deposits can overwhelm the sediment export of a river as large as the Narayani (A = 30’000 km^2; average sediment export = 150 Mt/yr) during several centuries, and secondly that numerous massive fill terraces preserved along the Lesser Himalayan intramontane reaches are not climatically induced, but rather represent transient storage following giant landslide material export.

^{10}Be - Sr - Nd applied on Bengal fan Expedition 353-354: A record of Late Cenozoic Himalayan erosion

Lenard S[1], Lavé J[1], France-Lanord C[1]

[1]CRPG, CNRS, Univ. of Lorraine, Nancy, France

Global records of erosion have led to conjecture that the Quaternary climatic transition was linked to an acceleration of erosion on Earth (Zhang et al. 2001, Herman et al. 2013). However, the reality of this increase of the erosion rates remains debated (e.g. Willenbring and von Blanckenburg 2010). In order to implement the debate at the scale of a major orogen, we have applied to the Himalaya a distinct approach, which is not affected by the same possible bias than for previously developed methods.

We present a new record of Himalayan erosion from IODP drilled cores in the Bengal fan. The fan mainly consists of sand-rich turbidites that originate from sediments eroded in the Himalaya and transported by the Ganga and the Brahmaputra since at least 20 Ma onwards. IODP Expeditions 353 and 354 (Clemens et al. 2016, France-Lanord et al. 2016) recently drilled 1 site at 14°N and a transect of seven sites at 8°N in the fan. These cores were dated by magnetostratigraphy and biostratigraphy.

The provenance of Plio-Pleistocene sediments was traced using $^{87}Sr/^{86}Sr$ and $^{143}Nd/^{144}Nd$ ratios from bulk silicates. Contrasted isotopic signatures characterize the Himalayan formations and the Transhimalaya, which results in distinct compositions for modern Ganga and Brahmaputra river sediments. Sr and Nd isotopic ratios range from 0.72 to 0.76 and from -17 to -13. They imply significant variations in the provenance mixture between Himalayan and Transhimalayan formations since 6 Ma. In particular, we notice a higher proportion of Transhimalayan provenance for the last 0.2 Ma.

Past erosion rates (mean values over timescales of ~1 kyr) were traced using in-situ cosmogenic ^{10}Be paleo-concentrations in the quartz of the sandy 75-250 µm fraction (e.g. Charreau et al. 2011). ^{10}Be paleo-concentrations vary in a range similar to the concentrations measured on the Brahmaputra and Ganga modern sands (Lupker et al. 2012; 2017). Although paleo-concentrations appear rather variable before 2 Ma and steadier afterwards, the time-averaged signal is relatively constant over the whole Plio-Pleistocene period and highlights a steadiness of the Himalayan erosion rates. Even if dominant sources of sediments seem to fluctuate in the Brahmaputra-Ganga watershed, our dataset suggests that the Himalayan erosion may not have been sensitive to climate cooling at the Quaternary transition, and that its erosion patterns may be mainly controlled by regional tectonics.

References

Charreau J, Blard PH, Puchol N, Avouac JP, Lallier-Vergès E, Bourlès D, Braucher R, Gallaud A, Finkel R, Jolivet M, Chen Y, Roy P (2011) Paleo-erosion rates in Central Asia since 9 Ma: A transient increase at the onset of Quaternary glaciations? Earth Planet Sci Lett 304: 85-92.

Clemens SC, Kuhnt W, LeVay LJ, Anand P, Ando T, Bartol M, Bolton CT, Ding X, Gariboldi K, Giosan L (2016) Expedition 353 summary. Proceedings of the IODP 353: 1-32.

France-Lanord C, Spiess V, Klaus A, Schwenk T (2016) The Expedition 354 Scientists. Expedition 354 summary. Proceedings of the IODP 354: 1-35.

Herman F, Seward D, Valla PG, Carter A, Kohn B, Willett SD, Ehlers TA (2013) Worldwide acceleration of mountain erosion under a cooling climate. Nature 504: 423-426.

Lupker M, Blard PH, Lavé J, France-Lanord C, Leanni L, Puchol N, Charreau J, Bourlès D (2012) 10Be-derived Himalayan denudation rates and sediment budgets in the Ganga basin. Earth Planet Sci Lett 333-334: 146-156.

Lupker M, Lavé J, France-Lanord C, Christl M, Bourlès D, Carcaillet J, Maden C, Wieler R, Rahman M, Bezbaruah D, Xiaohan L (2017) 10Be systematics in the Tsangpo-Brahmaputra catchment: the cosmogenic nuclide legacy of the eastern Himalayan syntaxis. Earth Surf Dyn 5: 429-449.

Willenbring JK, von Blanckenburg F (2010) Long-term stability of global erosion rates and weathering during late-Cenozoic cooling. Nature 465: 211-214.

Zhang PZ, Molnar P, Downs WR (2001) Increased sedimentation rates and grain sizes 2–4 Myr ago due to the influence of climate change on erosion rates. Nature 410: 891-897.

^{10}Be - Sr - Nd erosion patterns in the Narayani watershed, Central Nepal, viewed through the Valmiki Siwalik section

Lenard S[1], Lavé J[1], Charreau J[1], France-Lanord C[1], Gajurel A[2], Kaushal R[3], Pik R[1]

[1]CRPG, CNRS, Univ. of Lorraine, Nancy, France [2]Dept. of Geology, Tribhuvan Univ., Kathmandu, Nepal [3]IIT Gandhinagar, India

Climate variability and glacial extension may have led to a global increase of erosion rates at the Quaternary transition (Zhang et al. 2001). This potential increase may have impacted mountain building and also climate through feedback effects. However, the existence of strengthened erosion during the Quaternary is debated, particularly for the Himalaya. While the high relief of the range drives monsoonal precipitations that produce a major erosional flux on Earth (Milliman and Syvitski 1992), the existing records yield contrasting results. Addressing the question of Quaternary accelerated erosion both requires the application of new approaches and investigation of new archives.

Here, we present a new Siwalik record. The sections are located in the central Himalaya, South of Chitwan Dun, where local rivers have entrenched the Himalayan sediments exhumed by the uplifting Siwalik fold. The sections expose sediments of a paleo-fan that we assume to have been fed by the Narayani-Gandak river, one of the major Transhimalayan rivers. The studied sections present a cumulated thickness of ~4000 m and consist in almost continuous sandy to fine fractions of sedimentary rocks. The depositional ages were constrained by a magnetostratigraphy analysis and range from ca. 8 Ma to < 0.8 Ma.

To determine the paleo-erosion, we quantified the in-situ ^{10}Be cosmogenic nuclide concentrations in the 125-250 µm quartz fraction of the sedimentary rocks (e.g. Charreau et al. 2011). By measuring ^{36}Cl in feldspar, we checked that the contribution of recent exposure to ^{10}Be concentration was minor. We computed paleo-concentrations, which range from 5000 to 40’000 at/g and average 10’000 at/g.

We then analysed the provenance stability and potential recycling with Sr-Nd isotopes and major elements respectively. Major elements show a transition at ca. 1 Ma, with SiO_2 increasing from 75 to > 85% and Na/Al decreasing from 20% to < 10%. Na depletion in young sediments reflects an increase of weathering and may be indicative of a transition from direct deposition of sediments from the Himalaya to recycling of proximal sources, i.e. from Siwalik fold denudation.

The εNd and ^{87}Sr/^{86}Sr isotopic signatures of the sediments range from -19.5 and -17.5, and from 0.75 to 0.78 respectively. These signatures are similar to modern Narayani-Gandak sands (-19 and 0.75 on average respectively). They are interpreted as resulting from a rather steady mix of Himalayan formations, with 50 to 90% High Himalayan contributions.

Based on these results we assumed the cosmogenic production rates during the past were similar to the present value across the Narayani watershed at least until 1 Ma. The derived paleo-erosion rates of the Narayani watershed range from 0.5 to 4 mm/yr, around an average of 1.8 mm/yr. This corresponds to an average time scale of 1 kyr. The average paleo-erosion rate is similar to modern values (Lupker et al. 2012). However, the paleo-concentrations and the paleo-erosion rates display significant dispersion, with large (+100%) fluctuations of at high frequency (< 0.3 Ma). This dispersion could highlight the naturally stochastic character of erosion even for a large watershed in a range apparently dominated by tectonic processes.

References

Charreau J, Blard PH, Puchol N, Avouac JP, Lallier-Vergès E, Bourlès D, Braucher R, Gallaud A, Finkel R, Jolivet M, Chen Y, Roy P (2011) Paleo-erosion rates in Central Asia since 9 Ma: A transient increase at the onset of Quaternary glaciations? Earth Planet Sci Lett 304: 85-92.

Lupker M, Blard PH, Lavé J, France-Lanord C, Leanni L, Puchol N, Charreau J, Bourlès D (2012) 10Be-derived Himalayan denudation rates and sediment budgets in the Ganga basin. Earth Planet Sci Lett 333-334: 146-156.

Milliman JD, Syvitski JPM (1992) Geomorphic/Tectonic Control of Sediment Discharge to the Ocean: The Importance of Small Mountainous Rivers. J Geol 100: 525-544.

Zhang PZ, Molnar P, Downs WR (2001) Increased sedimentation rates and grain sizes 2–4 Myr ago due to the influence of climate change on erosion rates. Nature 410: 891-897.

A 3500-yr-long paleoseismic record for the Himalayan Main Frontal Thrust, Western Bhutan

Le Roux-Mallouf R[1], Ferry M[2], Ritz JF[2], Cattin R[2], Drukpa D[3], Pelgay P[3]

[1]Géolithe Co., Crolles, France [2]Geosciences Montpellier, Univ. of Montpellier, France [3]Dept. of Geology and Mines, Thimphu, Bhutan

The unusually large displacements of several meters associated with great Himalayan earthquakes point out the limits of classical trenching studies that do not allow the characterization of a long rupture history and may only document one or two events during the last millennium. Here, we present geomorphologic and paleoseismic studies conducted over a large river-cut exposure along the Main Himalayan Front in south-western Bhutan near the village of Piping (Fig. 1). This site reveals an important cumulative deformation of almost 30 m characterized by a well-developed uplifted terrace system associated with a pluri-decametric fault-propagation fold (Fig. 2). Paleoseismic excavation along with 16 radiocarbon ages chrono-stratigraphic modelling reveal the occurrence of at least six major and great earthquakes between 1070 ± 270 BC and 1714 A.D. with an average recurrence interval of 550 ± 300 yr. The slip-per-event analysis based on these new findings does not suggest a constant magnitude but rather a bimodal distribution, which includes (1) great earthquakes with decametric vertical offsets and (2) relatively smaller ones with metric vertical offsets.

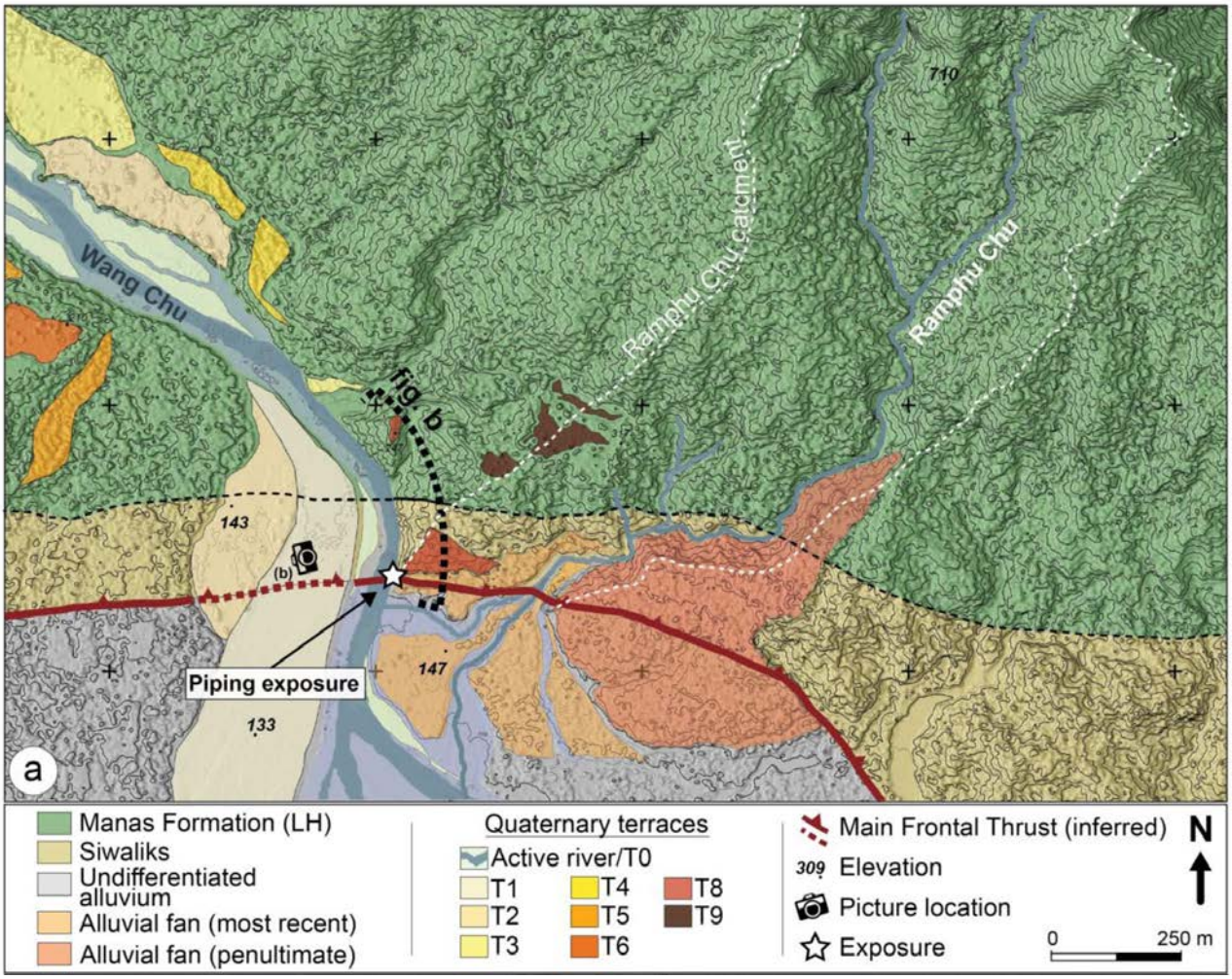

Figure 1. Geomorphological map of the Main Frontal Thrust, in the Piping area, superimposed on 2-m-resolution Pleiades-derived Digital Elevation Model (DEM). Alluvial terraces are labeled from T0 (active channel) to T9 (oldest). The camera pictogram indicates the location of the panorama in Figure 2. Star indicates the location of the Piping exposure. Spacing of elevation contours is 20 m. Black dots indicate spot elevations extracted from the Pleiades DEM.

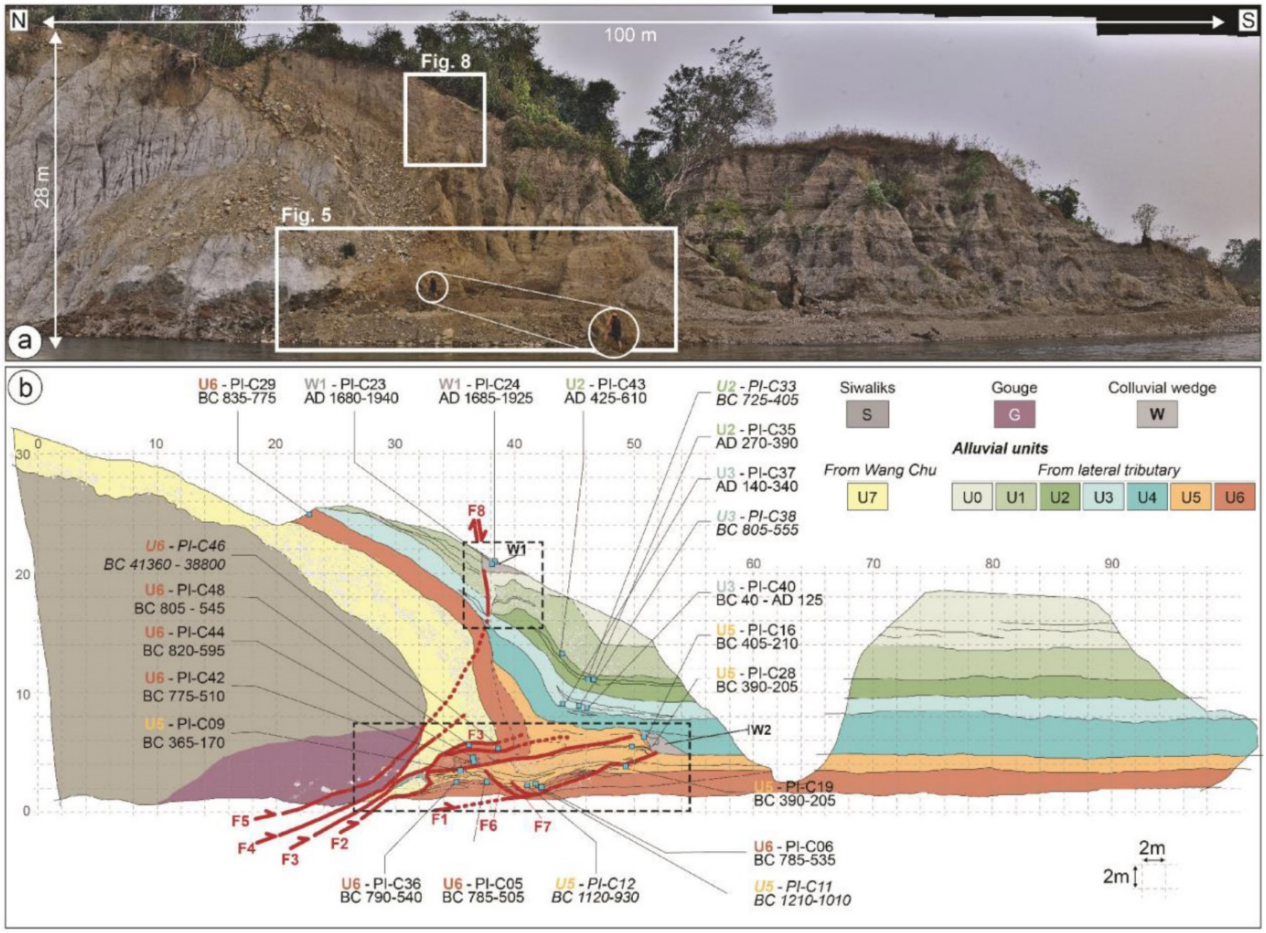

Figure 2. Piping paleoseismic exposure. (A) Orthorectified photomosaic of the left-bank of the Wang Chu (southernmost section of Fig. 2b) showing the contact between the Siwalik units (light grey) and Rampu Chu fan deposits (well-stratified beige to grey units). White rectangles indicate the locations of a normal-geometry fault (N.F.) and the figure of the lower part (L.P.). (B) Detailed log over a 2-m grid. Solid and dashed red lines are main faults (certain and suspected, respectively). Blue squares indicate the locations and 2σ-calibrated calendar ages of 22 detrital charcoal samples.

Source parameters and seismogenic structure of the 2017 Mw 6.5 Mainling earthquake in Tibet, China

Li W[1], Xu C[1], Yi L[1], Wen Y[1], Zhang X[2]

[1]Wuhan Univ., China [2]China Earthquake Administration, China

On November 18th, 2017, a moderate to strong earthquake occurred at Mainling County, Nyingchi City, Tibet, which was the first moderate earthquake in the Eastern Himalayan Syntaxis (EHS) region in the past five decades. To gain a better understanding of the rupture mechanism and seismogenic structure of this earthquake, the rupture process through a joint inversion of far-field body wave data and Interferometric Synthetic Aperture Radar (InSAR) data was present in this study. In addition, the three-dimensional (3D) crustal density structure of the EHS area was inverted using the gravity data. According to the joint inversion results of the rupture process, the Mainling earthquake lasted approximately 18 s and released energy of 8.32×10^{18} N m (Mw 6.5). The rupture was dominated by the thrust movement. The maximum slip was approximately 0.83 m, and the slip distribution was mainly concentrated at depths of 5 to 15 km. According to the results of gravity inversion, the density structure has good constraints on the source depth. The Mainling earthquake's epicentre was located near the junction of high and low density areas. The rupture extended over nearly 40 km in the ESE direction along the fault strike. In addition, the density structure also clearly shows a uniform density anomaly in the region, which may be beneficial to the release of seismic energy. The clockwise deformation of the erosion effect in the EHS superimposed over the uplifting and thrusting motion of the Namche Barwa (NB) area, and the Northward Indentation effect of the Indian block. All of these processes have strengthened folding deformation and the accumulated of stress and an abnormally high-density concentration within the NB area. The sudden release of accumulated stress led to the occurrence of the Mainling earthquake. These are the seismogenic structure of the NB zone. The regional structure and material characteristics indicates that the Dongjiu segment of the Dongjiu-Mainling Shear Zones (DMSZ) lies in the density anomaly gradient belt, with high density, low velocity, and high resistance media on its northeastern side, which benefits the stress accumulation. The earthquake activity and risks of this segment merits further attention.

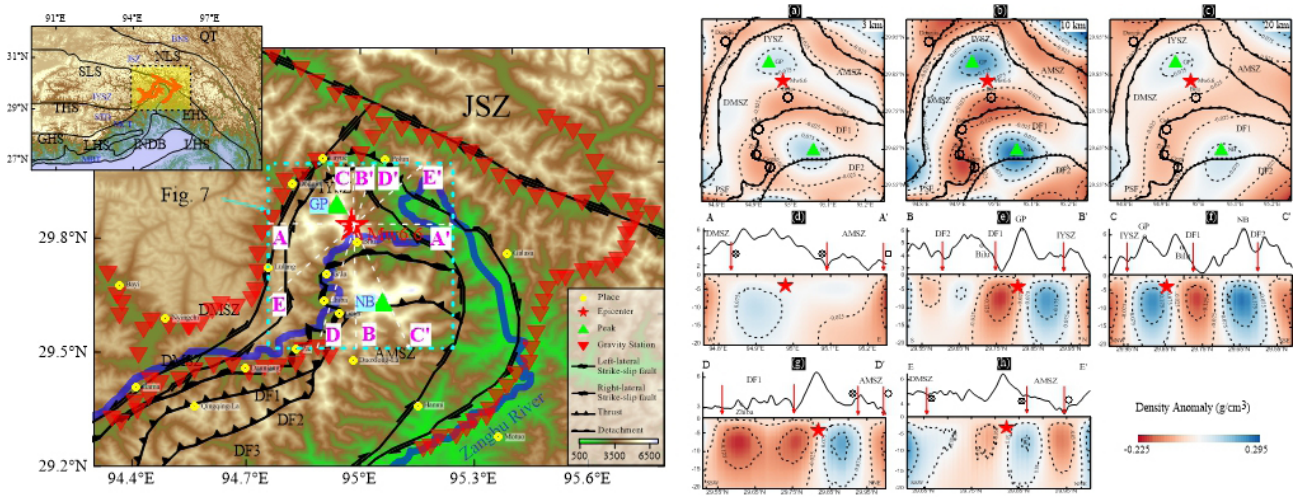

Graphical abstract.

Provenance of Thal Desert sands, Central Pakistan

Liang W[1], Andò S[1], Clift P[2], Garzanti E[1], Limonta M[1], Resentini A[1], Vermeesch P[3], Vezzoli G[1]

[1]Dept. of Earth and Environmental Sciences, Univ. of Milano-Bicocca, Italy [2]Dept. of Geology and Geophysics, Louisiana State Univ., Baton Rouge, USA [3]London Geochronology Centre, Dept. of Earth Sciences, Univ. College London, UK

The Thal Desert, a triangular dune field located in northern Pakistan and delimited by the Indus River in the west, the Jhelum River in the east, and the Salt Range foothills in the north, stores crucial information useful to unravel the recent evolution of the Indus River system and the erosional history of the western Himalayan syntaxis. Provenance of Thal Desert sand has been determined by a multi-technique approach based on high-resolution petrographic and heavy-mineral analyses, bulk-sediment geochemical and Nd isotope data, U-Pb age-spectra of zircon grains, integrated with Raman spectroscopy and SEM data on single detrital minerals including amphiboles, pyroxenes, and garnets. Thal Desert sands are litho-feldspatho-quartzose to quartzo-feldspatho-lithic, and contain up to very-high-rank metamorphic rock fragments (MI 253 ± 33) and very rich heavy-mineral assemblages (tHMC 12 ± 2) dominated by amphibole associated with epidote, garnet, clino- and orthopyroxene. Thal Desert sand compares closely petrographically, mineralogically, and geochemically with modern Indus River sand. Sediment sources were thus located chiefly within and around the western Himalayan syntaxis (Garzanti et al. 2005), and included the Kohistan Arc, the Karakorum and Hindukush ranges, whereas Himalayan sources were limited because contribution from the Jhelum and other Punjab rivers was minor, if any. The abundance of feldspars (Q/F ratio is 1.1 ± 0.1) and amphibole in dune sands indicates contributions from igneous and meta-igneous gabbroic to granitoid rocks. εNd displays moderately negative values with significant variability (εNd -9.1 ± 4.1) indicating major contributions from both Karakorum and Kohistan arc sources. These signatures are much less negative than those of Pleistocene Indus Delta (εNd -13.2 ± 1.0; Clift et al. 2010) and Indus Fan (εNd -13.3 ± 1.0; Clift et al. 2001), which chiefly reflects much higher Himalayan contribution via the Punjab rivers. The Thal dune field thus represents a repository of Pleistocene paleo-Indus sediments at a time when erosion was even more focused than at present on the glaciated high mountains of the western syntaxis, where granitoid rocks and mafic arc crust were actively eroded in Transhimalayan tectonic domains.

References

Clift PD, Shimizu N, Layne GD, Blusztajn JS, Gaedicke C, Schluter HU, Clark MK, Amjad S (2001) Development of the Indus Fan and its significance for the erosional history of the Western Himalaya and Karakoram. GSA Bull 113: 1039-1051.

Clift PD, Giosan L, Carter A, Garzanti E, Galy V, Tabrez AR, Pringle M, Campbell IH, France-Lanord C, Blusztajn J, Allen C, Alizai A, Lückge A, Danish M, Rabbani MM (2010) Monsoon control over erosion patterns in the Western Himalaya: possible feed-backs into the tectonic evolution. In: Clift PD, Tada R, Zheng H (Eds.) Monsoon evolution and tectonic-climate linkage in Asia. Geol Soc London Spec Publ 342: 185-218.

Garzanti E, Vezzoli G, Ando S, Paparella P, Clift PD (2005) Petrology of Indus River sands: a key to interpret erosion history of the Western Himalayan Syntaxis. Earth Planet Sci Lett 229: 287-302.

Cenozoic evolution of the Burmese subduction margin and implications for the history of India-Asia convergence

Licht A[1], Dupont-Nivet G[2], Win Z[3], Kaythi M[4], Swe H[4], Roperch P[2], Ugrai T[1], Littell V[1], Park D[1], Westerweel J[2], Jones D[1], Poblete F[2], Wa Aung D[4], Huang H[5], Hoorn C[5], Sein K[6]

[1]Univ. of Washington, Seattle, USA [2]Geosciences Rennes, Univ. of Rennes, France [3]Dept. of Geology, Univ. of Shwebo, Myanmar [4]Geology Dept., Univ. of Yangon, Myanmar, [5]Univ. of Amsterdam, The Netherlands [6]Myanmar Geosciences Society, Yangon, Myanmar

The geological history of the Burmese subduction margin, where India obliquely subducts below Indochina, remains poorly documented although it is key to deciphering geodynamic models for the evolution of the broader Tibetan-Himalayan orogen. Various scenarios have been proposed, including an ephemeral collision of India with Myanmar in the Paleogene, a significant extrusion of Myanmar and Indochina from the India-Asia collision zone, or very little change in paleogeography and subduction regime since the India-Asia collision. This talk proposes an overview of the Cenozoic history of the Burmese subduction margin based on new and unreleased data from the Myanmar Paleoclimate and Geodynamics Research Group (MyaPGR), including sedimentological, geochemical, petrographical, and geochronological data from the forearc basin and volcanic arc of central Myanmar.

Our results show that the Burmese margin acted as a regular Andean-type subduction margin until the late Middle Eocene, with a forearc basin open to the trench and fed by the denudation of the Andean volcanic arc. We show that the modern tectonic configuration of central Myanmar was formed 39-37 million years ago, when the Burmese margin shifted from an Andean-type margin to a hyper-oblique margin. The forearc basin was quickly partitioned into individual pull-apart basins, bounded to the west by a quickly emerged accretionary prism, and to the east by synchronously exhumed basement rocks including coeval high grade metamorphics. We interpret this shift as resulting from the onset of strike-slip deformation on the subduction margin leading to the formation of a paleo-sliver plate, with a paleo fault system in the accretionary prism, pull apart basins in the forearc, and another paleo fault system in the backarc. This evolution implies that hyper-oblique convergence below the Burmese margin is at least twice older – and therefore much more important – than previously thought. Our results reject any India-Asia convergence scenario involving an early Paleogene collision of India with Myanmar. They rather validate conservative geodynamic models arguing for a close-to-modern precollisional paleogeography for the Indochina Peninsula, and indicate that any postcollisional rotation of Indochina, if existed, must have been achieved by the late Middle Eocene.

Contact metamorphism of the Upper Mustang massif, west-central Nepal

Lihter I[1], Larson K[1], Shrestha S[1], Cottle J[2]

[1]Earth, Environmental and Geographic Sciences, Univ. of British Columbia, Okanagan, Canada [2]Dept. of Earth Science, Univ. of California, Santa Barbara, USA

The Upper Mustang “massif” is a little investigated exposure of garnet ± staurolite bearing schists and leucogranitic plutonic body. It crops out within the Tethyan sedimentary sequence in the restricted-access Upper Mustang region of west-central Nepal. A single reconnaissance study reported that these metamorphic rocks may be part of a domal culmination that exposes exhumed, former midcrustal rocks of the Greater Himalayan sequence. Potentially similar culminations are found along the North Himalayan antiform in along-strike regions of southern Tibet.

New field observations within the Upper Mustang “massif” identify intrusion of the pluton into the surrounding metasedimentary rocks and a gradual decrease in apparent metamorphic grade with distance away from the plutonic body. Preliminary P-T phase diagrams indicate metamorphic conditions ranging between 550-650°C and 3.5-7.5 kbar. New U/Th-Pb geochronology of monazite in igneous and metamorphic specimens outlines overlapping ^{232}Th-^{208}Pb weighted mean ages. Monazite from three leucogranite specimens analysed yields last crystallization ages of 1) 20.5-22.5 Ma, and 2) with dominant population ranging between 19.5 and 23.0 Ma and 3) between 20.0 and 23.0 Ma. These compare with ages from the surrounding schists with dominant populations of each specimen between 19.0-23.0 Ma, 18.0-22.0 Ma and 19.0-24.0 Ma.

In contrast to previous interpretations that suggested the Upper Mustang “massif” reflected regional metamorphism, new field and laboratory data presented herein are consistent with metamorphism in the “massif” reflecting contact metamorphism similar to that observed in the Bura Buri granite in the neighbouring Dolpo region. If correlative with the Bura Buri, then the emplacement of the Upper Mustang granite may also provide a constraint on the final movement across the STDS in this region.

Structural and temporal insights into the South Tibetan Detachment System shear zone in Dinggye area, Central Himalaya: Implications for the evolution from crustal thickening to ductile extrusion of the mid-crust during the Himalayan orogeny

Liu SR[1,2], Zhang JJ[1], Wang JM[3], Ling YY[1]

[1]Key Laboratory of Orogenic Belts and Crustal Evolution, School of Earth and Space Sciences, Peking Univ., Beijing, China [2]Geosciences Montpellier, Univ. of Montpellier, France [2]State Key Laboratory of Lithospheric Evolution, Inst. of Geology and Geophysics, Chinese Academy of Sciences, Beijing, China

The South Tibetan Detachment System (STDS) is a critical extensional system linking deformation, magmatism and metamorphism in the evolution of the Himalayan orogen (Burchfiel 1992). Previous studies revealed a two-stage deformation history of the STDS (Jessup et al. 2016; Kohn 2014; Larson and Cottle 2015; Searle 2013; Yin 2006; Yu et al. 2015; Zhang et al. 2012). In order to elucidate the rheological and magmatic processes of the STDS, we performed integrated methods using field observations, geochronology, geothermometry and electron backscattered diffraction (EBSD) measurements to investigate the entire deformation history of the South Tibetan Detachment System (STDS) in Dinggye area. We observed the STDS shear zone tilted by a number of north-south trending grabens related to the North-South Trending Rift (NSTR). The shear zone directly beneath the detachment (STDS) consists of deformed metasedimentary rocks intruded by mylonitic leucogranite sills, undeformed leucogranites and pegmatites at the top; mylonitic leucogranites in the middle and deformed augen orthogneiss at the bottom. Based on our studies, the STDS shear zone has experienced a protracted deformation history with continuous magmatism. The crustal thickening and early partial melting (D1) is from Oligocene to early Miocene (ca. 32-21 Ma) in mid-high temperature (ca. 525-600°C) with top-down-to-the-south shear sense and quartz X-maxima c-axis fabrics preserved in augen orthogneiss. The regional extension and extrusion of the GHC rocks in mid-crust (D2) in mid-high temperature (ca. 425-525°C) lasted to Middle Miocene (ca. 15 Ma) before the NSTR became active and tilted the STDS shear zone in upper crust. The top-down-to-the-NNE shear sense and quartz c-axis fabrics varying from crossed girdles to Y-maxima are preserved in upper part of the shear zone. Our findings complement the evolution of the STDS and are important towards a better understanding the role of the extensional structures in the collisional orogens.

References

Burchfiel BC, Chen Z, Hodges KV, Liu Y, Royden LH, Deng C, Xu J (1992) The South Tibetan Detachment System, Himalayan Orogen: Extension Contemporaneous With and Parallel to Shortening in a Collisional Mountain Belt. GSA Spec Paper 269.

Jessup MJ, Langille JM, Cottle JM, Ahmad T (2016) Crustal thickening, Barrovian metamorphism, and exhumation of mid-crustal rocks during doming and extrusion: Insights from the Himalaya, NW India. Tectonics 35: 160-186.

Kohn MJ (2014) Himalayan Metamorphism and Its Tectonic Implications. Annual Review Earth and Planetary Science 42: 381-419.

Larson KP, Cottle JM (2015) Initiation of crustal shortening in the Himalaya. Terra Nova 27: 169-174.

Searle M (2013) Crustal melting, ductile flow, and deformation in mountain belts: Cause and effect relationships. Lithosphere 5: 547-554.

Yin A (2006) Cenozoic tectonic evolution of the Himalayan orogen as constrained by along-strike variation of structural geometry, exhumation history, and foreland sedimentation. Earth-Sci Rev 76: 1-131.

Yu HJ, Webb AAG, He D (2015) Extrusion vs. duplexing models of Himalayan mountain building 1: Discovery of the Pabbar thrust confirms duplex-dominated growth of the northwestern Indian Himalaya since Mid-Miocene. Tectonics 34: 313-333.

Zhang JJ, Santosh M, Wang XX, Guo L, Yang XY, Zhang B (2012) Tectonics of the northern Himalaya since the India-Asia collision. Gondwana Res 21: 939-960.

^{10}Be systematics in the Tsangpo-Brahmaputra catchment: The cosmogenic nuclide legacy of the eastern Himalayan syntaxis

Lupker M[1], Lavé J[2], France-Lanord C[2], Christl M[1], Bourlès D[3], Carcaillet J[4], Maden C[1], Wieler R[1], Rahman M[5], Bezbaruah D[6], Xiaohan L[7]

[1]Geological Inst., Dept. of Earth Sciences, ETH Zurich, Switzerland [2]CRPG, CNRS, Univ. of Lorraine, Nancy, France [3]CEREGE, Aix-Marseille Univ, Aix en Provence, France [4]ISTerre, Univ. Grenoble-Alpes, France [5]Dhaka Univ., Bangladesh [6]Dibrugarh Univ., India [7]Chinese Academy of Sciences, China

We report on a ^{10}Be data-set from the Tsangpo-Brahmaputra basin in the eastern Himalaya (Lupker et al. 2017). The Tsangpo-Brahmaputra River drains the eastern part of the Himalayan range and flows from the Tibetan Plateau through the eastern Himalayan syntaxis downstream to the Indo-Gangetic floodplain and the Bay of Bengal. As such, it is a unique natural laboratory to study how denudation and sediment production processes are transferred to river detrital signals. In this study, we present a new ^{10}Be data set to constrain denudation rates across the catchment and to quantify the impact of rapid erosion within the syntaxis region on cosmogenic nuclide budgets and signals. The measured ^{10}Be denudation rates span around 2 orders of magnitude across individual catchments (ranging from 0.03 to > 4 mm/yr) and sharply increase as the Tsangpo-Brahmaputra flows across the eastern Himalaya. The increase in denudation rates, however, occurs ~150 km downstream of the Namche Barwa–Gyala Peri massif (NBGPm), an area which has been previously characterized by extremely high erosion and exhumation rates. We suggest that this downstream lag is mainly due to the physical abrasion of coarse-grained, low ^{10}Be concentration, landslide material produced within the syntaxis that dilutes the up-stream high-concentration ^{10}Be flux from the Tibetan Plateau only after abrasion has transferred sediment to the studied sand fraction. A simple abrasion model produces typical lag distances of 50 to 150 km compatible with our observations. Abrasion effects reduce the spatial resolution over which denudation can be constrained in the eastern Himalayan syntaxis.

Reference

Lupker M, Lavé J, France-Lanord C, Christl M, Bourlès D, Carcaillet J, Maden C, Wieler R, Rahman M, Bezbaruah D, Xiaohan L (2017) 10Be systematics in the Tsangpo-Brahmaputra catchment: the cosmogenic nuclide legacy of the eastern Himalayan syntaxis. Earth Surf Dyn 5: 429-449.

Thermal evolution and provenance of the Himalayan foreland basin of western India constrained from apatite fission track analyses and U-Pb detrital zircon ages

Maitra A[1], Anczkiewicz R[1], Anczkiewicz A[1], Porebski S[2], Mukhopadhyay D[3]

[1]Inst. of Geological Sciences, Polish Academy of Sciences, Kraków, Poland [2]Dept. of Geology, Geophysics and Environmental Protection, AGH University of Science and Technology, Kraków, Poland [3]Dept. of Earth Sciences, IIT Roorkee, India

The Subathu Basin of Himachal Pradesh in western India exposes sedimentary record of India-Asia collision since late Paleocene. The basin fill coarsens upward and begins with the Subathu Formation (57- 41 Ma) composed of early-collisional shelfal facies of the closing Tethys ocean. The overlying Dagshai Formation (~31-24 Ma) comprises paralic facies. It is followed upward by the fluvial Kasauli Formation (24-13 Ma) and chiefly alluvial-fan Siwalik Group (13-1 Ma) both recording uplift and exhumation of the Himalayan core. We conducted detrital zircon analyses of the entire basin-fill succession to constrain early collisional process and the rise of the Himalaya. The focus was on marine-continental transitions, which were densely sampled and sedimentologically logged along selected sections. We also studied the thermal history of the main units using apatite fission track analyses (AFT) in order to constrain deformation of the foreland basin.

High-resolution study of the two cross sections with well exposed transition between the Subathu and the Dagshai formations does not show any significant changes in detrital material source areas, even across the main 3-10 Ma hiatus zone, which is thought to reflect the advent of Himalayan exhumation. Although both sections are internally consistent, they show a marked difference expressed by the presence of strong trans-Himalayan signal throughout the whole northern section, which suggests important along strike variations. Preliminary results obtained for the Kasauli Formation show zircon age spectrum dominated by the Higher and the Tethyan Himalayan zircons. Throughout the Siwaliks, all zircon age spectra are similar and show a distinct signal of the trans-Himalaya. It denotes that the Himalaya did not form a physical barrier that would prevent fluvial transport across the orogen. Our observations document an increase in abundance of high-grade minerals within the Kasauli-Siwalik transition, which corresponds to the gradual exhumation of the deeper levels of the mountain core and complies with earlier studies.

The whole succession was intensely deformed by internal thrusting and nappe stacking that induced thermal perturbation. The pre-Siwalik sediments show AFT ages that are consistently younger than the respective depositional ages. The shortened track lengths point to only partial age resetting, whereas thermal modelling suggests that the sediments underwent heating up to ~90°C. Fairly rapid cooling of the pre-Siwalik units occurred after 4 Ma and is correlated with the movement along the frontal thrusts accommodating shortening across the shallow foreland basin wedge. The AFT ages in the Siwalik samples are older or contemporaneous with the depositional ages, which together with the confined track length distributions imply source areas in the Himalayan domains including recycled Paleogene-Early Miocene deposits of the foreland basin itself. Prolonged link to hinterland by antecedent rivers facilitated supply of the detritus from the trans-Himalaya to the foreland basin throughout the entire Cenozoic.

A model to quantify sediment mixing across alluvial piedmonts with cycles of aggradation and incision

Malatesta L[1], Berger Q[2], Avouac JP[3]

[1]Univ. California, Santa Cruz, USA [2]Sorbonne Univ., Paris, France [3]California Inst. of Technology, Pasadena, USA

The accurate interpretation of clastic sedimentary records hinges on a good understanding of the timescale and mode of sediment transport from source to sink. An environmental signal can be accurately recorded in the stratigraphy if it is transported quickly without being mixed with older sediments, or it can be entirely shredded by a slow transport and significant mixing along the way. Both transformations can happen in alluvial piedmonts by successive episodes of aggradation and incision. For example, in the Tian Shan the sediment flux reaching the foreland basin is mixed with sediments of up to 0.5 Ma age, mixing and blurring the environmental signals it carries.

We present here a numerical model that reproduces cycles of aggradation and incision on an alluvial fan and keeps track of the age composition in the sediment outflow. The model is based on three fundamental time- and length-scales: the period of aggradation-incision cycles, the depth of incision with respect to net aggradation, and the pattern of lateral migration. All three parameters can be reasonably easily surveyed in the field and with remote sensing. For simple geometries, we replace the numerical model with a probabilistic light analytical model. The output of both models quantifies sediment mixing in terms of the probability of finding a given minimum proportion of sediments of age “T” or older in the output flux.

We apply and test the analytical and numerical models to the Eastern Tian Shan where we can rely on independent measurements of mixing and buffering. There, rivers repeatedly aggraded and incised 100’s of meters every 20 to 30 kyr with two main effects: 1) the delivery of coarse sediments to the basin is delayed by at least 7 to 14 kyr between being first evacuated from the mountain and later re-eroded and transported basinward; 2) the outflux of coarse sediments from the piedmont contains a significant amount of recycled material that was deposited on the piedmont as early as the Middle Pleistocene. These initial field constraints are matched and completed with a probabilistic model. It is possible to identify which system is likeliest to preserve environmental signals and to which degree the environmental is modified based on the three model parameters that we can estimate in the field (incision frequency, incision depth, and lateral migration). The model can be used to inform future sampling strategies in foreland basins and also to revisit existing sediment records.

Variations in the basement structure of the Indian plate along the Himalayan Arc: Results from magnetotelluric study

Manglik A[1], Thiagarajan S[1], Suresh M[1], Adilakshmi L[1], Babu M[1], Chakravarthy N[1]

[1]CSIR, National Geophysical Research Inst, India

Geophysical studies in different segments of the Himalaya reveal along-strike variations in the wedge structure as well as the décollement surface (top of the Indian plate). These structural and compositional variations in turn lead to heterogeneous rheological structure and manifest themselves in terms of spatiotemporal variations in the seismicity. It is therefore important to understand the complexities of the Indian plate underthrusting the Himalaya. Some studies have been carried out earlier, especially for hydrocarbon exploration at the foothills of the Himalaya, to decipher the sedimentary structure overlying the Indian plate. Here, we present the results of a systematic magnetotelluric (MT) study carried out in the central Ganga basin to delineate the basement structure of the Indian plate south of the Main Frontal Thrust (MFT). The MT data were acquired at about 160 sites along six profiles spread across the central Ganga basin covering a total area of about 2×10^5 km^2. The region falls south of the Himalayan seismogenic zone encompassing the 1505 and the 2015 earthquakes. The average inter-station spacing was 6-8 km, except in the areas where big towns are located. The results reveal significant variations in the basement structure of the Indian plate. The basement depth is more than 9 km in the western part of the study region between the longitudes 80°09'E and 81°44'E The signatures of the Faizabad Ridge, which is buried underneath the sediments, are obtained at the depth of less than 4 km around the longitude 82°31'E. Further east, the basement depth is about 6 km around the Raxaul area (84°47'E) (south of the Hi-CLIMB profile). These structural variations are inferred to be controlling the earthquake genesis in the central segment of the Himalaya and need to be considered in developing any deformation/seismotectonic model of the Himalayan Collision Belt.

Evaluating the impact of earthquake-triggered landslides on riverine sediment and organic carbon export in the Central Himalaya

Märki L[1], Lupker M[1], Gajurel A[2], Haghipour N[1], Schide K[1], France-Lanord C[3], Lavé J[3], Morin G[4], Gallen S[5]

[1]Geological Inst., Dept. of Earth Sciences, ETH Zurich, Switzerland [2]Dept. of Geology, Tribhuvan Univ., Kathmandu, Nepal [3]CRPG, CNRS, Univ. of Lorraine, Nancy, France [4]Univ. Pierre et Marie Curie, Villefranche-sur-mer, France [5]Colorado State Univ., USA

In April 2015, the Gorkha earthquake (Mw 7.8) hit central Nepal, causing a large number of landslides in the steep valleys of the Higher Himalaya (Roback et al. 2018). Following the earthquake, we acquired suspended sediment samples during 3 monsoon seasons (2015-2017) at six sampling stations in trans-Himalayan rivers. The focus is laid on the Narayani River where daily samples provide high-resolution time-series and where a set of samples from the monsoon 2010 gives a pre-earthquake reference point. The Narayani River is one of the major outlets of the Central Himalaya and its eastern part was heavily affected by the earthquake providing a broader scale test of the impact of the earthquake on biogeochemical cycles. Combining suspended sediment load data with total organic carbon (TOC) as well as its stable and radiocarbon isotopic compositions, we try to reconstruct the sources of organic carbon in suspended sediments.

First results show that total sediment fluxes remained below the 40-year average during the weak 2015 monsoon immediately following the earthquake. In contrast, the stronger monsoon in 2016 was characterized by sediment concentrations that largely exceed the pre-earthquake average. This exceptional sediment load could be a consequence of the earthquake-triggered landslides in the Upper Himalaya. On the other hand, bulk radiocarbon data and TOC concentrations of suspended sediment samples provide an important tool for disentangling the sources of organic carbon in river sediments. First evaluations of a mixing model show similar results before and after the earthquake suggesting uniform sources of organic carbon. This new model proposes a weak impact of earthquake-triggered landslides on the export of riverine organic carbon in the active landscape of the Central Himalaya.

Reference

Roback K et al. (2018) The size, distribution, and mobility of landslides caused by the 2015 Mw 7.8 Gorkha earthquake, Nepal. Geomorphology 301: 121-138.

Web based landslide management system for Nepal

Meena SR[1,2], Westen C[2], Mavrouli O[2]

[1]Z_GIS, Univ. of Salzburg, Austria [2]ITC, Univ. of Twente, The Netherlands

Landslide inventory in Nepal is currently not done continuously and coherently, and efforts are made after major triggering events only, such as the 2015 Gorkha earthquake. There is a lack of sharing of knowledge and cooperation among stakeholders to cope with significant disaster events. This research will focus on filling the gaps by designing an approach for sustainable landslide inventory mapping in Nepal. The overall framework of research is to make a conceptual design of a Nepalese landslide information system and to show how different stakeholders can be involved. The use of a Nepalese landslide information system, to report and provide landslide data would benefit the stakeholders involved in data collection and landslide management. Several stakeholders could be considered such as road department, land management authority, forestry department, disaster management department and army. These stakeholders have different data requirements and are determined in this research. The landslide database system should be designed in such a way that it can incorporate information about different landslide characteristics and types. Availability and extraction of landslide data from the database are the important aspects. The landslide characteristics to be comprised in the database are defined, such as the completeness, the form of representation, the date of occurrence, the subdivision in scarp and accumulation areas, and the type of landslides.

For the reporting of landslides directly in the system, a web portal is proposed that will be connected to the internet and the central database (Fig. 1). Stakeholders who can contribute to the reporting of landslides are identified by field interviews and questionnaires. For example, primary users like school teachers can report a landslide event by pointing it out in the system as schools at the district level have the required infrastructure and internet facilities. Also, different methods for generating the inventory data are analysed in this research, and the applicability and efficiency of various collection methods are tested, including, image interpretation, the use of field-based Tablet PC, interviews and field survey. Interviews were carried out focusing on farmers and village residents and local police officers. Landslide inventories for Gorkha event were collected to see the spatial coverage of landslides in the country. Effects of different quality and completeness levels of landslide inventories, using tools such as Frequency Area Distribution and spatial overlap were carried out. Based on field investigations and literature reviews the optimal format of the database is determined for the Nepalese landslide information system.

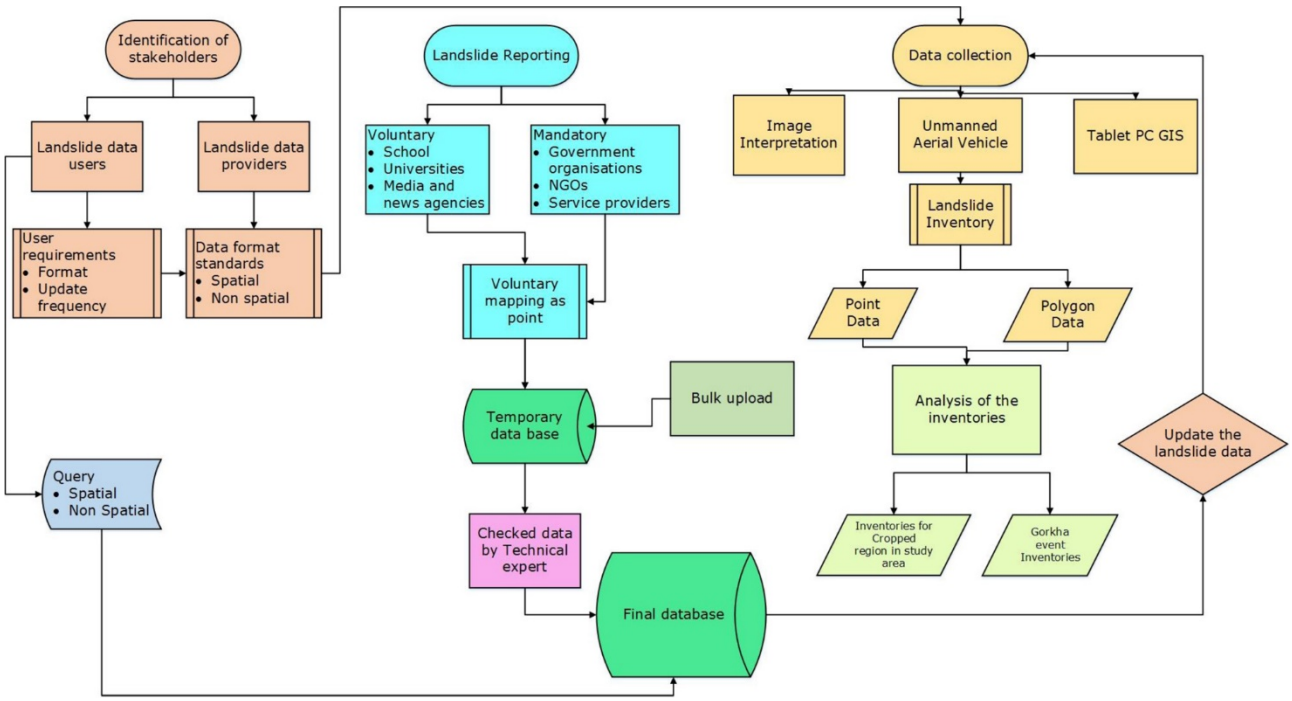

Figure 1. Methodological flowchart.

Fracture analysis and discrete fracture network modelling of Early Eocene Sakesar limestone, Eastern Salt Range, Potwar Plateau, Pakistan

Miraj M[1], Mehmood H[1], Kashif M[1], Zaidi S[1], Ahsan N[1]

[1]Inst. of Geology, Univ. of the Punjab, Lahore, Pakistan

Salt range is the youngest and southernmost part of the Himalayan Fold and Thrust Belt. Tectonically it is bounded by Jehlum Fault (left lateral) in the east, Kalabagh Fault (right lateral) in the west, Main Boundary Thrust (MBT) and Salt Range Thrust (SRT) in the north and south respectively. In carbonate reservoirs natural fractures plays an important role for fluid flow and can have a dramatic influence on reservoir performance. Our goal is to evaluate the natural fracture network pattern in Sakesar Limestone of Early Eocene, which is the leading reservoir rock in the Potwar Plateau, Pakistan. In study area the observed formation (Sakesar Limestone) is predominantly composed of limestone with chert in the upper part and highly fossiliferous having low to high fractures density. We adopted circle inventory method and collected data (fracture length, width, orientation and dip azimuth) at 24 different outcrop sections of Sakesar Limestone in Eastern Salt range. We observed different fracture network pattern mainly NW-SE which is parallel to the bedding plane. We also used FracaFlowTM of BeicipFranlab for Discrete Fracture Network (DFN) modelling, which is an effective tool to examine mechanical properties (Fluid Flow and Migration) of naturally fractured carbonate rocks. We built a 3D (DFN) model of different fracture and fault sets and the results show that the fracture set 1 which is E-W oriented is less dense than the other two fracture sets (NE-SW, N-S). We calibrated DFN modelling results with field data and concluded that highly fractured facies have high mean value (high density) and permit flow easily as compared to low fractured facies. The results depict that integrated workflow used in this study is handy for building DFN Model for naturally fractured carbonate reservoirs.

The Growth of the Tibetan Plateau

Molnar P[1]

[1]*Univ. of Colorado, Boulder, USA*

Although an Andean margin bounded southern Eurasia before the India-Eurasia collision occurred, the major process that built the Tibetan Plateau was the thickening of crust as India penetrated deeply into Eurasia since collision at ~50 Ma. The second most important event in Tibet's growth occurred at ~15-10 Ma, when east-west extension of the plateau and, more importantly, normal faulting and thinning of Tibetan crust began. Extrapolations of present-day strain rates back to 15-10 Ma imply ~5-10 km of thinning of Tibetan crust, and such thinning in isostatic equilibrium would require a drop in the mean elevation of ~1 km: from ~6000 m at 15-10 Ma to ~5000 m today. I will argue that the surface of Tibet rose, perhaps 1000 m near 15-10 Ma, because gravity acting on its thickened mantle lithosphere and resulting convective flow – somehow – removed at least part of that lithosphere. Removal of mantle lithosphere calls for a number of testable hypotheses, not just the onset of extension and thinning of crust: (1) marked lateral variations in the uppermost mantle, (2) enhanced volcanism, (3) accelerated crustal shortening in surrounding regions, (4) slowing of Indian-Eurasia convergence, and (5) surface uplift of Tibet, followed by subsidence as crust thins. I will show evidence that removal of mantle lithosphere passes the first four tests, and does not (yet) fail the fifth. If such removal of thickened mantle lithosphere did occur, questions that remain include: (1) How many times has such lithospheric removal occurred – just once at 15-10 Ma or earlier too?, and (2) How has such removal occurred – by a long sheet of downwelling mantle lithosphere under southern Tibet, by little drips beneath much of Tibet, or by some other process?

Among future directions of exciting research in geodynamics, I see environmental consequences of geodynamic processes as a promising one. At roughly, or slightly later than, the postulated rise of the Tibetan Plateau, climatic changes seemed to have occurred in regions surrounding Tibet. The rise of Tibet may have accelerated loess deposition in China and aridified the northwestern part of the Indian Subcontinent. The processes by which Tibet's growth affected these changes, however, differ from one another, with loess deposition being a geodynamic teleconnection and aridification of NW India an atmospheric teleconnection. The South Indian monsoon, however, apparently did not strengthen at ~10 Ma in response to a rise of Tibet, as many, including me, have argued.

Microstructural and geochronological investigations of the Main Central Thrust Zone and the South Tibetan Detachment System in the Alaknanda–Dhauli Ganga Valleys, NW India

Montemagni C[1], Carosi R[2], Iaccarino S[2], Montomoli C[3], Jain A[4], Villa IM[1,5]

[1]Univ. of Milano-Bicocca, Italy [2]Univ. of Torino, Italy [3]Univ. of Pisa, Italy [4]CSIR, Central Building Research Inst., India [5]Inst. of Geological Sciences, Univ. of Bern, Switzerland

Shear zones play a major role in the tectonic evolution of the orogens and in the exhumation of crystalline rocks. In the Himalaya, two crustal scale shear zones having opposite kinematics bound the Greater Himalayan Sequence (GHS), the metamorphic core of the orogen, along the entire belt: the Main Central Thrust zone (MCTz) and the South Tibetan Detachment System (STDS). The activity time-span of these shear zones has been addressed by many studies, which unsurprisingly give very scattered results, as each study focused on different geological features and followed different mapping, sampling, analytical and interpretive strategies. In the Alaknanda–Dhauli Ganga valleys (Garhwal, NW India) both the STDS and the MCTz crop out in the same transect. The MCTz is a > 1-km thick zone delimited by two distinct thrusts, the Munsiari Thrust at the base and the Vaikrita Thrust, the MCT sensu stricto in the study area, at the top.

We selected three representative samples from the Vaikrita Thrust, which crops out in the South of the transect, and three from the STDS, which crops out in the North of the study area, in order to compare the timing of their activity along the same transect using the same analytical and interpretive approach. Microstructural observations on one garnet-staurolite-bearing quartzite and two garnet-bearing mylonitic micaschists from the Vaikrita Thrust prove the occurrence of three different textural generation of micas: a rare relict foliation, a main mylonitic foliation, and a late generation of static micas forming coronites after garnet breakdown. $^{40}Ar/^{39}Ar$ step-heating coupled with EMP analyses and with Ca-Cl-K correlation diagrams constrain mica growth on the main foliation around 9 Ma, and coronitic micas at ca. 6 Ma (Montemagni et al. 2018b).

The STDS deforms the small Malari granite. Deformation microstructures vary according to structural level. In the uppermost sample, a pegmatite intruding the Malari main body, low temperature deformation features are expressed by bulging recrystallization in quartz, bent twins in plagioclase, and kink bands in muscovite. $^{40}Ar/^{39}Ar$ dating on muscovite give 16.46 ± 0.06 Ma. Structurally below, another pegmatite, intruding the HT-mylonites, was formed during a later, waning deformation stage. It shows undulose extinction in quartz and rare kink bands in mica which yields a younger $^{40}Ar/^{39}Ar$ age of ca. 16.0 Ma. The structurally lowest sillimanite-bearing migmatite shows high temperature deformation microstructures (chessboard extinction and grain boundary migration recrystallization in quartz), followed by static growth of undeformed muscovite, which yields a $^{40}Ar/^{39}Ar$ age of 14.36 ± 0.06 Ma. This is the minimum age for the cessation of ductile deformation (Montemagni et al. 2018a).

Our results demonstrate a diachroneity of STDS and MCT in the Garhwal Himalaya. Any model of exhumation of the GHS should account for this lack of contemporaneity.

References

Montemagni C, Iaccarino S, Montomoli C, Carosi R, Jain AK, Villa IM (2018a) Age constraints on the deformation style of the South Tibetan Detachment System in Garhwal Himalaya. Ital J Geosci 137: 175-187.

Montemagni C, Montomoli C, Iaccarino S, Carosi R, Jain AK, Massonne HJ, Villa IM (2018b) Dating protracted fault activities: microstructures, microchemistry and geochronology of the Vaikrita Thrust, Main Central Thrust zone, Garhwal Himalaya, NW India. Geol Soc London Spec Publ 481, in press, doi:10.1144/SP481.3

Ductile to brittle deformation in the South Tibetan Detachment System, Himalaya: A telescoped regional “contact” metamorphism?

Montomoli C[1], Iaccarino S[3], Nania L[1], Leiss B[2], Carosi R[3]

[1]Dept. di Scienze della Terra, Univ. of Pisa, Italy [2]Abteilung Strukturgeologie und Geodynamik, Univ. Göttingen, Germany [3]Dept. di Scienze della Terra, Univ. of Torino, Italy

The South Tibetan Detachment System (STDS) is a system of regional ductile-to-brittle top-to-the E and NE normal shear zone and faults developed for more than 2000 km along the Himalaya strike. The STDS gets in contact the very-low- to low-grade metamorphic rocks of the Tethyan Himalayan Sequence (THS), in the hanging-wall, from the medium to high-grade metamorphic rocks of the Greater Himalayan Sequence (GHS), in the footwall. We investigate, four different sections of the STDS cropping out from West to East in Lower Dolpo (western Nepal), Kali Gandaki and Marsyangdy valleys (central Nepal) and Dinggye area (south Tibet).

The ductile shear zone is very well developed in all the study sections and it affects both tectonic units, i.e. THS and GHS. Due to the carbonate-rich nature of THS and GHS rocks along the study transects, identifying and mapping the STDS is not a simple task (e.g. Carosi et al. 2002).

Along all the structural sections, we densely sampled impure marble and calcsilicate from both units deformed by the STDS related ductile-shearing.

Ductile deformation is heterogeneous, leading to the development of calcmylonites associated to a mylonitic foliation striking parallel to the STDS and dipping at low-angle to the N and NE. All kinematic indicators confirm a top-to-the N and NE sense of shear.

Finite strain analyses have been performed in marbles on sections parallel to XZ plane of finite strain ellipsoid and point out to a finite strain increase moving from top to bottom. Microstructural and petrofabric analysis of calcite and quartz was carried out and reveal both SPO and LPO in almost all samples, supporting intracrystalline creep and dynamic recrystallisation as main deformation mechanisms.

Vorticity of flow (Wk), estimated by different vorticity gauges, highlights a non-coaxial deformation regime, with a main pure shear component, acting during the STDS activity both in high- and medium-temperature and low-temperatures mylonites. In addition, a condensed metamorphic field gradient has been clearly detected though deformation mechanism and microstructures. The shortening perpendicular to the shear zone is also responsible for the telescoping of the metamorphic isograds at the base of the THS due both to shear heating and heating from the lower and hotter GHS.

Reference

Carosi R, Montomoli C, Visonà D (2002) Is there any detachment in the Lower Dolpo (western Nepal)? C R Geosci 334: 933-940.

A geodynamic perspective of the west and the east Himalayan syntaxes: Inferences from seismic sources

Mozhikunnath Parameswaran R[1], Rajendran K[2], Rajendran CP[1]

[1]Jawaharlal Nehru Centre for Advanced Scientific Research, Bangalore, India [2]Indian Inst. of Science, Bangalore, India

The great India-Eurasia continental collision boundary along the Himalayan arc, hinges near Nanga-Parbat (west Himalayan syntaxis) to swing south and meet the Makran subduction zone in the west, while in the east it pivots near Namche Barwa (east Himalayan syntaxis) to make its way south to the Andaman-Sumatra subduction zone across the Indo-Burman subduction. While both continental and oceanic interfaces of the Indian plate boundary are better understood, the seismotectonics of the axle points, namely the west and the east Himalayan syntaxes (WHS and EHS, respectively) remain less so. Seismic history of the EHS is highlighted by the Assam Earthquake (1950, Mw 8.7) with a strike-slip fault plane solution, which is in general coherent with the focal mechanisms of earthquakes in the region as opposed to the compressional nature along the Himalayan arc. Unlike the rest of the Higher Himalaya, the region also seems to be the home of temporally spaced low-magnitude earthquake swarms within given spatial clusters. The seismic source of these swarms is mapped to low P- and S-wave velocity patches resulting from horizontal and vertical flow of mobile rocks and consequent decompressional melting (Mukhopadhyay and Dasgupta 2015). The reported variations in heterogeneities are also captured by 3D resistivity imaging studies that classify it as evidence for crustal flow below Namche Barwa (Lin et al. 2017). A potent theory for this observed mantle upwelling arises from P-wave tomography of the region that points to the Indian slab tearing beneath the EHS, which could facilitate the upwelling and may even have played a role in the creation of the syntaxis (Peng et al. 2016). Meanwhile, in the WHS, the current seismic output far outranks its eastern counterpart. Based on numerical slab simulations and teleseismic tomographic models, the large seismic productivity here at intermediate depths is now believed to be the result of strain localization on a thinning subducting slab that is prepping for a tear/break-off (Magni et al. 2012; Kufner et al. 2016; 2017). Therefore, this work attempts to review the seismic maturity and output of the two syntaxes based on their earthquake histories and the corresponding potential seismic sources identified from tomographic results.

References

Kufner SK, Schurr B, Haberland C, Zhang Y, Saul J, Ischuk A, Oimahmadov I (2017) Zooming into the Hindu Kush slab break-off: A rare glimpse on the terminal stage of subduction. Earth Planet Sci Lett 461: 127-140.

Kufner SK, Schurr B, Sippl C, Yuan X, Ratschbacher L, Ischuk A, Murodkulov S, Schneider F, Mechie J, Tilmann F (2016) Deep India meets deep Asia: Lithospheric indentation, delamination and break-off under Pamir and Hindu Kush (Central Asia). Earth Planet Sci Lett 435: 171-184.

Lin C, Peng M, Tan H, Xu Z, Li Z.H, Kong W, Tong T, Wang M, Zeng W (2017) Crustal structure beneath Namche Barwa, eastern Himalayan syntaxis: New insights from three-dimensional magnetotelluric imaging. J Geophys Res 122: 5082-5100.

Magni VV, van Hunen J, Funiciello F, Faccenna C (2012) Numerical models of slab migration in continental collision zones. Solid Earth 3: 293-306.

Mukhopadhyay B, Dasgupta S (2015) Earthquake swarms near eastern Himalayan Syntaxis along Jiali Fault in Tibet: A seismotectonic appraisal. Geoscience Frontiers 6: 715-722.

Peng M, Jiang M, Li ZH, Xu Z, Zhu L, Chan W, Chen Y, Wang Y, Yu C, Lei J, Zhang L (2016) Complex Indian subduction style with slab fragmentation beneath the Eastern Himalayan Syntaxis revealed by teleseismic P-wave tomography. Tectonophys 667: 77-86.

Uplift of the Indo−Burman Ranges and palaeodrainage of the eastern Himalayan region: A combined provenance and age elevation profile study, western Myanmar

Najman Y[1], Sobel E[2], Ian Millar I[3], Stockli D[4], Garzanti E[5], Corley R[6], Ando S[5], Vezzoli G[5], Barfod D[7], Zhang P[8], Mei L[8]

[1]Lancaster Environment Centre, Lancaster Univ., UK [2]Inst. of Earth and Environmental Science, Univ. of Potsdam, Germany [3]British Geological Survey, UK [4]Univ. of Texas, Austin, USA [5]Univ. of Milano-Bicocca, Italy [6]Chevron, Texas, USA [7]SUERC, Univ. of Glasgow, UK [8]China Univ. of Geosciences, Wuhan, China

The Indo-Burman Ranges (IBR) is an accretionary prism that stretches the length of western Myanmar, between the Sunda Trench to the west and the Myanmar Central Basin (CMB) to the east. Determination of the timing of uplift of the IBR is necessary to understand the wider palaeodrainage of the eastern Himalaya. We carried out an age elevation profile across the range, using AFT and ZHe techniques, combined with a provenance study of new (petrography and heavy minerals, detrital rutile U-Pb, zircon U-Pb with Hf, bulk Sr-Nd) and published (Wang et al. 2014; Robinson et al. 2014; Licht et al. 2014; Naing et al. 2014; Allen et al. 2008) data, of rocks from east and west of the range to determine if and when provenance diverged.

Our age elevation profile shows exhumation of the IBR was occurring by the Mid Eocene, and a major episode of exhumation of the IBR occurred during the latest Oligocene to Oligo-Miocene boundary times. The latter is consistent with our provenance data that shows, at this time: (1) a provenance change between regions east and west of the IBR, and (2) input of material from the Mogok Metamorphic Belt (MMB) to the CMB.

The divergence of provenance east and west of the IBR we interpret as indicating formation of a mountain barrier between the regions. The majority of the MMB lies in the northern mountainous region of the modern Irrawaddy River's headwaters, extending as a thin sliver southward, adjacent to the Sagaing Fault. We consider the MMB detritus we record in the CMB rocks to be derived from the northern part of the MMB since this is where much of the MMB is located; palaeogeographic considerations would suggest southerly palaeodrainage from their exhuming highlands; some, (albeit not all), of the CMB sample locations are located north of the southern extension of the MMB; the southern MMB region is in close proximity to carbonates, for which we see no evidence in our Oligocene to Mio-Pliocene CMB petrographic data. Thus, we interpret the appearance of MMB detritus in our CMB samples as indicating onset of through-going north-to-south Irrawaddy drainage in the Basin at this time (Zhang et al. in review), which would have required the IBR to be emergent, to form the river valley's western flank.

This work, combined with our previous work (Zhang et al. in review), indicates that the palaeo-Yarlung River did not flow into the Irrawaddy drainage as previously proposed (e.g. Clark et al. 2004). Since the palaeo-Yarlung did not flow into the Bay of Bengal until the Early Miocene (Bracciali et al. 2015), we suggest that the Himalayan Yarlung Tsangpo Suture Zone was internally drained during the Paleogene.

References

Allen R, Najman Y, Carter A, Parrish R, Bickle M, Paul M, Garzanti E, Reisberg L, Chapman H, Vezzoli G, Ando S (2008) Provenance of the Tertiary sedimentary rocks of the Indo- Burman Ranges, Burma (Myanmar): Burman arc or Himalayan-derived? J Geol Soc London 165: 1045-1057.

Bracciali L, Najman Y, Parrish RR, Akhter SH, Millar I (2015) The Brahmaputra tale of tectonics and erosion: Early Miocene river capture in the Eastern Himalaya. Earth Planet Sci Lett 415: 25-37.

Clark MK, Schoenbohm LM, Royden L, Whipple KX, Burchfiel BC, Zhang X, Tang W, Wang E, Chen L (2004) Surface uplift, tectonics, and erosion of eastern Tibet from large-scale drainage patterns. Tectonics 23: TC1006.

Licht A, Reisberg L, France-Lanord C, Naing Soe A, Jaeger JJ (2014) Cenozoic evolution of the central Myanmar drainage system: insights from sediment provenance in the Minbu sub-basin. Basin Research 28: 237-251.

Naing TT, Bussien DA, Winkler WH, Nold M, Von Quadt A (2014) Provenance study on Eocene-Miocene sandstones of the Rakhine Coastal Belt, Indo-Burman Ranges of Myanmar: geodynamic implications. In: Scott RA, Smyth HR, Morton AC, Richardson N (Eds.) Sediment Provenance Studies in Hydrocarbon Exploration and Production, pp. 195-216.

Robinson RAJ, Brezina CA, Parrish RR, Horstwood MSA, Oo NW, Bird MI, Thein M, Walters AS, Oliver GJH, Zaw K (2014) Large rivers and orogens: The evolution of the Yarlung Tsangpo-Irrawaddy system and the eastern Himalayan syntaxis. Gondwana Res 26: 112-121.

Wang JG, Wu FY, Tan XC, Liu CZ (2014) Magmatic evolution of the Western Myanmar Arc documented by U-Pb and Hf isotopes in detrital zircon. Tectonophys 612: 97-105.

Thermal history of the Higher Himalayan Crystallines and over- and underlying sediments in west-central Nepal: LA-ICP-MS zircon fission-track analyses

Nakajima T[1], Sakai H[1], Iwano H[2], Danhara T[2]

[1]Univ. of Kyoto, Japan [2]Kyoto Fission-Track Co. Ltd., Japan

Zircon fission-track (ZFT) dating was carried out along 80 km long transect across the Himalaya: from Mt. Annapurna to the Main Boundary Thrust (MBT) in west-central Nepal. We newly obtained 17 ZFT ages from the Higher Himalayan Crystallines (HHC), the underlying Lesser Himalayan sediments (LHS), and the overlying Tibetan Tethys Sediments (TTS). The HeFTy thermal modelling was carried out based on ZFT age and FT length distribution. We discuss cooling process of each geotectonic units and comprehensive cooling process of the Himalaya since early to middle Miocene.

The ZFT ages of the LHS show northward younging linear distribution from the oldest age in the frontal zone near the MBT (13.4 ± 1.0 Ma) to the youngest age in the root zone (1.5 ± 0.2 Ma). Partially reset ZFT ages (~450 Ma) from the autochthonous LHS suggest that the LHS has undergone inverted thermal metamorphism caused by hot metamorphic nappe. The LHS in west-central Nepal is not covered by metamorphic nappe, however, these partially reset ages indicate that northern part of the LHS was once covered by the metamorphic nappe, and at present it was eroded out. The t-T path of LHS calculated by HeFTy show that LHS has undergone two major cooling phases: first rapid cooling (ca. 150 °C/Myr) and subsequent gradual cooling (ca. 30 °C/Myr).

On the other hand, the ZFT ages from the HHC and the TTS range from 10.9 ± 0.8 Ma to 1.7 ± 0.4 Ma and show southward younging distribution. The ZFT age distribution along NNE-SSW transect shows a concave upward pattern with the youngest ZFT age located near the MCT. This distribution pattern well corresponds to present uplift rate distribution, which suggests that the ZFT age distribution pattern reflects regional vertical velocity (Grandin et al. 2012). Inter-seismic vertical velocity distribution is considered to be controlled by kinematics and geometry of the MHT which is the main active decollement, thus the ZFT age distribution pattern seems to reflect exhumation and cooling of the hanging wall of the MHT.

Reference

Grandin R, Doin MP, Bollinger L, Pinel-Puysségur B, Ducret G, Jolivet R, Sapkota SN (2012) Long-term growth of the Himalaya inferred from interseismic InSAR measurement. Geology 40: 1059-1062.

Non-coaxial flow and time constraints of the South Tibetan Detachment System in Central Himalaya: An example from the Lower Dolpo and the Kali Gandaki Valley, Nepal

Nania L[1,2], Montomoli C[2], Iaccarino S[3], Leiss B[4], Di Vincenzo G[5], Carosi R[3]

[1]Dottorato Regionale in Scienze della Terra Pegaso, Firenze, Italy [2]Dept. di Scienze della Terra, Univ. of Pisa, Italy [3]Dept. di Scienze della Terra, Univ. of Torino, Italy [4]Geoscience Centre, Univ. Göttingen, Germany [5]CNR, Ist. di Geoscienze e Georisorse, Pisa, Italy

The South Tibetan Detachment System (STDS) is a main tectonic structure within the Himalayan Belt, regarded as extensional top-down-to-the-north ductile to brittle shear zones. In the Lower Dolpo Region (Western-Central Nepal) and Kali Gandaki Valley (Central Nepal), the STDS juxtaposes carbonate-rich rocks of the Tethyan Himalayan Sequence (THS) tectonically above the Greater Himalayan Sequence (GHS) where heterogeneous ductile deformation leads to the development of a strong mylonitic foliation (S2), partially overprinting an older D1 event (Carosi et al. 2007; Godin 2003). All meso- and micro-kinematic indicators related to the STDS are coherent with a top-to-the N-NE sense of shear.

Moving toward the core of the high strain zone, marbles are affected by an increase in new grains coupled by an increase of size for the old grains, previously deformed by grain boundary migration mechanisms. These microstructures are partially overprinted by a late e-twins development in the high strain zone, typical of low-to medium temperature deformation, and by a deformative annealing toward higher structural levels. Furthermore, micas have experienced a late static growth, forming large poikiloblasts with remnants of the main foliation S2.

Calcite and quartz crystallographic preferred orientations (CPO) have been measured by X-ray texture goniometry on oriented samples. Our investigation reveals the occurrence of strong CPOs, indicating dislocation slip and dynamic recrystallisation as the main deformation mechanisms. Slip systems suggest low deformation temperatures for the mylonitic shearing. The vorticity of flow analyses highlight a non-coaxial plane deformation regime, with a strong pure shear component, acting during the STDS activity. The asymmetric preferred orientation of calcite and quartz c-axis in respect to the mylonitic foliation S2 are in coincidence with the shear sense as suggested by the other kinematic indicators. Temperature and kinematic vorticity increase southward, approaching to the contact between the TSS and the GHS. For a critical approach in determining deformation temperatures, cathodoluminescence microanalyses have been carried out, pointing to a fluid-assisted deformation related to the late ductile activity of the STDS.

Isotopic age of poikiloblastic biotite grains through ^{40}Ar-^{39}Ar laserprobe analyses coupled with electron microprobe microanalyses on micas point to a late static thermometamorphic event, postdating the ductile activity of the STDS.

References

Carosi R, Montomoli C, Visonà D (2007) A structural transect in the Lower Dolpo: Insights on the tectonic evolution of Western Nepal. J Asian Earth Sci 29: 407-423.

Godin L (2003) Structural evolution of the Tethyan sedimentary sequence in the Annapurna area, central Nepal Himalaya. J Asian Earth Sci 22: 307-328.

High-temperature ductile deformation and inverse thermal metamorphic gradient in the Main Central Thrust zone: An example from the Lower Dolpo Region, Western Nepal

Nania L[1,2], Montomoli C[2], Iaccarino S[3], Leiss B[4], Carosi R[3]

[1]Dottorato Regionale in Scienze della Terra Pegaso, Firenze, Italy [2]Dept. di Scienze della Terra, Univ. of Pisa, Italy [3]Dept. di Scienze della Terra, Univ. of Torino, Italy [4]Geoscience Centre, Univ. Göttingen, Germany

The Greater Himalayan Sequence (GHS) is regarded as the mid-crustal metamorphic core of the Himalayan Belt, overlapping southward the low- to medium-metamorphic grade Lesser Himalayan Sequence (LHS) and underlying northward the low- to non-metamorphic Tethyan Himalayan Sequence (THS). The GHS is well exposed all along the Himalayan belt for nearly 2500 km, and it is bounded by two opposite shear zones: the contractive top-to-the-S Main Central Thrust zone (MCTz) and the low-angle top-down-to-the-N-NE extensional South Tibetan Detachment System (STDS).

One of the "classical" features of the Himalaya is the presence of an inverse metamorphic field gradient at the bottom of the GHS (Searle et al. 2008). Moreover, a new system of ductile contractional top-to-the-south high-temperature shear zones (named High Himalayan Discontinuity, HHD) has been recognized within the GHS, inferring that this unit did not behave as a single tectonic block (Montomoli et al. 2013). These features make the GHS a key example for studying exhumation processes for deep-seated metamorphic cores, covering a main topic in structural geology and tectonics.

In this work, we investigated the MCTz along a N-S transect near Dunai, in the Lower Dolpo Region (Western-Central Nepal), where the main lithotypes are, from north to south, kyanite + garnet mylonitic paragneisses and quartz-rich mylonites. All kinematic indicators, such as S-C-C' fabric, snowball garnet, several mineral fish and clasts with asymmetric strain shadows, confirm a top-to-the S sense of shear. Chessboard microstructures in quartz and myrmekites in feldspars indicate high temperature deformation in structurally higher located samples, supporting a northward increase of deformation temperature, from the base of the MCTz to the core of the GHS. Petrofabric analyses of quartz emphasize this trend as well as the high-temperature deformation regime in general. Going structurally upward, the activation of prism <a> and prism <c> slip systems increases, whereas rhomb <a> and basal <a> slip systems tend to disappear from the base of the GHS to the core of the Unit. The asymmetric distribution of c-axes is coherent with a top-to-the S sense of shear connected to the MCT kinematic, inferring that dislocation slip acted as the main deformation mechanism during non-coaxial deformation flow.

References

Montomoli C, Iaccarino S, Carosi R, Langone A, Visonà D (2013) Tectonometamorphic discontinuities within the Greater Himalayan Sequence in Western Nepal (Central Himalaya): insights on the exhumation of crystalline rocks. Tectonophys 608: 1349-1370.

Searle MP, Law RD, Godin L, Larson KP, Streule MJ, Cottle JM, Jessup MJ (2008) Defining the Himalayan main central thrust in Nepal. J Geol Soc 165: 523-534.

Forearc basin record of continental collision in Southern Tibet

Orme D[1]

[1]*Dept. of Earth Sciences, Montana State Univ., USA*

The Xigaze forearc basin in southern Tibet, one of the largest and best-preserved forearc basins on Earth, records upper-plate processes active prior to and following the inter-continental collision between India and Asia. This presentation addresses the Late Cretaceous to Miocene history of the Xigaze forearc by reconstructing the sedimentary environments of the southern margin of Asia prior to collision and determining the subsequent thermal history of the basin following cessation of deposition (Orme and Laskowski 2016; Orme et al. 2015). The timing of initial collision between Asia and India is no later than 58 Ma based on the based on the similarity of the U-Pb detrital zircon age spectra and sandstone compositions between the Xigaze forearc and strata deposited atop the passive margin of India at that time (Orme et al. 2015). Thermochronologic results determine the maximum burial temperature of the basin following the onset of collision to ~140-200°C, which corresponds to depths attainable by sedimentation in the forearc region by a Paleogene foreland basin succession (Orme 2017 in press). In addition, the thermochronologic dataset indicates rapid exhumation of the Xigaze forearc from ~21 Ma to 15 Ma (Orme 2017 in press). The timing of exhumation appears to be regionally extensive, affecting all the lithotectonic units of the India-Asia collision zone, and coincides with movement along the north-vergent Great Counter Thrust System (e.g. Carrapa et al. 2014). Thrusting, coupled with enhanced erosion possibly related to the paleo-Yarlung River, likely drove Early Miocene cooling of the India-Asia collision zone.

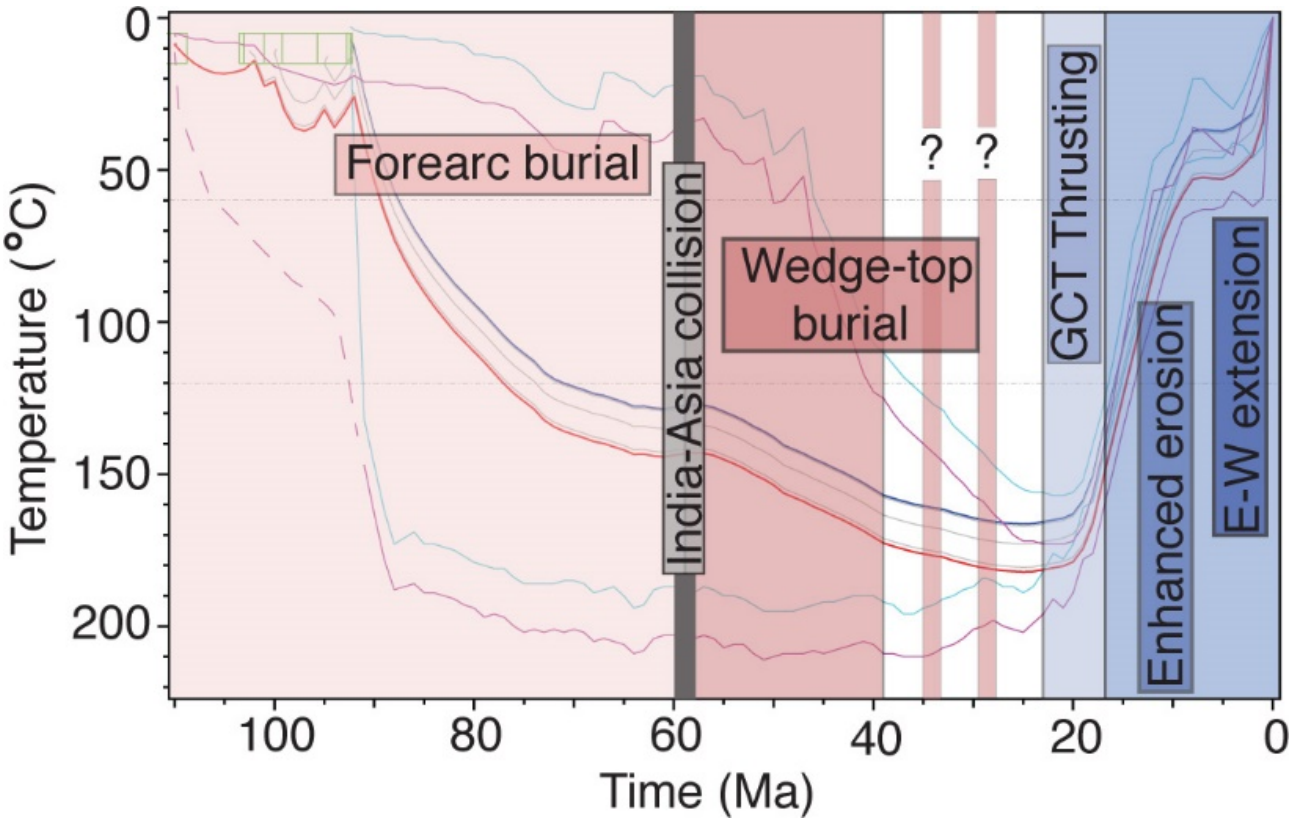

Figure 1. Thermal history for the oldest (i.e. stratigraphically deepest) rocks of the Xigaze forearc basin, southern Tibet (Orme 2017 in press).

References

Carrapa B, Orme D.A, Kapp P, DeCelles PG, Cosca M, Waldrip R (2014) Rapid Miocene Burial and Exhumation of the Indus-Yarlung Suture Zone in Tibet. Geology 42: 443-446.

Orme DA, Carrapa B, Kapp PK (2015) Sedimentology, Provenance and Geochronology of the western Xigaze Forearc, Southern Tibet. Basin Research 27: 287-411.

Orme DA, Laskowski AK (2016) Basin Analysis of the Albian-Santonian Xigaze forearc, south-central Tibet. J Sediment Res 86: 894-913.

Orme DA (2017) Burial and exhumation history of the Xigaze Forearc, Yarlung Suture Zone, Tibet. Geoscience Frontiers, in press.

The 17th century great earthquake at Hime village, Subansiri River Valley, Eastern Himalayan Front, India

Pandey A[1], Jayangondaperumal R[1], Singh Rao P[2], Singh I[1], Lochan Mishra R[3], B Srivastava H[4], Srivastava P[1]

[1]Wadia Inst. of Himalayan Geology, Dehradun, India [2]Geological Survey of India, Kolkata, India [3]Dept. of Geology, Ravenshaw Univ., Cuttack, India [4]Dept. of Geology, Banaras Hindu Univ., Varanasi, India

Many historical earthquakes have been documented in the eastern Himalaya, but their geological evidences are still lacking. Although sincere attempts have been taken by many workers in order to assert the precision of these historically reported events but yet the paleoearthquake catalogue in this area is still in infantry stage. In order to address this issue, we dug a trench adjacent to the eastern bank of the Subansiri River at Himebasti village (27.54°N, 94.36°E).

At Himebasti, a fault scarp was discovered with an E-W strike. It lies 2 km east of the Subansiri River along HFT (Himalayan Frontal thrust). A micro-topographic survey of the fault scarp was carried out using RTK-GPS (Real Time Kinematics-Global Positioning System) and RTS (Robotics Total Station) reveal variable scarp height (8-12 m) along 0.5 km long fault scarp. Sub-aerial photography of the youngest disjointed surface at the trench site was performed using Drone to generate a high resolution digital elevation model (DEM). A trench (26 m long × 8 m wide × 9 m deep) was excavated across the fault scarp to investigate the style of faulting and paleoearthquake history.

Near the trench site along Subansiri River, the youngest terrace shows several emplaced drifted wood logs. 19 Charcoal samples were collected from both trench walls, these samples were dated using the AMS (Accelerator Mass Spectrometry), conceding ages ranging from 43’000 BP to 1960 A.D. These ages are modelled using Bayesian statistics along with structural and stratigraphic observations of trench exposure. Wood logs (three samples) emplaced in the youngest terrace yielded consistent ages ranging from 1655 to 1826 A.D. The collective information of these results suggests that the most recent rupture at Himebasti occurred after 1450-1650 A.D. to produce a scarp of roughly 6.8 m vertical separation with a minimum observed dip-slip displacement of 11.2 m. Our inferred surface rupture event is related to the historically documented 1697 A.D. Sadiya earthquake, which shook the major cities of eastern Himalaya and destructed a town named Sadiya with continued aftershocks for six months. The present study suggests that adjoining eastern Himalayan segments have been ruptured by two great earthquakes at close time interval of approximately 250 years.

Seismic tomographic constraints for the Jurassic-to-present plate tectonic evolution of the Tethyan realm and the Himalayan-Alpine orogenic belt

Parsons A[1], Hosseini K[1], Sigloch K[1]

[1]*Dept. of Earth Sciences, Univ. of Oxford, UK*

Seismic tomography may be used to identify slabs of oceanic lithosphere that have subducted into the upper and lower mantle. Correlation of this information with constraints from the bedrock geological record provides a means to test and develop new and existing paleogeographic and tectonic plate reconstruction models. Here, we present a visual summary of positive seismic velocities in the mantle beneath Asia and the Indian Ocean. Many of these anomalies can be attributed to the remnants of Neo-Tethys and Paleo-Tethys oceanic lithosphere subducted beneath active margins and intra-oceanic arcs since the Jurassic.

We employ two important and commonly accepted assumptions that allow for identification of paleo-subduction zone trench location in paleogeographic and tectonic plate reconstruction models. Firstly, we assume that a given slab sinks vertically within the mantle (e.g. van der Meer et al. 2010; Butterworth et al. 2014; Sigloch and Mihalynuk 2013) and therefore marks the location and length of the overlying paleo-subduction zone trench from which it derived. Secondly, we assume that slabs within the mantle sink at rate of approximately 1 cm/yr (e.g. van der Meer et al. 2010; Butterworth et al. 2014; Sigloch and Mihalynuk 2013). This allows for a depth-to-age conversion, whereby the depth of a given slab with respect to the core-mantle boundary may be used to calculate the time at which subduction of that slab occurred. As such, slab geometries provide constraints on the absolute location and timing of active paleo-subduction zones of the geological past.

Ten different P-wave global tomography models were used to identify subducted slabs in the mantle (Hosseini et al. 2018). Our catalogue of subducted slabs from the Tethyan realm highlights the timing and position of active paleo-subduction zones that were responsible for the subduction of the Paleo-Tethys and Neo-Tethys oceans between Jurassic to present times. The distributions of these paleo-subduction zones provide important constraints for many ongoing debates including, (1) the relative timing and subduction zone configuration for collisions between India, Eurasia and the Kohistan-Ladakh arc (e.g. Searle et al. 1999; Khan et al. 2009; van Hinsbergen 2012; Sun et al. 2016); (2) the size and significance of the “Tethyan intra-oceanic arc” (e.g. Aitchison et al. 2007; Zang et al. 2014; Gibbons et al. 2015); and (3) the significance of Mesozoic ophiolite populations observed across the Tethyan realm (e.g. Robertson 2004; Searle and Treloar 2010; Gibbons et al. 2015). The implications of our findings are discussed in light of these and other important questions relating to the tectonic evolution of Tethyan realm and the Himalayan-Alpine orogenic belt.

References

Aitchison JC, McDermid IRC, Ali JR, Davis AM, Zyabrev SV (2007) Shoshonites in Southern Tibet Record Late Jurassic Rifting of a Tethyan Intraoceanic Island Arc. J Geol 115: 197-213.

Butterworth NP, Talsma AS, Müller RD, Seton M, Bunge HP, Schuberth BSA, Shephard GE, Heine C (2014) Geological, tomographic, kinematic and geodynamic constraints on the dynamics of sinking slabs. J Geodyn 73: 1-13.

Gibbons AD, Zahirovic S, Müller RD, Whittaker JM, Yatheesh V (2015) A tectonic model reconciling evidence for the collisions between India, Eurasia and intra-oceanic arcs of the central-eastern Tethys. Gondwana Res 28: 451-492.

Hosseini K, Matthews KJ, Sigloch K, Shephard GE, Domeier M, Tsekhmistrenko M (2018) SubMachine: Web-based tools for exploring seismic tomography and other models of Earth's deep interior. Geochem Geophys Geosyst, in press.

Khan SD, Walker DJ, Hall SA, Burke KC, Shah MT, Stockli L (2009) Did the Kohistan-Ladakh island arc collide first with India? GSA Bull 121: 366-384.

Robertson A (2004) Development of concepts concerning the genesis and emplacement of Tethyan ophiolites in the Eastern Mediterranean and Oman regions. Earth-Sci Rev 66: 331-381.

Searle MP, Khan MA, Fraser JE, Gough SJ, Jan MQ (1999) The tectonic evolution of the Kohistan-Karakoram collision belt along the Karakoram Highway transect, north Pakistan. Tectonics 18: 929-949.

Searle MP, Treloar PJ (2010) Was Late Cretaceous–Paleocene obduction of ophiolite complexes the primary cause of crustal thickening and regional metamorphism in the Pakistan Himalaya? In: Kusky TM, Zhai MG, Xiao W (Eds.) The Evolving Continents: Understanding Processes of Continental Growth. Geol Soc London Spec Publ 338: 345-359.

Sigloch K, Mihalynuk MG (2013) Intra-oceanic subduction shaped the assembly of Cordilleran North America. Nature 496: 50-56.

Sun J, Xiao W, Windley BF, Ji W, Fu B, Wang J, Jin C (2016) Provenance change of sediment input in the northeastern foreland of Pamir related to collision of the Indian Plate with the Kohistan-Ladakh arc at around 47 Ma. Tectonics 35: 315-338.

van der Meer DG, Spakman W, van Hinsbergen DJ, Amaru ML, Torsvik TH (2010) Towards absolute plate motions constrained by lower-mantle slab remnants. Nat Geosci 3: 36-40.

van Hinsbergen DJ, Lippert PC, Dupont-Nivet G, McQuarrie N, Doubrovine PV, Spakman W, Torsvik TH (2012) Greater India Basin hypothesis and a two-stage Cenozoic collision between India and Asia. Proc Nat Acad Sci 109: 7659-7664.

Zhang LL, Liu, CZ, Wu FY, Ji WQ, Wang JG (2014) Zedong terrane revisited: An intra-oceanic arc within Neo-Tethys or a part of the Asian active continental margin? J Asian Earth Sci 80: 34-55.

Paleostress reconstruction from fault slip analysis in the Main Boundary Thrust zone, foothill Darjeeling Himalaya

Patra A[1], Saha D[1]

[1]*Indian Statistical Inst., Geological Studies Unit, Kolkata, India*

The present state of stress along the Himalayan terrain is revealed by recent studies but there is very little information for the geological past, particularly from the Eastern Himalaya. In the present work, results of fault slip analysis are presented to constrain paleostresses associated with the Main Boundary Thrust (MBT) zone in the foothill Darjeeling Himalaya.

Two steep northerly dipping, subparallel splays of the MBT, namely MBT-1 (northern splay; alternatively named as North Kalijhora Thrust or Ramgarh Thrust) and MBT-2 (southern splay; cf. MBT) (Mukul 2000; Mitra et al. 2010) are respectively associated with ductile to brittle-ductile and shallow-crustal brittle deformation. The Proterozoic Daling rocks occur on hanging-wall of MBT-1, Upper Paleozoic Gondwana rocks between MBT-1 and MBT-2, and Neogene Siwalik succession on the footwall of MBT-2, indicating greater exhumation along the MBT-1. Lower Gondwana rocks in the area are represented by the Talchir Formation (Roy 1976) and the Barakar Formation (Pascoe 1959). Only the middle and upper divisions of the Siwalik Group are present in the study area. While folds and other ductile structures are common in the Daling Group, the Gondwana rocks show fault related folds, and the Siwalik strata are deformed by brittle faults and local warps.

A total of 665 mesoscale faults with stepped slickensides, mineralised slickenfibres and ridge-and-groove structures have been measured for dynamic analysis. The dynamic analysis was carried out by using mainly PBT method incorporated in the Win_Tensor software (Delvaux and Sperner 2003), taking into account heterogeneity of fault-slip data in different lithologic units and spatial position with respect to the main MBT splays. The following successive tectonic evolution is proposed from the reduced paleostress tensors (Table 1).

(1) A pre-Himalayan extensional regime with broad NW-SE maximum principal extension (σ3) is indicated by tensor solutions obtained from the Talchir Formation occurring in the MBT-1 footwall. (2) Tensor solutions related to Himalayan orogeny show two successive compressional regimes and one strike-slip regime. The first stage (2a) of N-S maximum principal compression (σ1) was associated with thrust movement along MBT-1, juxtaposing folded Daling Group over the Gondwana succession at a time when there was little tilting of the Gondwana rocks. The ongoing thrust shortening led to formation of the MBT-2 in a foreland propagating thrust system, and tilting, fracturing and folding of the Gondwana rocks. Tensor solutions based on tilt-corrected data from the hanging-wall and footwall of MBT-2 again show N-S σ1 (2b). The switch over to a strike-slip regime (2c) recorded in the Gondwana and Siwalik strata was possibly due to flip between σ2 and σ3 as tectonic loading led to increased vertical component of stress. The tensor solutions of compressional regime with N-S (mean N11°W) σ1 is comparable with the present convergence direction of N17°E ± 2° (Kreemer et al. 2003). Other tensor solutions with E-W extension indicating apparent orogen-parallel stretching and pure strike-slip regime under E-W compression appear to be of local importance.

	Tectonic regime	*Subset*	*Stratigraphic unit/ River section*	*Plunge/ plunge direction*			*Synoptic Paleostress orientation*	*Stress regime*
				σ_1	σ_2	σ_3		
1	Extension	P192_1	Talchir Fm./ Ramthi	85/ 321	01/ 224	05/ 134		Pure Extension
2a	Compression 1 (MBT-1 related)	D217*	Daling Gr./ Ramthi	22/ 169	24/ 269	57/ 041		Pure Compression
		P129_2	Talchir Fm./ Lish	06/ 157	18/ 249	71/ 048		Pure Compression
		B226_2	Barakar Fm./ Suke	31/ 032	00/ 302	59/ 211		Pure Compression
2b	Compression 2 (MBT-2 related)	P126_2*	Talchir Fm./ Lish	05/ 001	40/ 095	49/ 265		Oblique Compression
		B248*	Barakar Fm./ Gish	29/ 204	23/ 307	51/ 069		Pure Compression
2c	Strike-slip	P129_1*	Talchir Fm./ Lish	02/ 006	63/ 099	27/ 275		Pure Strike-slip
		B303_3*	Barakar Fm./ Mangzing	26/ 174	62/ 018	10/ 269		Pure Strike-slip
		U148	Upper Siwalik/ Lish	08/ 031	67/ 141	22/ 298		Pure Strike-slip

Table. 1. Reduced stress tensors obtained from fault-slip analysis for main stages of deformation in the foothill Darjeeling Himalaya. Principal stresses, σ1-σ2-σ3 orientations after tilt correction, except those subsets with asterix marks. Prefix in subset numbers related to distinctive lithounits: D = Daling, P = Talchir Formation, B = Barakar Formation, M = Middle Siwalik, U = Upper Siwalik; numerical digits for location number and suffix _1/2/3 represent subsets extracted from raw measurements in individual locations. Solid arrows for maximum principal compression (σ1) and unfilled arrows for minimum principal compression (σ3)

References

Delvaux D, Sperner B (2003) New aspects of tectonic stress inversion with reference to the TENSOR program. In: Nieuwland DA (Ed.) New Insights into Structural Interpretation and Modeling. Geol Soc London Spec Publ 212: 75-100.

Kreemer C, Holt WE, Haines AJ (2003) An integrated global model of present-day plate motions and plate boundary deformation. Geophys J Int 154: 8-34.

Mitra G, Bhattacharyya K, Mukul M (2010) The Lesser Himalayan Duplex in Sikkim: Implications for Variations in Himalayan Shortening. J Geol Soc India 75: 289-301.

Mukul M (2000) The geometry and kinematics of the Main Boundary Thrust and related neotectonics in the Darjiling Himalayan fold-and-thrust belt, West Bengal, India. J Struct Geol 22: 1261-1283.

Pascoe EH (1959) A Manual of The Geology of India and Burma. GSI 16 II, Gov of India Press: 485-1338.

Roy KK (1976) Some problems of stratigraphy and tectonics of the Darjeeling and Sikkim Himalayas. GSI Misc Publ 24: 379-394.

The petrogenesis of kyanite leucogranites in Bhutan, Eastern Himalaya

Phillips S[1], Argles T[1], Harris N[1], Warren C[1], Roberts N[2]

[1]The Open Univ., Milton Keynes, UK [2]NERC Isotope Geosciences Laboratory, British Geological Survey, Nottingham, UK

Dramatic exhumation of high-grade rocks from orogenic cores is commonly explained by variants of the “channel flow” model (Beaumont et al. 2001). This model requires weakening of the mid-crust via partial melting to trigger the change from burial to exhumation. The evidence for this melting is often sparse and is commonly overprinted by subsequent deformation, recrystallisation and decompression melting. Prograde crustal melts, or cryptic evidence of them, are however being increasingly reported in the Himalaya, in kyanite-grade rocks of the Greater Himalayan Series (GHS) (Groppo et al. 2010; Iaccarino et al. 2015; Imayama et al. 2012; Prince et al. 2001; Rubato et al. 2013). These leucogranites are commonly formed during the Oligocene, thus pre-dating the more voluminous and better-studied Miocene granites that formed through decompression melting. This implies that the formation of these Oligocene leucogranites weakened the mid-crust, and thus was the driver of the change from the burial of the GHS to its rapid exhumation.

Deformed kyanite leucogranites from eastern Bhutan are found at the deepest structural levels of the Greater Himalayan Series in kyanite-grade biotite schists just above the Main Central Thrust (MCT). Field observations indicate that they are small-scale, cm-dm sized lenses of melt that formed in situ within the host schists. Thin section textures reveal evidence for both prograde and retrograde mineral reactions. Individual kyanite grains have been further investigated using cathodoluminescence (CL) imaging combined with trace element mapping and spot analysis (Kendrick and Indares 2017).

Kyanite in the schist is commonly tabular in shape with complex internal structures revealed by CL imaging. In the leucosome adjacent to the schist, kyanite grains show similar internal textures, but have corroded, skeletal shapes which are rimmed by optically continuous “moats” of coarse muscovite. We interpret these kyanite crystals to be xenocrysts incorporated into the melt from the schist, thus inheriting the complex texture of the kyanite from the schist. The muscovite rim is interpreted to be a late-stage reaction product due to the back-reaction between kyanite and the melt, a reversal of the dry muscovite dehydration reaction. Also found in the leucosome, typically further away from the schist margin, are thin, bladed kyanite crystals with little to no internal zonation. These crystals are thought to represent “igneous” kyanite that formed either peritectically or by crystallisation from the melt.

To further characterise these different mineral populations, kyanite and muscovite trace element concentrations will be analysed by EPMA and LA-ICP-MS. This will bring greater insight to what is controlling the complex kyanite internal CL textures and will further elucidate the reaction history preserved in these rocks. Understanding the genesis of the kyanite is important for constraining future P-T-t modelling of the leucogranites and is crucial for the tectonic interpretation of these melts as drivers for the exhumation of the orogenic mid-crust.

References

Beaumont C, Jamieson RA, Nguyen MH, Lee B (2001) Himalayan tectonics explained by extrusion of a low-viscosity crustal channel coupled to focused surface denudation. Nature 414: 738-742.

Groppo C, Rubatto D, Rolfo F, Lombardo B (2010) Early Oligocene partial melting in the Main Central Thrust Zone (Arun valley, eastern Nepal Himalaya). Lithos 118: 287-301.

Iaccarino S, Montomoli C, Carosi R, Massonne HJ, Langone A, Visonà D (2015) Pressure–temperature–time–deformation path of kyanite-bearing migmatitic paragneiss in the Kali Gandaki valley (Central Nepal): investigation of Late Eocene-Early Oligocene melting processes. Lithos 231: 103-121.

Imayama T, Takeshita T, Yi K, Cho D.L, Kitajima K, Tsutsumi Y, Kayama M, Nishido H, Okumura T, Yagi K, Itaya T, Sano Y (2012) Two-stage partial melting and contrasting cooling history within the Higher Himalayan Crystalline Sequence in the far-eastern Nepal Himalaya. Lithos 134-135: 1-22.

Kendrick J, Indares A (2017) The reaction history of kyanite in high-P aluminous granulites. J Metam Geol 36: 125-146.

Prince C, Harris N, Vance D (2001) Fluid-enhanced melting during prograde metamorphism. J Geol Soc 158: 233-242.

Rubatto D, Chakraborty S, Dasgupta S (2013) Timescales of crustal melting in the Higher Himalayan crystallines (Sikkim, Eastern Himalaya) inferred from trace element-constrained monazite and zircon chronology. Contrib Mineral Petrol 165: 349-372.

The ASTER data is used to predict ore prospecting in Liuyuan area of Gansu Province

Ping Z[1]

[1]*The China Unversity of Geoscience, Beijing, China*

The Liu Yuan area in Gansu province is located on the Heishan–Xianquanzi deep fault zone with many hydrothermal deposits. In this paper, by using ASTER data and principle component analysis (PCA) method, the mineralized anomalies such as iron staining, hydroxy alteration and carbonation are extracted, and the abundances of SiO_2 abundances are obtained by quantitative inversion of the abundances. Combined with previous geological data and field verification, it is found that the coincidence between the results of remote sensing mineralization anomalies and the actual situation can reach 88.9%. In the end, 2 metallogenic target areas have been successfully delineated in combination with the origin theory of known deposits, regional tectonic analysis and lithologic distribution, which provides a scientific basis for prospecting and prospecting in this area.

Tectonic development of Potwar Plateau and Salt Range, NW Himalayas, Pakistan

Qayyum A[1], Willem Poesse J[2], Ahsan N[3], Kaymakci N[1], Langereis C[2]

[1]Dept. of Geological Engineering, Middle East Technical Univ., Ankara, Turkey [2]Paleomagnetic Laboratory Fort Hoofddiijk, Utrecht Univ., The Netherlands [3]Inst. of Geology, Univ. of the Punjab, Lahore, Pakistan

Potwar and Salt Range (see map below) formed as a result of ongoing convergence and indentation of Indian Plate into the Eurasian Plate. Tectonic loading and resultant tectonic wedge developed a décollement surface at Eo-Cambrian evaporites on the Indian shield. We have sampled Oligocene to recent sediments for paleomagnetic purpose at 86 different locations to check the vertical axis rotations in the tectonic wedge. The results have shown that 10 to 30 degrees counter clockwise rotations are observed in the Potwar Plateau and Salt Range. The age of the rotations are calibrated by magnetostratigraphic studies. The Anisotropy of magnetic susceptibility (AMS) studies were carried on the same samples, before demagnetization procedure, and the results are compared with the paleostress configurations obtained from fault slip data obtained from the fault planes in the field. Results show that major principal stress axis (σ1) in the Potwar Plateau and the Salt Range changes from NNW to NNE. We also combined balanced cross-sections based on seismic interpretations on several key seismic lines orthogonal to the main structures in the region. It is observed that Salt Range Thrust is developed due to a basement step at the leading edge of the Potwar Plateau which obstructed further southern movement and resulted N-S shortening of the plateau. The eastern and western margins of the plateau and the Salt Range is delimited by two major strike slip faults that acted as lateral ramps accommodating their southwards motion.

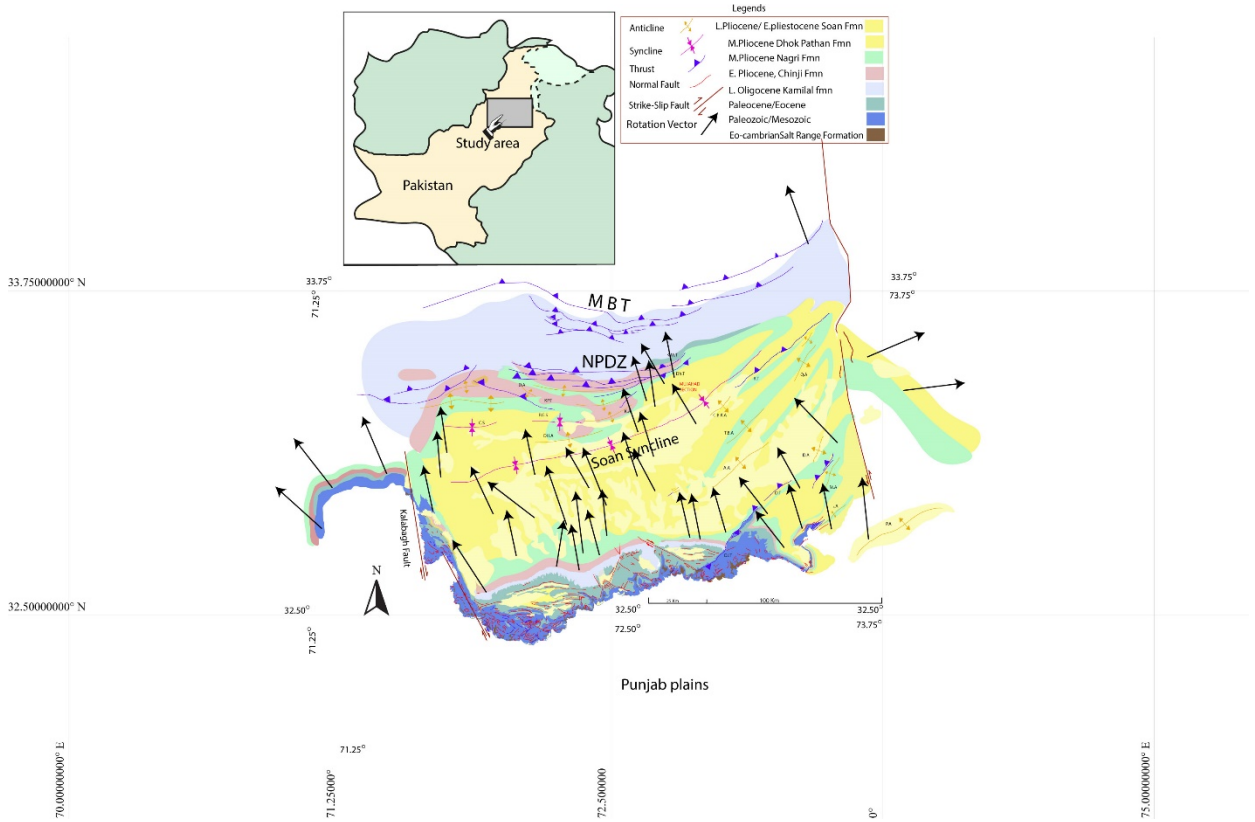

The medieval cluster of great earthquakes: Implications for earthquake recurrence in the Central Himalaya

Rajendran CP[1], Rajendran K[2], John B[3], Sanwal J[1], Karthikeyan A[1]

[1]Jawaharlal Nehru Centre for Advanced Scientific Research, Bangalore, India [2]Indian Inst. of Science, Bangalore, India [3]National Inst. of Rock Mechanics, India

The timing and size of the last great earthquake in the central Himalaya continues to excite scientific interest, and the paleoseismological studies in the region often reaching conflicting conclusions. Here we review the available database from the region to determine the timing of the last faulting event on the frontal thrust of the central Himalaya and how the overlapping segments in the region have been behaving in terms of generating large and great earthquakes. From the historic perspective, the Indian sources hint at a restoration phase for the mid-14th century monuments located in Delhi and a contemporaneous destruction to the ancient temples located in the central Indian Himalaya. The constraints generated from such earthquake proxies and the data from multiple trenches across the frontal thrust in the central Himalaya converge on a mid-14th century rupture that extends for a length of about 600 km of the central Indian Himalaya, with an average slip of 15 m, consistent with moment magnitude of Mw 8.5. The regional data from Nepal and India, in general, indicate evidence for a medieval cluster of great earthquakes (14th, 13th and 11th centuries) spreading across the adjacent segments along the central Himalayan front, followed by quiescence extending to the present. The medieval cluster of great earthquakes within the central Himalaya indicates episodic nature of earthquake occurrence separated by long temporal gap of 700 to 1000 years.

Assessing the rupture modes of the Himalayan earthquakes: Historical and recent examples

Rajendran K[1], Mozhikunnath Parameswaran R[2], Rajendran CP[2]

[1]Centre for Earth Sciences, Indian Inst. of Science, Bangalore, India [2]Jawaharlal Nehru Centre for Advanced Scientific Research, Bangalore, India

The Himalaya, a product of the Indo-Eurasian plate collision is seismically productive in terms of generating large and great earthquakes. Notable among the seismogenic structures of this plate boundary are the Main Frontal Thrust (MFT), the Chaman Fault (CF), the Sagaing Fault (SF), and the western and eastern syntaxes. The prolonged ongoing lull in the generation of great earthquakes, as against the postulated slip deficit in the central segment of the Himalaya has remained a point of discussion. The earliest and widely discussed model adopts a mechanism wherein great earthquakes originate on the Main Himalayan Thrust (MHT) and the rupture propagates up-dip in the southward direction, sometimes rupturing the MFT or ending up as a blind thrust. Recent understanding of the source zones of some of the historical earthquakes (1803, 1833, 1905, and 1934), however, provides some contrarian arguments about the existence of surface ruptures. The source models of the well-studied MHT earthquakes imply southeastward-directed slip (e.g. Gorkha 2015 Mw 7.8, Uttarkashi 1991 Mw 6.8, and Chamoli 1999 Mw 6.5), concurring also with their postulated origin on the MHT. The 2005 Mw 7.6 Kashmir earthquake on the other hand was associated with an out-of-sequence thrust, and also broke the surface. An analysis of the source models of the modern-day earthquakes provides some insights into their varied rupture mechanisms. We find that not all ruptures sourced on the MHT are necessarily related all the way to the MFT (as with the 2015 event), while those sourced on the out-of-sequence thrust systems may lead to significant surface deformation. These variable rupture modes of the earthquakes need to be taken into account in any effort towards constraining the Himalayan seismogenesis.

Metamorphism and CO_2-production in collisional orogens: Case studies from the Himalayas

Rapa G[1], Groppo C[1,2], Rolfo F[1,2], Mosca P[2]

[1]Univ. of Torino, Italy [2]CNR, Ist. di Geoscienze e Georisorse, Italy

The aim of this contribution is to achieve a deeper understanding of the role exerted by the Himalayan orogeny on the long-term global carbon cycle, clarifying the abundance, distribution and types of CO_2-source rocks in selected sectors of the Himalayan orogen, the nature of the metamorphic CO_2-producing reactions, the amounts of CO_2 produced and the chronology of these reactions.

In the Lesser and Greater Himalayan Sequence (LHS and GHS), three different chemical groups of CO_2-source rocks have been recognized, and they can be described in terms of relatively complex chemical systems: (1) CFMAST-HC (CaO-FeO-MgO-Al_2O_3-SiO_2-TiO_2-H_2O-CO_2) group, significantly more abundant in the Upper-GHS; (2) NCFMAST-HC (Na_2O-CaO-FeO-MgO-Al_2O_3-SiO_2-TiO_2-H_2O-CO_2) and (3) NKCFMAST-HC (Na_2O-K_2O-CaO-FeO-MgO-Al_2O_3-SiO_2-TiO_2-H_2O-CO_2) groups, widespread in both the GHS (Lower-GHS and Upper-GHS) and LHS. In all groups, mineral assemblages vary with increasing metamorphic grade from lower to upper structural levels. Different petrographic types have been distinguished for each chemical group, based on the mineral assemblages (i.e. Types 1A to 1D; Types 2A-2B; Types 3A to 3F).

The phase petrology approach was used to investigate the most relevant CO_2-producing reactions in different types of CO_2-source rocks (Types 1C, 3C and 3F) and to quantify the amounts of CO_2 that were released through these reactions. Decarbonation reactions were modelled using different types of phase diagrams: P/T-XCO_2 pseudosections, P/T-XCO_2 sections and mixed-volatile P-T phase diagrams.

In Type 1C rocks (likely derived from bentonite), the CO_2-producing process was a continuous process and mostly occurred at relatively high-T conditions. The final CO_2 production was < 1 wt%, and more likely almost negligible. In Type 3C rocks (derived from carbonate-rich pelite) the CO_2 productivity was < 3.5 wt% and the majority of CO_2 was released through continuous reactions occurred at relatively low P-T conditions, during the early prograde evolution. In Type 3F lithologies (derived from marly protoliths) CO_2 was produced through distinct, short-lived events, which occurred at specific P-T conditions along the whole prograde metamorphic evolution, and especially at relatively high-T. The predicted amounts of produced CO_2 are quite high (2-8 wt%). Most of the CO_2-producing reactions modelled in the Type 3F CO_2-source rocks also produced titanite.

The results of thermometric determinations (Zr-in-Ttn thermometry) and U-Pb geochronology suggest that titanite grains in type 3F lithologies grew during two nearly consecutive episodes of titanite formation: a near-peak event at 730-740°C, 10 kbar, 30-26 Ma, and a peak event at 740-765°C, 10.5 kbar, 25-20 Ma (Rapa et al. 2017).

A first-order extrapolation of such CO_2 amounts to the orogen scale provides metamorphic CO_2 fluxes ranging between 1.4 and 19.4 Mt/yr; this estimated metamorphic CO_2 flux is of the same order of magnitude as present-day degassing from hot springs, thus suggesting that CO_2-producing processes similar to those occurred in the past still occur along the active Himalayan orogen, and should be considered in any future attempts of estimating the global budget of non-volcanic carbon fluxes from the lithosphere.

Reference

Rapa G, Groppo C, Rolfo F, Petrelli M, Mosca P, Perugini D (2017) Titanite-bearing calc-silicate rocks constrain timing, duration and magnitude of metamorphic CO2 degassing in the Himalayan belt. Lithos 292-293: 364-378.

Natural Hazards and their impacts on downstream areas in Nepal Himalaya

Regmi D[1], Kargel J[2]

[1]The Himalayan Research Expeditions Pvt. Ltd., Kathmandu, Nepal [2]Planetary Science Inst., Tucson, USA

Nepal, which represents the highest elevation difference within the shortest distance, is under the threat of several types of natural hazards in different elevation zones. Every year different type of natural hazards claim lives as well as property worth millions of dollars. With the rise is temperature and changing precipitation patterns, the natural Earth surface process activities such as avalanches, rock falls, landslides, Glacial Lake Outburst Floods (GLOFs), and other floods are becoming more intensive in recent years. There are more than 2000 glacier lakes in Nepal; while most pose no significant hazard to people, a comparative few are very dangerous, such as Tso Rolpa, Imja, Barun and Thulagi glacier lakes. The objectives of this study are to present 1) a review of major natural hazards and its impact in downstream area in the recent past; 2) review of prior glacier lake studies that have been carried out in the Nepal Himalaya; 3) recent research results, including bathymetric studies of the lakes; 3) a summary of possible infrastructure damages, especially multi-million-dollar hydropower projects, that are under threat of GLOFs; 4) the outcome of the recently completed Imja lake lowering project, which is the highest altitude lake ever controlled by lowering the water level. This project is being undertaken as a response to a scientific ground-based bathymetric and geophysical survey funded by the United Nations Development Program. The objective of the Imja Lake GLOF mitigation project was to lower the water level by three meters to reduce the lake volume, increase the freeboard, and improve the safety of tourism, downstream communities, and the infrastructure of Nepal's Everest region. This GLOF mitigation step taken by Nepal's government to reduce the risk of an outburst flood is a good step to reduce the chances of a GLOF or the magnitude of a disaster if a GLOF nonetheless occurs despite our best efforts. We will also present the prospects for the future of Imja and Thulagi lakes, including an outline of possible steps that could further reduce the hazards faced by downstream communities and infrastructure.

Recent activity on the Main Boundary Thrust in western Nepal: Neo-tectonic constraints from high-resolution Pleiades satellite images

Riesner M[1], Bollinger L[2], Hubbard J[1], Guérin C[2], Almeida R[1], Bradley K[1], Sapkota S[3], Tapponnier P[1]

[1]Nanyang Technological Univ., Singapore [2]CEA, France [3]Dept. of Mines and Geology, Kathmandu, Nepal

The largest (M8+) known earthquakes in the Himalaya have ruptured the upper locked segment of the Main Himalayan Thrust zone, producing slip at the surface along the Main Frontal Thrust at the range front. This active deformation has been well documented, with an emphasis on the more accessible central and eastern Nepal. However, out-of-sequence active structures have received less attention. Here, we focus on an active fault, with clear geomorphological signature of recent deformation, that closely follows the surface trace of the Main Boundary Thrust (MBT), the Surkhet-Gorahi fault (Nakata 1989). Hossler et al. (2016) used fluvial terraces offset analysis to study slip on this fault and suggested that this fault may have slipped in the great 1505 earthquake that shook western Nepal, but much about this fault remains unclear. Across most of its length, this fault appears geomorphologically as a normal fault, raising questions about why the crust would be extending in the hanging wall of the MHT, whether slip events are linked to larger earthquakes that also rupture the MFT, as suggested by Hossler et al. (2016), and if so, what impact this has on seismic hazards. Here, we study the reactivation of the MBT on a 120 km-long surface trace between Surkhet and Gorahi, using a high-resolution Digital Elevation Model generated from pairs of very high-resolution Pleiades images in order to map the fault scarp and the terrace incision to quantify tectonic uplift.

References

Hossler T, Bollinger L, Sapkota SN, Lavé J, Gupta RM, Kandel TP (2016) Surface ruptures of large Himalayan earthquakes in western Nepal: evidence along a reactivated strand of the Main Boundary Thrust. Earth Planet Sci Lett 434: 187-196.

Nakata T (1989) Active faults of the Himalaya of India and Nepal. GSA Spec Paper 232: 243-264.

Geologic mapping, modelling, and kinematic reconstructions from far-western Nepal

Robinson D[1], McQuarrie N[2], Battistella C[1], Ghoshal S[2]

[1]Dept. of Geological Sciences, The Univ. of Alabama, Tuscaloosa, USA [2]Univ. of Pittsburgh, USA

New geologic mapping in far western Nepal is combined with existing geochronologic, thermochronologic and sedimentology data as well as ongoing thermokinematic modelling to produce an integrated view of the tectonic evolution of far western Nepal. We have drawn multiple balanced cross sections, and kinematic models are produced from these reconstructed sections. The reconstructed sections are then sequentially deformed in ~10 km increments with flexural loading and erosional isostatic unloading applied to each step, which are then combined with thermokinematic modelling to determine the most correct cross section. We produce cross sections that agree with all the available data in far western Nepal. In addition, we will discuss how the geologic data in far western Nepal integrates with data from Kumaon, northwest India.

Incorporating geochronologic and thermochronologic data with geologic mapping in far western Nepal: Implications for tectonic models

Robinson D[1], McQuarrie N[2], Battistella C[1], Ghoshal S[2]

[1]Dept. of Geological Sciences, The Univ. of Alabama, Tuscaloosa, USA [2]Univ. of Pittsburgh, USA

Robinson et al. (2006) present a geologic map and tectonic model for far western Nepal between the Indian border and west of the Karnali River. The map was approximately 200 km^2 and had very little geochronologic and thermochronologic data. Since 2006, a wealth of data have been produced and published both in the thrust belt rocks and in the synorogenic sedimentary rocks as well as additional geologic mapping. It is time to update what is known of this remote part of the Himalayan thrust belt. We present an integrated view of the existing published geochronologic and thermochronologic ages and discuss the viability of the 2006 critical taper model, analyse the fit of other tectonics models and possible deviations as necessitated by these new data. We also present new mapping and data in Kumaon, northwest India, and discuss how the geologic data in far western Nepal integrates with northwest India.

Reference

Robinson DM, Decelles PG, Copeland P (2006) Tectonic evolution of the Himalayan thrust belt in western Nepal: Implications for channel flow models. GSA Bull 118: 865-885.

The Shikar Beh nappe: An enigmatic but factual NE-verging structure in the NW Indian Himalaya – In honour of Albrecht Steck

Robyr M[1]

[1]*ISTE, FGSE, Univ. of Lausanne, Switzerland*

From the early eighties, Prof Steck and collaborators undertook to unravel the geological framework of a complete and continuous traverse across the NW Indian Himalaya, from the Indus suture zone to the frontal part of the belt. Over the last 35 years, several segments along the initial transect have been investigated by his research group using a multidisciplinary approach combining mapping, structural analyses, metamorphic petrology, and geochronology. Through his long term commitment to detailed studies in the northwestern Himalaya, Prof Steck has contributed greatly to our understanding of not only the Himalaya, but of collisional process and mountains building in general. One of his major impacts in our understanding of the Himalayan geology of NW India is the highlighting of an early NE-directed Eohimalayan phase of metamorphism and deformation associated with the emplacement of a thrust sheet that he termed the Shikar Beh nappe.

NE-vergent folds and thrust faults are an enigmatic feature of the High Himalayan Crystalline in NW India, as these structures are in marked contrast to the SW-directed thrusts and fold vergences that predominate in the rest of the Himalaya since the continental collision between India and Asia. It is however still controversial whether these unusual NE-vergent structures reflect local heterogeneities in strain during the main SW-vergent deformation, or whether they are associated with a postulated NE-directed early Eocene deformation phase collectively termed the Shikar Beh nappe. Some groups working in the region did not recognize the Shikar Beh nappe and the existence of this early Eocene NE-directed deformation phase is still questioned.

Recent investigations along the Miyar Valley (Upper Lahul) provide evidences attesting that the metasediments forming now the High Himalayan Crystalline of NW India have been affected by a NE-directed crustal thickening phase. This tectono-metamorphic event is well recorded as sigmoidal inclusion trails in garnet porphyroblasts indicating a NE-directed sense of shearing during garnet growth. In addition, microstructural analysis and monazite geochronology along the Miyar Valley section reveal that this deformational phase occurred before 40 Ma, likely slightly after continental collision at ca. 55 Ma. These data clearly identify that the kinematic evolution of the High Himalayan Crystalline in NW India was initially controlled by an early Eocene NE-directed crustal thickening phase attesting the statement made by Prof Steck 25 years ago. Consequently, the SW-verging kinematic evolution widely accepted for the High Himalayan Crystalline in the central and eastern Himalayan sections should be reconsidered for the western part of the Indian Himalaya. In a broader sense, these data reveal that crustal shortening during the initial stage of continental subduction is not exclusively accommodated by foreland-directed folding and thrusting but may also be adapted by deformation involving opposite-directed vergence.

High Central Tibet at the onset of Indo-Asian collision derived from leaf-wax hydrogen and palynology data

Rohrmann A[1], Barbolini N[2], Meijer N[1], Yang Z[3], Dupont-Nivet G[4]

[1]Inst. of Earth and Environmental Science, Univ. of Potsdam, Germany [2]Inst. for Biodiversity and Ecosystem Dynamics, Univ. of Amsterdam, The Netherlands [3]School of Earth and Space Sciences, Peking Univ., Bejing, China [4]Geosciences Rennes, Univ. of Rennes, France

Reconstructions of topographic growth of mountain belts increasingly rely on leaf-wax hydrogen isotope data (δDwax), a paleo-hydrology proxy obtained from organic material in sedimentary rocks. In Tibet common to many models of plateau formation is the assumption that most of the plateau was near sea level prior to the India-Asia collision at 55-50 Ma, and that the plateau grew northward and eastward away from the Indus-Yarlung suture. Instead, over the recent years a growing body of evidence implies that plateau-like conditions began to develop in central Tibet during the Late Cretaceous and were regionally extensive no later than 45 Ma. Investigation into the early Tibetan Plateau formation history is hampered by the lack of sediments covering this time period suitable for the reconstruction of topography.

Here, we present δDwax results and new palynoassemblages recovered from the Nangqian Basin sediments of east-central Tibet (32°08'N, 96°30'E) to reconstruct the paleoelevation and eco-hydrologic conditions at that time. Previously, the studied fluviolacustrine deposits were assigned a mid-Cretaceous age, however, our new palynological evidence combined with magnetostratigraphy indicate a pre-50 Ma Paleogene age (66-56 Ma). The obtained δDwax record ranges from -194 to -219‰ with a marked negative shift within the middle of the section. We show that the Nangqian Basin at the time possessed: (a) near modern topography of ca. 3.5 km based on our δDwax data; (b) abundant high-altitude gymnosperms; and (c) eco-hydrological conditions of a wetter climate than today. We also compare our δDwax results from the Nangqian Basin with time-equivalent δDwax data from the low-elevation Xining Basin located towards the NE. We observe a 30‰ difference in δDwax that suggest a ca. 1.5-2 km elevation difference between both basins, assuming a modern water-isotope lapse rate. Our results highlight the existence of Paleogene high elevation in central Tibet and corroborate the idea of the establishment of an Andean-style plateau in central Tibet at the onset of collision.

Tibetan Plateau paleolatitude and tectonic rotations: Paleomagnetic constraints

Roperch P[1], Dupont-Nivet G[1,2], Guillot S[3], Goussin F[3], Huang W[4], Replumaz A[3], Yang Z[5]

[1]Geosciences Rennes, CNRS, Univ. of Rennes, France [2]Inst. of Earth and Environmental Science, Univ. of Potsdam, Germany [3]ISTerre, Univ. Grenoble-Alpes, France [4]Univ. of Rochester, USA [5]Peking Univ., China

Knowledge of the latitudinal position of the southern margin of Asia in the Paleogene is fundamental to understanding the India-Asia collision and associated N-S convergence and shortening. Paleomagnetism is in principle the perfect tool for that. Unfortunately, in Asia the persistence of seemingly too low inclinations by 10-15° from 50-30 Ma hinders precise paleolatitude determinations and has given rise to different reference Paleomagnetic poles (APWP). Some authors compare their data with the expected direction from the APWP of stable Eurasia (Torsvik et al. 2012). Others use the APWP for the deformed Eurasia (Cogné et al. 2013). This results in conflicting reports about the timing and paleomagnetically-derived magnitude of shortening in Tibet. In addition, sedimentary datasets are either corrected or not corrected for depositional inclination shallowing that can often amount to more than 15 to 20°. Close inspection of previously published data for Tibet clearly indicates that the largest inclination anomalies arise from Cenozoic continental red bed sequences with magnetizations of detrital origin affected by inclination shallowing that should either not be used or properly corrected prior to further estimates of N-S shortening.

To constrain the paleolatitude and rotation of the Central Tibetan Plateau, supposedly uplifted and rotated in the early stage of the collision, we obtained paleomagnetic results from 2 distinct volcanic fields, unaffected by inclination shallowing, from the Eastern Qiangtang terrane (~32°N, 96°W) that are complemented by a thorough review of existing regional paleomagnetic data.

The oldest one (Xialaxiu) dated at ~50 Ma is located 50 km north of the Nangqian volcanic field (~37-39 Ma) (Spurlin et al. 2005). Additional paleomagnetic results from Paleogene sedimentary basins are used to better constrain the timing and spatial variations of tectonic rotations within the region. Clockwise rotations are spatially variables and associated with strike-slip deformation that started at the time of volcanic emplacement. The results do not support a regional rotation of Eastern Qiantang. Paleomagnetic results in the Nangqian basin indicate that primary magnetization in Eocene red beds record a ~13° latitude anomaly compared to the ~37 Ma volcanics.

Compared to the stable Eurasia APWP, results from Nangqian provide paleolatitude lower than expected by ~7° of which 2 to 4° can possibly be accounted by NS shortening north of Nangqian since the late Eocene. On the other hand, the deformed Eurasia APWP provides lower expected inclinations than the Nangqian observations. This suggests that the proposed deformation between Eastern and Western Eurasia has been overestimated.

References

Cogne JP, Besse J, Chen Y, Hankard F (2013) A new Late Cretaceous to Present APWP for Asia and its implications for paleomagnetic shallow inclinations in Central Asia and Cenozoic Eurasian plate deformation. Geophys J Int 192: 1000-1024.

Spurlin MS, Yin A, Horton BK, Zhou J, Wang J (2005) Structural evolution of the Yushu-Nangqian region and its relationship to syncollisional igneous activity, east-central Tibet. GSA Bull 117: 1293-1317.

Torsvik TH, van der Voo R, Preeden U, Mac Niocaill C, Steinberger B, Doubrovine PV, van Hinsbergen DJJ, Domeier M, Gaina C, Tohver E, Meert JG, McCausland PJA, Cocks LRM (2012) Phanerozoic polar wander, palaeogeography and dynamics. Earth-Sci Rev 114: 325-368.

Brittle structures and liquefaction features in Mio-Pliocene strata in the foothill Darjeeling Himalaya: Are these seismogenic?

Saha D[1], Patra A[1]

[1]Indian Statistical Inst., Kolkata, India

Historical records are replete with earthquakes (M 4-7) in Darjeeling-Sikkim Himalaya as in other parts of the active orogen. Historical earthquakes leave signs of damage to life and property and widespread liquefaction features in the Holocene sediments. However, geologically older events must be read from rock records. We present some brittle deformation features in Mio-Pliocene Siwalik rocks now occurring as folded/tilted strata within thrust sheets bounded by the Main Boundary Thrust (MBT), its splays and the Main Frontal Thrust in Eastern Himalaya. Some of these may be potential paleoseismic indicators for Mio-Pliocene and younger earthquakes.

The Middle Siwalik sandstones in river sections cutting across the MBT and its splays in the foothill Darjeeling Himalaya often show soft sediment deformation structures ranging from ball and pillow, load casts, sand dyke, lateral sand injection, cm-m scale faults and associated broken strata, and small growth faults (Fig. 1a-b). While such structures can well be interpreted as a consequence of fast sedimentation and fluid entrapment, these are spatially close to the then active fault like the MBT formed under compressive regime. Occurrence of such structures cover strike length of ~30 km and are restricted to a stratigraphic interval (upper part of Middle Siwalik) indicating deformation events of short duration but wide areal extent within the depositional system. Signatures of liquefaction and fluidization, and their recurrent occurrence within a short stratigraphic interval within shallow water sedimentary strata of the middle Siwalik subgroup (fluvial to tidal-intertidal) suggest possible seismic trigger. Given the magnetostratigraphic age constraint of Middle Siwalik in the Eastern Himalaya (Chirouze et al. 2012), the synsedimentary liquefaction/fluidisation events would be around 10 Ma.

Post-lithification brittle deformation structures are observed in Gondwana and Siwalik strata in the vicinity of the MBT and its splay. Two strands of north dipping faults, MBT-1 and MBT-2, border the Gondwana thrust slice. The Siwalik rocks occur in the footwall of the MBT-2. Mesoscopic faults with displacement on mm to cm scale offset strata in both the rock groups. While the deformation may be partly aseismic, the deformation bands in the vicinity of the MBT-2 contain cataclasite/gouge with grain scale textures of pulverization (Fig. 1c-d; Dor et al. 2006; Rockwell et al. 2009). The cataclasite seams, particularly those with fine matrix, show small apophyses cutting into the wall rock. While the cataclasite bands with porphyroclasts show angular clasts with intragranular fractures, the fine quartz clasts in ultracataclasite show considerable rounding, and are set in a very fine to clayey matrix, locally with spaced foliation. These deformation bands of different orientations are locally associated with slickensides and show mutual offset and microfaults in larger clasts, indicating shearing deformation. The fault rock textures are similar to those obtained from the neighbourhood of seismogenic faults, for example San Andreas Fault and San Jacinto Fault strands (e.g. Whearty et al. 2017). We suggest possible cyclic switch between aseismic brittle slip and seismic damage in controlling long term evolution of the fault zone rocks associated with MBT-1 and MBT-2.

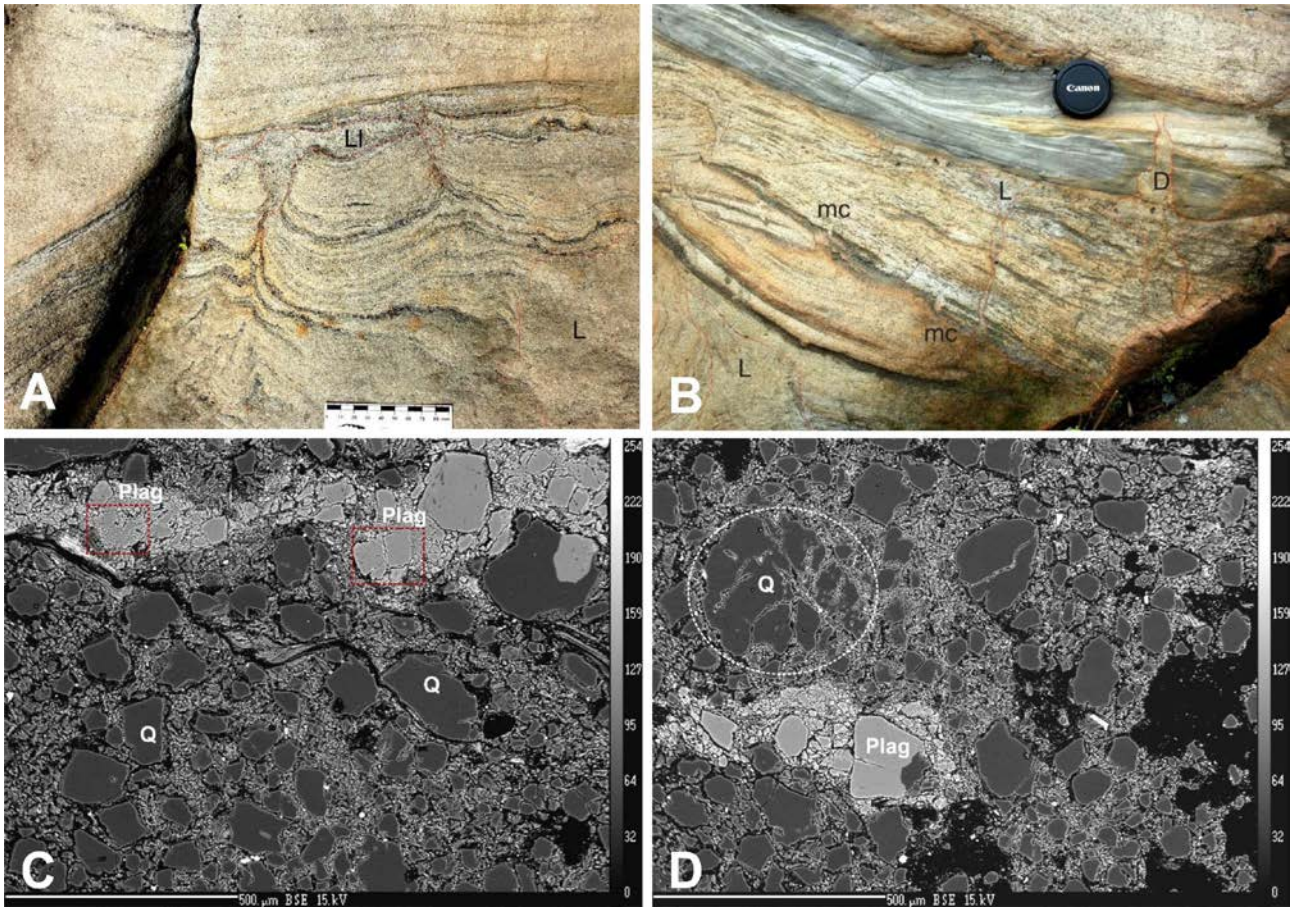

Figure 1. Liquefaction and brittle deformation features in Siwaliks and stones triggered by past earthquakes. (A) Liquefaction (L) and soft sediment deformation; note lateral injection (Ll) of massive sand capped by a thin relatively impermeable layer. (B) Liquefaction below a thicker muddy layer (dark grey), small faults (dash-dot lines) and sand dyke (D) cutting the muddy layer; note sand filled mud cracks (mc). (C) Pulverization in plagioclase (Plag) clasts in boxed areas; note dispersed fragmentary quartz (Q) clasts well separated by finer matrix due to slow shearing deformation. (D) Pulverization in large quartz clast; subgrains fit as in a zig-saw puzzle. (a)-(b) outcrop photos, (c)-(d) BSE images.

References

Chirouze F, Dupont-Nivet G, Huyghe P, van der Beek P, Chakraborti T, Bernet M, Erens V (2012) Magnetostratigraphy of the Neogene Siwalik Group in the far eastern Himalaya: Kameng section, Arunachal Pradesh, India. J Asian Earth Sci 44: 117-135.

Dor O, Ben-Zion Y, Rockwell TK, Brune JK (2006) Pulverized rocks in the Mojave section of the San Andreas fault zone. Earth Planet Sci Lett 245: 642-654.

Rockwell K, Sisk M, Girty GH, Dor O, Wechsler N, Ben-Zion Y (2009) Chemical and physical characteristics of pulverized Tejon Lookout granite adjacent to the San Andreas and Garlock faults: Implications for earthquake physics. Pure Appl Geophys 166: 1725-1746.

Whearty JJ, Rockwell TK, Girty GH (2017) Incipient pulverization at shallow burial depths along the San Jacinto Fault, Southern California. In: Thomas MY, Mitchell TM, Bhat HS (Eds.) Fault Zone Dynamic Processes: evolution of Fault properties During Seismic Rupture. AGU Geophysical Monograph Series 227.

Evidence of early Paleozoic Andean-type orogeny along the northern Indian Plate based on U-Pb zircon dating and geochemistry of granites in northern Pakistan

Sajid M[1], Andersen J[2], Rocholl A[3], Wiedenbeck M[3]

[1]Univ. of Peshawar, Pakistan [2]Camborne School of Mines, Penryn, Cornwall, UK [3]GFZ Potsdam, Germany

The zircon ages and detailed geochemistry of the Utla and Mansehra granites in north-western Pakistan is thoroughly investigated and compared with regional magmatic history of the northern Indian plate. This detailed comparison has led to novel insights about the early Paleozoic magmatism and related tectonism along the northern margin of the Indian plate and the role of this magmatism within the framework of northern Gondwana evolution.

The Precambrian Tanawal formation hosts the Utla and Mansehra granites which are broadly megacrystic, however, fine to medium grained aplites intruding the main granites are also observed. Their early Paleozoic emplacement i.e. 478.8 ± 2.3 Ma and 479.5 ± 5.8 Ma respectively, is revealed by SIMS U-Pb zircon geochronology followed by the intrusion of aplite dykes in 476 ± 4.1 Ma. These granitoids are both S-type and strongly peraluminous (A/CNK values > 1.11). Fractional crystallization as the dominant geochemical process is recorded by the change in composition of plagioclase from the megacrystic granites to aplite dykes, zoned plagioclase megacrysts and the higher silica content of aplite dykes. These two granites are enriched in light rare-earth elements (LREEs), showing similar REE patterns with pronounced negative Eu anomalies. Geochemical modelling indicates that these granites were derived mainly from the partial melting of pelitic sources followed by the evolution of the melt during the fractional crystallization of feldspars, biotite, muscovite, apatite, and/or zircon, with the aplite dykes representing the very last fractionation product. The analogous composition, source rock characteristics and U-Pb geochronology point to an affinity with other Cambro-Ordovician granitoids from the Himalayas (e.g. Tso Morari granites) and northern Gondwana terranes (e.g. western Yunnan).

Based on these observations, this wide-scale magmatism is related to an Andean-type orogenic event in the early Paleozoic that could have been initiated by the subduction of the Proto-Tethys oceanic lithosphere beneath the northern Gondwana continental margin. The supporting evidences include a) coeval radiometric ages for regionally dispersed but geochemically similar magmatic suites, b) the presence of a regionally extensive, unconformable contact marked by conglomerate beds between Cambro-Ordovician strata and older rock units, c) development of metamorphic fabric in the Precambrian strata and d) the unmetamorphosed overlying sedimentary units.

Thermochronological constraints on the tectono-thermal evolution of Dibang valley, Eastern Himalaya

Salvi D[1], Mathew G[1], Borgohain B[1], Pande K[1]

[1]IIT Bombay, India

New in-situ apatite fission track, zircon (U-Th)/He and biotite ($^{40}Ar/^{39}Ar$) temperature thermochronometric data from the Dibang valley are used to constrain the time of emplacement of major thrusts, development of an upper-crustal duplex and formation of dome and basin structure in the Dibang valley of north-east Himalaya. Together with field and petrographic studies, modifications are proposed to the structural cross-section of the Dibang valley. Biotite $^{40}Ar/^{39}Ar$ ages ranging from 24.8-30.6 Ma from the eastern Lohit Plutonic Complex exposed in and around Anini town are inferred to represent exhumation ages for the batholith. Zircon (U-Th)/He ages support previously proposed indications for the formation of four horsebacks forming the high-angled antiformal duplex stack at mid-crustal depths around 10-14 Ma. Thermal history modelling of apatite fission track data indicate that the north-eastern samples located close to Anini town underwent a late Miocene ~10 Ma phase of rapid cooling, followed by slow cooling. This thermal history contrasts with samples in the southwestern Dibang valley that cooled and uplifted rapidly only after ~4 Ma. Older biotite $^{40}Ar/^{39}Ar$ ages from Hunli and 3D thermo-kinematic modelling of the data indicate less mass removal around Hunli than other parts of Dibang valley. These results disagree with the previously proposed ~16.2 km uplift near Hunli. Apatite fission track ages from the Hunli window indicate that the region has witnessed modest uplift of only 4-5 km since ~4 Ma. Brittle duplexing of the lower Lesser Himalayan Sequence at Hunli and upper Lesser Himalayan Sequence at Mayodia caused warping of the overlying litho-units and resulted in the translation of Greater Himalaya Sequence and suture zone rocks westwards towards the foreland. Subsequent erosion resulted in development of the Mayodia klippe and Hunli window.

Role of tectonics on abundance of C3-C4 plants: Evidence from the Mio-Pliocene Siwalik deposits of Central Himalaya

Sanyal P[1], Roy B[1], Ghosh S[1]

[1]*Indian Inst. of Science Education and Research, Kolkata, India*

The collision between Indian and Eurasian plate resulted in building up of Himalaya. Along the southern flanks of the Himalaya, a wedge-shaped basin commonly known as Himalayan foreland basin (HFB) developed in response to flexural loading of the lithosphere by thrust propagation. Foredeep of this basin provided adequate space to accommodate the eroded hinterland sediments carried by the Himalayan Rivers. The sediments deposited in the HFB known as Siwalik Group of sediments. The tectonic activity in the hinterland during the sedimentation strongly influenced the sediment characters, stratigraphy and structure of the foreland. Effects of the hinterland orogeny were reflected in the paleocurrent direction, sedimentation rate. High sediment accumulation in the Bengal fan during Miocene-Pliocene times also confirms exhumation and denudation of the rising Himalayas. However, the sediment accumulation within the foreland basin was not uniform. Continued convergence of India with Eurasia resulted in the southward propagation of fault systems thus affecting the sedimentation of the foreland deposits. During the middle-late Miocene or Pliocene times, active movement along the major thrust planes of Main Boundary Thrust (or MBT) and Main Frontal Thrust (or MFT) resulted in exhumation of the foreland deposits while the sedimentation was going on. Therefore, in comparison to the distal areas, the proximal part of the fluvial megafan would have been elevated. Relatively higher elevation in proximal part would have induced difference in climatic and environmental condition which could have affected the indigenous vegetation.

In order to track the vegetation distribution as a result of surface exhumation, reconstruction of paleovegetation and climate was done from the Siwaliks of Central Himalayas (Surai Khola, Nepal). The carbon isotopic composition of bulk organic matter along with long chain n-alkane and n-alkanoic acid showed enrichment in $\delta^{13}C$ values around ca. 7.5 Ma implying C4 plants expansion. However, from ca. 4 to < 1 Ma, the $\delta^{13}C$ values showed depletion indicating an increase in the abundance of C3 plants. Previously, it was interpreted that increased summer monsoon seasonality favoured expansion of C4 vegetation. In contrast, the rainfall intensity measured from hydrogen isotopic composition of molecular proxies (dD) does not show any direct control in the distribution of vegetation type. The abundance of C3 vegetation increased in an elevated area as a result of accelerated exhumation in the Himalayas and also the Siwaliks. The topographic elevation gave rise to a cool and arid climatic condition which favoured C3 vegetation growth. Further, the Late Miocene-Pliocene signature of the increased C3 vegetation in the Siwalik was also observed in the distal part of the Bengal fan sediments.

Evaluating the role of coseismic landsliding on cosmogenic nuclides, erosion rates, and topographic evolution in mountainous landscapes: A case study of the Mw 7.8 Gorkha earthquake, Nepal

Schide K[1], Lupker M[1], Gallen S[2], Märki L[1], Gajurel A[3], Haghipour N[1], Christl M[4], Willett S[1]

[1]Geological Inst., Dept. of Earth Sciences, ETH Zurich, Switzerland [2]Dept. of Geosciences, Colorado State Univ., Fort Collins, USA [3]Dept. of Geology, Tribhuvan Univ., Kathmandu, Nepal [4]Laboratory of Ion Beam Physics, ETH Zurich, Switzerland

The Mw 7.8 2015 Gorkha earthquake presents a unique opportunity to study the effects of coseismic landsliding on sediment transport and landscape response in the years immediately following a large earthquake. The effects of these infrequent mass wasting events on longer-term erosion rates is still not fully understood and recent studies question whether these large earthquakes build or destroy topography at the orogen-scale (Marc et al. 2016; Parker et al. 2008). In this study, we repeatedly sample river sediments in earthquake affected valleys of central Nepal for terrestrial cosmogenic nuclides (TCN). Assuming landslides mobilize deeper material with lower TCN concentrations, we expect an “earthquake signal” in the export of these lower concentration sediments (West et al. 2014). However, preliminary data do not show such a clear response after the Gorkha earthquake and using our measurements of ^{10}Be in sands and pebbles, we model how concentrations of cosmogenic nuclides respond to coseismic landsliding and longer-term erosion rates. In addition, we measure landslide geometries using high resolution digital surface models created by camera-equipped unmanned aerial vehicles (UAVs) and terrestrial lidar. Comparing landslide volumes with the amount of landslide material in the river channel will allow us to quantify storage on hillslopes and understand the relationship between channel connectivity and export. This project investigates how large, infrequent events effect basin-averaged erosion rates on both long and short timescales.

References

Marc O, Hovius N, Meunier P (2016) The mass balance of earthquakes and earthquake sequences. Geophys Res Let. 43: 1-9.

Parker RN, Densmore AL, Rosser NJ, de Michele M, Li Y, Huang R, Whadcoat S, Petley DN (2011) Mass wasting triggered by the 2008 Wenchuan earthquake is greater than orogenic growth. Nat Geosci 4: 449-452.

West AJ, Hetzel R, Li G, Jin Z, Zhang F, Hilton RG, Densmore AL (2014) Dilution of 10Be in detrital quartz by earthquake-induced landslides: Implications for determining denudation rates and potential to provide insights into landslide sediment dynamics. Earth Planet Sci Lett 396: 143-153.

High differential stress in upper crust is required to maintain the relief of the Tibetan Plateau

Schmalholz S[1], Duretz T[2], Hetényi G[1], Medvedev S[3]

[1]ISTE, FGSE, Univ. of Lausanne, Switzerland [2]Geosciences Rennes, Univ. of Rennes, France [3]Univ. of Oslo, Norway

The magnitudes of differential stress in the lithosphere, and especially the upper crust, are still disputed, primarily due to the difficulty of direct measurements. Stress drops from earthquakes indicate median values < 10 MPa whereas in situ borehole measurements and grain size piezometers indicate values > 100 MPa. Lateral variation of gravitational potential energy (GPE) across significant relief is an alternative approach. Such an analysis indicates stress magnitudes of ca. 100 MPa in average across a 100 km thick lithosphere between the Indian lowland and the Tibetan plateau. We present analytical results, which show that lateral variations in GPE can also cause bending stresses of several hundreds of MPa. To evaluate stress estimates based on GPE variations and to quantify stress magnitudes in the lithosphere, we perform two-dimensional thermomechanical numerical simulations (1) to quantify crustal stress magnitudes that are required to maintain the topographic relief between lowland and plateau for ca. 10 Ma and (2) to quantify the corresponding relative contribution of crustal strength to the total lithospheric strength. The numerical model includes viscoelastoplastic deformation, gravity and heat transfer. The model configuration consists of a lithosphere with normal crustal thickness, mimicking the Indian lowland, and with larger crustal thickness, mimicking the Tibetan plateau. The configuration is based on density fields from the CRUST 1.0 data set and from a geophysically and petrologically constrained density model. The numerical results indicate that maximal values of differential stress in the upper crust must be > 150 MPa, corresponding to a friction angle of ca. 10°, to maintain the relief between India and Tibet for > 10 Ma. Crustal friction angles > 10° generate higher crustal stresses, which, however, do not further decrease the horizontal surface velocity between lowland and plateau and, hence, do not further increase the stability of the plateau with respect to gravitational collapse. The relative contribution of crustal strength to total lithospheric strength varies considerably laterally. In the region between lowland and plateau and inside the plateau the depth-integrated crustal strength is approximately equal to the depth-integrated strength of the mantle lithosphere. Simple analytical formulae predicting the lateral variation of depth-integrated stresses agree with numerically calculated stress fields, which show both the accuracy of the numerical results and the applicability of simple analytical predictions to highly-variable stress fields. Our results indicate that (1) crustal strength is locally equal to mantle lithosphere strength and that (2) crustal stresses must be at least one order of magnitude larger than median stress drops in order to support plateau relief for a duration of ca. 10 Ma.

Evidence for east-west extension across Lake Nam Co, Tibetan Plateau: Results from high-resolution 2D seismic data

Schulze N[1], Spiess V[1], van der Woerd J[2], Daut G[3], Haberzettl T[4], Wang J[5], Zhu L[5]

[1]Univ. of Bremen, Dept. of Geosciences, German y [2]Inst. de Physique du Globe de Strasbourg, CNRS, Univ. of Strasbourg, France [3]Univ. Jena, Inst. of Geography, Germany [4]Univ. of Greifswald, Inst. of Geography and Geology, Germany [5]Chinese Academy of Sciences, Inst. of Tibetan Plateau Research, Beijing, China

It is mostly accepted that north-south crustal shortening and thickening, in a state of isostatic equilibrium, has built the Tibetan Plateau (e.g. Tapponnier et al. 2001) and that a major change in its development occurred long after collision, when north-south trending graben structures developed across southern Tibet (e.g. Armijo et al. 1986). The onset of normal faulting is locally different with estimates ranging from 14 to 2.5 Ma (e.g. Armijo et al. 1986; Blisniuk et al. 2001). Also, rates of normal faulting vary by one or two orders, e.g. 0.1-0.06 mm/yr in the Shuang Hu graben (Blisniuk and Sharp 2003) or 1-2 mm/yr in the Dinggye graben (Kali et al. 2012).

The Nam Co basin is located in the Karakorum-Jiali-Fault Zone, which separates the southern part of the Tibetan Plateau with predominant rifting from the northern part where normal faulting is subordinate to minor strike-slip faulting (Armijo et al. 1986). Nowadays, the basin extents are limited by a chain of hills and the dextral NW-SE Beng Co strike-slip fault towards the north, to the east by a mountain range and the extensional proximal N-S Gulu half-graben, which connects to the sinistral SW-NE strike-slip and normal Damxung fault system of the Nyainqêntanglha Mountain Range in the south (Fig. 1).

Using high-resolution 2D seismic data, acquired in 2016, we were able to reveal a narrowly spaced pattern of normal faults within Lake Nam Co. The fault planes strike mainly N-S and dip steeply with 60°-80° west and east.

By measuring the vertical offset (throw) of the normal faults, two clusters of major faults became visible. The clusters describe two secondary graben structures within the centre of the lake, with fault offsets of up to 40 m. These grabens acted as depocenters for sediments. According to our interpretation the sedimentation rate of deposits younger than Marine Isotope Stage (MIS) 5 age inside the grabens is 1.5 mm/yr in contrast to the sedimentation rate outside the graben structure of 1.1 mm/yr.

By plotting cumulative fault throw versus stratigraphic horizons in T-H-plots, as introduced by Hongxing and Anderson (2007), we were able to assess styles, timing, and kinematic history of the normal faults. The initiation of the tectonic activity started approximately 200-100 ka ago (between MIS 7 and 5). Older sedimentary deposits show post-depositional faulting, while from MIS 5 until Upper Pleistocene times, active synsedimentary faulting takes place. Holocene sediments bury the majority of the faults, indicating a modern inactive tectonic phase.

Calculated cumulative vertical displacement rates of maximal 0.3 mm/yr are in the range of slip-rate measurements of more distributed extension like the Shuang Hu graben in north central Tibet (Blisniuk and Sharp 2003). However, they are distinctly lower than the slip rate of 1-2 mm/yr inferred for normal faults bounding the Gulu or Dinggye graben systems (Kali et al. 2010; Armijo et al. 1986), which is in agreement with the absence of prominent deformation or faulting around Lake Nam Co.

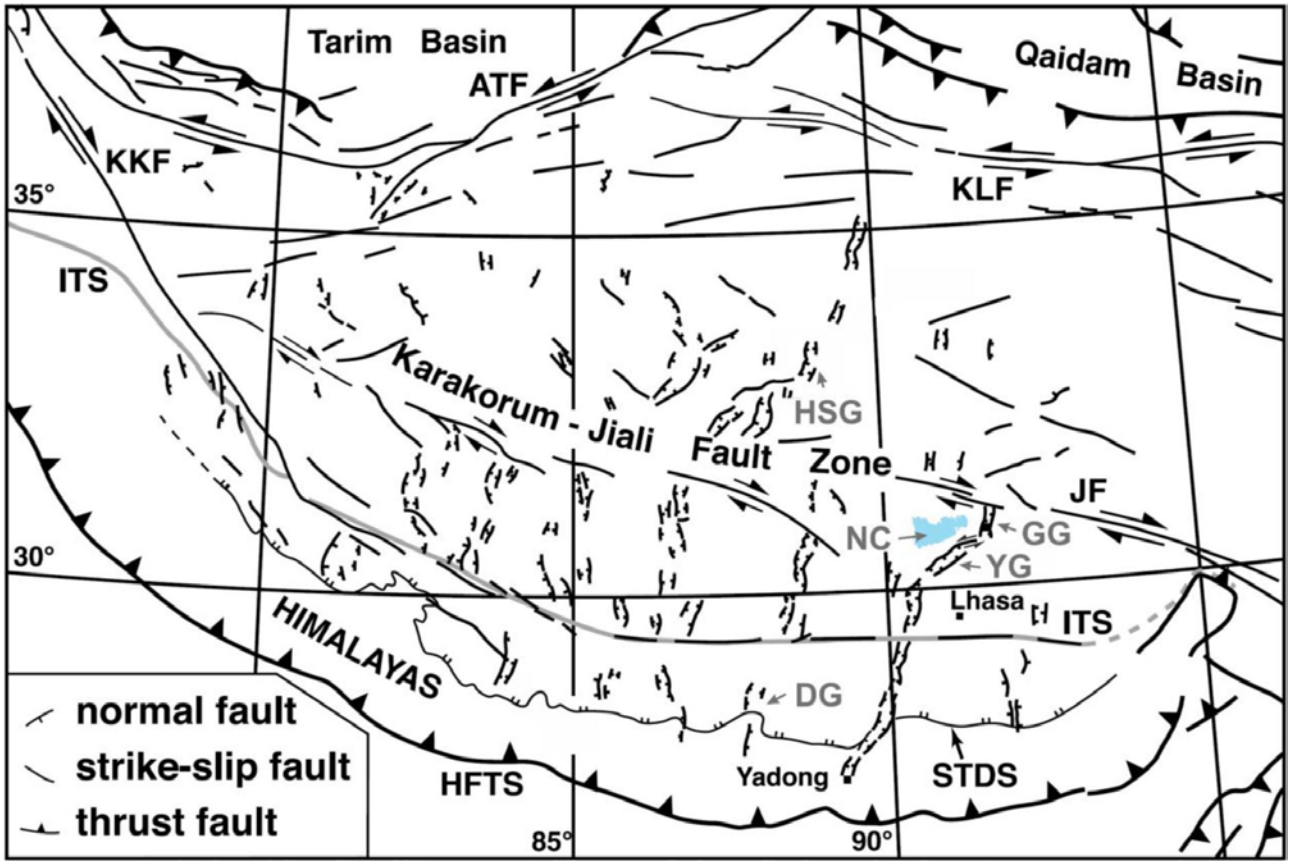

Figure 1: Overview map of the Tibetan Plateau and adjacent regions. Major faults with demonstrated Cenozoic displacement are highlighted Abbreviations: ATF: Altyn Tagh fault, HFTS: Himalayan Frontal Thrust System, ITS: Indus-Tsangpo suture, KKF: Karakorum fault, KLF: Kunlun fault, STDS: South Tibetan Detachment System, SHG: Shuang Hu graben, YG: Yangbajian graben, GG: Gulu graben; DG: Dinggye graben, NC: Nam Co (after Blisniuk and Sharp 2003).

References

Armijo R, Tapponnier P, Mercier J, Han TL (1986) Quaternary extension in southern Tibet: Field observations and tectonic implications: J Geophys Res 91: 13803-13872.

Blisniuk P, Hacker BR, Glodny J, Ratschbacher L, Bi S, Wu Z, McWilliams MO, Calvert A (2001) Normal faulting in central Tibet since at least 13.5 Myr ago. Nature 412: 628-632.

Blisniuk PM, Sharp WD (2003) Rates of late Quaternary normal faulting in central Tibet from U-series dating of pedogenic carbonate in displaced fluvial gravel deposits. Earth Planet Sci Lett 215: 169-186.

Hongxing G, Anderson JK (2007) Fault throw profile and kinematics of Normal fault: conceptual models and geologic examples. Geol J China Univ 13: 75-88.

Kali E, Leloup P, Arnaud N, Mahéo G, Liu D, Boutonnet E, van der Woerd J, Liu X, Liu-Zeng J, Li H (2010) Exhumation history of the deepest central Himalayan rocks, Ama Drime range: Key pressure-temperature-deformation-time constraints on orogenic models. Tectonics 29: TC2014.

Kali E, van der Woerd J, Liu-Zeng J, LeBéon M, Leloup PH, Mahéo G, Tapponnier P, Thuizat R (2012) Active normal faults and river damming: the importance of tectonics and climate in shaping the landscape of the southern Tibetan plateau. EGU General Assembly Conference Abstracts, p. 11051.

Tapponnier P, Zhiqin X, Roger F, Meyer B, Arnaud N, Wittlinger G, Jingsui Y (2001) Oblique stepwise rise and growth of the Tibet Plateau. Science 294: 1671-1677.

Structural and metamorphic evolution of the Karakoram and Pamir following India-Kohistan-Asia collision

Searle M[1], Hacker B[2]

[1]Dept. of Earth Sciences, Univ. of Oxford, UK [2]Dept. of Earth Science, Univ. of California, Santa Barbara, USA

Following the ~50 Ma India–Kohistan arc–Asia collision, crustal thickening and shortening resulted in uplift of the Himalaya (Indian plate) and the Karakoram, Pamir and Tibetan plateau (Asian plate). Whereas surface geology of Tibet shows limited Cenozoic metamorphism and deformation and only localised crustal melting, the Karakoram and Pamir show extensive regional sillimanite- and kyanite-grade metamorphism, crustal melting resulting in major granitic intrusions (Baltoro granites), and extreme deformation. U/Th-Pb dating shows that metamorphism along the Hunza Karakoram peaked at ~83-62 Ma and 44 Ma with intrusion of the Hunza dykes at 35 Ma and 32-30 Ma, and along the Baltoro Karakoram peaked at ~28-22 Ma but continued until 5.4-3.5 Ma (Dassu dome). Widespread crustal melting along the Baltoro batholith spanned 26.4-13 Ma. In the Pamir a series of gneiss domes (metamorphic core complexes) record regional prograde metamorphism between 37-20 Ma. We suggest that continuous crustal thickening, melting, and exhumation of lower crust occurred throughout the mid-Eocene–Miocene and these processes are almost certainly continuing at depth today along the Asian side of the India-Asia collision. This Karakoram-Pamir-Tibet region may be in the early stages of cratonization.

Thermodynamic modelling of phosphate minerals: Implications for the development of P-T-t histories recorded in garnet and monazite bearing metapelites

Shrestha S[1], Larson K[1], Duesterhoeft E[2], Soret M[1], Cottle J[3]

[1]Earth and Environmental Sciences, Univ. of British Columbia, Okanagan, Canada, [2]Inst. of Geosciences, Univ. of Kiel, Germany [3] Dept. of Earth Science, Univ. of California, Santa Barbara, USA

Monazite, xenotime and apatite are accessory phosphate minerals commonly used as geochronometers to provide timing constraints on metamorphic events recorded by the rocks within which they occur. They are also used to investigate trace element partitioning between minerals to understand the behaviour of co-existing mineral phases. Despite widespread use, the growth and formation of these accessory minerals, and their interaction with major mineral phases, are still poorly understood. Thus, linking the ages obtained from these accessory minerals to the metamorphic pressure-temperature (P-T) path obtained primarily from major phases such as garnet remains one of the major challenges in geosciences.

This study incorporates phosphate minerals into one of the most commonly used thermodynamic dataset for phase equilibria modelling to understand the behaviour of these phases in context of growth and dissolution of major minerals. P-T-time (t) paths were built for two different rock specimens from the Himalaya using this methodology, one that experienced sub-solidus conditions and one that records evidence of supra-solidus metamorphism. The results obtained from this modelling provide direct information on the behaviour of monazite and xenotime growth/breakdown along the calculated P-T path. This information not only provides a tool to evaluate the validity of commonly used empirical trace element partitioning between garnet and monazite, but also allows the tying of ages obtained from accessory phases directly to the specific sections of the P-T paths derived from the composition of major phases. Construction of these well-constrained P-T-t paths can provide detailed insights into tectonic processes that may facilitate the further interpretation of the tectonometamorphic evolution of the studied rocks.

The Greater Himalayan thrust belt: Insight into the assembly of the exhumed Himalayan metamorphic core, Modi Khola Valley, Central Nepal

Shrestha S[1], Larson K[1], Martin A[2], Cottle J[3], Smit M[4]

[1]Earth and Environmental Sciences, Univ. of British Columbia, Okanagan, Canada [2]División de Geociencias Aplicadas, IPICYT, San Luis Potosi, Mexico [3] Dept. of Earth Science, Univ. of California, Santa Barbara, USA [4]Dept. of Earth, Ocean and Atmospheric Sciences, Univ. of British Columbia, Vancouver, Canada

The identification of multiple strike-parallel discontinuities within the exhumed Himalayan metamorphic core has significantly improved our understanding of convergence accommodation processes within the former mid-crust now exposed in the Himalaya. This study aims to unravel the structure and the kinematics of the exhumed midcrustal rocks exposed within Greater Himalayan sequence (GHS) in the Modi Khola valley of central Nepal to enhance our understanding of these structures and to better constrain how convergence has been accommodated during the India-Eurasia collision.

Based on an integrated approach comprising Lu-Hf garnet geochronology, Quartz-in-Garnet (QuIG) barometry and Th-Pb monazite petrochronology, this study confirms and characterizes multiple structural breaks within the GHS in the Modi Khola valley, bounding at least four lithotectonic rock packages with unique histories. The breaks approximately coincide with previously recognized features, which include from north to south, the Sinuwa thrust (ST), Bhanuwa fault (BF) and Main Central thrust (MCT). Lu-Hf garnet ages obtained from the thrust sheets separated by these structures yield prograde ages of ca. 35 Ma, 27 Ma, 35 Ma and 17 Ma, respectively down structural section. Pressure estimates from QuIG barometry, utilizing previously published peak temperature conditions, are also compatible with significant metamorphic breaks across the identified structures. Maximum entrapment pressure above the ST is ~13 kbar. Below the ST and above the BF, pressures drop to ~11.5 kbar before increasing again to ~14 kbar below the BF. Unique prograde and retrograde histories informed by monazite (re-)crystallization ages are also consistent with the occurrence of these structural breaks.

This new integrated data set, combined with similar data from other transects along the Himalaya, shows that the assembly of the GHS is a result of progressive deformation and juxtaposition of different thrust sheets through a combination of both in and out-of-sequence thrusting. We refer to this as the Greater Himalayan thrust belt, which is broadly consistent with the results of the published geometric prediction from thermo-mechanical model of the Himalaya.

India-Asia collision and biotic exchange: Evidences from Cenozoic plant megaremains

Shukla A[1], Mehrotra R[1]

[1]Birbal Sahni Inst. of Palaeosciences, Lucknow, India

Himalayan origin, uplift of the Tibetan plateau and initiation of extant Asian monsoon system (AMS) are outcomes of the India-Asia collision at about ~55–50 Ma when the wandering Indian plate travelled all the way from south of the equator to the north. On a geological timescale, biotic interchange is considered to be a key factor that shaped the current composition of global biodiversity. The collision between India and Asia opened the dispersal corridors which not only allowed range expansions, but also species diversification in deep time. Several major events that allowed the sudden expansion of terrestrial floras and faunas are known from the Cenozoic, such as the Great American Biotic Interchange after the Neogene closure of the Isthmus of Panama, the Pleistocene closure of the Bering Strait and the Eocene Indian–Eurasian collision. It is evident that during these events not only the physical connection of continental plates influenced biotic exchange but also ecological factors that either promote or hamper dispersal. The resulting rise of the Himalaya and Tibetan plateau triggered environmental changes of global impact following the development of the extant Asian monsoon system. Consequently, the Indian subcontinent and adjacent Asia underwent several environmental shifts between humid tropical and arid climates. The Indian subcontinent known as “Biotic ferry” was carrying ancient Gondwanan forms and upon collision with Asia these forms were dispersed into Asia; this theory is called as “Out-of-India” hypothesis. It was suggested that peninsular India was not completely isolated during its northward journey and that floral/faunal links were maintained with Africa and Madagascar till the collision of the Indian and Eurasian plates. As a result, many African elements also dispersed into India.

Paleoproterozoic distinct mafic intrusive rocks from the Himalayan Mountain Belt, India: Implications for their connection to a widespread ~1.9 Ga large igneous province event of the Indian Shield and Western Australia

Srivastava RK[1]

[1]*Banaras Hindu Univ., Varanasi, India*

Paleoproterozoic mafic intrusive rocks are well exposed all along the Himalayan Mountain Belt of India (Ahmad 2008; Ahmad et al. 1999; Miller et al. 2000). They occur as small bodies of dykes, sills and lenses and exposed in the Higher as well as the Lesser Himalaya sequences. Geochemical characteristics suggest that a group of rocks with low-Ti content are derived from melts generated through a high percentage of melting (~20-25%) of a lherzolite mantle source in spinel stability field, whereas other group having comparatively high-Ti content are thought to be derived from a low percentage melting (~5-10%) of a similar mantle source but generated in garnet stability field (Srivastava and Samal 2018). The similar picture is also observed in the Karoo and Emeishan basalts where both low-Ti and high-Ti basalts coexists but represent single LIP event (Ernst 2014). It is suggested that both groups were originally spatially separated at the time of their emplacement and believed that probably they have been juxtaposed during the Himalayan orogeny by crustal shortening through development of imbricated thrusts. The studied mafic intrusive rocks are emplaced either in MORB-like (i.e. the low-Ti rocks) or in within-plate tectonic setting (i.e. the high-Ti rocks). Widespread ~1.88-1.89 Ga mafic events in the Indian shield, which includes Bastanar dyke swarm in the Bastar, the Hampi dyke swarm in the eastern Dharwar craton and Pulivendla sills in the Cuddapah basin (Halls et al. 2007; French et al. 2008; Ernst and Srivastava 2008; Shellnutt et al. 2018) and similar event in dykes from the Yilgarn Craton of Western Australia (Stark et al. 2018) together with mafic intrusive and extrusive rocks in the Himalayan Mountain Range suggest presence of a large igneous province (LIP) at ~1.9 Ga. Probably the low-Ti rocks are emplaced at the northern margin of the Indian plate, whereas the high-Ti rocks are produced during a rifting event within the Indian plate. However, absolute ages for emplacement of these two distinct suites are warranted for a complete picture. It is pointed out that the global ~1.9 Ga event, that includes the Superior craton (“Circum-Superior” LIP), Slave, Kaapvaal, Siberian, and possibly East European cratons, is an important LIP and probably suggest more than one centre of mantle upwelling (e.g. plume) of this age (French et al. 2008; Ernst and Srivastava 2008).

References

Ahmad T (2008) Precambrian mafic magmatism in the Himalayan Mountain Range. J Geol Soc India 72: 85-92.

Ahmad T, Mukherjee PK, Trivedi JR (1999) Geochemistry of Precambrian mafic magmatic rocks of the Western Himalaya, India: petrogenetic and tectonic implications. Chem Geol 160: 103-119.

Ernst RE (2014) Large Igneous Provinces. Cambridge Univ. Press, Cambridge, 653 p.

Ernst RE, Srivastava RK (2008) India's place in the Proterozoic world: constraints from the large igneous provinces (LIP) record. In: Srivastava RK, Sivaji Ch, Chalapathi Rao NV (Eds.) Indian Dykes: Geochemistry, Geophysics, and Geochronology, pp. 41-56.

French JE, Heaman LM, Chacko T, Srivastava RK (2008) 1891-1883 Ma Southern Bastar-Cuddapah mafic igneous events, India: A newly recognized large igneous province. Precambrian Res 160: 308-322.

Halls HC, Kumar A, Srinivasan R, Hamilton MA (2007) Paleomagnetism and U-Pb geochronology of easterly trending dykes in the Dharwar craton, India: feldspar clouding, radiating dyke swarms and the position of India at 2.37 Ga. Precambrian Res 155: 47-68.

Miller C, Klotzli U, Fran W, Thoni M, Grasemann B (2000) Proterozoic crustal evolution in the NW Himalaya (India) as recorded by circa 1.80 Ga mafic and 1.84 Ga granitic magmatism. Precambrian Res 103: 191-206.

Shellnutt JG, Hari KR, Liao AC, Denyszyn SW, Vishwakarma N (2018) A 1.88 Ga giant radiating mafic dyke swarm across Southern India and Western Australia. Precambrian Res, in press.

Srivastava RK, Samal AK (2018) Geochemical characterization, petrogenesis, and emplacement tectonics of Paleoproterozoic high-Ti and low-Ti mafic intrusive rocks from the western Arunachal Himalaya, northeastern India and their possible relation to the ~1.9 Ga LIP event of the Indian shield. Geol J, in press.

Stark JC, Wang X, Denyszyn SW, Li ZX, Rasmussen B, Zi JW, Sheppard S, Liu Y (2018) Newly identified 1.89 Ga mafic dyke swarm in the Archean Yilgarn Craton, Western Australia suggests a connection with India. Precambrian Res, in press.

The "Seismology-at-school in Nepal" project

Subedi S[1], Hetényi G[1], Sauron A[2]

[1]ISTE, FGSE, Univ. of Lausanne, Switzerland [2]HES-SO Valais, Sion, Switzerland

Nepal is located above the convergent plate boundary between India and Eurasia. As a result, it has experienced devastating earthquakes throughout its history, claiming lives and causing significant damage. The most recent large earthquake in 2015, named Gorkha, killed nearly 9000 people and injured approximately 22’000. It was the most critical natural disaster to hit Nepal since the 1934 earthquake. Still, these casualties and damage were far under the expectations. After the Gorkha earthquake, Nepali people are thirsty to know more about earthquakes and vividly seek safety.

Schools play a vital role in the society and are essential elements of the values and culture of the society. A proper education through the schools not only teaches the children but also reaches deep into the community through the parents and teachers. Earthquake education reaching a broad group of the population early in their life is strongly needed, but seismology is not part of curriculum in Nepali schools. Our initiative aims to install low-cost sensor network with the specific focus on using it as educational tool and also for crowdsourcing.

Beyond teaching adapted classes, we strive for “learning-by-doing” using low-cost seismometers in schools. We start this scheme in the western region by installing inexpensive seismometers in schools and then seek that the example is spread to other areas. We are testing several types of low-cost sensors in the lab before installing one type in schools to record data in real-time. The data will be used to make shake maps and will also be shared openly. The primary practical challenges we face include load-shedding, limited internet access and mobile phone coverage, high noise-level near cities, no street connection to the countryside and lack of the computers in schools. Two pilot stations are installed in 2018, and numerous stations will follow in 2019.

We aim to develop several educational activities within this initiative. The class content will be adapted to the Nepali school system (levels and languages) and the topic will bear on earthquakes as a process (what creates them, how do we measure them, what can be expected, hazard and risk), as well as on preparedness (how to construct a safer home, what to do in case of an earthquake, what to do after an earthquake, perform earthquake drills). Moreover, the seismometer in each school will allow students to daily check and see whether an earthquake has happened in the region, and what was the respective shaking. The so collected seismic data will be available freely, so we hope that this type of crowdsourcing will also be useful for scientific goals.

Western Nepal crustal structure from P-to-S converted seismic waves

Subedi S[1], Hetényi G[1], Vergne J[2], Bollinger L[3], Lyon-Caen H[4], Farra V[5], Adhikari L[6], Gupta R[7]

[1]ISTE, FGSE, Univ. of Lausanne, Switzerland [2]Ecole et Observatoire des Sciences de la Terre, Strasbourg, France [3]CEA, France [4]Laboratoire de Géologie, Ecole Normale Supérieure, Paris, France [5]Inst. de Physique du Globe de Paris, France [6]National Seismological Centre, Dept. of Mines and Geology, Kathmandu, Nepal [7]Regional Seismological Centre, Dept. of Mines and Geology, Surkhet, Nepal

The structure of the crust in Western Nepal is investigated by performing P-to-S receiver function analysis from teleseismic earthquakes recorded at 16 temporary broadband seismic stations. A gentle deepening of the Moho is imaged between the Lesser and Higher Himalaya, from ca. 40 km depth beneath the foothills to ca. 58 km beneath the high range. A mid-crustal low-velocity zone is observed in the upper crust along ca. 55 km distance and is interpreted as the signature of fluids expelled from rocks thrusted under the Main Himalayan Thrust. Our new image allows comparison of the Moho and the Main Himalayan Thrust geometry along the strike of the Himalayas. This reveals non-negligible lateral variations, even over relatively short distances. The general crustal architecture observed in our study resembles that of Central Nepal, therefore Western Nepal is expected to be able to host large (Mw > 8) megathrust earthquakes.

Influence of paleogeography on Asian Cenozoic climate

Tardif D[1], Fluteau F[1], Donnadieu Y[2], Le Hir G[1], Ladant JB[2], Poblete F[3]

[1]Inst. de Physique du Globe de Paris, France [2] CEREGE, Aix-Marseille Univ, Aix en Provence, France [3]Inst. de Ciencias de la Ingeniería, Univ. de O'Higgins, Rancagua, Chile

The Late Eocene/Early Oligocene climatic transition from the so called "greenhouse" to "icehouse" world is marked by a decrease in atmospheric CO_2 concentrations, important oceanic circulation modifications and the inception of the Antarctic ice sheet. This climatic transition is coeval with paleogeographical changes, notably the shrinkage of the Tethysian ocean, the retreat of the Paratethys sea and the uplift of the Tibetan Plateau.

The combination of these factors may have controlled the regional climatic changes observed in Asia across this interval, such as a marked continental aridification and the possible inception of monsoon-like climatic patterns.

Based on newly acquired data in China and Myanmar, Licht et al. (2014) proposed an early development of the Asian monsoon in the Late Eocene, way before the commonly accepted onset around the Early Miocene (22 Ma, Guo et al. 2002). However, possible causes of the onset of Asian monsoons in conditions such as those in the late Eocene (40-34 Myr ago) are still poorly understood. Moreover, the reconstructed patterns of precipitation/moisture variations in Asia suggest a complex interplay between the Westerlies and Asian monsoon.

To better decipher the role of paleogeography on the observed climate and its possible implication in monsoon onset in Asia, we use an IPCC-like Earth System model (IPSL-CM5A2) to perform simulations using several 40 Ma paleogeography reconstructions based on the main ongoing theories (Cogné et al. 2013, Müller et al. 2016, van Hinsbergen et al. 2012), to assess their relative effect on the Asian climate system. These paleogeographies will allow us to understand the importance of some key parameters such as the Tibetan Plateau elevation and latitude on climate and possibly on monsoons inception.

References

Cogne JP, Besse J, Chen Y, Hankard F (2013) A new Late Cretaceous to Present APWP for Asia and its implications for paleomagnetic shallow inclinations in Central Asia and Cenozoic Eurasian plate deformation. Geophys J Int 192: 1000-1024.

Guo ZT, Ruddimas WF, Hao QZ, Wu HB, Qiao S, Zhu R.X, Liu TS (2002) Onset of Asian desertification by 22 Myr ago inferred from loess deposits in China. Nature 416: 159-163.

Licht A, van Cappelle M, Abels HA, Ladant JB, Trabucho-Alexandre J, France-Lanord C, Terry Jr D (2014) Asian monsoons in a late Eocene greenhouse world. Nature 513: 501-506.

Müller RD, Seton M, Zahirovic S, Williams SE, Matthews KJ, Wright NM, Bower DJ (2016) Ocean Basin Evolution and Global-Scale Plate Reorganization Events Since Pangea Breakup. Annu Rev Earth Planet Sci 44: 107-138.

van Hinsbergen DJJ, Lippert PC, Dupont-Nivet G, McQuarrie N, Doubrovine PV, Spakman W, Torsvik TH (2012) Greater India Basin hypothesis and a two-stage Cenozoic collision between India and Asia. Proc Nat Acad Sci 109: 7659-7664.

Fault activity, tectonic segmentation, and deformation patterns in the western Himalaya on geological timescales inferred from landscape morphology and thermochronology: A summary

Thiede RC[1], Bookhagen B[2], Scherler D[3,4], Dey S[5], Eugster P[2], Nennewitz M[2], Sobel E[2], Stübner K[2], Arrowsmith R[6], Jain V[5], Strecker M[2]

[1]Univ. Kiel, Inst. for Geosciences, Germany [2]Inst. of Earth and Environmental Science, Univ. of Potsdam, Germany [3]GFZ Potsdam, Germany [4]Freie Univ. Berlin, Germany [5]IIT Gandhinagar, Gujarat, India [6]Arizona State Univ., Tempe, USA

The distribution of tectonic activity in the Himalaya has been debated for decades and several aspects remain unknown. For instance, the amount of crustal shortening that ultimately sustains Himalayan topography and the activity of major fault zones remains poorly quantified over geological-timescales. In our work, we study landscape morphology and combine surface exposure and thermochronologic dating methods with models to address the spatial and temporal pattern of deformation in the western Himalaya. Of particular interest is a 30 to 40-km-wide orogen-parallel belt of rapid exhumation that extends from central Nepal to the western Himalaya. This belt has been linked to a mid-crustal ramp in the basal décollement, to out-of-sequence basement thrusts, and to the growth of Lesser Himalayan duplex structures. Further goals are constraining fault activity of the Main Boundary Thrust fault (MBT) and deformation within the Sub-Himalaya.

From our results we conclude that all major deformation zones in the western Himalaya are active and some portion of crustal shortening is accommodated by active out-of-sequence faulting sustaining topography, despite rapid erosion. We have published several new studies containing new apatite fission-track and zircon (U-Th)/He cooling ages from the western Himalayan region, particular in the vicinity of the transition from the central to the western Himalaya (~77°-78°E). We analyzed the spatial distribution of the relative change of river steepness using averaged basin wide river steepness indexes (ksn) from both along and across strike to gain information about the regional distribution of differential uplift patterns and to relate this to the activity of distinctive fault segments. Our results indicate the existence of three orogenic segments with distinctive landscape morphology, structural architecture, and fault geometry along the western Himalaya: Garhwal-Sutlej, Chamba, and Kashmir Himalaya (from east to west). We observe a positive correlation of averaged ksn values with long-term exhumation rates derived from recently published regional thermochronologic datasets combined with thermal modelling as well as with millennial timescale denudation rates based on cosmogenic nuclide dating. These results are in agreement with significant lateral changes in exhumation between the Dhauladar Range to the west, the Beas-Lahul region, and the Sutlej-Garhwal area to the east. Moreover, our data recognize distinctive fault segments, suggesting varying differential uplift along the strike of the Main Frontal Thrust (MFT), the Main Boundary Thrust (MBT), and in the vicinity of the steep topographic transition between the Lesser and Greater Himalaya. In this region, we relate out-of-sequence deformation along major basement thrust ramps such as the Munsiari Thrust (MT) combined with deformation along mid-crustal ramp along the basal décollement as the main driver of exhumation along the southern Himalayan front. This implies that some portion of crustal shortening is accommodated here on Quaternary if not longer timescales. Our results allow us to spatially correlate the western termination of the rapid exhumation belt with a mid-crustal ramp. Furthermore, it suggests that exhumation in the far west is focused at the frontal parts of the mountain range and associated with the hanging wall of the MBT.

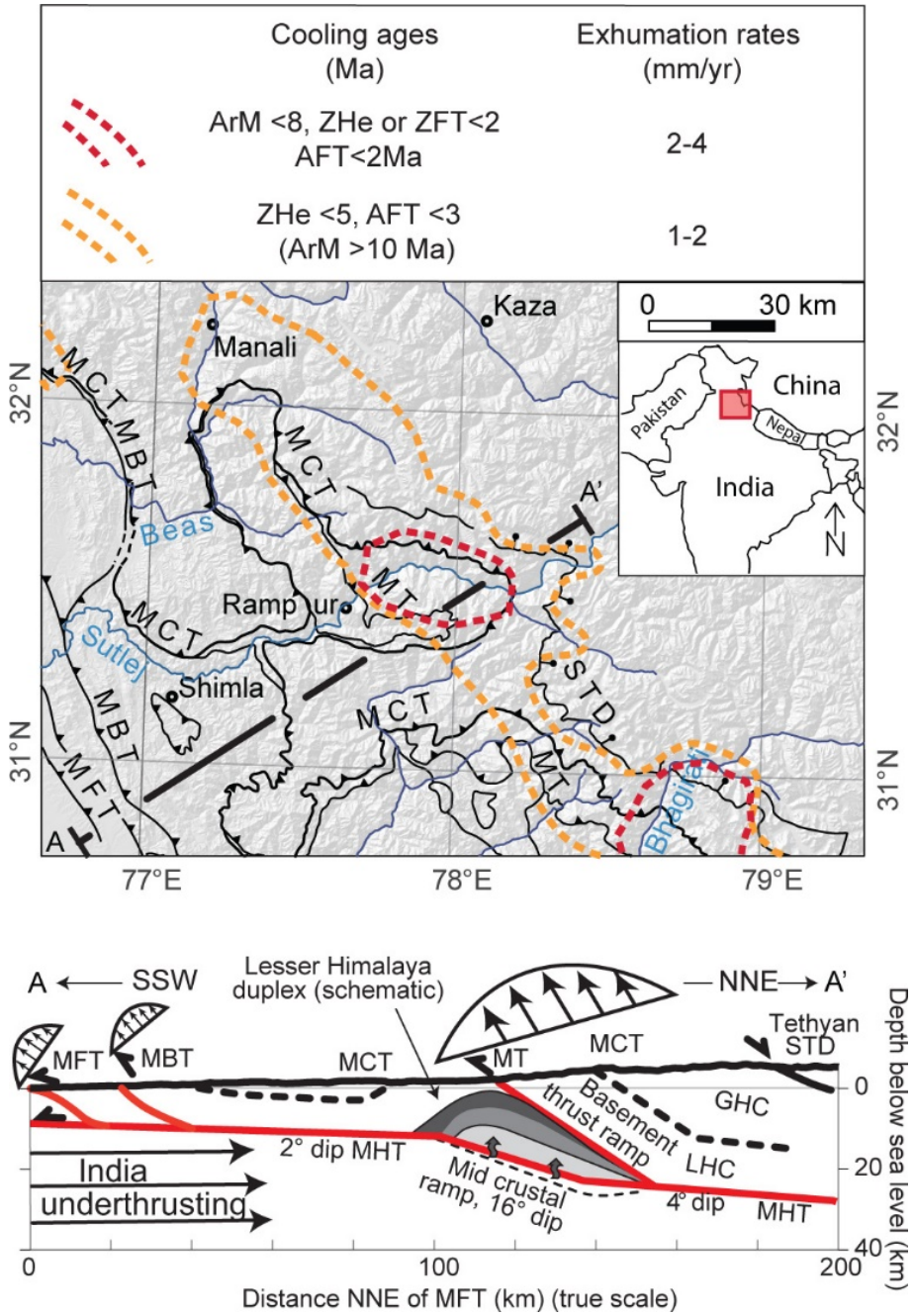

Figure 1. Schematic pattern of tectonic deformation and exhumation across the Indian southern Himalayan front since the late Miocene until present day based on thermochronologic data and thermal modelling (Thiede and Ehlers 2013; Thiede et al. 2017; Stübner et al. 2018) (A) in map view and (B) cross section (redrawn from Caldwell et al. 2013). Black arrows indicate contribution of overthrusting within the Himalayan wedge (~25% of total shortening) and underthrusting component of India (75%) (Lavé and Avouac 2001). Profile crossing the Himalaya along the Sutlej Valley (Profile A-A') is representative of the western end of the central Himalaya. Here, the rapid exhumation (1-4 mm/yr) of the high-grade metamorphic core along the southern front of the High Himalaya accommodates about ~50-75% of total overthrusting component. Abbreviations: ArM: $^{40}Ar/^{39}Ar$ – white mica, ZHe: zircon U-Th/He dating; ZFT and AFT: zircon and apatite fission track; MBT: Main Boundary Thrust; MCT: Main Central Thrust; MFT: Main Frontal Thrust; MHT: Main Himalayan Thrust; STD: South Tibetan Detachment System; MT: Munsiari Thrust; GHC: Greater Himalayan Crystalline; LHC: Lesser Himalayan Crystalline.

Reconstructing Greater India: Paleogeographic, kinematic, and geodynamic perspectives

van Hinsbergen D[1], Li S[2], Lippert P[3], Huang W[4], Advokaat E[1], Spakman W[1]

[1]Dept. of Earth Sciences, Utrecht Univ., The Netherlands [2]State Key Laboratory of Lithospheric Evolution, Inst. of Geology and Geophysics, Chinese Academy of Sciences, Beijing, China [3]Univ. of Utah, Salt Lake City, USA [4]Univ. of Rochester, USA

Key in understanding the geodynamics governing subduction and orogeny is reconstructing the paleogeography of “Greater India” (Fig. 1), the Indian plate lithosphere that subducted since Tibetan Himalayan continental collision with Asia. Here, we discuss this reconstruction from paleogeographic, kinematic, and geodynamic perspectives and isolate the evolution scenario that is consistent with all three. We follow recent constraints suggesting a ~58 Ma initial collision and update a previous kinematic restoration of intra-Asian shortening with a recently proposed Indochina extrusion model that reconciles long-debated large and small estimates of Indochina extrusion. The reconstruction is tested against Tibetan paleomagnetic rotation data, and against seismic tomographic constraints on paleo-subduction zone locations. The resulting restoration shows ~1000-1200 km of post-collisional intra-Asian shortening, leaving a 2600-3400 km wide Greater India. From a paleogeographic, sediment provenance perspective Eocene sediments in the Lesser Himalaya and on undeformed India may suggest that all Greater Indian lithosphere may have been continental but may also source from the Paleocene-Eocene western Indian orogen unrelated to the India-Asia collision. A quantitative kinematic, paleomagnetic perspective prefers major Cretaceous extension and “Greater India Basin” opening within Greater India, but data uncertainty may speculatively allow for minimal extension. Finally, from a geodynamic perspective, assuming a fully continental Greater India would require that the highest subduction rates recorded in the Phanerozoic would have been driven by a subduction of a lithosphere-crust assemblage more buoyant than the mantle, which seems physically improbable. We conclude that the Greater India Basin hypothesis is the only scenario sustainable from all perspectives. We infer that old pre-collisional lithosphere rapidly entered the lower mantle sustaining high subduction rates, whilst post-collisional continental and young Greater India basin lithosphere did not, inciting the rapid India-Asia convergence deceleration ~8 Myr after collision. Subsequent absolute northward trench migration and slab overturning terminated Gangdese arc activity despite ongoing oceanic subduction.

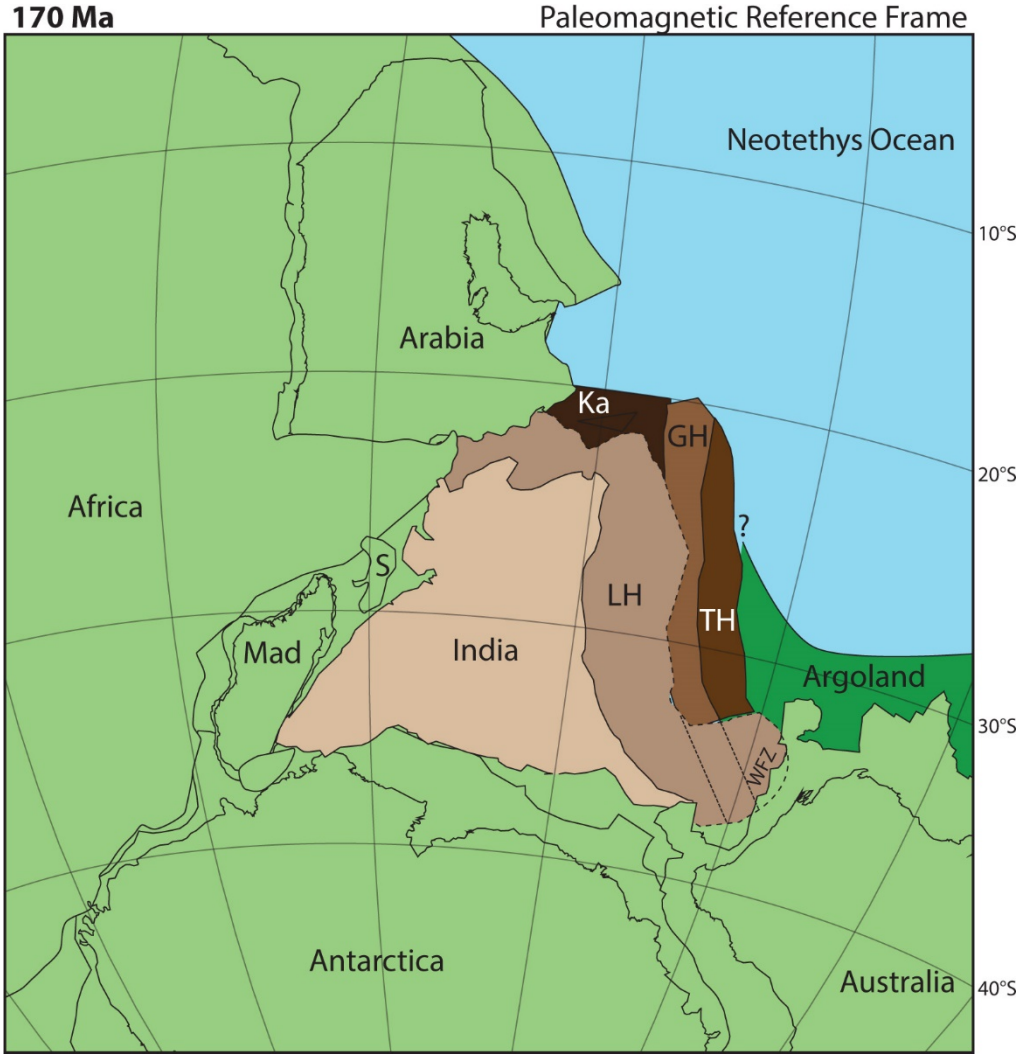

Figure 1. Reconstruction of Greater India in Gondwana at 170 Ma cast in the paleomagnetic reference frame of Torsvik et al. (2012). Reconstruction of Argoland follows Gibbons et al. (2012). WFZ: Wallaby Fracture Zone.

Himalayan geochronology: A road map for the next 15 years

Villa IM[1,2]

[1]Centro Datazioni e Archeometria, Univ. of Milano-Bicocca, Italy [2]Inst. of Geological Sciences, Univ. of Bern, Switzerland

New approaches and new analytical tools have the potential to substantially improve our understanding of Himalayan geochronology beyond the first half-century of Himalayan studies.

1. Mapping. The Alps have been mapped for over 200 years (nearly twenty generations of field geologists), yet a systematic understanding of petrologic disequilibria and tectonic discontinuities is still elusive. As most of the Himalaya is unaccessed, 10-m-scale mapping is vastly incomplete, even if it would be needed to catch up with better-studied orogens. Similarly, mapping the candidate source rocks of a sedimentary basin needs to take into account rock fertility before a mass balance budget (a forgotten requirement of the lag-time approach) can be credibly assessed.

2. Microstructural characterization. As a complement to megastructural mapping (which in recent years has recognized an increasing number of tectonic discontinuities in the Greater Himalayan Sequence), petrography reveals multistage deformations at the µm scale. The uniform "Formation 1 gneisses" of the 1970s have become a mosaic of multiple mineral generations reflecting diachronous petrogenesis.

3. Microchemical characterization. Each mineral generation is chemically different from the others in the same rock. Once one knows what to look for, chemical variations in index and accessory minerals can be found and interpreted in terms of open-system deformation.

4. Thermobarometry. Estimating P-T-A-X (pressure-temperature-activity-molar fraction) conditions assumes that chemical compositions of minerals stayed frozen in at the metamorphic peak, without subsequent modification by diffusion, retrogression, deformation-aided mass transfer, coupled dissolution-reprecipitation, etc. Retrograde reactions and petrological disequilibrium are expected, and indeed observed whenever looked for, in deformation events. If disequilibrium is observed, diffusive re equilibration was less efficient than the much faster reaction rates.

5. Integrated petrology. Keeping track of the reactions leading to the present-day paragenesis allows understanding the isotope retention behaviour of new petrochronometers, such as micas, relative to established ones, such as monazite. The challenge of dating each of the observed mineral generations is labour-intensive, but can be, and has been, met. A change of paradigm is slowly taking place: geochronology and petrochronology require hard work. First, the petrogenetic framework for each rock must be established, and any possible prograde and retrograde reaction assigned a point in P-T-A-X space; then a mineral chronometer in equilibrium with the surrounding rock volume must be identified, separated, and dated, giving a P-T-A-X-D-t point. This is much more labour-intensive than the (sometimes wishful thinking) attempts of the early days, but the payoff is reaching a robust understanding of the entire petrogenetic sequence.

6. Dating. Mathematical models are not an end in themselves, up to the point that they require neglecting data and twisting observations. Instead, legitimate models must fit all available data in the correct context. Once petrology is understood, geochronology is straightforward. In-situ dating can help if the appropriate questions are asked: intra-grain age maps are only useful if they are connected to compositional data (especially of trace elements) and if their resolution is sufficiently high (1 µm) to establish the mechanisms controlling the rate of chemical and isotopic exchange.

Geodetic evidence for a subhorizontal underthrusting of the India plate beneath the Himalaya

Wang Q[1], Chen G[1]

[1]China Univ. of Geosciences, Wuhan, China

The 2015 Gorkha Nepal earthquake (Mw 7.8) is a fresh and grim reminder of seismic potential induced by underthrusting the India subcontinent beneath the Himalaya and thus provide a rare opportunity to illuminate puzzles regarding mountain building and seismicity, for which we knew little as yet. Himalayan earthquakes are assumed to suddenly release elastic strain energy built up on the basal decollement, a megathrust fault along which the Indian plate is descending. However, their growth to achieve greatness is impeded usually by complex structures on the megathrust. Here, by analysis of near-field displacements (at 55 sites in Nepal and south Tibet) observed by GPS geodesy, we show that coseismic slip of > 1 meter in 2015 has propagated northward for 160 km at the depth range of 10-20 km below the Himalaya, extending substantially into south Tibet. The Gorkha rupture thus unravels a shallowly-dipping plate interface that was commonly proposed to stretch along a deep seismic reflector (the Main Himalayan Thrust) imaged at 25-45 km beneath the Tethys Himalaya. Our modelling distinguishes a mid-crustal shear zone of Indian upper crust in between the overly plate-interface and the deep seismic reflector, which underlies a tapered accretionary wedge, and exclude an active mid-crustal ramp fault beneath the topographic front of the high Himalaya for uplift. Our finding sheds insight into two puzzling features in the Himalaya: why the mid-crustal seismicity is absent in the continental subduction, and high Himalayan metasedimentary rocks are much younger than the Indian basement. In addition, the planar surface of the megathrust and its seismogenic downdip width of at least 200 km highlight a potential for generating giant earthquakes (Mw ~9). We conclude that any model adopting a mid-crustal ramp-decollement geometry as the plate interface for India underthrusting beneath the Himalaya and Tibet should be revised.

The Main Central thrust–South Tibet fault branch line: A closely-spaced structural survey across a controversial feature

Webb A[1], Dong H[2], Xu Z[3]

[1]Univ. of Hong Kong, Hong Kong [2]Inst. of Geology, Chinese Academy of Geological Science, China [3]Nanjing Univ., China

Perhaps the most controversial structural element in the Himalayan orogen over the last ~15 years has been the potential branch line of the Main Central thrust and the South Tibet fault, bounding the leading edge of the Greater Himalayan Crystalline complex (Yin 2006). The branch line is controversial because (1) the overall structural geometry would show South Tibet fault as a backthrust, not a normal fault, and (2) the preservation of this feature would require that the leading edge of the Greater Himalayan Crystalline complex was not eroded in the early to middle Miocene. These two aspects contradict the central components of extrusion models, which include the South Tibet fault as a normal fault that exhumes the Greater Himalayan Crystalline complex during the early Neogene.

The history of inference, discovery, and dispute concerning the Main Central thrust–South Tibet fault branch line can be condensed as follows: (1) The "tunnelling" stage of Beaumont et al.'s (2001) channel flow model could be considered to propose such a structure, because during tunnelling the basal and upper shear zones bounding the channel merge at the southern tip of the channel. (2) Yin (2006) inferred that such a structure is preserved today in the western Himalaya, on the basis of very preliminary mapping as well as the simple, long standing observation that across the southern parts of this region, Tethyan Himalayan sequence rocks are thrust directly atop the Lesser Himalayan sequence rocks along the Main Central thrust (e.g. Thakur and Rawat 1992; Fuchs and Linner 1995; Steck 2004). Emplacement of Tethyan rocks atop Lesser Himalayan rocks along the Main Central thrust requires the commonly intervening Greater Himalayan Crystalline complex to pinch out in some fashion. (3) Integrated geological investigations were able to tightly constrain the position of the branch line in the Sutlej region of the western Himalaya (Webb et al. 2007; 2011a) and the NW Kathmandu half-klippe in the central Himalaya (Webb et al. 2011b). (4) A suite of further studies have variously challenged (Antolin et al. 2013; Khanal et al. 2015; Long et al. 2017; Soucy La Roche et al. 2016; 2017) and confirmed (He et al. 2015; 2016; Rapa et al. 2016) the existence of the branch line, such that today the general Himalayan geologist may be somewhat confused as to its pertinence.

Here we present (1) preliminary results of <a> a closely-spaced structural survey across the key discovery area in the NW Kathmandu half-klippe and <b> a more broadly spaced structural transect across the western Kathmandu half-klippe, and (2) a synthesis of prior work along each transect previously investigated in order to test the branch line concept. We show that the branch line can be viably interpreted in the context of the geology along each studied transect. The new findings from the Kathmandu half-klippe demonstrate that here, the branch line is actually exposed: a remarkably lucky occurrence amidst the dense vegetated cover of the southern Himalaya.

References

Antolin B, Godin L, Wemmer K, Nagy C (2013) Kinematics of the Dadeldhura klippe shear zones (W Nepal): implications for the foreland evolution of the Himalayan metamorphic core. Terra Nova 25: 282-291.

Fuchs G, Linner M (1995) Geological traverse across the western Himalaya; a contribution to the geology of eastern Ladakh, Lahul, and Chamba. Jahrbuch der Geologischen Bundesanstalt Wien 138: 655-685.

He D, Webb AAG, Larson P, Martin AJ Schmitt AK (2015) Extrusion vs. duplexing models of Himalayan mountain building 3: duplexing dominates from Oligocene to present. Int Geol Rev 57: 1-27.

He D, Webb AAG, Larson KP, Schmitt AK (2016) Extrusion vs. duplexing models of Himalayan mountain building 2: The South Tibet detachment at the Dadeldhura klippe. Tectonophys 667: 87-107.

Khanal S, Robinson DM, Kohn MJ, Mandal S (2015) Evidence for a far-traveled thrust sheet in the Greater Himalayan thrust system, and an alternative model to building the Himalaya. Tectonics 34: 31-52.

Long SP, Gordon SM, Soignard E (2017) Distributed north-vergent shear and flattening through Greater and Tethyan Himalayan rocks: insights from metamorphic and strain data from the Dang Chu region, central Bhutan. Lithosphere 9: 774-795.

Rapa G, Groppo C, Mosca P, Rolfo F (2016) Petrological constraints on the tectonic setting of the Kathmandu Nappe in the Langtang-Gosainkund-Helambu regions, Central Nepal Himalaya. J Metam Geol 34: 999-1023.

Soucy La Roche R, Godin L, Cottle JM, Kellett DA (2016) Direct shear fabric dating constrains early Oligocene onset of the South Tibetan detachment in the western Nepal Himalaya. Geology 44: 403-406.

Soucy La Roche R, Godin L, Crowley JL (2017) Reappraisal of emplacement models for Himalayan external crystalline nappes: The Jajarkot klippe, western Nepal. GSA Bull 130: 1041-1056.

Thakur VC, Rawat BS (1992) Geologic map of Western Himalaya: Dehra Dun, India, Wadia Inst. of Himalayan Geology, scale 1:1’000’000.

Webb AAG, Yin A, Harrison TM, Célérier J, Burgess WP (2007) The leading edge of the Greater Himalayan Crystallines revealed in the NW Indian Himalaya: implications for the evolution of the Himalayan Orogen. Geology 35: 955-958.

Webb AAG, Yin A, Harrison TM, Célérier J, Gehrels GE, Manning CE, Grove M (2011a) Cenozoic tectonic history of the Himachal Himalaya (northwestern India) and its constraints on the formation mechanism of the Himalayan orogen. Geosphere 7: 1013-1061.

Webb AAG, Schmitt AK, He D, Weigand EL (2011b) Structural and geochronological evidence for the leading edge of the Greater Himalayan Crystalline complex in the central Nepal Himalaya. Earth Planet Sci Lett 304: 483-495.

Yin A (2006) Cenozoic tectonic evolution of the Himalayan orogen as constrained by along-strike variation of structural geometry, exhumation history, and foreland sedimentation. Earth-Sci Rev 76: 1-131.

Himalayan tectonics in three dimensions: Slab dynamics controlled mountain building, monsoon intensification, and asymmetric arc curvature

Webb A[1], Guo H[2], Clift P[3], Husson L[4], Müller T[5], Costantino D[5], Yin A[6], Xu Z[7], Wang Q[7]

[1]Univ. of Hong Kong, Hong Kong [2]Lehigh Univ., Bethlehem, USA [3]Louisiana State Univ., Baton Rouge, USA [4]ISTerre, Univ. Grenoble-Alpes, France [5]Univ. of Leeds, UK [6]Univ. of California, Los Angeles, USA [7]Nanjing Univ., China

There is remarkable diversity in Oligocene-Miocene Himalayan crustal tectonics models, ranging from channelized flow of partially molten crust extruding to the surface under the influence of monsoon-driven erosion to making the entire mountain belt via simple thrust stacking / duplexing. Nonetheless nearly every tectonic model that addresses Himalayan crustal tectonics has two problematic commonalities: (1) these are developed in two dimensions, i.e. in cross section view, and (2) they involve static mantle geometries. Concerning the two dimensionality, the models assume uniformity along the length of the Himalaya. However, significant along-strike tectonic variations occur. For example, the cessation of motion along the South Tibet fault is non-uniform along the length of the arc (e.g. ~20-19 Ma in the Zanskar region, ~14-12 Ma along the northern borders of Sikkim and Bhutan). Concerning the static mantle geometries, the issue is not that the mantle is not involved – convergence happens in all models – but rather that the mantle undergoes no dynamic change. In contrast, tomographic and volcanic records suggest that the mantle lithosphere has participated in cycles of underthrusting, (relative) rollback, (laterally propagating) detachment, and renewed underthrusting throughout the Himalayan orogeny. Such cycles would have involved first-order changes in the weight distributions across the orogenic system, and thus should have similarly major impacts on crustal tectonics.

Clearly, new models are required that consider along-strike variations and mantle dynamics. We present an early attempt at such work (see also: Webb et al. 2017). First, we illustrate strong temporal correlation of southward motion of the Indian slab relative to the overriding Himalayan orogen, lateral migration of slab detachment, and subsequent dynamic rebound with major changes in Himalayan metamorphism, deformation, and exhumation. We propose that anchoring of the Indian continental subducted lithosphere from 30 to 25 Ma steepened the dip of the Himalayan sole thrust, resulting in duplexing deep within the Himalayan orogenic wedge. During the subsequent ~13 Myr, slab detachment propagated inward from both Himalayan syntaxes. Resultant dynamic rebound terminated deep duplexing and caused a rapid rise of the mountain range, and the increased orography intensified the South Asian monsoon. Decreased compressive forces in response to slab detachment may explain an observed ~25% decrease in the India-Eurasia convergence rate. The asymmetric curvature of the arc, i.e. broadly open, but tighter to the east, may have been caused by faster slab detachment migration from the west than from the east.

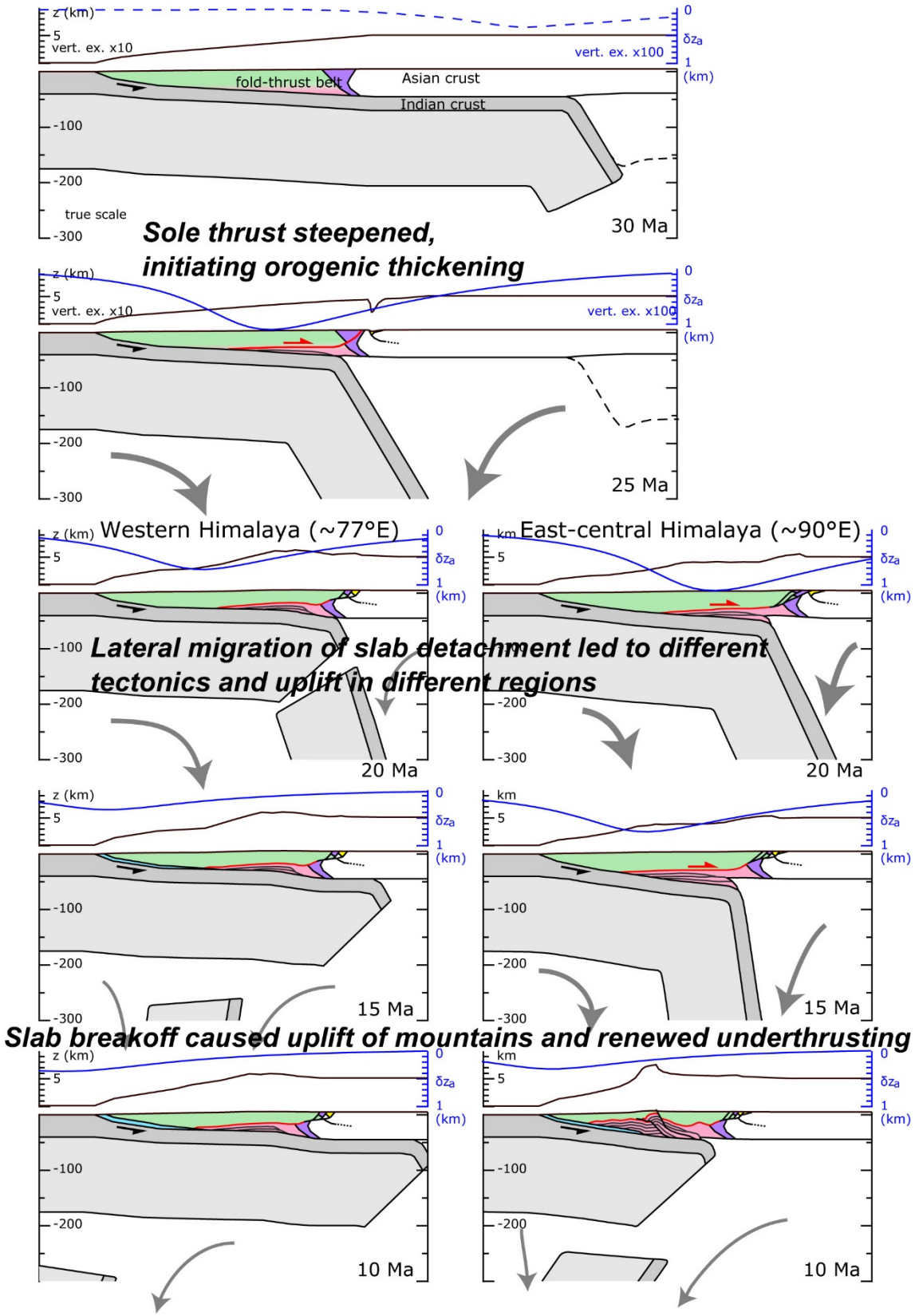

Graphical abstract.

Reference

Webb AAG, Gao H, Clift P, Husson L, Müller T, Costantino D, Yin A, Xu Z, Cao H, Wang Q (2017) The Himalaya in 3D: slab dynamics controlled mountain building and monsoon intensification. Lithosphere 9: 637-651.

Meteoric fluid-rock interaction in the footwall of the South Tibetan Detachment, Sutlej Valley and Zanskar, NW India

Webster T[1], Gébelin A[1], Law R[2], Stahr D[2], Mulch A[3,4]

[1]School of Geography, Earth and Environmental Sciences, Plymouth Univ., UK [2]Dept. of Geosciences, Virginia Tech, Blacksburg, USA [3] Senckenberg Biodiversity and Climate Research Centre, Frankfurt/Main, Germany [4]Inst. of Geosciences, Univ. Frankfurt, Frankfurt/Main, Germany

The South Tibetan Detachment (STD) is one of the most fundamental structures within the Himalayan orogenic belt. It exposes a thick mylonitic zone, over a distance of > 1500 km along strike that is hundreds of metres thick and which separates upper plate Palaeozoic sediments (Tethyan Himalayan sequence, THS) from high-grade metamorphic rocks and syntectonic leucogranites below (Greater Himalayan series, GHS).

Infiltration of meteoric fluids has been documented in the deformed footwall of the STD at ~15-17 Ma in the Mt. Everest area where hydrous minerals equilibrated with surface-derived fluids during deformation (Gébelin et al. 2013; Gébelin et al. 2017). Such minerals provide important information on the fluid source and migration pathways associated with shear zones, as well as the fluxes of fluids involved in fluid-rock interaction that in turn place limits on the thermomechanical behaviour of the STD. In addition, such fluids allow to obtain paleoaltimetry estimates for the world's highest point of our planet (Gébelin et al. 2013), based on a technique that recovers the isotopic composition of ancient meteoric water that scales with elevation (e.g. Poage and Chamberlain 2001).

Here, we present hydrogen isotope data combined with microstructural observations from the Zanskar detachment zone (ZDZ) (Haptal river, NW India) and the Sangla detachment (SD) (Sutlej Valley, NW India) that extend the spatial distribution of records acquired in the Mt. Everest region.

Hydrogen isotope ratios of synkinematic biotite, muscovite, and chlorite collected within the top 450 m of the ZDZ footwall indicate δD values as low as -146‰, -127‰, -140%, respectively (Fig. 1). These results suggest that these rhomboidal shaped mica fish interacted with meteoric fluids during (re-)crystallization / deformation which took place between ~26 and ~18 Ma (Dèzes et al. 1999; Searle et al. 2001). In contrast, below 450 m, biotite and muscovite yield higher δD values that range from -80‰ to -97‰, and from -60‰ to -68‰, respectively. These δD values are correlated with microstructures that developed during high temperature deformation (≥ 650°C) such as lobate quartz grain boundaries, myrmekites, and magmatic biotites (Stahr 2013).

In contrast, samples from the SD do not suggest interaction with surface-derived fluids, but rather, indicate (re-)crystallization in the presence of metamorphic/magmatic fluids (δDminerals > -76‰) which is in good agreement with the associated magmatic microstructures. However, it is worth noting, that one sample collected at ~10 m below the detachment provides low δDbiotite values of -120‰ that can only be explained by interaction with meteoric fluids.

The hydrogen isotope data obtained from the ZDZ indicate that samples in the footwall interacted during high temperature deformation with meteoric fluids sourced at high elevation between ~26 and ~18 Ma. These results suggest that the Zanskar region was likely lower when compared to the Mt Everest region at ~17 Ma but still represented a regional topographic high.

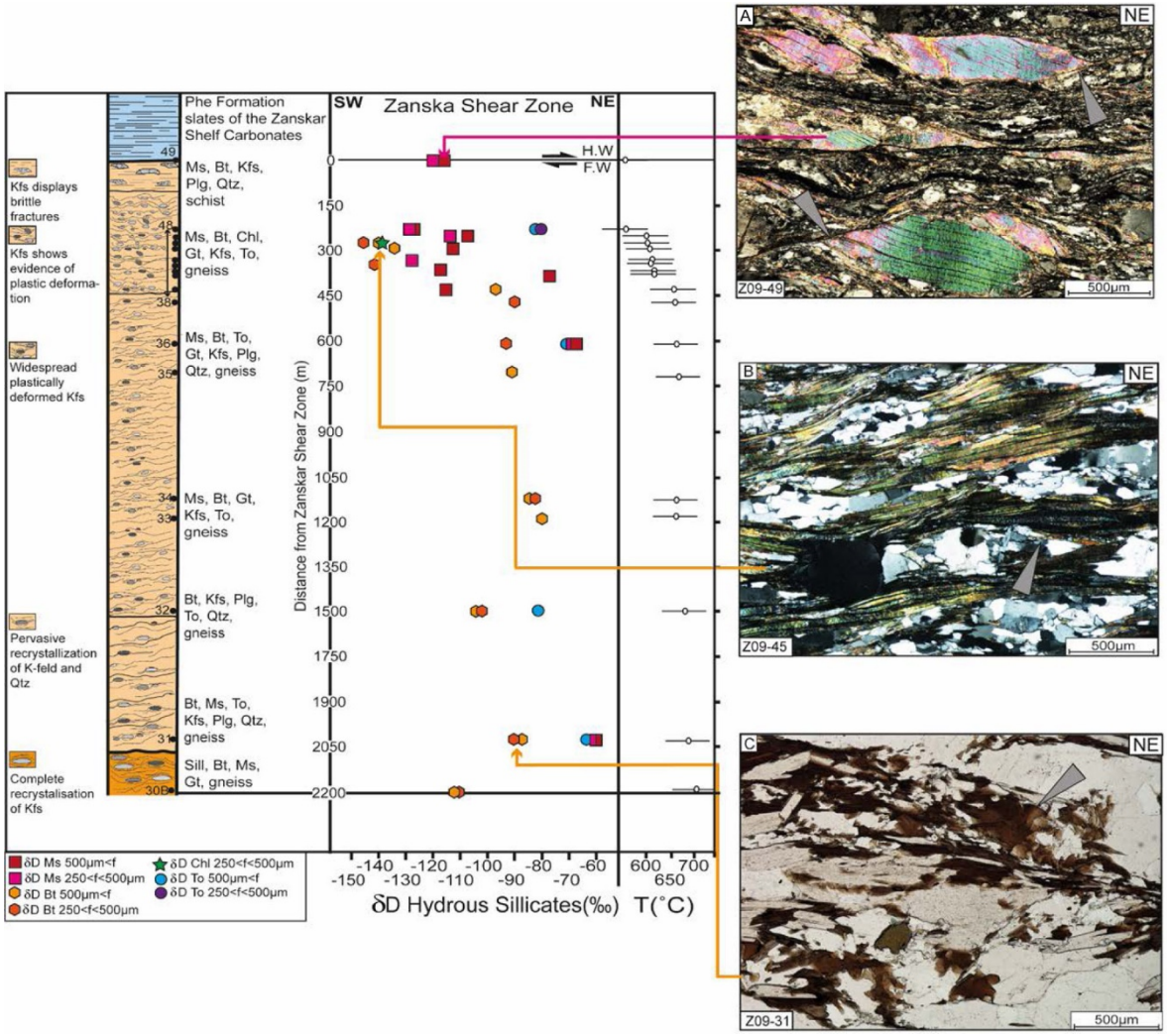

Figure 1. Left: Tectono-stratigraphic column showing locations of samples. Middle: Structural distance (m) vs. δD hydrous silicate values (‰). Right: Representational microstructures, (A) Rhomboidal muscovite fish, with truncated cleavage, (B) Thin elongated muscovite and biotite shear bands, (C) Magmatic biotite.

References

Gébelin A, Mulch A, Teyssier C, Jessup MJ, Law RD, Brunel M (2013) The Miocene elevation of Mount Everest. Geology 41: 799-802.

Gébelin A, Jessup M, Teyssier C, Cosca MA, Law RD, Brunel M, Mulch A (2017) Infiltration of meteoric water in the South Tibetan Detachment (Mt Everest, Himalaya): When and Why? Tectonics 36: 1-24.

Poage MA, Chamberlain PC (2001) Empirical Relationships Between Elevation and the Stable Isotope Composition of Precipitation and Surface Waters: Considerations for Studies of Paleoelevation Change. Am J Sci 301: 1-15.

Dèzes PJ, Vannay JC, Steck A, Bussy F, Cosca M (1999) Synorogenic extension: Quantitative constraints on the age and displacement of the Zanskar shear zone (northwest Himalaya). GSA Bull 111: 364-374.

Searle MP, Stephenson B, Walker J, Walker C (2007) Restoration of the Western Himalaya: implications for metamorphic protoliths, thrust and normal faulting, and channel flow models. Episodes 30: 242-257.

Stahr D (2013) Kinematic evolution, metamorphism, and exhumation of the Greater Himalayan Series, Sutlej River and Zanskar regions of NW India. PhD thesis, Virginia Tech.

First paleomagnetic constraints on the latitudinal displacement of the West Burma block

Westerweel J[1], Roperch P[1], Licht A[2], Dupont-Nivet G[1,3], Win Z[4], Poblete F[1,5], Huang H[6], Littell V[2], Swe H[7], Kai Thi M[7], Hoorn C[6], Wa Aung D[7]

[1]Geosciences Rennes, Univ. of Rennes, France [2]Dept. of Earth and Space Sciences, Univ. of Washington, Seattle, USA [3]Inst. of Earth and Environmental Science, Univ. of Potsdam, Germany [4]Dept. of Geology, Univ. of Shwebo, Myanmar [5]Univ. de O'Higgins, Rancagua, Chile [6]Univ. of Amsterdam, The Netherlands [7]Dept. of Geology, Univ. of Yangon, Myanmar

On the eastern side of the India-Asia collision zone, the West Burma block exhibits a unique geodynamic evolution within this system, influenced by oblique subduction of the Indian plate and significant strike-slip motion along the dextral Sagaing Fault. Furthermore, it is at a key location for paleoenvironmental reconstructions (Cai et al. 2016; Licht et al. 2013) and has been a biodiversity hotspot since Mid-Cretaceous times evidenced by exceptional Burmese amber fossils (Poinar 2018). Despite this, robust paleomagnetic data constraining the geodynamic evolution of the West Burma block remains largely absent.

Here we report new paleomagnetic, petrological and U-Pb age data to constrain the latitudinal displacement of the West Burma block. To this end, 45 sites were drilled in the intrusives, extrusives and sediments of the Wuntho arc, Myanmar. Paleomagnetic results were obtained at 30 sites. In addition, 175 paleomagnetic results were obtained from a Late-Eocene homoclinal sedimentary section in the Chindwin basin, Myanmar.

Wuntho arc U-Pb ages cluster in the 110-90 Ma range, indicating an early Late-Cretaceous age. Paleomagnetic results from this area show declination values of around 50-100°, implying clockwise rotation of the overall arc dispersed by local-block rotations related to faulting, and inclination values close to zero, corresponding to near-equatorial paleolatitude. Tilt corrections are not available for sites in intrusive rocks. However, the sampling is distributed over a large area (1000 km^2) and the results are found inconsistent with regional tilting of the arc. The occurrence of remagnetization after tilting of the country rocks in several sites by the intrusive batholith provide paleo-horizontal constraints that further support the clockwise rotations and the low paleolatitude. In the Late Eocene sediments, normal and reverse polarity magnetizations indicate a primary detrital or a very early diagenetic origin for the acquisition of the magnetization. The low inclination after tilt correction is coherent with the inferred near-equatorial position from the older Wuntho arc rocks and suggests a significant northward motion of the West Burma block since the Late-Eocene. The ~10° clockwise rotation in the Eocene sediments indicates that the Wuntho arc rotated clockwise prior to the Late-Eocene. These results, combined with a regional compilation of available geological data, enables us to establish a geodynamic evolution of the Burma block significantly different from previous models, with important implications for regional tectonism, paleoenvironment and paleobiogeography.

References

Cai F, Ding L, Laskowski AK, Kapp P, Wang H, Xu Q, Zhang L (2016) Late Triassic paleogeographic reconstruction along the Neo-Tethyan Ocean margins, southern Tibet. Earth Planet Sci Lett 435: 105-114.

Licht A, France-Lanord C, Reisberg L, Fontaine C, Soe AN, Jaeger JJ (2013) A palaeo Tibet–Myanmar connection? Reconstructing the Late Eocene drainage system of central Myanmar using a multi-proxy approach. J Geol Soc 170: 929-939.

Poinar G (2018) Burmese amber: evidence of Gondwanan origin and Cretaceous dispersion. Hist Biol, 1-6.

Is differential landscape evolution in the Bhutan Himalaya driven by arc segmentation?

Wood M[1], Pelgay P[2], Sandiford M[1], Kohn B[1], Li G[1]

[1]The Univ. of Melbourne, Australia [2]Dept. of Geology and Mines, Thimphu, Bhutan

The principal structural elements of the Himalayan arc can be traced more or less continuously for nearly 2,500 km. It is therefore understandable that along-strike variations in structure (and resultant denudation) have not received the same scientific attention as equivalent arc-normal trends. However, it is now clear that lateral variations in the geometry of the Main Himalayan Thrust (MHT) are responsible for first-order arc segmentation. The Bhutan Himalaya has a distinctive physiography and hosts nominal modern seismicity despite experiencing long-term strain accommodation of the same magnitude as the wider arc. This enigmatic section of the orogen presents an opportunity to test the case for local arc segmentation through applied tectonic geomorphology.

Using a combination of low temperature thermochronology and cosmogenic radionuclide methods, which are sensitive to orogenic processes over varying, but overlapping timescales, this study documents the spatial and temporal variability of denudation within Eastern Bhutan. Partitioning of deformation across crustal structures is inferred from integrated erosional histories and quantitative landscape morphometrics. Laboratory methods include apatite fission track (AFT), and (U-Th)/He dating of zircon and apatite (ZHe and AHe respectively), from in situ bedrock, synorogenic sediments and modern detrital samples. Additionally, ^{10}Be concentrations from detrital quartz samples adds to a nation-wide compilation of previously published data.

Results suggest prominent along- and across-strike variation in deformation within Eastern Bhutan. Elevated relief and hillslope characterise a prominent east-west trending zone of elevated millennial-scale erosion rates in the Lesser Himalaya of Bhutan. Here termed the Naka Zone, this geomorphic region is coincident with the estimated rupture extent of an early 18th century great earthquake and terminates to the east in the vicinity of the Kuru Chu reentrant in the Main Central Thrust (MCT).

Longer-term landscape evolution signals revealed by thermochronometry have strong gradients in the arc-normal direction. Greater Himalaya basement rocks show a phase of rapid, monotonic cooling, the timing of which is largely latitude-dependent. Northward decreasing cooling ages are consistent with exhumation above a mid-crustal ramp on the MHT ~100 km from the front, followed by horizontal translation at orogenic shortening rates above a relatively flat décollement. This framework explains the decoupling of AFT ages in sampled catchments from millennial-scale erosion rates.

Small catchments that straddle the MCT show bimodal distributions in single grain AFT ages, suggestive of activity on the MCT during the late Miocene. Further, central ages show a marked decrease towards Arunachal Pradesh, suggesting that in far eastern Bhutan the mid-crustal ramp extends towards the foreland, possibly invoking a lateral ramp.

Synorogenic detrital thermochronometers are not thermally reset and thus provide information on source area bedrock cooling and provenance. ZHe and AFT age distributions in the Siwaliks are bimodal. Comparisons with large modern drainage systems (and accounting for lag times since deposition), links a young age peak (Mio-Pliocene) to the Greater Himalaya and a dominant older age peak (Mid Miocene) to the Lesser Himalaya. Siwaliks paleodrainage is likely to be comparable to the modern range front, pointing to persistent elevated topography in the Lesser Himalaya east of Kuru Chu.

Impacts of marine cloud brightening scheme on the Tibetan Plateau

Xie M[1]

[1]*College of Global Change and Earth System Science, Beijing Normal Univ., China*

Geoengineering, which is the deliberate and large-scale manipulation of the Earth's climate, has been proposed as a way to mitigate or offset the impacts of anthropogenic global warming, Marine cloud brightening (through sea spray injection to increase the albedo of the cloud) is considered as the most effective geoengineering scheme with its high feasibility. In this study, we will use the simulated data from the three Earth system models (HadGEM2-ES, MIROC-ESM, CanESM2) to analyze the impact of marine cloud brightening scheme on various climate factors in the Tibetan Plateau, i.e. we will evaluate the spatial and temporal evolution of precipitation, temperature, radiation flux, cloud optical thickness with/without marine cloud brightening implement.

Provenance and paleodrainage signature in Bengal Fan deposits

Yoshida K[1], Osaki A[1], France-Lanord C[2]

[1]Faculty of Science, Shinshu Univ., Matsumoto, Japan [2]CRPG, CNRS, Univ. of Lorraine, Nancy, France

The Bengal Fan is the largest submarine fan in the world. It has developed as a result of the collision of India with Asia, reflecting the orogeny of the Himalayas. The changes in the mineral assemblages of fan sediments record the uplift history of the Himalayan orogenic system. In the deepest site, U1451A and U1451B of IODP Expedition 354, a complete sequence of fan deposits from the Oligocene was recovered (France-Lanord et al. 2015). The sediments drilled at this site consisted of mica and quartz-rich sand, silt, and clay, with the exception of the lower Oligocene-Eocene section. In this study, we examined the heavy mineral assemblage in the sediments in the Bengal Fan with a chemistry of detrital garnets, amphibole and chromian spinels. Heavy mineral fractions were isolated from core samples, which range in age from earliest Miocene to present.

It is already reported that the heavy mineral assemblage of the Early Miocene silt-sands was mainly characterized by the predominance of garnet and amphibole grains with a small amount of kyanite, sillimanite and staurolite by Yoshida et al. (2016). The most sand layers in the lower Miocene contain tourmaline, apatite, rutile and amphibole grains with relatively Mg-rich almandine garnets correlatable to the metamorphic garnets in the High Himalayan Crystalline complex. However, several sand layers contain sodic amphibole and chromian spinels, which show very low TiO_2 content (< 0.05 wt%) suggestive of depleted ultramafic rock origin. In the Middle Miocene sequence, most of the sand layers contain Mg-rich almandine garnet and amphiboles, however, several sand layers contain sodic amphibole and chromian spinels with almandine garnet. Pliocene and Pleistocene sands frequently include pyroxene, olivine, sodic amphibole and chromian spinels.

The sand layers including both sodic amphibole and chromian spinels were possibly derived from ophiolite zone in Yarlung Tsangpo suture zone. These heavy minerals might be carried by "paleo-Brahmaputra river" and supplied to Bengal Fan. Though the Ganges river, which carried the most of detritus from central and western Himalayas, constantly supplied a large amount of detritus into Bengal Fan, the paleo-Brahmaputra river could supply the detritus from eastern Himalaya and Burman mountain ranges in the early Miocene period. The relative richness of the sodic amphibole and chromian spinels in Pliocene and Pleistocene sands is considered to be caused by strong uplift around the Eastern Himalayan syntaxis.

Reference

France-Lanord C, Spiess V, Klaus A (2015) Expedition 354 Preliminary Report Bengal Fan Neogene and late Paleogene record of Himalayan orogeny and climate: a transect across the Middle Bengal Fan. IODP.

Yoshida K, Nakajima T, Osaki A, Matsumto Y, Gyawali BR, Regmi AD, Rai L, Sakai H (2016) Heavy mineral assemblages in Bengal Fan sediments, IODP Exp. 354, and foreland basin fill of Himalaya. 123th Ann Meet Geol Soc Japan, R8-P-7.

Mineralizing epochs, exhumation, and preservation of the Hariza-Halongxiuma polymetallic ore district in Eastern Kunlun Mountains, Northeastern Tibetan Plateau, China

Yuan W[1], Zhou P[2]

[1]Inst. of Earth Sciences, China Univ. of Geosciences, Beijing, China [2]School of Earth Sciences and Resources, China Univ. of Geosciences, Beijing, China

The Ganzi-Litang gold belt, a part of the Sanjiang Tethys orogen, is located between the Yidun block and Songpan Garze block in eastern Qinghai-Tibetan plateau and experienced the oceanic slab subduction, continent-arc collision and intracontinental convergence since Indosinian Epoch. A series of gold ore deposits have been found in the recent years within the region. The gold ore mineralization was closely related to the alkaline magmatic hydrothermalism in Yanshanian Period. In this paper the fission track (FT) method has been used to reveal the tectonic evolution, mineralizing episodes and preservation of the gold ore deposits. The new geochronological data and new evidences are presented.

The zircon FT analysis results are composed of 4 age groups of 217-213 Ma, 190-160 Ma, 155-93 Ma and 72-67 Ma. The 4 age groups represent 4 distinct episodes of gold mineralization in which the middle two predominate. The auriferous volcanic rocks were formed since the subduction in 217-213 Ma. The mineralization episode of 190-160 Ma corresponds to the formation of both, the auriferous volcanic rocks and the Ganzi-Litang ductile shear belt in intracontinental collisional convergent stage. The episodes of 155-93 Ma and 72-67 Ma were related to a period of post collisional quiescence during tectonic evolution. It was the age of 217-213 Ma that the Ganzi-Litang Meso-Tethys Ocean entered into the subduction episode. The age groups of 190-160 Ma and 155-67 Ma recorded an integral time period of the intracontinental collision-convergence events and post-collision intracontinental evolution with weak tectonic activities, respectively.

The apatite fission track ages show 4 groups of 92-88 Ma, 34-26 Ma, 17-15 Ma and 8.1 Ma, according better with tectonic-magmatic activity and their developing periods. The uplifting amplitude and the uplifting rate are quantitatively calculated, revealing different orders of magnitude and the uneven uplifting. The uplifting rate could be divided into 4 orders of 0.07 mm/yr, 0.18-0.24 mm/yr, 0.32-0.43 mm/yr, and 0.81 mm/yr. The uplifting amplitude has 3 magnitude orders, that is, 5405 m, 6023-6272 m and 6519-6576 m. The exhumation amount is about 2100 m averagely. The ore deposits belong to the medium-epithermal gold deposits, and formed in the condition of higher oxygen fugacity, middle-shallow depths and middle-low temperature of 165-250 ºC based on various mineragenetic indexes. It is shown that the most ore deposits are better preserved except for a small portion has been denuded partially.

This work was supported by the National Natural Science Foundation of China (Nos. 41730427 and 41172088) and the National Basic Research Program of China (No. 2015CB452606).

Zircon SHRIMP U-Pb dating of high potassium rhyolite at Caze area of Tibet and its geological significance

Zhou S[1], Qiu RZ[2], Ren XD[2], Qiu L[1], Zhao LK[1], Zhu QL[1]

[1]China Univ. of Geosciences, Beijing, China [2]Development and Research Center, China Geological Survey, Beijing, China Zhou S1, Qiu R Zhao2, Ren X Dong1, Qiu L1, Zhao L Ke1, Zhu Q Long 1

The Miocene volcanic rocks in Gangdese belt are less exposed and were previously interfused into the Palaeocene-Eocene group. Based on previous work, we conducted field geological investigation, laboratory study, and the zircon SHRIMP U-Pb dating of the Neogene volcanic rocks in the southern part of Caze graben. Compared with previous studies, the samples of LZ06023 and LZ06023-1 have higher SiO_2 content and lower total alkali content, which is different from that of the intermediate-basic potassic-ultra-potassic volcanic rocks studied by previous researchers. Zircons with good crystal shape, no cracks and no inclusions were dated on the SHRIMP-II instrument in the centre of Beijing ion probe. SHRIMP U-Pb dating results of the zircons are mainly distributed between the Concordia ages with a weighted mean $^{206}Pb/^{238}U$ age of 12.82 ± 0.69 Ma (MSWD = 2.8) and 12.81 ± 0.68 Ma (MSWD = 1.7), indicating that the volcanic activity occurred in the middle Miocene.

The results of the high potassium rhyolite dating in the Caze area determined was within the age range of most of the existing Miocene potassic-ultra-porassic volcanic rocks (14.1-11.5 Ma) at the southern range of the Dangreyong graben. This result provides new constraints for clarifying the temporal and spatial distribution of the Neogene volcanic rocks there and is great significance for studying the composition and evolution of the lithospheric mantle in the Neogene period of the Tibet Plateau.

This work is jointly funded with the National Natural Science Foundation of China (40572048) and the National key research and development Project (2016YFC0600304) and the international Science & Technology cooperation Program of China (2011DFA22460), the National Science and Technology support program of the 12th five-year plan (2015BAB061302-2).

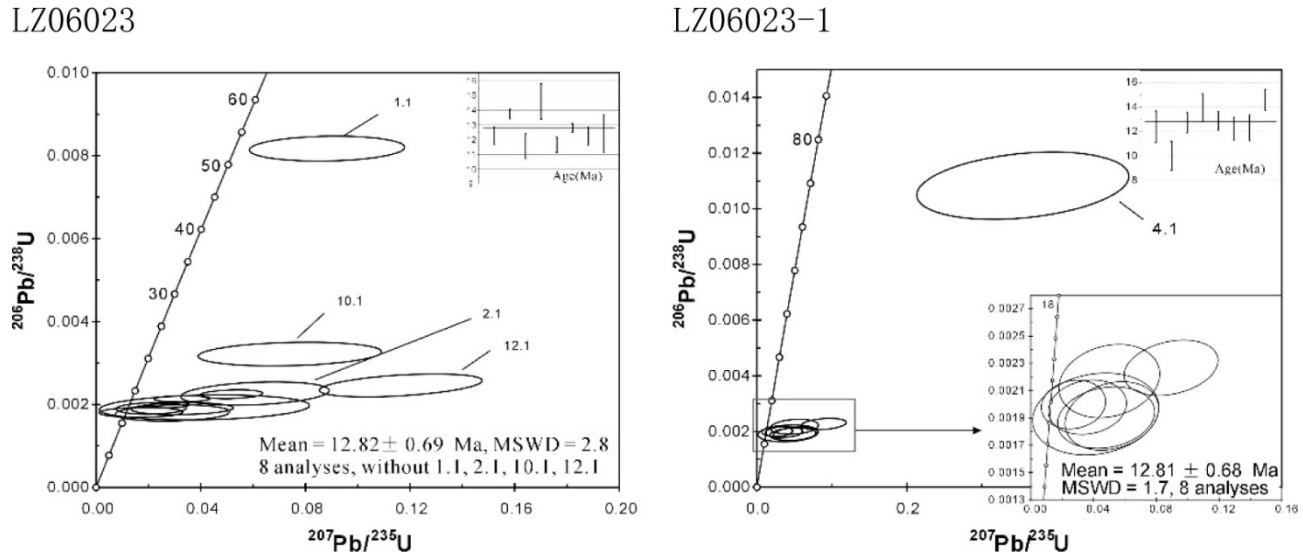

Figure 1. Zircon SHRIMP U-Pb Concordia diagram of high potassium rhyolite in Caze Area.

List of workshop participants and their affiliations

Family name	Given name	Institution	Country
Ahsan	Naveed	Univ. of the Punjab	Pakistan
Airaghi	Laura	ISTeP Sorbonne Univ.	France
Ali	Sheikh Nawaz	Birbal Sahni Inst. of Palaeosciences	India
Battistella	Claire	Univ. Alabama	USA
Baud	Aymon	Baud Geological Consultant	Switzerland
Beaumont	Chris	Dalhousie Univ.	Canada
Bhattacharya	Gourab	Univ. Alabama	USA
Bollinger	Laurent	CEA	France
Bouscary	Chloé	Univ. Bern	Switzerland
Braden	Zoe	Queen's University	Canada
Buchs	Nicolas	Univ. Lausanne	Switzerland
Burg	Jean-Pierre	ETH Zurich	Switzerland
Carosi	Rodolfo	Univ. Torino	Italy
Chen	Gang	China Univ. of Geosciences, Wuhan	China
Chen	Yating	Beijing Normal Univ.	China
Clark-Lowes	Danny	Nubian Consulting	United Kingdom
Coutand	Isabelle	Dalhousie Univ.	Canada
Dal Zilio	Luca	ETH Zurich	Switzerland
de Palézieux	Larissa	ETH Zurich	Switzerland
de Sigoyer	Julia	Univ. Grenoble-Alpes	France
Devkota (Regmi)	Sabina	Nepal Agriculture Research Council	Nepal
Diehl	Tobias	ETH Zurich	Switzerland
Dini	Benedetta	ETH Zurich	Switzerland
Dupont-Nivet	Guillaume	CNRS, Potdsam Univ.	Germany
Epard	Jean-Luc	Univ. Lausanne	Switzerland
Fluteau	Frédéric	CNRS, Inst. de Physique du Globe de Paris	France
Fort	Monique	Univ. Paris Diderot	France
France-Lanord	Christian	CNRS, CRPG Univ. Lorraine	France
Furlong	Kevin	Penn State Univ.	USA
Gajurel	Ananta	Tribhuvan Univ.	Nepal
Gébelin	Aude	Univ. Plymouth	United Kingdom
Ghangas	Vandana	Ministry of Earth Sciences	India
Ghani	Humaad	Univ. Potsdam	Germany
Ghosh	Abhijit	Univ. California, Riverside	USA
Ghoshal	Suryodoy	Univ. Pittsburgh	USA
Godard	Vincent	Aix-Marseille Univ.	France
Grujic	Djordje	Dalhousie Univ.	Canada
Guillermin	Zoé	Univ. Lausanne	Switzerland
Guillot	Stephane	Univ. Grenoble-Alpes	France
Hazarika	Devajit	Wadia Inst. of Himalayan Geology	India
Hermanns	Reginald L.	Geological Survey of Norway	Norway
Hetényi	György	Univ. Lausanne	Switzerland
Hubbard	Mary	Montana State Univ.	USA
Huber	Marius	ETH Zurich	Switzerland
Husson	Laurent	CNRS, Univ. Grenoble-Alpes	France

Family name	Given name	Institution	Country
Huyghe	Pascale	Univ. Grenoble-Alpes	France
Iaccarino	Salvatore	Univ. Torino	Italy
Imayama	Takeshi	Okayama Univ. of Science	Japan
Iturrizaga	Lasafam	Univ. Potsdam	Germany
Iwano	Hideki	Kyoto Fission-Track Co.	Japan
Jamieson	Rebecca	Dalhousie Univ.	Canada
Jiang	Xiaodian	Ocean Univ. of China	China
Jordan	Maud	Univ. Lausanne	Switzerland
Kargel	Jeffrey	Planetary Science Inst.	USA
Karki	Alina	Nepal Electricity Authority	Nepal
Kaya	Mustafa	Univ. Potsdam	Germany
Kelly	Sean	Dalhousie Univ.	Canada
King	Georgina	Univ. Bern	Switzerland
Kufner	Sofia-Katerina	GFZ Potsdam	Germany
Kumar	Naresh	Wadia Inst. of Himalayan Geology	India
Laskowski	Andrew	Montana State Univ.	USA
Lavé	Jérôme	CNRS, CRPG Univ. Lorraine	France
Law	Richard	Virginia Tech	USA
Le Roux-Mallouf	Romain	Géolithe	France
Lenard	Sebastien	CRPG Univ. Lorraine	France
Li	Wei	Wuhan Univ.	China
Liang	Wendong	Univ. Milano Bicocca	Italy
Licht	Alexis	Univ. Washington	USA
Lihter	Iva	Univ. British Columbia	Canada
Liu	Jinmei	Univ. of Chinese Academy of Sciences	China
Liu	Shiran	Peking Univ.	China
Lupker	Maarten	ETH Zurich	Switzerland
Maitra	Akeek	Inst. of Geological Sci., Polish Acad. of Sci.	Poland
Malatesta	Luca	Univ. California, Santa Cruz	USA
Manglik	Ajai	CSIR, National Geophysical Research Inst.	India
Märki	Lena	ETH Zurich	Switzerland
McQuarrie	Nadine	Univ. Pittsburgh	USA
Meena	Sansar Raj	Univ. Salzburg	Austria
Miraj	Muhammad A. F.	Univ. of the Punjab	Pakistan
Molnar	Peter	Univ. Colorado	USA
Montemagni	Chiara	Univ. Milano Bicocca	Italy
Montomoli	Chiara	Univ. Pisa	Italy
Mozhikunnath Parameswaran	Revathy	Jawaharlal Nehru Centre for Adv. Sci. Res.	India
Najman	Yani	Lancaster Univ.	United Kingdom
Nakajima	Toru	Univ. Kyoto	Japan
Nania	Laura	Univ. Florence	Italy
Neustadtl	Sara	Guest	USA
Orme	Devon	Montana State Univ.	USA
Pandey	Arjun	Wadia Inst. of Himalayan Geology	India
Pantet	Adrien	Univ. Lausanne	Switzerland
Parsons	Andy	Univ. Oxford	United Kingdom
Patra	Abhijit	Indian Statistical Inst.	India

Family name	Given name	Institution	Country
Phillips	Stacy	The Open Univ.	United Kingdom
Ping	Zhou	China Univ. of Geosciences, Beijing	China
Qayyum	Abdul	Middle East Technical Univ., Ankara	Turkey
Rajendran	C. P.	Jawaharlal Nehru Centre for Adv. Sci. Res.	India
Rajendran	Kusala	Centre for Earth Sci., Indian Inst. of Sci.	India
Rapa	Giulia	Univ. Torino	Italy
Raymond	Gerald	Univ. Lausanne	Switzerland
Regmi	Dhananjay	The Himalayan Research Expeditions	Nepal
Riesner	Magali	Nanyang Technological Univ.	Singapore
Robinson	Delores	Univ. Alabama	USA
Robyr	Martin	Univ. Lausanne	Switzerland
Rohrmann	Alexander	Univ. Potsdam	Germany
Roperch	Pierrick	CNRS, Géosciences Rennes	France
Saha	Dilip	Indian Statistical Inst.	India
Sajid	Muhammad	Univ. Peshawar	Pakistan
Salvi	Dnyanada	IIT Bombay	India
Sanyal	Prasanta	IISER Kolkata	India
Schide	Katie	ETH Zurich	Switzerland
Schmalholz	Stefan	Univ. Lausanne	Switzerland
Schulze	Nora	Univ. Bremen	Germany
Searle	Mike	Univ. Oxford	United Kingdom
Shrestha	Sudip	Univ. British Columbia	Canada
Shukla	Anumeha	Birbal Sahni Inst. of Palaeosciences	India
Singh	Sandeep	IIT Roorkee	India
Steck	Albrecht	Univ. Lausanne	Switzerland
Subedi	Shiba	Univ. Lausanne	Switzerland
Tardif	Delphine	CNRS, Inst. de Physique du Globe de Paris	France
Thiede	Rasmus C.	Univ. Kiel	Germany
van Hinsbergen	Douwe	Utrecht Univ.	The Netherlands
Villa	Igor M.	Univ. Milano Bicocca / Univ. Bern	Italy / Switzerland
Wang	Qi	China Univ. of Geosciences, Wuhan	China
Wason	Hans Raj	IIT Roorkee	India
Webb	A. Alexander G.	Univ. Hong Kong	Hong Kong
Webster	Tim	Plymouth Univ.	United Kingdom
Westerweel	Jan	CNRS, Géosciences Rennes	France
Wood	Matthew	Univ. Melbourne	Australia
Xie	Mengdie	Beijing Normal Univ.	China
Xu	Caijun	Wuhan Univ.	China
Yoshida	Kohki	Shinshu Univ.	Japan
Yuan	Wanming	China Univ. of Geosciences, Beijing	China
Zhou	Su	China Univ. of Geosciences, Beijing	China